U.S. Department
of Commerce

Volume 109
Number 1
January 2011

Fishery Bulletin

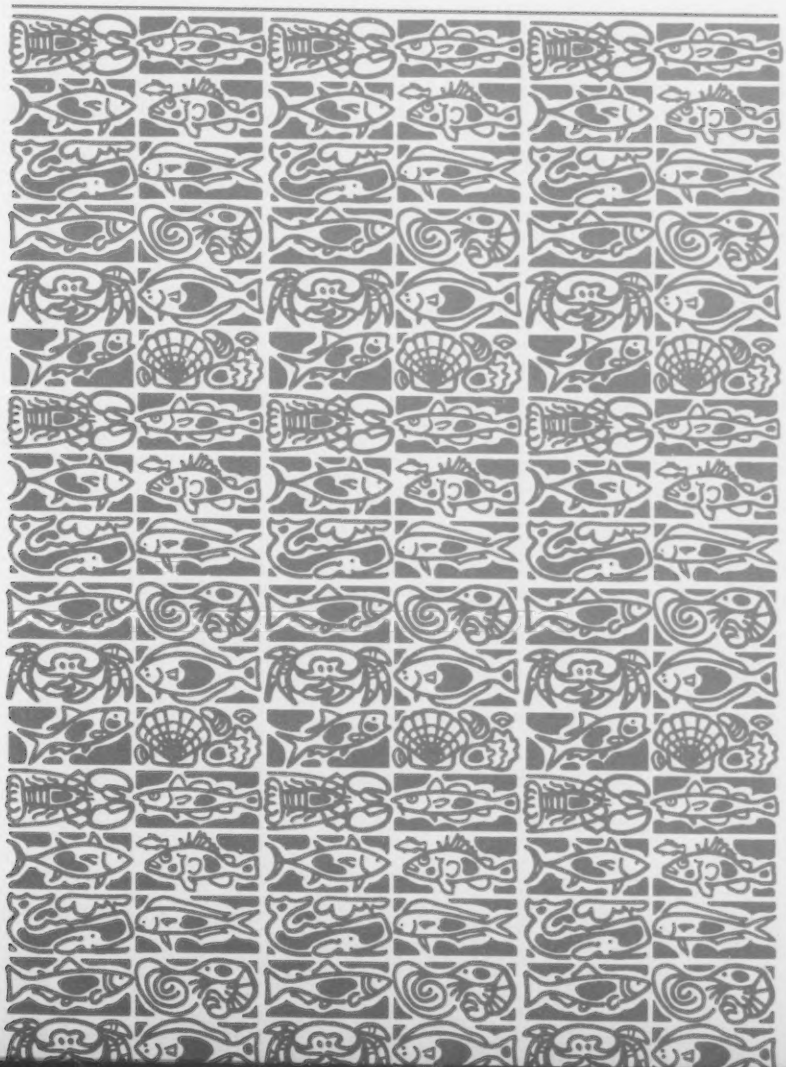

U.S. Department of Commerce
Gary Locke
Secretary of Commerce

National Oceanic and Atmospheric Administration
Jane Lubchenco, Ph.D.
Administrator of NOAA

National Marine Fisheries Service
Eric C. Schwaab
Assistant Administrator for Fisheries

Fishery Bulletin

Scientific Editor
Richard D. Brodeur, Ph.D.

Associate Editor
Julie Scheurer

National Marine Fisheries Service
Northwest Fisheries Science Center
2030 S. Marine Science Dr.
Newport, Oregon 97365-5296

Managing Editor
Sharyn Matriotti

National Marine Fisheries Service
Scientific Publications Office
7600 Sand Point Way NE
Seattle, Washington 98115-0070

Editorial Committee

John Carlson	National Marine Fisheries Service, Panama City, Florida
Kevin Craig	Florida State University, Tallahassee, Florida
Jeff Leis	Australian Museum, Sydney, New South Wales, Australia
Rich McBride	National Marine Fisheries Service, Woods Hole, Massachusetts
Rick Methot	National Marine Fisheries Service, Seattle, Washington
Adam Moles	National Marine Fisheries Service, Auke Bay, Alaska
Frank Parrish	National Marine Fisheries Service, Honolulu, Hawaii
Dave Somerton	National Marine Fisheries Service, Seattle, Washington
Ed Trippel	Department of Fisheries and Oceans, St. Andrews, New Brunswick, Canada
Mary Yoklavich	National Marine Fisheries Service, Santa Cruz, California

***Fishery Bulletin* web site: www.fisherybulletin.noaa.gov**

The *Fishery Bulletin* (ISSN 0090-0656) is published quarterly by the Scientific Publications Office, National Marine Fisheries Service, NOAA, 7600 Sand Point Way NE, BIN C15700, Seattle, WA 98115-0070. Periodicals postage is paid at Seattle, WA. POSTMASTER: Send address changes for subscriptions to Fishery Bulletin, Superintendent of Documents, Attn.: Chief, Mail List Branch, Mail Stop SSOM, Washington, DC 20402-9373.

Although the contents of this publication have not been copyrighted and may be reprinted entirely, reference to source is appreciated.

The Secretary of Commerce has determined that the publication of this periodical is necessary according to law for the transaction of public business of this Department. Use of funds for printing of this periodical has been approved by the Director of the Office of Management and Budget.

For sale by the Superintendent of Documents, U.S. Government Printing Office, Washington, DC 20402. Subscription price per year: $36.00 domestic and $50.40 foreign. Cost per single issue: $21.00 domestic and $29.40 foreign. **See back for order form.**

The *Fishery Bulletin* carries original research reports and technical notes on investigations in fishery science, engineering, and economics. It began as the Bulletin of the United States Fish Commission in 1881; it became the Bulletin of the Bureau of Fisheries in 1904 and the *Fishery Bulletin* of the Fish and Wildlife Service in 1941. Separates were issued as documents through volume 46; the last document was No. 1103. Beginning with volume 47 in 1931 and continuing through volume 62 in 1963, each separate appeared as a numbered bulletin. A new system began in 1963 with volume 63 in which papers are bound together in a single issue of the bulletin. Beginning with volume 70, number 1, January 1972, the *Fishery Bulletin* became a periodical, issued quarterly. In this form, it is available by subscription from the Superintendent of Documents, U.S. Government Printing Office, Washington, DC 20402. It is also available free in limited numbers to libraries, research institutions, State and Federal agencies, and in exchange for other scientific publications.

U.S. Department of Commerce
Seattle, Washington

Volume 109
Number 1
January 2011

Fishery Bulletin

Contents

Articles

1-19 **Campfield, Patrick A., and Edward D. Houde**
Ichthyoplankton community structure and comparative trophodynamics in an estuarine transition zone

20–33 **Friess, Claudia, and George R. Sedberry**
Age, growth, and spawning season of red bream (*Beryx decadactylus*) off the southeastern United States

34–47 **Cox, M. Keith, Ron Heintz, and Kyle Hartman**
Measurements of resistance and reactance in fish with the use of bioelectrical impedance analysis: sources of error

48–55 **Sturdivant, S. Kersey, and Kelton L. Clark**
An evaluation of the effects of blue crab (*Callinectes sapidus*) behavior on the efficacy of crab pots as a tool for estimating population abundance

56–67 **Merritt, Daniel, Mary K. Donovan, Christopher Kelley, Lynn Waterhouse, Michael Parke, Kevin Wong, and Jeffrey C. Drazen**
BotCam: a baited camera system for nonextractive monitoring of bottomfish species

68–78 **Able, Kenneth W., Mark C. Sullivan, Jonathan A. Hare, Gretchen Bath-Martin, J. Christopher Taylor, and Roland Hagan**
Larval abundance of summer flounder (*Paralichthys dentatus*) as a measure of recruitment and stock status

79–89 **Kurita, Yutaka, Yuichiro Fujinami, and Masafumi Amano**
The effect of temperature on the duration of spawning markers—migratory-nucleus and hydrated oocytes and postovulatory follicles—in the multiple-batch spawner Japanese flounder (*Paralichthys olivaceus*)

The National Marine Fisheries Service (NMFS) does not approve, recommend, or endorse any proprietary product or proprietary material mentioned in this publication. No reference shall be made to NMFS, or to this publication furnished by NMFS, in any advertising or sales promotion which would indicate or imply that NMFS approves, recommends, or endorses any proprietary product or proprietary material mentioned herein, or which has as its purpose an intent to cause directly or indirectly the advertised product to be used or purchased because of this NMFS publication.

The NMFS Scientific Publications Office is not responsible for the contents of the articles or for the standard of English used in them.

90–100 **Ballagh, Aaron C., David Welch, Ashley J. Williams, Amos Mapleston, Andrew Tobin, and Nicholas Marton**
Integrating methods for determining length-at-age to improve growth estimates for two large scombrids

101–112 **Booth, Anthony J., Alan J. Foulis, and Malcolm J. Smale**
Age validation, growth, mortality, and demographic modeling of spotted gully shark (*Triakis megalopterus*) from the southeast coast of South Africa

113–122 **Lane, Hillary A., Andrew J. Westgate, and Heather N. Koopman**
Ontogenetic and temporal variability in the fat content and fatty acid composition of Atlantic herring (*Clupea harengus*) from the Bay of Fundy, Canada

123–134 **DeMartini, Edward E., Alan R. Everson, and Ryan S. Nichols**
Estimates of body sizes at maturation and at sex change, and the spawning seasonality and sex ratio of the endemic Hawaiian grouper (*Hyporthodus quernus*, F. Epinephelidae)

135 Errata

136 Guidelines for authors

Subscription form (inside back cover)

Ichthyoplankton community structure and comparative trophodynamics in an estuarine transition zone

Patrick A. Campfield (contact author)*

Edward D. Houde

Email address for contact author: pcampfield@asmfc.org

University of Maryland Center for Environmental Science
Chesapeake Biological Laboratory
1 Williams Street
Solomons, Maryland 20688, USA

*Present address: Atlantic States Marine Fisheries Commission
1050 N. Highland Street
Arlington, Virginia 22201

Abstract—Surveys were conducted to evaluate and compare assemblage structure and trophodynamics of ichthyoplankton, and their variability, in an estuarine transition zone. Environmental gradients in the salt-front region of the Patuxent River subestuary, Chesapeake Bay, were hypothesized to define spatiotemporal distributions and assemblages of ichthyoplankton. Larval fishes, zooplankton, and hydrographic data were collected during spring through early summer 2000 and 2001. Larvae of 28 fish species were collected and species richness was similar each year. Total larval abundance was highest in the oligohaline region down-estuary of the salt front in 2000, but highest at the salt front in 2001. Larvae of anadromous fishes were most abundant at or up-estuary of the salt front in both years. Two ichthyoplankton assemblages were distinguished: 1) riverine—characterized predominantly by anadromous species (Moronidae and Alosinae); and 2) estuarine—characterized predominantly by naked goby (*Gobiosoma bosc*) (Gobiidae). Temperature, dissolved oxygen, salinity-associated variables (e.g., salt-front location), and concentrations of larval prey, specifically the calanoid copepod *Eurytemora affinis* and the cladoceran *Bosmina longirostris*, were important indicators of larval fish abundance. In the tidal freshwater region up-estuary of the salt front, there was substantial diet overlap between congeneric striped bass (*Morone saxatilis*) and white perch (*M. americana*) larvae, and also larvae of alewife (*Alosa pseudoharengus*) (overlap= 0.71–0.93). Larval abundance, taxonomic diversity, and dietary overlap were highest within and up-estuary of the salt front, which serves to both structure the ichthyoplankton community and control trophic relationships in the estuarine transition zone.

Manuscript submitted 30 January 2010.
Manuscript accepted 30 August 2010.
Fish. Bull. 109:1–19 (2011).

The views and opinions expressed or implied in this article are those of the author (or authors) and do not necessarily reflect the position of the National Marine Fisheries Service, NOAA.

Anadromous and estuarine fishes migrate in the spring months to oligohaline and freshwater regions of tidal tributaries in Chesapeake Bay to spawn, potentially leading to overlapping distributions and diets of their larvae. Spawning seasonality overlaps broadly for anadromous alosines (shads and herrings [*Alosa* spp.]) and moronids (striped bass [*Morone saxatilis*], white perch [*M. americana*]). Estuarine species such as naked goby (*Gobiosoma bosc*) and bay anchovy (*Anchoa mitchilli*) also spawn during late spring and early summer in tidal tributaries, and their larvae occur in oligohaline regions, often near the salt front (Shenker et al., 1983; Loos and Perry, 1991).

There is limited information on foraging by larval fishes in Chesapeake Bay and the influences hydrographic features may have on foraging. Successful larval foraging improves with ontogeny as swimming ability and mouth gape increase, leading to shifts in types and sizes of zooplankton prey selected (Shirota, 1970; Arthur, 1976; Pepin and Penney, 1997). With some exceptions, larvae of closely related estuarine fishes in Chesapeake Bay often have similar diets (Setzler-Hamilton et al.[1]) that could result in resource competition within larval fish assemblages. Feeding habits of alewife (*Alosa pseudoharengus*) larvae in freshwater lakes (Norden, 1968), in laboratory experiments (Miller et al., 1990), and of congeneric larval alosines (American shad [*A. sapidissima*] and blueback herring [*A. aestivalis*]) in estuaries have been described (Crecco and Blake, 1983). Laboratory experiments on prey selection by naked goby larvae (Harding, 1999) and feeding by naked goby larvae in the Patuxent River (Breitburg, 1991) also are described. Foods and feeding by striped bass and white perch larvae have been reported (Setzler et al., 1981; Limburg et al., 1997; Chick and Van den Avyle, 1999; Shoji et al., 2005; Martino and Houde, 2010).

We refer to the frontal region where fresh and oligohaline waters merge as the estuarine transition zone, a region potentially important in controlling occurrences and feeding by fish larvae. This frontal region often contains an estuarine turbidity maximum (ETM) and is an important nursery area for young fish (North and Houde, 2001, 2003; Winkler et al., 2003; Shoji and Tanaka, 2006; Boynton et al.[2]). Previous research

[1] Setzler-Hamilton, E. M., P. W. Jones, G. E. Drewry, F. D. Martin, K. L. Ripple, M. Beaven, and J. A. Mihursky. 1982. A comparison of larval feeding habits among striped bass, white perch and Clupeidae in the Potomac Estuary. Rep. Md. Univ. Chesapeake Biol. Lab., no. 81–87, p. 1–127.

[2] Boynton, W. R., W. Boicourt, S. Brant, J. Hagy, L. Harding, E. D. Houde, D. V. Holliday, M. Jech, W. M. Kemp, C. Lascara, S. D. Leach, A. P. Madden, M. R. Roman, L. P. Sanford, and E. M. Smith. 1997. Interactions between physics and biology in the estuarine turbidity maximum (ETM) of Chesapeake Bay, USA. ICES Council Meeting Documents 1997/S:11. (www.ices.dk/products/cmdocsindex.asp).

in the mainstem of Chesapeake Bay has shown above-mean concentrations of zooplankton and larvae of anadromous striped bass and white perch near the salt front and associated ETM, where physical processes act to trap and concentrate plankton (North and Houde, 2001; Roman et al., 2001). Here, we identify ichthyoplankton assemblages and analyze the feeding ecology of larval fishes in the Patuxent River subestuary. We tested two hypotheses: 1) environmental gradients define spatiotemporal distributions and assemblages of ichthyoplankton in the estuarine transition zone; and 2) the salt front plays a key role in controlling assemblage structure and trophic interactions of larval fish communities.

In analyzing trophic relationships of fish larvae co-occurring in the estuarine transition zone, we addressed the following questions:

- Are diets controlled by the types of zooplankton prey available?
- Is there significant dietary overlap among co-occurring larval fishes?
- Do the salt front and estuarine transition zone control diets?
- Does selection of prey types and sizes shift during ontogeny?

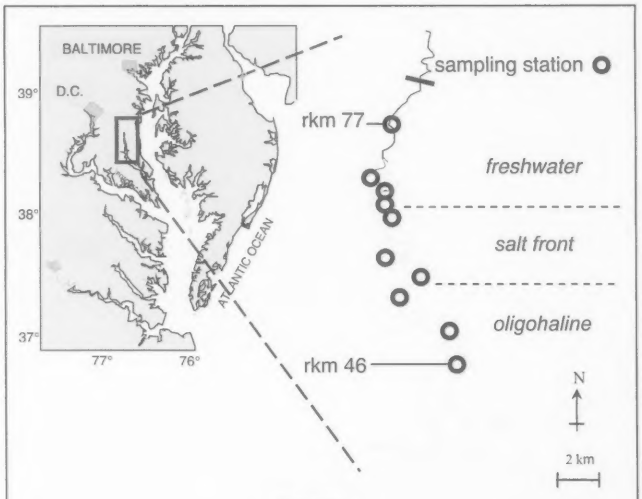

Figure 1

Patuxent River study area with sampling stations and regions for the years 2000 and 2001. The area between river kilometers (rkm) 46–77 defines the estuarine transition zone. Dashed lines in the enlarged map are conceptual partitions of freshwater, salt-front, and oligohaline regions. For individual surveys, the regions and numbers of stations within each region varied depending on the location of the salt front.

Materials and methods

Study area and sampling procedures

Ichthyoplankton surveys on the tidal Patuxent River were conducted at 3–7 day intervals between 24 April and 5 July (13 surveys in 2000 and 17 surveys in 2001) to identify larval assemblages and shifts in seasonal abundances. Sampling was conducted from late spring to early summer to coincide with the peak seasonal spawning and larval production periods of anadromous and estuarine fishes. Samples were taken at 10 designated stations along the channel in the estuarine transition zone (Fig. 1). Stations were located at 2–7 river-kilometer intervals where depths ranged from 2 to 10 m. Surveys were conducted during daylight and were of 8–10 hours duration.

Sampling stations were located up-estuary, within, and down-estuary of the salt front in the estuarine transition zone (Fig. 1). The location of the salt front, defined by conductivities of 800–1000 µS (approximate salinities 0.4–0.5), was determined in each survey. Ichthyoplankton distributions, concentrations, and sizes were evaluated with respect to the salt front and site of intersection of the 2.0 isohaline with the bottom (referred to as X_2 by Jassby et al., 1995). Most surveys were conducted from an 8-m boat (11 surveys in 2000; 14 in 2001). Ichthyoplankton was sampled by towing a 60-cm diameter, paired bongo net with 333-µm meshes at 1 m/s in 5-min oblique tows from the surface to the bottom. Flow meters in net mouths measured volumes of water sampled for use in calculating larval concentrations (no./m^3). The mean volume filtered in each tow (combined paired-net samples) was 137 m^3 (±9 m^3 standard deviation [SD]). In the final weeks of the survey during each year, juveniles and large larvae were sampled from a 16-m (2000) or a 19-m vessel (2001) with a 2-m^2 mouth-opening Tucker-trawl with 700-µm meshes (23 June and 5 July 2000, and 31 May, 27 June, and 3 July 2001). Oblique tows were of 5-min duration from near-bottom to surface at approximately 1 m/s and filtered a mean volume of 575 m^3 (±71 m^3 SD). Ichthyoplankton samples were preserved in ethanol.

Zooplankton (potential prey for fish larvae) was collected at each station by pumping 20 liters of water from surface, middle, and bottom depths (60 liters total). Water from the three depths was combined and filtered onto a 35-µm sieve to concentrate zooplankton before preserving samples in 5% formalin. In the laboratory, zooplankters were identified, enumerated, and measured.

At each station, measurements of temperature, salinity, conductivity, and dissolved oxygen were made at surface, mid-water, and near-bottom for analysis of ichthyoplankton occurrence and abundance. Surface pH was measured at alternate stations. River-flow data were obtained from a U.S. Geological Survey gauge at river kilometer 130, near Bowie, Maryland (USGS, http://waterdata.usgs.gov, accessed April 2010).

Processing of samples

In the laboratory, fish larvae and juveniles were identified to species and enumerated. Total lengths (up to 100 individuals of each species per sample) were measured to the nearest 0.1 mm. Zooplankton concentrations (no./L) were estimated for several taxonomic categories, including copepodites and adults of the calanoid copepods *Eurytemora affinis* and *Acartia* sp., cyclopoid copepods, copepod nauplii, invertebrate eggs, rotifers, and the cladoceran *Bosmina longirostris*. Lengths of zooplankters were measured under microscope to the nearest 0.1 mm with an ocular micrometer.

Ichthyoplankton distributions, abundances, and assemblages

Larval concentrations (no./m^3) at each sampling site were calculated from numbers per tow and measured tow volumes. Total larval abundances in river segments representative of each sampling site were estimated by expanding larval concentrations at sites to abundances in documented river-segment volumes (Cox et al.[3]). Abundances were analyzed with respect to hydrographic gradients. Species richness and Shannon-Wiener diversity (H') (Magurran, 1988) were calculated to compare ichthyoplankton assemblages among river regions. Habitat use and spatial overlap were examined in principal components analysis (PCA) of catch per unit of effort (CPUE, no. of larvae/tow) and hydrographic data to identify and describe associations (Miller, 2002).

Ichthyoplankton concentrations were analyzed for stations grouped into three designated regions within the estuary: freshwater, salt front, and oligohaline. Freshwater stations had no detectable salinity. Salt front stations had salinities of 0.2–1.0 and oligohaline stations had salinities >1.0. In each survey, a region typically included 3–4 stations (Fig. 1). Zooplankton and hydrographic variables were included in multivariate analyses to evaluate these factors with respect to larval concentrations of alewife, striped bass, white perch, and naked goby. In statistical analysis, the normality assumption generally was met by applying $\log_{10}(x+1)$ transformations to larval fish and zooplankton concentrations. Multiple regressions with larval concentration as the dependent variable were run on combinations of independent variables in a stepwise procedure (forward-backward) to select variables for inclusion as descriptors of larval concentration. Independent variables considered were temperature, salinity, conductivity, dissolved oxygen, pH, river flow, salt front location, and the concentrations of copepod nauplii, calanoid copepods, and *Bosmina*. The probability threshold for including or removing variables was 0.10. The quality of model fits was assessed by using Akaike's information criterion (AIC). The model with lowest AIC value was retained for each larval taxon (Kleinbaum et al., 1998).

Diet composition

Digestive tracts of larval alewife, striped bass, white perch, and naked goby from the three designated regions were analyzed to determine feeding incidence, kinds of prey, prey numbers, prey sizes, prey selection, and dietary overlap. Larvae were grouped into 1-mm (naked goby) or 2-mm (other taxa) length intervals for diet analyses. In prey selection and dietary overlap comparisons, larvae were analyzed in broader length classes (<10 mm or >10 mm total length [TL]), except for naked goby which was analyzed as a single class (5–12 mm TL). All prey in larval guts were identified, enumerated, and measured with an ocular micrometer. Maximum lengths or widths of each prey taxon were recorded from each larval gut.

Diets of 633 larvae were analyzed (135 alewife; 165 striped bass; 200 white perch; 133 naked goby). Diets and zooplankton concentrations were evaluated from sampling sites throughout the estuarine transition zone (Fig. 1), and from the salt front and intersection of the 2.0 isohaline with bottom. Trophic niche breadth (S), a measure of variability in sizes of prey in the larval diet (Pearre, 1986) was defined as the standard deviation of mean logarithmic ($\log_e$) prey size. An ontogenetic index (O_L) (Fuiman et al., 1998) was calculated to characterize and compare feeding with respect to developmental state of larvae. Mean prey size and niche breadth estimates were regressed on larval length and ontogenetic state to examine patterns in the sizes of prey consumed.

Selection of prey types and sizes in larval diets was evaluated by applying Strauss's (1979) prey selection index:

$$L = r_i - p_i, \tag{1}$$

where r_i = the proportion of zooplankton prey type i in larval guts;
p_i = its proportion in the environment; and
L can range from –1.0 to +1.0.

Positive values indicate prey preference and negative values avoidance. The standard error of L was estimated (Strauss, 1982) and t-tests were conducted to determine whether L differed significantly ($P<0.05$) from 0.

The importance of prey types and sizes in larval diets was evaluated with a relative importance index (George and Hadley, 1979). For each fish species, the importance (A) of prey type a, for length class i was computed with the following equation:

$$A_{i,a} = \%\ \textit{frequency of occurrence} + \%\ \textit{total number} + \%\ \textit{total weight};$$

$$R_{i,a} = 100\left(A_{i,a} / \sum_{a=1}^{k} A_{i,a} \right). \tag{2}$$

[3] Cox, A. M., P. A. Waltz, and P. G. Robertson. 1980. Patuxent River Program. Bathymetric investigation of the Patuxent River system, p. 11–83. Maryland Department of Natural Resources, Water Resources Administration, Annapolis, MD.

$R_{i,a}$ (relative importance) is a measure of the importance of prey type a relative to other prey types. $R_{i,a}$ can range from 0 to 100, and high values indicate greater importance. Zooplankton length-weight relationships (Heinle, 1969) were used to estimate weights of prey in larval guts.

To evaluate possible competition, diet overlaps between larval taxa and length classes were evaluated from gut contents with Czechanowski's index: $O_{12}=O_{21}=1-0.5\ (\Sigma|P_{i1}-P_{i2}|)$ (Feinsinger et al., 1981). O_{12} is the overlap index value of species-length class 1 on species-length class 2, P_{i1} is the proportion of food type i eaten by species-length class 1, and P_{i2} is the proportion of food type i eaten by species-length class 2. Index values may range from 0.0 to 1.0. Values approaching 1.0 indicate strong overlap. Index values were tested for statistical significance by comparing them with null models following procedures of Albrecht and Gotelli (2001) and Gotelli and Entsminger (2003).

Results

Hydrographic conditions

There were strong gradients in hydrographic variables along the 31-rkm estuarine transition zone of the Patuxent River (Fig. 2). Highest temperatures were down-estuary. Salinities ranged from 0.0 to 10.0 and were highest down-estuary. Dissolved oxygen (DO) tended to be higher in the cooler and fresher up-estuary waters.

In 2000, precipitation and river flow were below the historical average and relatively constant. And, except for an unusual cooling episode in late May, river temperatures generally were >20°C during surveys and approached 29°C in early July (Fig. 3). In May, the salt-front location was stationary near river kilometer (rkm) 56 before shifting 5 rkm down-estuary in mid-June, coincident with small increases in precipitation and river flow. DO levels were >8.0 mg/L in May, but declined to approximately 6.0 mg/L as temperatures increased in June.

In 2001, hydrographic conditions were more variable (Fig. 3). Precipitation and river flow were below historical averages and more variable than in year 2000. River temperatures were <20°C in late April, fluctuated in early May, and gradually increased to >25°C by early summer. The salt front shifted 10 rkm up-estuary in early May, coincident with low precipitation and river flow, before moving 12 rkm down-estuary after high-flow events in late May–early June 2001.

The mean salt front locations were at rkm 56 in 2001 and rkm 54 in 2000. DO and pH levels were more variable in 2001. Although DO at mid-depth declined to 4.0 mg/L at down-estuary stations in early May 2001, DO generally ranged from 5 to 10 mg/L during the two years. The pH ranged from 7.0 to >9.0 and was consistently >7.0 in both years; on average, pH was slightly higher in 2001.

Species composition, diversity, and abundance of ichthyoplankton

In the two survey years, a total of 198,161 fish larvae were collected, representing 28 taxa (Appendix Tables 1 and 2). Twenty of the taxa occurred in both years. Species richness over the entire survey area was similar between years ($n_{spp.,\ 2000}=24$, $n_{spp.,\ 2001}=23$). Species diversity was higher in the freshwater and salt-front regions ($H'=0.72–0.86$) than in down-estuary oligohaline waters ($H'=0.25–0.50$). Larval white perch, alewife, gizzard shad (*Dorosoma cepedianum*), and striped bass were the most abundant taxa in freshwater. Naked goby, white perch, and striped bass larvae were the most abundant taxa in salt front and oligohaline regions.

In both years, ichthyoplankton abundance was dominated by larvae of naked goby and white perch, which together comprised 94% and 89% of the catches, respectively, in 2000 and 2001. In 2000, catch per unit of effort (CPUE, no. of larvae/tow) was highest in the oligohaline region (625.1) where naked goby larvae dominated (Appendix Table 1). CPUEs were lower and similar in the salt front (278.9) and in freshwater (212.2). The coefficient of variation (CV) in CPUE, an indicator of spatial heterogeneity, indicated that catches were most variable in freshwater ($CV_{FW}=315\%$) and least variable at the salt front (154%). In 2001, CPUE was highest at the salt front (842.1) (Appendix Table 2) and lowest in the oligohaline region (189.6), primarily because larvae of naked goby were concentrated at the salt front in 2001. Relative variability in CPUE was similar across the freshwater, salt-front, and oligohaline regions in 2001 (CV range 217–254%).

Larvae of several freshwater fishes (spottail shiner [*Notropis hudsonius*]; darters [*Etheostoma* spp.]; suckers [*Erimyzon* spp.]; yellow perch [*Perca flavescens*]) were far more abundant in 2001 than in 2000 (Appendix Tables 1 and 2). For example, the concentration of yellow perch larvae was 15 times higher in 2001. In contrast, larvae of gizzard shad, a freshwater species, were 4 times more abundant in 2000 than in 2001.

Additionally, in the freshwater region in 2001, concentrations of white perch larvae were >2 times higher and concentrations of striped bass larvae were >10 times higher than in 2000 (Fig. 4). Larvae of anadromous striped bass also were relatively abundant at the salt front in 2001 than in 2000. Larvae of naked goby, an estuarine species, although of comparable abundance in the two years, were concentrated in the oligohaline region in 2000, but at the salt front in 2001 (Appendix Tables 1 and 2, Fig. 4). The regional difference in goby abundance between years may be related to differences in the timing of production of these larvae in the two years (Fig. 5). Goby larvae occurred first on 2 May in 2001 and had time to disperse into the salt front region during June. In 2000, goby larvae did not occur until 24 May and then were mostly collected in the oligohaline region, downriver from the salt front.

Differing regional patterns in overall larval abundance between years were largely attributable to the

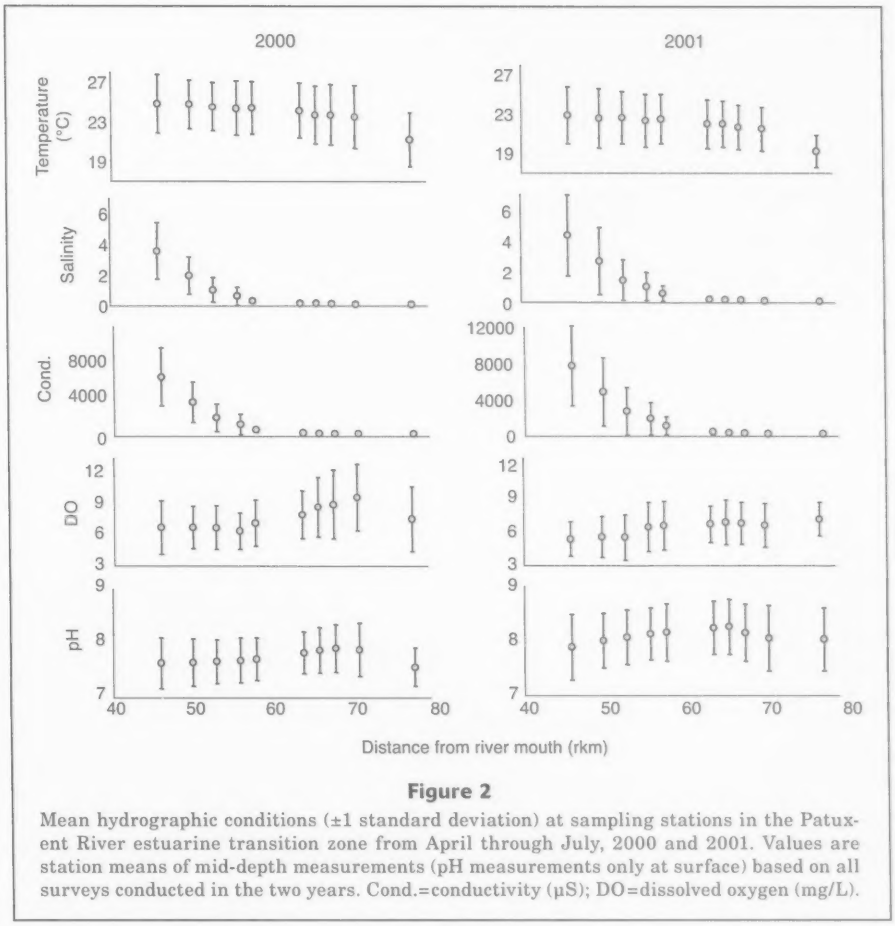

Figure 2

Mean hydrographic conditions (±1 standard deviation) at sampling stations in the Patuxent River estuarine transition zone from April through July, 2000 and 2001. Values are station means of mid-depth measurements (pH measurements only at surface) based on all surveys conducted in the two years. Cond.=conductivity (µS); DO=dissolved oxygen (mg/L).

two most abundant species, naked goby and white perch. In 2000, their mean combined-species CPUE increased directionally from freshwater to oligohaline regions (Appendix Table 1). In contrast, in 2001 their combined mean CPUE was highest at the salt front, intermediate in freshwater, and lowest in the oligohaline region (Appendix Table 2).

Occurrences and abundances of larvae of anadromous species differed with respect to location of the salt front. Yolk-sac larvae of striped bass occurred most frequently up-estuary of the salt front in tidal freshwater, whereas most feeding-stage larvae and small juveniles (<75 mm) were found either within or up-estuary of the salt front. White perch larvae were broadly distributed throughout the estuarine transition zone, overlapping with alosines (mostly alewife) and congeneric striped bass.

Larvae of alewife were consistently most abundant up-estuary of the salt front (Fig. 4). In 2001, larval white perch were clearly more abundant in freshwater than at the salt front or down-estuary, but in 2000 they were equally abundant at the salt front and in freshwater. Larval striped bass concentrations did not differ significantly among the three regions ($P>0.08$) or between 2000 and 2001 ($P>0.07$), although their numbers tended to be relatively high at the salt front and in freshwater in 2001 (Fig. 4).

Temporal patterns in abundances of alewife, striped bass, and white perch were broadly similar in both years. Abundance of white perch larvae was an order of magnitude higher than striped bass in the earliest seasonal collections in each year and generally was higher than that of striped bass throughout the survey periods (Fig. 5). Although larval naked goby were present earlier in the season during 2001, their abundance peaked in the second week of June in both years (Fig. 5), when temperatures in the oligohaline region reached 25°C.

In each year, catches of larvae and small juveniles of the estuarine- and coastal-spawning species became increasingly common later in the sampling period. Small juveniles of menhaden and bay anchovy dominated the late-season (June and July) collections in Tucker trawls. Naked goby larvae occurred first in the oligohaline

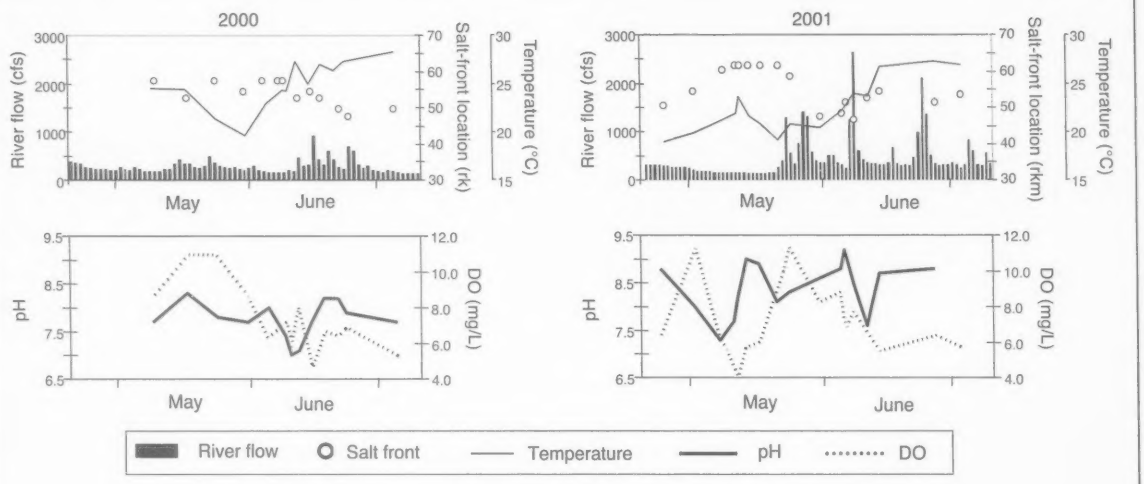

Figure 3

Hydrographic conditions for the Patuxent River in 2000 (left) and 2001 (right). The salt-front location (in river kilometers from river mouth, rkm) is defined by conductivity readings of 800–1000 µS. River flow data were obtained from a U.S. Geological Survey gauge at rkm 130. The plotted temperature, dissolved oxygen (DO), and pH data were collected from rkm 58, the mid-point of the Patuxuent River sampling area.

region in May and were dispersed up-estuary where large individuals (>10 mm) occurred in the salt-front and freshwater regions in June and July.

Assemblage analysis

A principal components analysis (PCA) defined riverine and oligohaline ichthyoplankton assemblages in the estuarine transition zone (Fig. 6). The first two principal components explained 60% and 59% of the variance in assemblage structure in years 2000 and 2001, respectively:

1 Riverine assemblage—comprised anadromous and freshwater taxa, predominantly white perch, striped bass, alewife and other alosines, and gizzard shad. Yolk-sac larvae were common in this assemblage, which tended to occur in fresher, cooler, more oxygenated water.
2 Oligohaline assemblage—estuarine-spawning species, such as naked goby, characterized this low-diversity assemblage. In late June, when water temperature reached 25 °C, juvenile Atlantic menhaden and bay anchovy joined this assemblage.

Overall, assemblage structure and species associations were similar for the two years. Oligohaline and riverine assemblages were defined each year, but several constituent taxa (moronids, naked goby, alosines, and gizzard shad) from each assemblage were found at the salt front. Overlap between the two assemblages occurred at the lower end of the salinity vector in each year's PCA (Fig. 6), coinciding with salinities of 0.2–1.0 that typically contain the salt-front feature.

Zooplankton distribution and abundance

Highest concentrations of combined zooplankton taxa occurred near and up-estuary of the salt front. Mean concentration was significantly higher in 2001 (t=–4.59, P<0.01), primarily because rotifers peaked at 4000/L. In 2000, when rotifers were less abundant, the seasonal trend in zooplankton abundance was driven by the cladoceran *Bosmina longirostris*.

Zooplankters that are potential prey for larval fish differed in their spatiotemporal patterns of distribution and abundance. Naupliar stages of copepods, mostly *Eurytemora affinis* or *Acartia tonsa*, were common throughout the sampling area, but were often most abundant near and down-estuary of the salt front. Mean nauplii concentration was higher in 2001 (t=6.01, P<0.01). The cladoceran *B. longirostris* was most abundant in the freshwater region (Fig. 7) and was uncommon at stations where salinity was >2. Its mean concentration did not differ significantly between years (t=–0.68, P=0.50).

Adult stages of the two abundant calanoid copepods, *Acartia tonsa* and *Eurytemora affinis*, had different distributions. *Acartia* occurred down-estuary of the salt front and abundance was similar in each year. *Eurytemora* were present throughout the estuarine transition zone, but usually were most abundant in the salt-front region, especially in 2001 (Fig. 7). The mean *Eurytemora* and *Acartia* concentrations did not differ

significantly between years (*Eurytemora*, t=–1.35, P=0.18; *Acartia*, t=0.71, P=0.48).

Cyclopoid copepods (primarily *Oithona* spp.) were more abundant (P<0.01) in 2000 than in 2001. Cyclopoid abundance was highest near or up-estuary of the salt front. In 2001, rotifers were the most abundant zooplankters and occurred in highest concentrations within or up-estuary of the salt front. Rotifer mean concentration was 12 times higher in 2001 than in 2000 (P<0.01).

Environmental factors and larval abundances

The descriptive analyses and PCA indicated that hydrographic factors and larval prey controlled ichthyoplankton distributions in the two years. Multiple regression models identified some environmental factors that explained variability in ichthyoplankton abundance (Table 1).

The model results indicated that alewife larvae were most abundant up-estuary of the salt front, where DO levels and *Bosmina* concentrations were highest (year 2000) and where temperatures were relatively cool (year 2001). For alewife, temperature, dissolved oxygen (DO), salt front location, and concentration of *Bosmina* were significant descriptors of larvae abundance.

For larval striped bass, concentrations of potential prey explained a significant proportion of variability in larvae abundance. In year 2000, salinity and concentrations of *Bosmina* and calanoid copepods were significant factors (Table 1). In 2001, potential prey, salt front location, DO, and temperature were positively related to striped bass abundance, which was highest near the salt front and coincident with high prey densities.

For white perch larvae, levels of salinity, DO, and temperature were positively related to white perch abundance in 2000, and highest concentrations were near the salt front, coincident with high prey concentrations (Table 1). The white perch regression model differed markedly in 2001 when only temperature and salinity explained a significant portion of variability in white perch larvae abundance.

For larvae of naked goby, concentration of copepod nauplii was a significant factor explaining goby abundance in year 2000 (Table 1) when concentrations were highest in oligohaline waters below the salt front that had relatively low DO levels, low *Bosmina* densities, and high copepod nauplii densities. In 2001, concentration of goby larvae was not significantly related to any prey-density variable, but larvae were most abundant in the relatively warm water within the salt-front region.

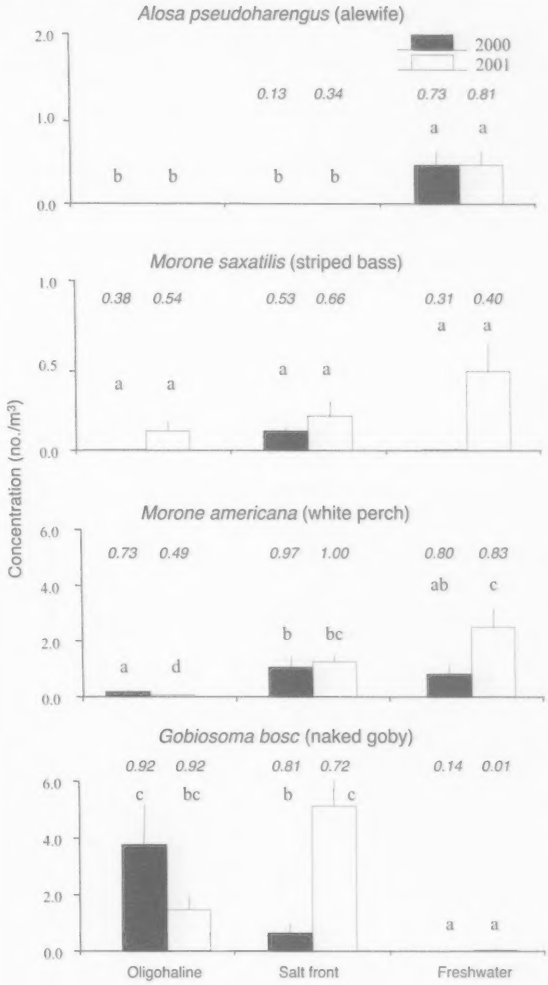

Figure 4

Larval concentrations (no./m^3) by region. Student t-tests with unequal variances were applied. Significant differences are indicated by different letters (P<0.05). Vertical lines are standard errors of the mean. Note differences in scale of y axes. Values in italics are frequencies of positive tows.

Diets and prey

Feeding incidence in the four taxa of fish larvae that we examined ranged from 72% to 97%. Feeding incidence did not differ significantly among the freshwater, salt-front, and oligohaline regions.

The diet of larval alewife was diverse (Fig. 8), differed between years, and shifted with ontogeny and growth. Copepod nauplii and rotifers represented >50% of diets in ≤11 mm alewife larvae. Invertebrate eggs and larger prey (i.e., *Eurytemora* and *Bosmina*) were more common in >11 mm alewife larvae. *Bosmina* and cyclopoid copepods were more frequent in alewife diets in 2000, whereas rotifers and *Eurytemora* were more common in 2001.

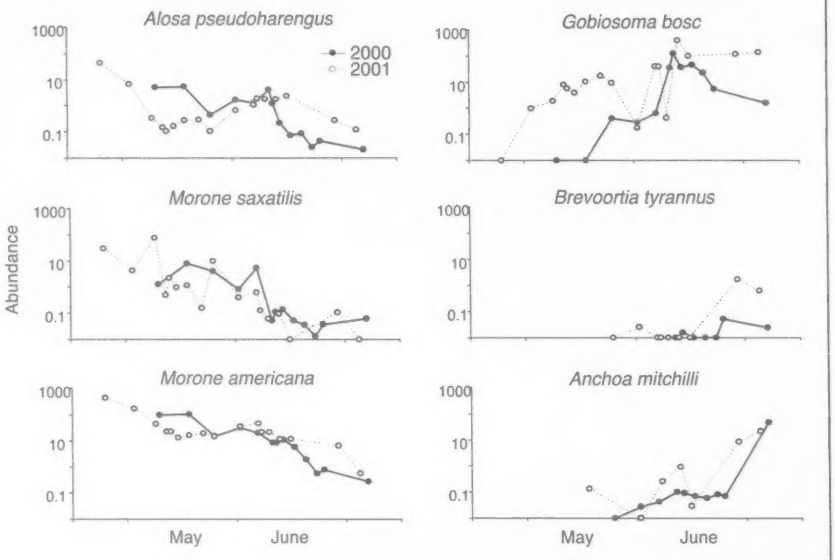

Figure 5

Temporal patterns in abundance ($\log_{10}$-scale) of anadromous (plots at left) and estuarine (plots at right) ichthyoplankton taxa in the Patuxent River, 2000–01. Abundance values= Σ([no./m^3 at station i]×[station i volume, m^3]).

Striped bass larvae primarily consumed relatively large zooplankters (*Eurytemora*, *Acartia*, and *Bosmina*; Fig. 8), with no obvious ontogenetic shift in prey size. Calanoid copepodites and adults were the dominant prey of striped bass larvae down-estuary of the salt front. In the salt-front and freshwater regions, *Bosmina* was common prey of 11–19 mm larvae. *Acartia* was eaten by >11-mm striped bass only in year 2000 and only in the oligohaline region.

Diets of small white perch larvae were relatively diverse, but larger larvae fed predominantly on *Bosmina* and the calanoid copepods *Eurytemora* and *Acartia* (Fig. 8). The calanoid copepods were dominant prey down-estuary of the salt front. As for striped bass, *Acartia* was eaten by white perch only in 2000.

Naked goby larvae had the least diverse diet. In the oligohaline region, they fed almost exclusively on copepod nauplii and calanoid copepods, including *Acartia*, in both years (Fig. 8). In the salt front region, the diet of goby larvae was more diverse.

Prey utilization, preference, and importance

Mean prey size increased with larval length and ontogenetic state in alewife, white perch, and naked goby, but not in striped bass (Table 2). Functional relationships between prey ingestion and either larval size or ontogenetic state differed among taxa. Niche breadth (standard deviation of mean logarithmic prey size) increased significantly in naked goby with respect to larval length or ontogenetic state, but not in the other species.

Larval prey preference and importance differed among the three regions of the estuarine transition zone and were generated primarily by prey availability and larval sizes. In general, *Eurytemora* was a preferred and important prey, especially for the moronid larvae and for large alewife larvae (>10 mm) (Table 3A). *Bosmina* was an important prey across taxa and larval sizes, but was only preferred by large white perch larvae and large striped bass larvae in the salt-front region. Rotifers and cyclopoid copepods were eaten, but were neither positively selected nor important prey for larvae of the four species. In the oligohaline region, *Acartia* was positively selected by naked goby and large (>10-mm) white perch larvae. Copepod nauplii were positively selected and important prey for small (<10-mm) alewife and naked goby larvae but were generally neither selected nor important for white perch and striped bass.

Overall, diets of large (>10-mm) larvae strongly overlapped among taxa (O=0.88–0.90). Diet overlaps among larval taxa and sizes were strongest in the freshwater region (Table 3B). However, the diet of small alewife in freshwater did not overlap significantly with diets of other taxa or size classes. At the salt front, the only significant overlap in diets of larval fish was between naked goby and small white perch (Table 3B). In the oligohaline region, diet overlap was

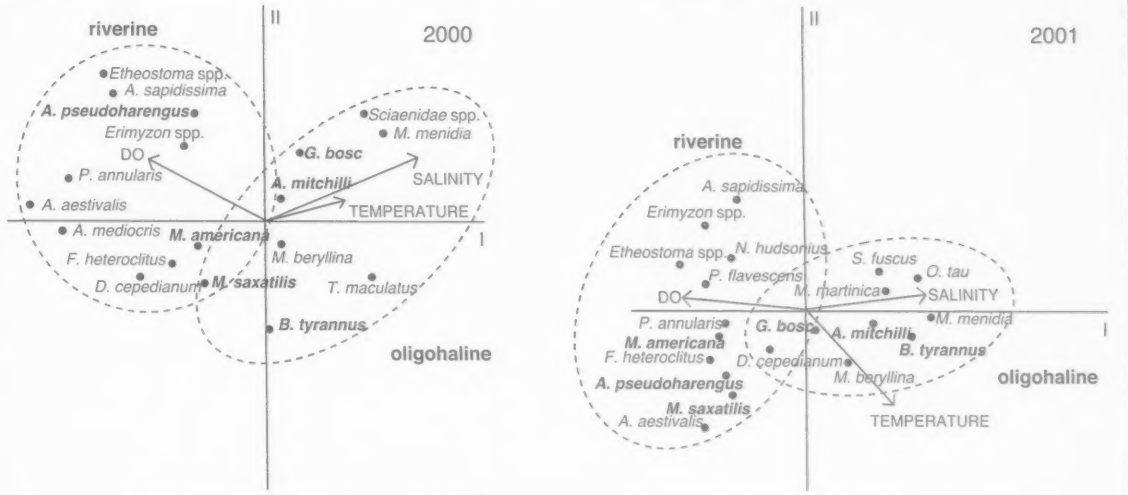

Component	1	2	3	4	5
Variance	0.39	0.21	0.13	0.09	0.06
Loading	–1.65	0.86	0.91	–1.95	2.18

Component	1	2	3	4	5
Variance	0.43	0.16	0.11	0.09	0.07
Loading	–0.13	–1.33	0.15	1.20	0.11

Figure 6

Plots of ichthyoplankton species within the first two components of principal components analysis, and loadings and variances explained by each component in year 2000 (at left) and year 2001 (at right). See Appendix I and II for full species names. Focal species of this study are shown in bold.

significant among large (>10-mm) white perch and striped bass larvae.

Discussion

Estuarine transition zones in coastal plain estuaries are regions of strong hydrographic gradients that control distributions of icththyoplankton and zooplankton and, potentially, their trophic interactions. We propose that the larval assemblage structure, zooplankton distributions, and trophodynamics observed in the Patuxent River provide insight into the role of salt front-ETM features and dynamics in other temperate estuaries that receive variable freshwater inputs and which support fishes with diverse life histories (estuarine-dependent, anadromous, and freshwater resident). We documented interannual variability of the ichthyoplankton assemblages in the estuarine transition zone of the Patuxent River in 2000 and 2001. Two larval assemblages, riverine and estuarine, were identified in each year. In 2000, abundance of ichthyoplankton was highest in the oligohaline region immediately below the salt front, but in 2001 highest abundance was at the salt front. Our two hypotheses were supported: 1) environmental gradients defined distributions and assemblages of larvae, and 2) the salt front was a factor controlling assemblage structure and trophic interactions.

Larval assemblages and environmental factors

Moronid and alosine larvae occurred in fresh to oligohaline waters of the Patuxent River subestuary. Although moronids are commonly found in salinities of 0–3 (North and Houde, 2001), the distribution centers of alosine larvae occur in freshwater further up-estuary (Setzler et al., 1981; Bilkovic et al., 2002). In addition to interannual differences in overall distributions, ontogenetic migrations or shifts are common, resulting in species distributions that are most discrete during the earliest larval stages and greater overlaps in taxa distributions during ontogeny. For example, larvae of alewife at all stages were confined to the freshwater region, and small naked goby larvae were confined to the oligohaline region. However, during ontogeny naked goby larvae dispersed up-estuary and its late-stage larvae were found with alewife in freshwater.

A salt front and estuarine turbidity maximum (ETM) often characterize coastal plain estuaries. In Chesapeake Bay, they typically occur in the 0–3 salinity region of the mainstem Bay and its tributaries (North and Houde, 2001, 2003; Sanford et al., 2001). As larval fishes develop, they may converge at the salt front-ETM through passive transport and retention related to hydrographic and circulation features. Convergence also could be facilitated by active tracking by larvae of elevated zooplankton prey concentrations, especially

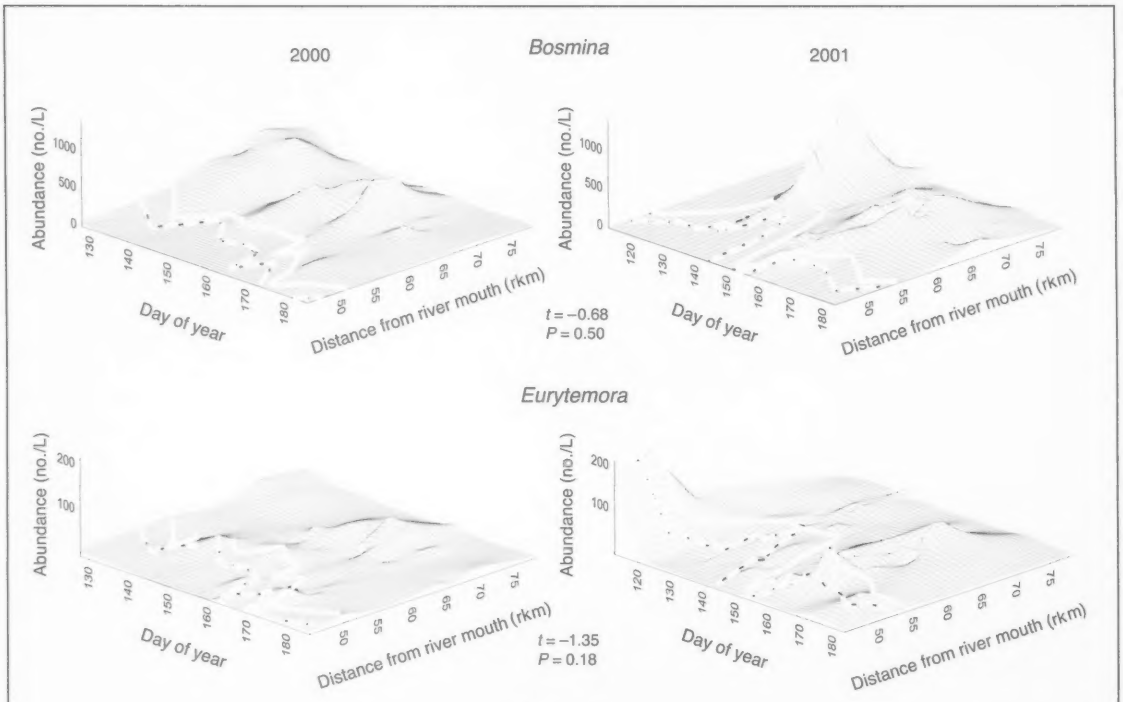

Figure 7

Spatiotemporal trends in concentrations of the cladoceran *Bosmina longirostris* and calanoid copepod *Eurytemora affinis* in the Patuxent River in 2000 (at left) and 2001 (at right). Student's *t*-tests with unequal variance were used to compare mean concentrations between years. Solid and dashed lines are the salt front and 2-psu isohaline positions, respectively. Day 130=10 May; day 160=9 June.

the copepod *Eurytemora affinis*, in the salt-front–ETM feature (Roman et al., 2001; North and Houde, 2006). Interannual differences in the timing and level of freshwater runoff control spatiotemporal variability in the salt front-ETM feature, and the occurrences, abundances, and distributions of striped bass larvae and their zooplankton prey (Martino and Houde, in press). The potential importance of the salt front as a retention feature has been recognized in previous research in Chesapeake Bay and its tributaries in which striped bass eggs or larvae, if advected below the salt front and ETM, apparently were lost to down-estuary dispersal (Secor et al., 1995; North and Houde, 2003; North et al., 2005; Secor and Houde[4]). Our survey results support these findings and, additionally, we have documented distributions and overlaps of larval taxa and zooplankton prey in this estuarine transition zone.

Larvae of striped bass and white perch were abundant above the salt front and in close proximity to it. Their yolk-sac larvae were virtually absent down-estuary of the 2.0 isohaline and abundance levels of all moronid larval stages declined to near-zero levels down-estuary of the 2.0 isohaline. Declines and absences do not conclusively demonstrate failed retention or advective loss. However, Secor et al. (1995) released millions of marked, hatchery-source striped bass larvae in the Patuxent River and recaptured larvae from all release groups except those released below the salt front, providing strong circumstantial evidence that the front serves as a retention feature.

We documented patterns in ichthyoplankton taxa occurrences, distributions, and peak abundances in the estuarine transition zone that indicate a predictable seasonal progression in assemblage structure and distribution. A PCA identified riverine and estuarine ichthyoplankton assemblages. The two assemblages were characterized best by their occurrences with respect to salinity and, secondarily, to temperature and dissolved oxygen. Some taxa could not be assigned unambiguously to either the riverine or estuarine assemblage because of extensive overlap of taxa in the transition zone. This ambiguity differs from reported ichthyoplankton assemblage structures often observed

[4] Secor, D. H., and E. D. Houde. 1996. Episodic water quality events and striped bass recruitment: larval mark-recapture experiments in the Nanticoke River. Final Report to Maryland Department of Natural Resources, 271 p. Center for Environmental Science, Univ. Maryland, Solomons, MD.

Table 1

Multiple regression models evaluating relationships between concentrations (no./m^3) of common larval taxa (alewife [*Alosa pseudoharengus*], striped bass [*Morone saxatilis*], white perch [*Morone americana*], and naked goby [*Gobiosoma bosc*]) and abiotic and biotic variables in 2000 and 2001. Organism concentrations were $\log_{10}(x+1)$-transformed. Independent variables were entered into models by using stepwise procedures. Parameter estimates and standard errors (in parentheses) are reported for independent variables that described a significant amount of variability in larval concentrations (*=P<0.10, **=P<0.05, ***=P<0.01). Akaike's information criterion (AIC) indicates quality of model fit. The salt-front location was modeled as a dichotomous variable (0 when the station located at or up-estuary of the salt front, 1 when below the salt front). $n_{\text{surveys, 2000}}$=11; $n_{\text{surveys, 2001}}$=14. r^2 = coefficient of determination.

	Independent variables							Model fit			
Dependent variables	Salinity	Temperature	Dissolved oxygen	Salt-front location	*Bosmina* cladocera	Calanoid copepods	Copepod nauplii	AIC	r^2	df_{model}	P
Alosa pseudoharengus											
2000			0.01 (0.01) *	−7.96 (3.20) **	1.17 (0.23) ***			4.76	0.88	3	<0.001
2001		−0.01 (0.01) *		−7.88 (1.16) ***				3.45	0.81	2	<0.001
Morone saxatilis											
2000	3.39 (0.62) ***				2.31 (0.43) ***	2.67 (1.39) *		15.15	0.86	3	0.002
2001		0.01 (0.01) *	0.03 (0.01) **	26.46 (4.14) ***	0.83 (0.23) ***	2.50 (0.59) ***		7.41	0.90	5	<0.001
Morone americana											
2000	1.28 (0.17) ***	0.01 (0.01) *	0.02 (0.01) **	11.62 (1.63) ***	1.62 (0.16) ***	2.40 (0.33) ***		0.61	0.99	6	<0.001
2001	−0.25 (0.03) ***	0.01 (0.01) *						2.22	0.84	2	<0.001
Gobiosoma bosc											
2000			−0.02 (0.01) **	6.65 (3.21) *	−1.12 (0.27) ***		0.90 (0.42) *	4.01	0.93	4	0.002
2001		0.01 (0.01) ***		8.64 (1.58) ***				7.45	0.76	2	<0.001

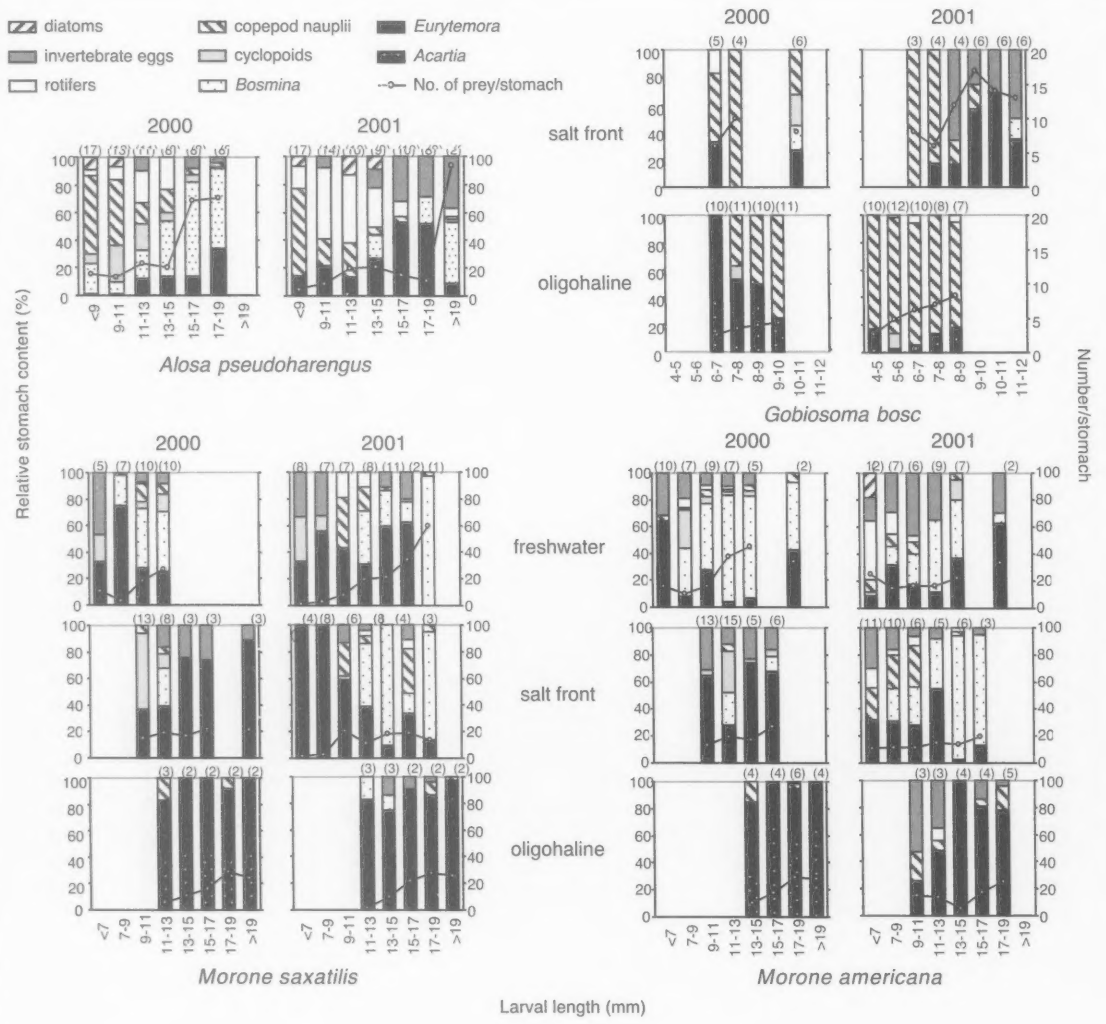

Figure 8

Relative stomach content (% by numbers; bars) and total stomach content (number of prey per stomach; lines) for 2-mm length classes of alewife (*Alosa pseudoharengus*) larvae (all sampled larvae were from freshwater stations), for 2-mm length classes of striped bass (*Morone saxatilis*) and white perch (*Morone americana*) larvae from freshwater, salt-front, and oligohaline stations, and for 1-mm length classes of naked goby (*Gobiosoma bosc*) larvae from salt-front and oligohaline stations. The number of larvae analyzed is shown in parentheses.

on continental shelves, where taxa in coastal and oceanic assemblages frequently have quite distinct distributions (Richardson et al., 1980; Young et al., 1986; Munk et al., 2004). In estuaries, gradients in larval and juvenile fish assemblages, often with overlaps, and seasonal shifts in taxonomic dominance are typically explained by salinity and temperature regimes (Rakocinski et al., 1996; Witting et al., 1999; Martino and Able, 2003) and this appears to be the case in the Patuxent River.

Strong gradients in water mass properties, especially temperature and salinity, combined with complex circulation processes at hydrographic fronts can act as hydrodynamic particle traps and provide favorable foraging habitat for fish larvae (Nakata et al., 1995; Munk, 1997; Hillgruber and Kloppmann, 1999; North and Houde, 2003; Islam and Tanaka, 2005). In estuaries, temperature and salinity often are the most important variables delineating ichthyoplankton distributions. As examples, in the St. Lucia estuary, South Africa, tem-

Table 2

Linear regressions evaluating larval total length (TL, mm) and ontogenetic state (O_L) in relation to logarithmic mean prey length (PL, µm) and trophic niche breadth (S) for common larval taxa in the Patuxent River, 2000–01. r^2=coefficient of determination.

	Model	r^2	P
Alosa pseudoharengus (alewife), n=135			
Log_e prey length on larval length	$PL = 1.90 + 0.02TL$	0.17	0.01
Niche breadth on larval length	$S = 0.15 + 0.01TL$	0.06	0.12
Log_e prey length on ontogenetic state	$PL = 1.54 + 0.01O_L$	0.16	0.01
Niche breadth on ontogenetic state	$S = 0.02 + 0.01O_L$	0.06	0.14
Morone saxatilis (striped bass), n=165			
Log_e prey length on larval length	$PL = 2.58 - 0.01TL$	0.02	0.43
Niche breadth on larval length	$S = 0.17 + 0.01TL$	0.07	0.08
Log_e prey length on ontogenetic state	$PL = 2.73 - 0.01O_L$	0.02	0.32
Niche breadth on ontogenetic state	$S = 0.01 + 0.01O_L$	0.06	0.11
Morone americana (white perch), n=200			
Log_e prey length on larval length	$PL = 1.94 + 0.04TL$	0.49	0.01
Niche breadth on larval length	$S = 0.39 - 0.01TL$	0.03	0.27
Log_e prey length on ontogenetic state	$PL = 1.49 + 0.01O_L$	0.45	0.01
Niche breadth on ontogenetic state	$S = 0.41 - 0.01O_L$	0.01	0.55
Gobiosoma bosc (naked goby), n=133			
Log_e prey length on larval length	$PL = 2.07 + 0.03TL$	0.18	0.05
Niche breadth on larval length	$S = 0.13 + 0.05TL$	0.60	0.01
Log_e prey length on ontogenetic state	$PL = 1.82 + 0.01O_L$	0.19	0.05
Niche breadth on ontogenetic state	$S = 0.50 + 0.01O_L$	0.56	0.01

perature was the most important variable explaining larval fish distributions and abundances (Harris et al., 1999) and salinity was most important in the Tanshui River estuary, Taiwan (Tzeng and Wang, 1993). Larval fish distributions and abundances in estuaries tend to be most responsive to salinity-related factors (e.g., salt-front location), which can be strongly linked to precipitation and freshwater flow. In the Patuxent River subestuary, we found that concentrations of particular zooplankton prey, which also are responsive to salinity and temperature conditions, were significant in explaining ichthyoplankton abundances and distributions.

In multiple regression models, the location of the salt front usually was a good indicator of larval concentrations for most taxa included in the models (Table 1). Additionally, concentrations of anadromous fish larvae were highest where densities of the cladoceran *Bosmina longirostris* and calanoid copepods were high. These zooplankters, which are important prey for fish larvae in Chesapeake Bay (Setzler et al., 1981; Shoji et al., 2005; North and Houde, 2006; Martino and Houde, 2010), were significant in explaining concentrations of larvae of anadromous species in the Patuxent River, but not the estuarine naked goby. Goby larvae tended to occur where concentrations of copepod nauplii were high down-estuary of the salt front.

Concentrations of zooplankton that are potential prey were significant explanatory variables in regression models for all ichthyoplankton taxa in 2000, but were less important in 2001. The reasons for the differences between years are unclear, but may be explained in part by the greater variability and intensity in estuarine physics (river flow, salt front location) in 2001. In the Hudson River, Limburg et al. (1999) reported that cohorts of larval moronids co-occurring temporally and spatially with zooplankton blooms, including *Bosmina*, had higher recruitment potential. In Chesapeake Bay and its tributaries, temperature and freshwater flow may be of equal or greater importance (Rutherford and Houde, 1995; North and Houde 2001), although recent evidence has identified a strong relationship between recruitment success of striped bass and a temporal-spatial match of zooplankton production in the ETM region (Martino and Houde, 2010).

Trophic interactions

Larval diets in the estuarine transition zone were influenced by the composition of the zooplankton community, which differed in 2000 and 2001. On average, the location of the salt front was similar in both years. But, more variable temporal trends in river flow and temperature in 2001 affected the timing, intensity, and spatial distribution of copepod and *Bosmina* production that in turn influenced larval diets. Cyclopoid copepods, which were 16 times more abundant in 2000 than in 2001, were common in larval fish diets only in 2000., Copepod nauplii and rotifers were relatively important in diets of larval moronids and naked goby in 2001 when these small zooplankters were most abundant

Table 3

(**A**) Prey preferences and importance of prey types and (**B**) dietary overlap for larval fish taxa and size classes common in the Patuxent River, 2000–01. Relative importance index Ri_a values are shown in italics. * indicates significant ($P<0.05$) Strauss's selection index L values. Significance of Czechanowski overlap index O values are indicated by *$P<0.05$ or **$P<0.01$. AP = alewife (*Alosa pseudoharengus*); MS = striped bass (*Morone saxatilis*); MA = white perch (*Morone americana*); GB = naked goby (*Gobiosoma bosc*).

	Freshwater							Salt front					Oligohaline	
A	AP <10 mm	AP >10 mm	MS <10 mm	MS >10 mm	MA <10 mm	MA >10 mm	GB	MS <10 mm	MS >10 mm	MA <10 mm	MA >10 mm	GB	MS >10 mm	MA >10 mm
Acartia												+0.11*	+0.07	+0.10*
												18.40	*31.98*	*38.11*
Eurytemora	+0.05	+0.17*	+0.41*	+0.16*	0.20*	+0.19*	+0.26*	+0.87*	+0.11*	+0.17*	+0.12*	+0.07	+0.35*	+0.30*
	13.03	*14.84*	*55.76*	*30.73*	*34.71*	*30.33*	*48.25*	*100.00*	*35.14*	*44.71*	*34.38*	*16.86*	*41.66*	*29.44*
Bosmina	−0.35*	−0.21*	−0.27*	−0.07	−0.19*	+0.10*	−0.14*	−0.17*	+0.13*	−0.06	+0.15*	−0.04	+0.02	−0.04
	18.50	*33.31*	*25.50*	*29.13*	*17.75*	*34.27*	*5.81*	*0.00*	*26.78*	*12.89*	*26.63*	*0.00*	*3.20*	*2.13*
Cyclopoids	+0.04	+0.01	−0.01	+0.01	+0.05	+0.01	−0.11*	−0.13	−0.04	−0.13*	+0.02	+0.03	−0.01	−0.01
	18.07	*12.02*	*2.59*	*12.07*	*11.20*	*9.41*	*3.63*	*0.00*	*13.04*	*0.00*	*20.40*	*14.08*	*0.00*	*3.22*
Copepod nauplii	+0.41*	0.00	−0.12*	−0.03	−0.08	−0.08	+0.03	−0.25*	−0.16*	0.00	−0.22*	+0.13*	−0.42*	−0.39*
	39.45	*17.04*	*9.61*	*11.30*	*10.15*	*10.54*	*28.25*	*0.00*	*10.02*	*23.38*	*4.46*	*46.70*	*8.72*	*9.99*
Rotifers	−0.13*	−0.04	−0.26*	−0.19*	−0.15*	−0.24*	−0.25*	−0.26*	−0.24*	−0.15*	−0.26*	−0.19*	−0.21*	−0.19*
	10.96	*18.14*	*0.00*	*6.72*	*11.08*	*5.58*	*1.94*	*0.00*	*3.52*	*11.15*	*2.31*	*3.96*	*0.00*	*0.00*
Invertebrate eggs	−0.12*	+0.01	+0.04	+0.10*	+0.15*	+0.01	+0.08	−0.04	+0.07	+0.06	+0.07	−0.02	+0.09	+0.07
	0.00	*4.64*	*6.54*	*10.05*	*15.11*	*9.87*	*12.12*	*0.00*	*11.49*	*7.87*	*11.82*	*0.00*	*14.44*	*17.12*

B	AP <10 mm	AP >10 mm	MS <10 mm	MS >10 mm	MA <10 mm	GB	MS <10 mm	MS >10 mm	MA <10 mm	GB	MS >10 mm
AP>10 mm	0.55										
MS<10 mm	0.44	0.73				0.58					
MS>10 mm	0.50	0.90**	0.71			0.71	0.52			0.35	
MA<10 mm	0.52	0.87*	0.71	0.93**		0.86**	0.46	0.46			
MA>10 mm	0.45	0.88*	0.79*	0.88*	0.85*	0.66	0.50	0.51	0.68	0.41	0.81**

in the plankton. Although mean concentrations of *Bosmina* and calanoid copepods did not differ significantly in 2000 and 2001, their representation in larval diets did differ. For example, larval alewife and white perch in the freshwater region consumed higher proportions of *Bosmina* in 2000, whereas larval striped bass in the salt-front region consumed more *Bosmina* in 2001. The calanoid copepod *Acartia* occurred down-estuary of the salt front in the oligohaline region and was equally abundant during the two years but was common in diets of moronid larvae only in 2000. We could not explain why consumption of *Acartia* differed between the two years but note that moronid larvae in 2001 strongly preferred *Eurytemora* as prey.

Feeding incidences (72–97%) in larvae and mean numbers of prey per gut (typically 5–50 zooplankters) were high in the salt front-ETM of the Patuxent River. In the estuarine transition zone, the two calanoid copepods *Eurytemora affinis* and *Acartia* sp. were important and generally were positively selected prey. Only small alewife larvae, which have small mouth gape, did not select these relatively large calanoid copepods. The abundant cladoceran *Bosmina* also was important prey of fish larvae, although it usually was not positively selected. Combined contributions of the important, larger prey *Bosmina* and *Eurytemora* to diets of larger larvae were highest within and up-estuary of the salt-front–ETM.

The copepod *Eurytemora affinis* was the most important food of white perch and striped bass larvae in the Patuxent River. It also was the most important prey consumed by these larvae in the salt-front–ETM of upper Chesapeake Bay and was particularly important in high freshwater-flow years (Shoji et al., 2005; Martino and Houde, 2010). This copepod is hypothesized to play a vital role in supporting the nutrition of larval fishes in the salt-front transition regions of Chesapeake Bay (North and Houde, 2006) and its tributaries, a role similar to that proposed for the calanoid copepod *Sinocalanus sinensis* and larval Japanese sea bass *Lateolabrax japonicus* in the transition region of the Chikugo River estuary (Islam and Tanaka, 2005; Shoji and Tanaka, 2007).

Although concentrations of fish larvae are often high, with taxa overlaps in the salt front-ETM region, it is not certain that feeding competition occurs. Larval fish populations generally are not capable of significantly grazing down zooplankton prey resources (Pepin and Penney, 2000). Still, it is possible that foraging interactions are intense where larvae are highly concentrated. In the estuary, diet overlaps among larvae may be of greatest consequence in the salt front-ETM region where larvae of estuarine species such as naked goby and anadromous species such as white perch and striped bass are abundant and have a common preference for *Eurytemora* as prey. Despite differences in the hydrographic conditions and prey available to larvae in the Patuxent River, the abundances of juvenile striped bass, white perch, and alewives in the summers of 2000 and 2001, based on monitoring surveys conducted by Maryland Department of Natural Resources (http://www.dnr.state.md.us/fisheries/juvindex/index.html, accessed April 2010), were similar, indicating that environmental conditions in these two years were not sufficiently different to generate the high (up to 100-fold) recruitment variability seen in the 25-yr survey time series.

Hydrographic features define assemblages and, in part, control trophic relationships of ichthyoplankton and zooplankton within estuarine transition zones. The larvae of many fish species and abundant zooplankton prey coexist here, within and up-estuary of the salt front and ETM. High dietary overlap is indicative of strong trophic interactions among larval fish taxa. Despite the potential for competition, larvae in this transition region may have a trophodynamic advantage derived from high prey densities and the benefits of hydrodynamic retention. Together, these conditions provide a relatively stable environment that is favorable for larval production and survival in the estuarine transition region.

Acknowledgments

The project was supported by Maryland Sea Grant (NOAA award no. NA16RG2207, Maryland Sea Grant R/F-90) and by National Science Foundation Oceanography Awards 0002543 and 0453905. J. Bichy, J. Boynton, A. Chandler, S. Gibson, E. Martino, E. North, B. Pearson, and J. Shoji assisted with various aspects of this research. We thank J. Olney (deceased) and D. Bilkovic at the Virginia Institute of Marine Sciences for assisting with larval fish identifications. We also thank members of the University of Maryland Center for Environmental Science Research Fleet for assistance in surveys aboard RV *Pisces*, RV *Orion*, and RV *Aquarius*. E. North and E. Martino reviewed early versions of the manuscript. This article is contribution no. 4444 of the University of Maryland Center for Environmental Science.

Literature cited

Albrecht, M., and N. J. Gotelli.
2001. Spatial and temporal niche partitioning in grassland ants. Oecologia 126:134–141.

Arthur, D. K.
1976. Food and feeding of larvae of three fishes occurring in the California Current, *Sardinops sagax*, *Engraulis mordax*, and *Trachurus symmetricus*. Fish. Bull. 74:517–530.

Bilkovic, D. M., J. E. Olney, and C. H. Hershner.
2002. Spawning of American shad (*Alosa sapidissima*) and striped bass (*Morone saxatilis*) in the Mattaponi and Pamunkey Rivers, Virginia. Fish. Bull. 100:632–640.

Breitburg, D. L.
1991. Settlement patterns and presettlement behavior of the naked goby, *Gobiosoma bosci*, a temperate oyster reef fish. Mar. Biol. 109:213–221.

Chick, J. H., and M. J. Van den Avyle
1999. Zooplankton variability and larval striped bass foraging: evaluating potential match/mismatch regulation. Ecol. Appl. 9:320–334.
Crecco, V. A., and M. M. Blake
1983. Feeding ecology of coexisting larvae of American shad and blueback herring in the Connecticut River. Trans. Am. Fish. Soc. 112:498–507.
Feinsinger, P., E. E. Spears, and R. W. Poole
1981. A simple measure of niche breadth. Ecology 62:27–32.
Fuiman, L. A., K. R. Poling, and D. M. Higgs
1998. Quantifying developmental progress for comparative studies of larval fishes. Copeia 1998(3):602–611.
George, E. L., and W. F. Hadley.
1979. Food and habitat partitioning between rock bass (*Ambloplites rupestris*) and smallmouth bass (*Micropterus dolomieui*) young of the year. Trans. Am. Fish. Soc. 108:253–261.
Gotelli, N. J., and G. L. Entsminger.
2003. EcoSim: Null models software for ecology, vers. 7. Acquired Intelligence Inc. and Kesey-Bear, Jericho, VT. Available at http://garyentsminger.com/ecosim.htm.
Harding, J. M.
1999. Selective feeding behavior of larval naked gobies *Gobiosoma bosc* and blennies *Chasmodes bosquianus* and *Hypsoblennius hentzi*: preferences for bivalve veligers. Mar. Ecol. Prog. Ser. 179:145–153.
Harris, S. A., D. P. Cyrus, and L. E. Beckley.
1999. The larval fish assemblage in nearshore coastal waters off the St Lucia Estuary, South Africa. Estuar. Coast. Shelf Sci. 49:789–811.
Heinle, D. R.
1969. Temperature and zooplankton. Chesapeake Sci. 10:186–209.
Hillgruber, N., and M. Kloppmann.
1999. Distribution and feeding of blue whiting *Micromesistius poutassou* larvae in relation to different water masses in the Porcupine Bank area, west of Ireland. Mar. Ecol. Prog. Ser. 187:213–225.
Islam, M. S., and M. Tanaka.
2005. Nutritional condition, starvation status and growth of early juvenile Japanese sea bass (*Lateolabrax japonicus*) related to prey distribution and feeding in the nursery ground. J. Exp. Mar. Biol. Ecol. 323:172–183.
Jassby, A. D., W. J. Kimmerer, S. G. Monismith, C. Armor, J. E. Cloern, T. M. Powell, J. R. Schubel, and T. J. Vendlinski.
1995. Isohaline position as a habitat indicator for estuarine populations. Ecol. Appl. 5:272–289.
Kleinbaum, D. G., L. L. Kupper, K. E. Muller, and A. Nizam.
1998. Applied regression analysis and other multivariable methods, 3rd ed., 816 p. Brooks/Cole Publishing Co., Pacific Grove, CA.
Limburg, K. E., M. L. Pace, and K. K. Arend.
1997. Consumption, selectivity, and use of zooplankton by larval striped bass and white perch in a seasonally pulsed estuary. Trans. Am. Fish. Soc. 126:607–621.
1999. Growth, mortality, and recruitment of larval *Morone* spp. in relation to food availability and temperature in the Hudson River. Fish. Bull. 97:80–91.
Loos, J. L., and E. S. Perry.
1991. Larval migration and mortality rates of bay anchovy in the Patuxent River. *In* Larval fish recruitment and research in the Americas: proceedings of the thirteenth annual larval fish conference; Merida, Mexico, 21–26 May 1989 (R. D. Hoyt, ed.), p. 65–76. NOAA Tech. Rep. NMFS 95.
Magurran, A. E.
1988. Ecological diversity and its measurement Princeton Univ. Press, Princeton, NJ, 192 p.
Martino, E. J., and K. W. Able.
2003. Fish assemblages across the marine to low salinity transition zone of a temperate estuary Estuar. Coast. Shelf Sci. 56:969–987.
Martino, E. J., and E. D. Houde.
2010. Recruitment of striped bass in Chesapeake Bay: spatial and temporal environmental variability and availability of zooplankton prey. Mar. Ecol. Prog. Ser. 409:213–228.
Miller, T. J.
2002. Assemblages, communities, and species interactions. *In* Fisheries science: the unique contributions of early life stages (Fuiman, L. A., and R. G. Werner, eds.), p. 183–205. Blackwell Publishing, Ames, IA.
Miller, T. J., L. B. Crowder, and F. P. Binkowski.
1990. Effects of changes in the zooplankton assemblage on growth of bloater and implications for recruitment success. Trans. Am. Fish. Soc. 19:483–491.
Munk, P.
1997. Prey size spectra and prey availability of larval and small juvenile cod. J. Fish Biol. 51 (suppl. A):340–351.
Munk, P., P. K. Bjørnsen, P. Boonruang, M. Fryd, P. J. Hansen, V. Janekarn, V. Limtrakulvong, T. G. Nielsen, O. S. Hansen, S. Satapoomin, S. Sawangarreruks, H. A. Thomsen, and J. B. Østergaard.
2004. Assemblages of fish larvae and mesozooplankton across the continental shelf and shelf slope of the Andaman Sea (NE Indian Ocean). Mar. Ecol. Prog. Ser. 274:87–97.
Nakata, K., H. Zenitani, and D. Inagake.
1995. Differences in food availability for Japanese sardine larvae between the frontal region and the waters on the offshore side of Kuroshio. Fish. Oceanogr. 4:68–79.
Norden, C. R.
1968. Food selectivity of larval alewives in Lake Michigan. Proc. Great Lakes Res. 10:70–78.
North, E. W., and E. D. Houde.
2001. Retention of white perch and striped bass larvae: biological-physical interactions in Chesapeake Bay estuarine turbidity maximum. Estuaries 24:756–769.
2003. Linking ETM physics, zooplankton prey, and fish early-life histories to striped bass *Morone saxatilis* and white perch *M. americana* recruitment. Mar. Ecol. Prog. Ser. 260:219–236.
2006. Retention mechanisms of white perch (*Morone americana*) and striped bass (*M. saxatilis*) early-life stages in an estuarine turbidity maximum: an integrative fixed-location and mapping approach. Fish. Oceanogr. 15:429–450.
North, E. W., R. R. Hood, S.-Y. Chao, and L. P. Sanford.
2005. The influence of episodic events on transport of striped bass eggs to the estuarine turbidity maximum nursery area. Estuaries 28:108–123.
Pearre, S.
1986. Ratio-based trophic niche breadth of fish, the Sheldon spectrum, and the size-efficiency hypothesis. Mar. Ecol. Prog. Ser. 27:299–314.
Pepin, P., and R. W. Penney.
1997. Patterns of prey size and taxonomic composition in larval fish: are there general size-dependent models? J. Fish Biol. 51 (suppl. A):84–100.

2000. Feeding by a larval fish community: impact on zooplankton. Mar. Ecol. Prog. Ser. 204:199–212.

Rakocinski, C. F., J. Lyczkowski-Shultz, and S. L. Richardson.
1996. Ichthyoplankton assemblage structure in Mississippi Sound as revealed by canonical correspondence analysis. Estuar. Coast. Shelf Sci. 43:237–257.

Richardson, S. L., J. L. Laroche, and M. D. Richardson.
1980. Larval fish assemblages and associations in the north-east Pacific along the Oregon coast, winter-spring 1972–1975. Estuar. Coast. Shelf Sci. 11:671–699.

Roman, M. R., D. V. Holliday, and L. P. Sanford.
2001. Temporal and spatial patterns of zooplankton in the Chesapeake Bay turbidity maximum. Mar. Ecol. Prog. Ser. 213:215–227.

Rutherford, E. S., and E. D. Houde.
1995. The influence of temperature on cohort-specific growth, survival, and recruitment of striped bass, *Morone saxatilis*, larvae in Chesapeake Bay. Fish. Bull. 93:315–332.

Sanford, L. P., S. E. Suttles, and J. P. Halka.
2001. Reconsidering the physics of the Chesapeake Bay estuarine turbidity maximum. Estuaries 24:655–669.

Secor, D. H., E. D. Houde, and D. M. Monteleone.
1995. A mark-release experiment on larval striped bass, *Morone saxatilis*, in a Chesapeake Bay tributary. ICES J. Mar. Sci. 52:87–101.

Setzler, E. M., J. A. Mihursky, K. V. Wood, W. R. Boynton, T. T. Polgar, and G. E. Drewry.
1981. Major features of ichthyoplankton populations in the upper Potomac Estuary: 1974–1976. Rapp. P.-v. Reun. Cons. Int. Explor. Mer 178:204–206.

Shenker, J. M., D. J. Hepner, P. E. Frere, L. E. Currence, and W. W. Wakefield.
1983. Upriver migration and abundance of naked goby, *Gobiosoma bosc*, larvae in the Patuxent River estuary, Maryland. Estuaries 6:36–42.

Shirota, A.
1970. Studies of the mouth size of fish larvae. Bull. Jpn. Soc. Fish. Oceanogr. 36:353–368.

Shoji, J., E. W. North, and E. D. Houde.
2005. The feeding ecology of white perch *Morone americana* larvae in the Chesapeake Bay estuarine turbidity maximum: the influence of physical conditions and prey concentrations. J. Fish Biol. 66:1328–1341.

Shoji, J., and M. Tanaka.
2006. Influence of spting river flow on the recruitment of Japanese seaperch *Lateolabrax japonicus* into the Chikugo estuary, Japan. Sci. Mar. (Barc.) 70 (S2):159–164.
2007. Growth and mortality of larval and juvenile Japanese seaperch *Lateolabrax japonicus* in relation to seasonal changes in temperature and prey abundance in the Chikugo estuary. Estuar. Coast. Shelf Sci. 73:423–430.

Strauss, R. E.
1979. Reliability estimates for Ivlev's electivity index, the forage ratio, and a proposed linear index of food selection. Trans. Am. Fish. Soc. 108: 344–352.
1982. Influence of replicated subsamples and subsample heterogeneity on the linear index of food selection. Trans. Am. Fish. Soc. 111:517–522.

Tzeng. W.-N., and Y.-T. Wang.
1993. Hydrography and distribution dynamics of larval and juvenile fishes in the coastal waters of the Tanshui River estuary, Taiwan, with reference to estuarine larval transport. Mar. Biol. 116:205–217.

USGS (United States Geological Survey).
2010. Water resources (National Water Information System (NWIS): daily stream flow for Maryland. April, 2010. http://waterdata.usgs.gov/md/nwis/discharge. Department of the Interior, U.S. Geological Survey, Bowie, MD.

Winkler, G., J. J. Dodson, N. Bertrand, D. Thivierge, and W. F. Vincent.
2003. Trophic coupling across the St. Lawrence River estuarine transition zone. Mar. Ecol. Prog. Ser. 251:59–73.

Witting, D. A., K. W. Able, and M. P. Fahay.
1999. Larval fishes of a Middle Atlantic Bight estuary: assemblage structure and temporal stability. Can. J. Fish. Aquat. Sci. 56:222–230.

Young, P. C., J. M. Leis, and H. F. Hausfield.
1986. Seasonal and spatial distribution of fish larvae in waters over the North West Continental Shelf of Western Australia. Mar. Ecol. Prog. Ser. 31:209–222.

Appendix Table 1

Year 2000. Larval fishes: species composition, frequency of occurrence (Freq=proportion of tows positive), no./tow, and standard error (SE) of no./tow by region in the Patuxent River estuarine transition zone from spring through early summer 2000. The salt front region includes stations ±3 rkm from the salt-front location (see Fig. 1). H'=Shannon-Wiener diversity index values (H'_{max}=2.0).

	Freshwater			Salt front			Oligohaline		
Species	Freq	no./tow	SE	Freq	no./tow	SE	Freq	no./tow	SE
Anguilla rostrata (American eel)	0.01	0.01	0.01	—	—	—	—	—	—
Anchoa mitchilli (bay anchovy)	0.01	0.01	0.01	0.19	0.31	0.15	0.35	0.73	0.26
Alosa aestivalis (blueback herring)	0.14	0.52	0.20	—	—	—	—	—	—
Alosa mediocris (hickory shad)	0.07	0.09	0.04	0.03	0.03	0.03	—	—	—
Alosa sapidissima (American shad)	0.10	0.13	0.05	0.03	0.03	0.03	—	—	—
Alosa pseudoharengus (alewife)	0.73	28.84	10.46	0.13	0.13	0.06	—	—	—
Dorosoma cepedianum (gizzard shad)	0.59	14.39	4.82	0.34	1.25	0.50	0.12	0.27	0.16
Notropis hudsonius (spottail shiner)	0.04	0.06	0.03	—	—	—	—	—	—
Etheostoma spp. (darters)	0.10	0.11	0.04	—	—	—	—	—	—
Fundulus heteroclitus (mummichog)	0.07	0.08	0.04	—	—	—	—	—	—
Fundulus majalis (striped killifish)	0.01	0.01	0.01	—	—	—	—	—	—
Erimyzon spp. (chubsuckers)	0.06	0.06	0.03	0.03	0.03	0.03	—	—	—
Ictalurus punctatus (channel catfish)	0.01	0.01	0.01	0.03	0.03	0.03	—	—	—
Menidia beryllina (inland silverside)	0.13	0.17	0.06	0.03	0.03	0.03	0.12	0.12	0.06
Menidia menidia (Atlantic silverside)	—	—	—	0.16	0.19	0.08	0.31	1.23	0.77
Syngnathus fuscus (Northern pipefish)	—	—	—	—	—	—	0.04	0.04	0.04
Lepomis gibbosus (pumpkinseed)	0.01	0.01	0.01	—	—	—	—	—	—
Perca flavescens (yellow perch)	0.03	0.06	0.04	—	—	—	—	—	—
Morone americana (white perch)	0.80	160.59	74.80	0.97	167.11	64.09	0.73	27.27	8.05
Morone saxatilis (striped bass)	0.31	5.61	2.28	0.53	11.14	4.12	0.38	3.21	1.46
Pomoxis annularis (white crappie)	0.24	0.45	0.13	0.06	0.09	0.07	—	—	—
Sciaenidae spp. (drums)	—	—	—	0.03	0.16	0.16	0.08	0.27	0.23
Gobiosoma bosc (naked goby)	0.14	1.00	0.46	0.81	98.30	42.99	0.92	591.90	227.69
Trinectes maculatus (hogchoker)	0.01	0.01	0.01	0.06	0.06	0.04	0.04	0.04	0.04
Total		212.2			278.9			625.1	
CV (%)		315			154			185	
Number of species		21			15			10	
H'		0.85			0.86			0.25	

Appendix Table 2

Year 2001. Larval fishes: species composition, frequency of occurrence (Freq= proportion of tows positive), no./tow, and standard error (SE) of no./tow by region in the Patuxent River estuarine transition zone from spring through early summer 2001. The salt-front region includes stations ±3 rkm from the salt-front location (see Fig. 1). H'=Shannon-Wiener diversity index values (H'_{max}=2.0).

	Freshwater			Salt front			Oligohaline		
Species	Freq	no./tow	SE	Freq	no./tow	SE	Freq	no./tow	SE
Anchoa mitchilli (bay anchovy)	—	—	—	0.14	0.34	0.22	0.13	1.31	0.97
Alosa aestivalis (blueback herring)	0.16	0.85	0.19	—	—	—	—	—	—
Alosa mediocris (hickory shad)	0.03	0.03	0.02	—	—	—	—	—	—
Alosa sapidissima (American shad)	0.11	0.13	0.05	—	—	—	—	—	—
Alosa pseudoharengus (alewife)	0.81	25.10	9.13	0.34	0.76	0.30	—	—	—
Dorosoma cepedianum (gizzard shad)	0.36	2.99	1.31	0.38	2.10	0.83	0.05	0.18	0.16
Notropis hudsonius (spottail shiner)	0.15	0.62	0.34	0.03	0.03	0.03	—	—	—
Etheostoma spp. (darters)	0.28	0.96	0.23	0.10	0.10	0.06	—	—	—
Fundulus heteroclitus (mummichog)	0.18	0.20	0.05	—	—	—	—	—	—
Erimyzon spp. (suckers)	0.42	4.11	1.28	0.10	0.14	0.08	0.03	0.03	0.03
Menidia beryllina (inland silverside)	0.14	0.39	0.23	0.31	0.45	0.14	0.31	1.49	0.54
Menidia menidia (Atlantic silverside)	0.11	0.13	0.04	0.28	1.17	0.61	0.59	4.87	1.41
Membras martinica (rough silverside)	—	—	—	0.07	0.07	0.05	—	—	—
Syngnathus fuscus (Northern silverside)	—	—	—	—	—	—	0.05	0.05	0.04
Opsanus tau (oyster toadfish)	—	—	—	—	—	—	0.05	0.05	0.04
Perca flavescens (yellow perch)	0.07	0.92	0.59	0.07	0.07	0.05	—	—	—
Morone americana (white perch)	0.83	429.34	128.28	1.00	194.07	39.55	0.49	8.05	2.49
Morone saxatilis (striped bass)	0.40	72.72	37.88	0.66	45.17	22.62	0.54	4.44	1.93
Micropterus salmoides (largemouth bass)	0.01	0.01	0.01	—	—	—	—	—	—
Pomoxis annularis (white crappie)	0.17	0.27	0.09	0.03	0.03	0.03	—	—	—
Sciaenidae spp. (drums)	0.01	0.03	0.03	—	—	—	—	—	—
Gobiosoma bosc (naked goby)	0.01	0.01	0.01	0.72	597.62	405.02	0.92	169.10	65.64
Trinectes maculatus (hogchoker)	0.01	0.01	0.01	—	—	—	0.03	0.03	0.03
Total		538.8			842.1			189.6	
CV (%)		223			254			217	
Number of species		19			14			11	
H'		0.72			0.78			0.50	

Age, growth, and spawning season of red bream (*Beryx decadactylus*) off the southeastern United States

Claudia Friess (contact author)[1*]

George R. Sedberry[2]

Email address for contact author: cfriess@oceanconservancy.org

[1] Grice Marine Laboratory
College of Charleston
205 Fort Johnson Road
Charleston, South Carolina 29412-9110
* Present address: Ocean Conservancy
106 E 6th St
Austin, TX 78701

[2] Gray's Reef National Marine Sanctuary
10 Ocean Science Circle
Savannah, Georgia 31411

Abstract—Red bream (*Beryx decadactylus*) is a commercially important deep-sea benthopelagic fish with a circumglobal distribution on insular and continental slopes and seamounts. In the United States, small numbers are caught incidentally in the wreckfish (*Polyprion americanus*) fishery which operates off the southeastern coast, but no biological information exists for the management of the U.S. red bream population. For this study, otoliths (n=163) and gonads (n=161) were collected from commercially caught red bream between 2003 and 2008 to determine life history parameters. Specimens ranged in size from 410 to 630 mm fork length and were all determined to be mature by histological examination of the gonads. Females in spawning condition were observed from June through September, and reproductively active males were found year-round. Sectioned otoliths were difficult to interpret, but maximum age estimates were much higher than the 15 years previously reported for this species from the eastern North Atlantic based on whole-otolith analysis. Estimated ages ranged from 8 to 69 years, and a minimum lifespan of 49 years was validated by using bomb radiocarbon dating. Natural mortality was estimated at 0.06/yr. This study shows that red bream are longer lived and more vulnerable to overfishing than previously assumed and should be managed carefully to prevent overexploitation.

Manuscript submitted 30 September 2009.
Manuscript accepted 28 September 2010.
Fish. Bull. 109:20–33 (2011).

The views and opinions expressed or implied in this article are those of the author (or authors) and do not necessarily reflect the position of the National Marine Fisheries Service, NOAA.

Red bream (*Beryx decadactylus*, Cuvier, 1829) is one of three species in the genus *Beryx* (Beryciformes: Berycidae). Similar to its congener, the splendid alfonsino (*B. splendens*), red bream have a circumglobal distribution in temperate to tropical waters and are commonly found on continental shelves and slopes, seamounts, and oceanic ridges at depths of at least 1240 m (Busakhin, 1982). The third species, *B. mollis*, is restricted to the western North Pacific region and is not further discussed in this article.[1] Red bream and splendid alfonsino are commercially exploited wherever they occur in abundance, particularly in the eastern North Atlantic around the Macaronesian Islands (Large et al., 2003); in the Pacific around New Caledonia (Lehodey et al., 1997), New Zealand (Massey and Horn, 1990) and Japan (Adachi et al., 2000); and in the Indian Ocean on Saya de Malha Bank and around the Kerguelen Islands. In the eastern North Atlantic, both alfonsino species are currently caught in a multispecies, multigear fishery that targets mainly blackspot seabream (*Pagellus bogaraveo*) at depths of 200–600 m (ICES[2]). In European waters alfonsinos are managed collectively because species-specific landings data rarely exist. The status of the European stocks is currently unknown owing to short catch time series, the lack of fishery-independent data, and unreliable estimates of mortality rates, but there are reports of serial depletion of alfonsino populations during the early years of the rapidly expanding deep-sea fisheries on and around seamounts in the eastern North Atlantic (Vinnichenko, 1997; ICES[2]).

In the western North Atlantic, alfonsinos are caught incidentally off the southeastern coast of the United States in the wreckfish (*Polyprion americanus*) fishery. The fishery operates in an area of high topographic relief known as the Charleston Bump, located on the Blake Plateau south-

[1] Because of the confusion created by regional differences in the use of common names for the *Beryx* species, the following nomenclature will be used throughout the rest of this article: *B. decadactylus* will be referred to by its American Fisheries Society (AFS) common name "red bream" (Nelson et al., 2004; FAO common name "alfonsino"), *B. splendens* by its FAO common name "splendid alfonsino" (Froese and Pauly, 2008; AFS common name "alfonsino"), and the two collectively will be called "alfonsinos."

[2] ICES (International Council for the Exploration of the Sea). 2008. Report of the working group on the biology and assessment of deep-sea fisheries resources, 3–10 March 2008, ICES Headquarters, Copenhagen. ICES CM 2008/ACOM:14., 531 p.

east of Charleston, South Carolina. The Charleston Bump is characterized by carbonate outcrops, scarps, scour depressions, and overhangs that are essential hard-bottom habitat for demersal fishes (Sedberry et al., 2001). In most global fisheries, splendid alfonsino is the most abundant *Beryx* species in the catch, but in the U.S. wreckfish fishery, red bream composes more than 95% of the alfonsino landings (senior author, personal observ.). Alfonsino landings in the United States are currently not monitored.

Life history data for red bream are sparse because research on alfonsinos has focused almost exclusively on the economically more important splendid alfonsino. A few studies have addressed both species, and it was concluded that distribution, feeding habits, reproductive parameters, age and growth, and larval development are similar (Busakhin, 1982; Mundy, 1990; Isidro, 1996; Dürr and Gonzalez, 2002). Alfonsinos are gonochoristic batch spawners (Isidro, 1996), their eggs and larvae are epipelagic, and juveniles are pelagic for several months (Mundy, 1990) before moving into deeper waters and assuming the adult benthopelagic lifestyle (Busakhin, 1982; Lehodey et al., 1994). In the eastern North Atlantic, female red bream reach sexual maturity at 276 mm fork length. The maximum age estimate for the Azores red bream population is 15 years, although ages for this species have never been validated (Isidro, 1996).

Basic biological information has not been published for the western North Atlantic red bream population. Many other deep-sea fishes have life history patterns characterized by slow growth, high longevity, and late maturity, all of which results in low productivity, high susceptibility to overfishing, and low resiliency (Merrett and Haedrich, 1997; Koslow et al., 2000; Cheung et al., 2007). Knowledge of red bream life history traits is essential for establishing the biological reference points needed for management and, in the absence of traditional stock assessments, for conducting risk assessments to evaluate vulnerability and prevent overfishing (Patrick et al., 2010).

The purpose of this study was to investigate the age, growth, and reproductive biology of red bream caught off the southeastern United States. We hypothesized that red bream attain a much higher maximum age than previously assumed, more similar to other deep-water fishes that occur on the Charleston Bump, such as barrelfish (*Hyperoglyphe perciformis*) and blackbelly rosefish (*Helicolenus dactylopterus*), which have estimated longevities of 85 and 30 years, respectively (White et al., 1998; Filer and Sedberry, 2008). Another goal of the study was to validate high red bream age estimates obtained through the interpretation of thin-sectioned otoliths. We used bomb radiocarbon dating, a method that has previously been successfully applied to validate ages for other long-lived fishes (Kalish et al., 1997; Kerr et al., 2005; Piner et al., 2005). We used age estimates to determine growth parameters and estimate natural mortality rate. The life history parameters presented here provide critical inputs for stock assessments, risk analyses, and for determining biological reference points. This information is needed if red bream become a target for the fishery and need to be included in a fishery management plan in the future.

Materials and methods

Collection of samples

Red bream landed by the commercial wreckfish fishery operating on the Charleston Bump (approximately 31°30′N, 79°W) were sampled from April 2003 to January 2008. All specimens were caught by vertical line fishing in depths of 450–600 m (Sedberry et al., 1999) and iced on the vessel until arrival at port. Every red bream caught on a fishing trip was sampled during a port sampling trip. For each specimen, total length (TL), fork length (FL), and standard length (SL) were measured to the nearest millimeter, and total body weight (TBW) was recorded in grams. Sagittal otoliths were extracted and stored dry in envelopes for age and growth analysis, and the entire gonad was removed and placed in 10% buffered formalin for histological analysis. In addition, otoliths and fork lengths from 22 small (FL≤400 mm) specimens collected from the Azores were provided by Gui Menezes of the Departamento de Oceanografia e Pescas (DOP), University of the Azores. These otoliths were examined to aid with aging technique development because initial counts of age increments for Charleston Bump otoliths were much higher than ages previously reported for eastern North Atlantic red bream.

Age and growth

Sagittal otoliths were weighed to the nearest milligram, and either the right or left otolith (depending on the condition of the otolith) was embedded in epoxy resin. A Buehler Isomet low-speed saw (Buehler Ltd., Lake Bluff, IL) with a diamond wheel was used to cut transverse sections of approximately 0.6–0.7 mm thickness through the focus. Sections were mounted on glass slides with Cytoseal mounting medium and viewed under a Nikon SMZ-U dissecting scope (Nikon Instruments Inc., Melville, NY) with transmitted and reflected light.

Exploratory readings were conducted along ventral and dorsal axes toward the proximal edge of the otolith. Increments were counted independently by two readers, without knowledge of fish length or sex, and both readers rated the readability of otoliths. After the exploratory readings, the first reader made two counts (readings) over the period of several weeks to assess within-reader precision, and the second reader made one count. When ages were compared between readings and readers, both readers decided to jointly recount all otoliths because of the large variation in assigned ages for some otoliths between the two readers. During the joint count, both readers agreed that there had been an error in the second reader's interpretation of the first growth bands and, therefore, the joint count was substituted for the second reader's count in all subse-

quent analyses and will be referred to as "reading 3" throughout the rest of this article.

Thin sections from two otoliths were polished to the core and presumed daily growth rings were counted under 40× magnification to help with the interpretation of what was thought to be the first annulus. Presumed daily growth rings were not validated. In addition to thin section interpretation, some of the uncut second otoliths were randomly selected and viewed whole under the dissecting microscope to qualitatively evaluate the ease of determining growth bands on the whole otolith surface.

To validate ages, eighteen of the uncut, second otoliths were selected for bomb radiocarbon analysis. These otoliths were chosen for readability and to span the range of observed ages that were based on thin section growth band counts, including otoliths from specimens with estimated birth years spanning the prebomb to postbomb period. The selected otoliths were embedded in epoxy resin and sectioned transversely through the core to 1 mm thickness. The sections were then taped to plates, and the cores were isolated by using a Dremel model 221 variable speed rotary tool (Robert Bosch Tool Corporation, Mt. Prospect, IL). Core isolation was visually aided because the central opaque area of the first year of growth in red bream otoliths is clearly visible on whole and sectioned otoliths.

The extracted cores were rinsed in 10% HNO_3 for 15–30 s, ultrasonically cleaned with a Branson ultrasonic cleaner B-22-4 (Branson Ultrasonics Corporation, Danbury, CT) with distilled water, air-dried, and weighed to the nearest 0.1 mg (Baker and Wilson, 2001). Each core was placed in a glass vial that had been cleaned with 10% HNO_3, and the samples were sent to the National Ocean Sciences Accelerator Mass Spectrometry (NOSAMS) laboratory at Woods Hole Oceanographic Institution. NOSAMS provided values of delta Carbon-14 ($\Delta^{14}C$) for each sample that were then plotted against otolith-derived birth years and compared to a reference chronology of validated ages for haddock (*Melanogrammus aeglefinus*) collected from Newfoundland (Campana, 1997). The timing of initial radiocarbon increase and mean year of increase were calculated with the deterministic model developed by Hamel et al. (2008) which models the pulse of radiocarbon from nuclear testing as a Gaussian curve over time and couples it with a continuous exponential decay process to describe radiocarbon dispersion and dilution.

Aging precision and bias between paired readings were examined graphically with age bias plots, and the coefficient of variation (CV) was calculated as a measure of the relative ease of aging red bream otoliths (Campana et al., 1995). Age frequencies were computed, and a standard linear regression relating increment count to otolith weight was also conducted. The von Bertalanffy growth function (VBGF; von Bertalanffy, 1938) was fitted to unweighted length-at-age data by using a random effects (RE) model with gamma population distribution likelihood as implemented in the program IGOR+, a Microsoft Excel®-based application developed by Cope and Punt (2007). The random effects model is based on a likelihood function that takes into account multiple reads for each otolith and thus incorporates both process and interpretation error into growth parameter estimations (Cope and Punt, 2007). Age and length information from all three readings could therefore be included in the estimation of the VBGF. The standard von Bertalanffy growth parameters k (the Brody coefficient), L_∞ (the theoretical mean maximum length), and t_0 (the theoretical age at length zero) were calculated with IGOR+ program. The model was run separately for males and females and for both sexes combined. The resulting sex-specific growth functions were compared by using likelihood tests (Kimura, 1980). An additional run was made including the age and length data for the 22 specimens from the Azores to assess how much the model parameters would change by including the smaller fish.

Natural mortality was estimated by using the equations developed by Hoenig (1983) and Pauly (1980) and by using the IGOR+ program. Hoenig's longevity-based estimator, $\ln Z = 1.46 - 1.01 \ln^*(t_{max})$, uses maximum age ($t_{max}$), and Pauly's equation, $\log_{10} M = -0.0066 - 0.279 \log_{10} L_\infty + 0.6543 \log_{10} k + 0.463 \log_{10} T$, uses von Bertalanffy growth parameters and water temperature, T, which in this case was the average annual water temperature for *Beryx* habitat from the literature. IGOR+ calculates total mortality by using the catch curve of the gamma-distributed "true ages" estimated in the RE model.

Reproductive biology

Gonads were weighed and processed according to the standard procedure used by the Marine Resources Monitoring Assessment and Prediction (MARMAP) Program at the Marine Resources Research Institute of the South Carolina Department of Natural Resources (White et al., 1998). A portion of the posterior gonad was removed, fixed in 10% formalin for 7–14 days, and transferred to 50% isopropanol for an additional 1–2 weeks. Tissues were then dehydrated, cleared, and blocked in paraffin under vacuum infiltration by using a Leica ASP300 tissue processor (Leica Microsystems Inc., Bannockburn, IL). Blocks were allowed to cool in a freezer, and three 7-µm cross sections were cut with a Leica RM2255 rotary microtome (Leica Microsystems Inc., Bannockburn, IL). These sections were then transferred to a microscope slide and allowed to dry overnight before they were stained with hematoxylin and eosin. The sections were viewed and interpreted under a Nikon Eclipse 55i compound microscope (Nikon Instruments Inc., Melville, NY), and reproductive stages were assigned independently by two readers without knowledge of specimen age, length, or collection date, according to criteria described by Harris et al. (2004). Females in spawning condition were identified by the presence of hydrated oocytes and postovulatory follicles. Specimens, for which interpretation between readers differed, were re-examined jointly, and a consensus was

reached. Spawning seasonality was determined by plotting monthly frequencies of reproductive stages.

Results

Data from samples

Of the 165 red bream sampled from the commercial fishery between April 2003 and January 2008, otoliths were collected from 163 specimens, gonads from 161, and fork length was measured for 164 fish (one specimen had a damaged tail). Otolith weights were obtained for 130 otoliths. No specimens could be sampled from the fishery in February and March in any year over the sample collection period because the wreckfish fishery is closed from January 15 through April 15. Sample sizes were highest for the months of July, August, September, and December (n=23–30) and lowest for April, October, and November (n=4–8). Because of low sample sizes, samples were pooled across years.

Fork lengths ranged from 410 to 630 mm and were not normally distributed (Shapiro-Wilk test; $P<0.001$; Fig. 1). Thus, the median FL more accurately describes the central tendency of the data set. Male FLs ranged from 410 to 601 mm (n=61), and female FLs ranged from 420 to 630 mm FL (n=98) (Fig. 1). The median FL for males (538 mm FL, standard error [SE]=7) was significantly different from that of females (550 mm FL, SE=5; 2-tailed Wilcoxon rank sum test, P=0.017). Strong linear relationships for both sexes were detected between FL and TL (males: TL=1.05FL+63.79, r^2=0.983; females: TL=1.03FL+73.32, r^2=0.973), FL and SL (males: SL=0.91FL+0.25, r^2=0.983; females: SL=0.91FL–5.44, r^2=0.970), and FL and TBW (males: TBW=17.52FL–5588.2, r^2=0.952; females: TBW=20.74FL–7323.1, r^2=0.949). The otoliths provided from the Azores corresponded to fork lengths ranging from 190 to 400 mm.

Age and growth

On whole otoliths, growth increments were best visible on the anterior edge of the antisulcal surface close to a large, central opaque area but became virtually indistinguishable closer to the otolith margin, especially in older specimens. Age determinations based on whole otoliths were therefore not attempted. In a few cases, one of the two otoliths collected from a specimen was misshapen, and crystals were clearly visible as lumps on the otolith surface. The second otolith would look normal and was used for aging.

Thin transverse sections of red bream otoliths contained a large central opaque area, and the count of assumed daily growth rings indicated that the translucent zone outside the central opaque area marks the first annulus (first otolith: 389 daily rings, second otolith: 371 daily rings). Thin sections of red bream otoliths contained a transition zone where increment width notably decreased and otoliths started increasing in thickness on the proximal surface rather than growing along the dorsoventral and anterioposterior axes (Fig. 2, A and B).

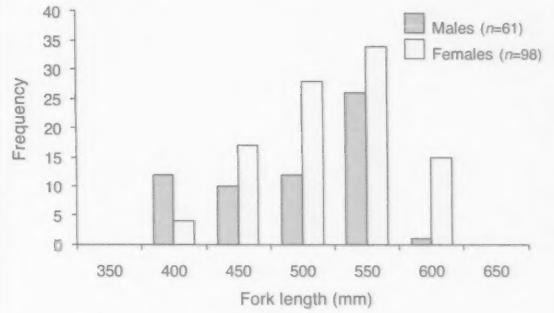

Figure 1

Length distribution of male and female red bream (*Beryx decadactylus*) sampled from the commercial wreckfish fishery off the southeastern United States from 2003 to 2008.

Thin sections of red bream otoliths had poor clarity and were difficult to interpret. Bands were often unclear, split, or irregularly spaced, and increments became thinner and harder to see toward the edge of the otolith. The dorsal axis next to the sulcus acousticus was chosen as the preferred axis for aging because the banding pattern was most distinct there. In many otoliths readability decreased at various points along the chosen axis, and counting had to be shifted away from the sulcus and toward the dorsal tip by following an increment over to the new axis. Often, increments, both close to the core and toward the edge of the otolith, were difficult to interpret in older as well as younger specimens because they were so poorly defined. In addition, semicrystalline fields were apparent in a number of thin sections, which added to difficulty in interpretation.

Even though red bream otoliths were overall difficult to age, there were no otoliths in the sample that were identified as unreadable by both readers and, therefore, all otoliths were aged and used in the analysis. Estimated ages ranged from 8 to 64 years for reading 1, 10 to 71 years for reading 2, and 9 to 69 years for reading 3. The age variation for individual otoliths between readings was high and ranged from 0 to 23 years, with a mean difference of 4 years. The age bias plots revealed that increment counts from reading 1 tended to underestimate age with respect to reading 2, increasingly so at ages 30 and higher (Fig. 3A). Reading 3 tended to underestimate ages 36 and higher with respect to reading 2 (Fig 3B), and reading 1 underestimated ages compared to reading 3, particularly ages up to 40 (Fig. 3C). Pairwise comparisons of CVs were highly variable across ages but tended to decrease with increasing age (Fig. 3, D–F). The mean pairwise CV was lowest between readings 2 and 3 at 8.6%, and high-

est between readings 1 and 2 at 12.2%. The mean CV across all three readings was 12.1%. Low aging precision was mostly due to overall poor clarity of otoliths and poorly defined bands. In addition, interpretation of growth bands close to the core was often particularly difficult, leading to high CVs, especially for younger fish. Bands towards otolith margins were also often difficult to distinguish.

Bomb radiocarbon analysis resulted in negative $\Delta^{14}C$ values ranging from −42.6‰ to −67.8‰ for fish estimated to have hatched before the mid-1960s, followed by rapid accumulation of $\Delta^{14}C$ over the period of atmospheric radiocarbon increase, to a peak of 93.4‰ in 1974 and a subsequent decline of $\Delta^{14}C$ levels in recent years (Table 1). The red bream $\Delta^{14}C$ chronology followed a similar pattern to that of the reference chronology for haddock from Newfoundland but was shifted by about five years to later years (Fig. 4). The year of initial radiocarbon increase was 1963, which is about five years later than that for haddock. Similarly, the mean year of radiocarbon increase for red bream was 1968, which is six years later than that for haddock (Table 2). Overall, bomb radiocarbon results supported the interpretation of growth increments as annual growth rings. In addition, a strong linear relationship was detected between otolith weight and age (r^2=0.845; n=130), which further supports otolith interpretation.

The von Bertalanffy growth curve fitted to males differed slightly from that fitted to females, and likelihood ratio tests indicated that growth functions were significantly different (χ^2=19.56, df=3, P<0.001; Fig. 5A), even though individual growth parameters were not. Sex-specific VBGFs were: $L_t=573.5(1-e^{-0.0.079(t-(-6.11))})$ for males, and $L_t=597.8(1-e^{-0.080(t-(-6.51))})$ for females. The combined VBGF for western North Atlantic red bream was: $L_t=583.1(1-e^{-0.094(t-(-3.69))})$. The growth coefficient was almost identical between males (k=0.079/yr, standard deviation [SD]=0.014) and females (k=0.080/yr, SD=0.017), but was higher for the combined sexes (k=0.094/yr, SD=0.013). In addition, females attained larger maximum theoretical lengths than did males (females: L_∞=597.8 mm, SD=10.310; males: L_∞=573.5 mm, SD=7.551). All three growth curves are depicted in Figure 5A and show that red bream growth is rapid in the first years of life, then slows down until asymptotic length is reached at about 580 mm FL or age 35 (Fig. 5A). The addition of the 22 specimens from the Azores (mean ages ranged from 1.5 to 10.5 years) did not have an appreciable effect on VBGF parameters; it merely increased k slightly to 0.100/yr.

The age-frequency distribution based on reading 3 was multimodal for both sexes. Most males caught on the Charleston Bump fell into the age groups between 11 and 20 years and 36 and 50 years and another slight peak occurred in the highest age group, 66–70 years. The females were most abundant in the age groups from 11 to 30 years and showed another slight increase in abundance from 41 to 50 years (Fig. 5B).

Mortality estimates were calculated for the combined sexes by using the maximum age estimate from reading 3 and von Bertalanffy growth parameters for the combined-sex growth curve. Total mortality (Z) based on Hoenig's equation was calculated as Z=0.06/yr by using 69 years, the maximum age estimate from growth band count, as t_{max}. With IGOR+ program, we also es-

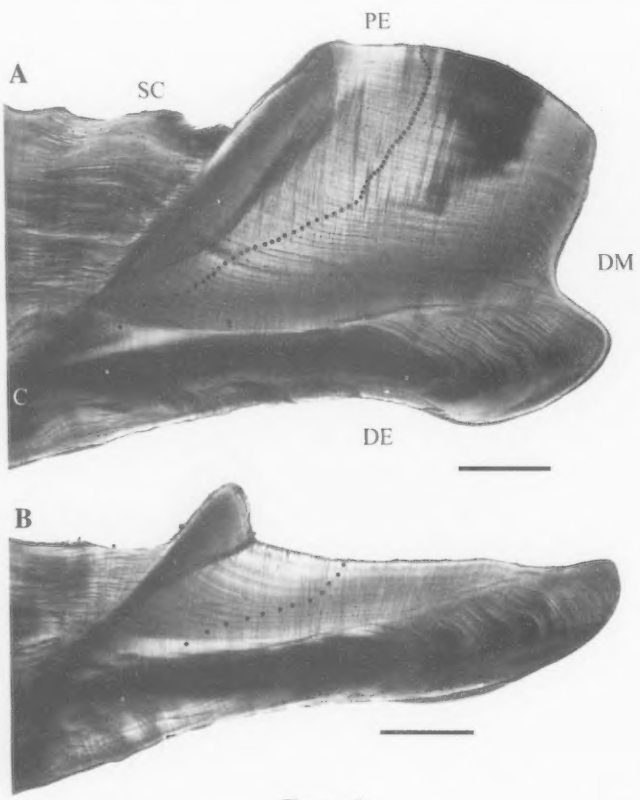

Figure 2

Transverse sections of sagittal otoliths under transmitted light showing (**A**) a male red bream (*Beryx decadactylus*) (fork length=567 mm) estimated to be 61 years old; C=core, SC=sulcus acousticus, DM=dorsal margin, PE=proximal edge, DE=distal edge; (**B**) a female specimen (fork length=502 mm) estimated to be 12 years old. Each dot represents a growth band (scale bar=1 mm).

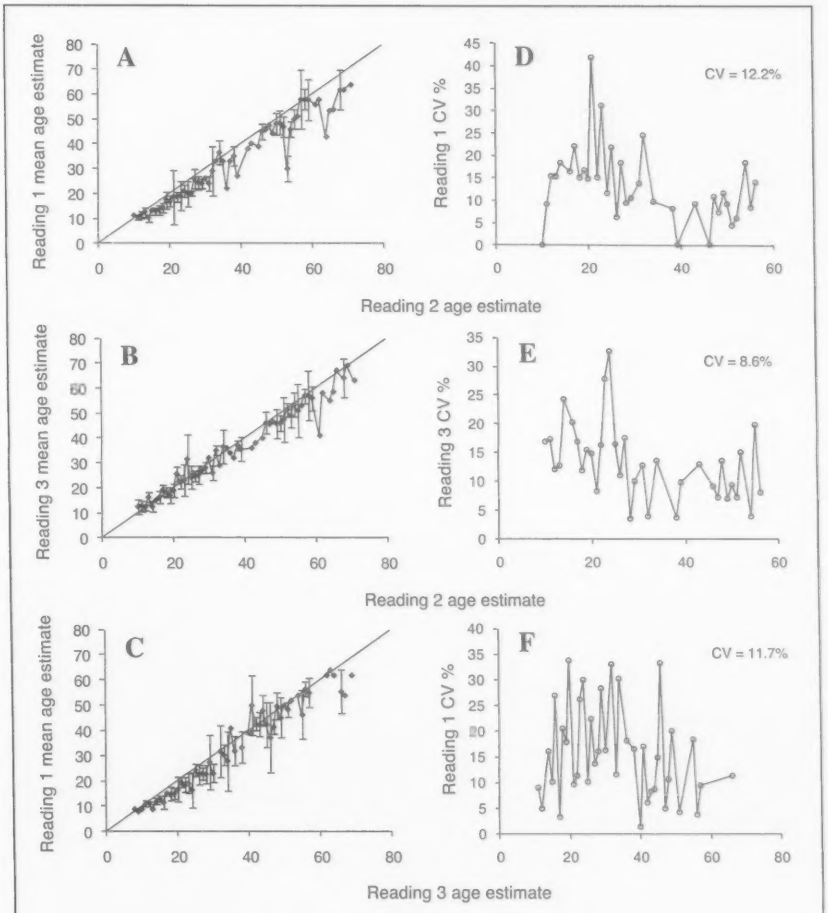

Figure 3

Pairwise comparisons of aging precision between readings of red bream (*Beryx decadactylus*) otoliths. (**A**) Mean age estimated in reading 1 for all fish assigned a given age in reading 2; (**B**) mean age estimated in reading 3 for all fish assigned a given age in reading 2; and (**C**) mean age estimated in reading 1 for all fish assigned a given age in reading 3. Error bars represent 95% confidence intervals and the solid line is the 1:1 relationship. (**D**) Coefficient of variation (CV) of reading 1 with respect to ages estimated in reading 2; (**E**) CV of reading 3 with respect to ages estimated in reading 2; and (**F**) CV of reading 1 with respect to ages estimated in reading 3. Mean CVs for pairwise readings are indicated on the individual panels.

timated a total mortality value of 0.06/yr. Estimates of M based on Pauly's equation were strongly influenced by the choice of mean water temperature value and ranged from 0.097 to 0.124/yr (Table 3).

Reproductive biology

Histological samples were obtained from 161 fish, of which 98 were female, 62 were male, and the sex of one specimen could not be determined. The overall sex ratio was 1:1.58 (M:F). All specimens sampled in this study were mature, and, therefore, a size and age at 50% maturity could not be established for the Charleston Bump red bream population.

Ovaries of resting females clearly showed characteristic thick, muscular walls, elongate lamellae with well-developed fibromuscular cords, and wide spaces between lamellae (Fig. 6A). Ripe females were often difficult to distinguish from individuals in the late developing stage because hydrated oocytes were few and always accompanied by oocytes in all stages of development (Fig. 6B). Female red bream in spawn-

Table 1

Summary of radiocarbon ($\Delta^{14}C$) results from red bream (*Beryx decadactylus*) otoliths collected off the southeast coast of the United States. NOSAMS accession no.= identification number assigned by the Woods Hole National Ocean Sciences Accelerator Mass Spectrometry Facility.

NOSAMS accession no.	Collection year	Birth year	Sample weight (mg)	Reading 1 age (yr)	Reading 2 age (yr)	Reading 3 (joint) age (yr)	$\Delta^{14}C$ (‰) (±error)
OS-67042	2007	1945	81.1	62	62	62	–61.5 (3.2)
OS-66866	2007	1951	40.6	58	59	56	–54.1 (4.0)
OS-66870	2006	1952	52	54	62	54	–62.1 (3.6)
OS-67041	2006	1958	56.5	48	50	48	–52.3 (2.9)
OS-66869	2007	1959	48.4	54	55	48	–67.7 (3.6)
OS-68036	2004	1959	74	38	43	45	–42.6 (3.3)
OS-68037	2005	1963	56.9	41	47	42	–67.8 (2.8)
OS-66868	2005	1964	86.6	44	50	41	–65.7 (3.2)
OS-68041	2004	1966	85.1	37	38	38	–18.7 (3.1)
OS-68142	2006	1966	152.3	40	43	40	–25.3 (3.7)
OS-68035	2003	1967	75.3	24	32	36	–14.4 (3.2)
OS-66867	2005	1969	42.7	33	38	36	–48.6 (3.6)
OS-68038	2006	1970	99	38	42	36	–34.3 (3.2)
OS-66998	2004	1974	39.6	23	29	30	–93.4 (4.1)
OS-68034	2005	1982	75.5	18	27	23	–67.0 (3.6)
OS-67038	2004	1989	35.6	11	11	15	–89.8 (4.1)
OS-68040	2003	1989	77.2	14	19	14	–85.7 (5.1)
OS-67040	2005	1991	70.6	10	11	14	–82.6 (3.4)

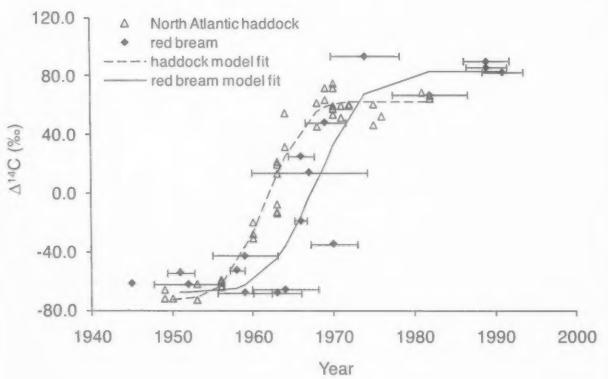

Figure 4

Radiocarbon ($\Delta^{14}C$) values plotted against otolith-derived estimates of birth year for red bream (*Beryx decadactylus*) from reading 3. Horizontal bars represent the CV of the age estimate for each sample. The reference chronology is shown for haddock (*Melanogrammus aeglefinus*) from Newfoundland (Campana, 1997). The best fit of Hamel et al.'s coupled-functions model to the otolith radiocarbon data is represented by the solid line for red bream and by the dashed line for haddock.

ing condition, based on the presence of hydrated oocytes and postovulatory follicles (Fig. 6C), were observed from June through September (Fig. 7A). There was one female for which reproductive stage could not be assigned because of poor quality of the histological sample.

There were five males that were determined to be mature, but reproductive stages could not be assigned even though spermatozoa were detected because the samples were mostly duct tissue. Consequently, those five males could not be included in the analysis of spawning seasonality. For one additional male there was not enough tissue to determine either a reproductive or maturity state, but it is unlikely that this male was immature, because it was neither one of the smallest nor one of the youngest males in the sample. Males in spawning condition, as indicated by the predominance of spermatozoa in ducts and lobules, were observed in all months for which male reproductive stages could be assigned. No resting males were present in the sample, but spent males were observed in July, August, November, December, and January (Fig. 7B).

Table 2

Estimated parameters and derived quantities from a deterministic coupled-functions model fitted to otolith radiocarbon series for red bream (*Beryx decadactylus*) and haddock (*Melanogrammus aeglefinus*) from the North Atlantic (Campana, 1997). Parameters are total inputted radiocarbon (k), mean year of increase (μ), standard deviation of the cumulative normal (σ), estimated timing of initial radiocarbon increase ($\mu-\sigma$), exponential rate of decay (r), minimum radiocarbon level observed (y_{min}), and maximum radiocarbon level that would occur in the absence of r (y_{asym}). Standard deviations (SD) are giving in parentheses, y_{min} has no SD because it is an observed point, and y_{asym} and k have the same SD.

Species	k (‰)	μ (year)	σ	$\mu-\sigma$ (year)	r	y_{min} (‰)	y_{asym} (‰)
Red bream	150.97 (8.64)	1967.94 (0.75)	4.87 (1..13)	1963.07 (1.59)	0	–67.8	83.17
Haddock	136.94 (6.24)	1961.81 (0.26)	3.93 (0.36)	1957.88 (0.49)	0.001 (0.004)	–72.8	64.14

Table 3

Estimates of natural mortality rates for red bream (*Beryx decadactylus*). Maximum ages used for Hoenig's estimator are 69 years based on otolith section interpretation and 49 years based on highest validated age in this study. L_∞ and k used for Pauly's equation were 583.1 mm and 0.094/yr, respectively, from the combined-sex von Bertalanffy growth function. The IGOR+ estimate is based on the random effects model with gamma-distributed population likelihood for all three readings and for both sexes combined.

Model		M (1/yr)
Hoenig (1983)	t_{max}=69 years	0.060
	t_{max}=49 years	0.085
Pauly (1980)	T=8.85°C *	0.097
	T=12.3°C †	0.113
	T=15.0°C ‡	0.124
IGOR+		0.060

* Average of the range (5.4–12.3°C) reported by Ross (2007) for southeastern U.S. deep-water coral habitat.

† Mean bottom temperature recorded on *Beryx* fishing habitat during submersible dives in August 2003 and 2004 (G. Sedberry, unpubl. data).

‡ Mean temperature recorded during submersible dives when red bream were present at site (G. Sedberry, unpubl. data).

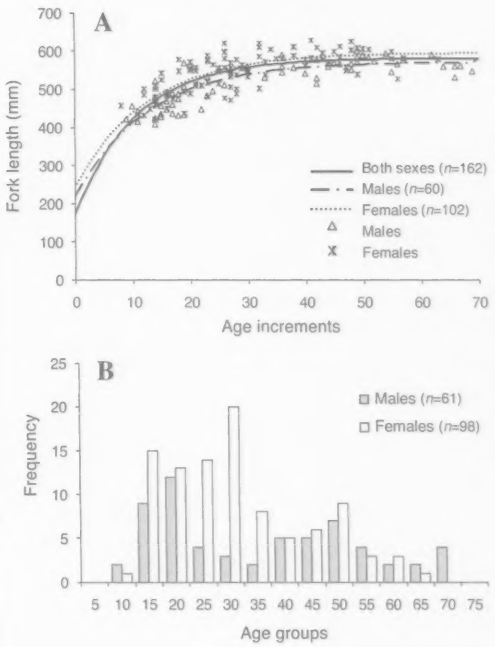

Figure 5

(**A**) Von Bertalanffy growth curves estimated from length-at-age data for Charleston Bump red bream (*Beryx decadactylus*), for males, females, and both sexes combined, and (**B**) age-frequency distribution of male and female red bream sampled from the commercial wreckfish fishery off the southeastern United States from 2003 to 2008.

Discussion

Age and growth

The presence of semicrystalline fields in a number of red bream otoliths is indicative of a partial replacement of the normal aragonite crystalline structure by vaterite, a calcium carbonate isomorph that has optical properties different from aragonite. The presence of vaterite in fish otoliths gives them a glassy and more translucent appearance and can mask usual growth banding patterns (Tomas et al., 2004; Solomon et al., 2006). Vaterite in red bream otoliths likely contributed to the aforementioned difficulties in aging that led to age estimation bias and lower aging precision than the average for otolith-derived age estimates reported by Campana (2001). The level of aging precision reported here for red bream was more similar to that achieved in other deep-sea teleost aging studies (Francis et al., 1998; Harris et al., 2004; Filer and Sedberry, 2008).

Even though interpretation error in the current study was present and significant, bomb radiocarbon

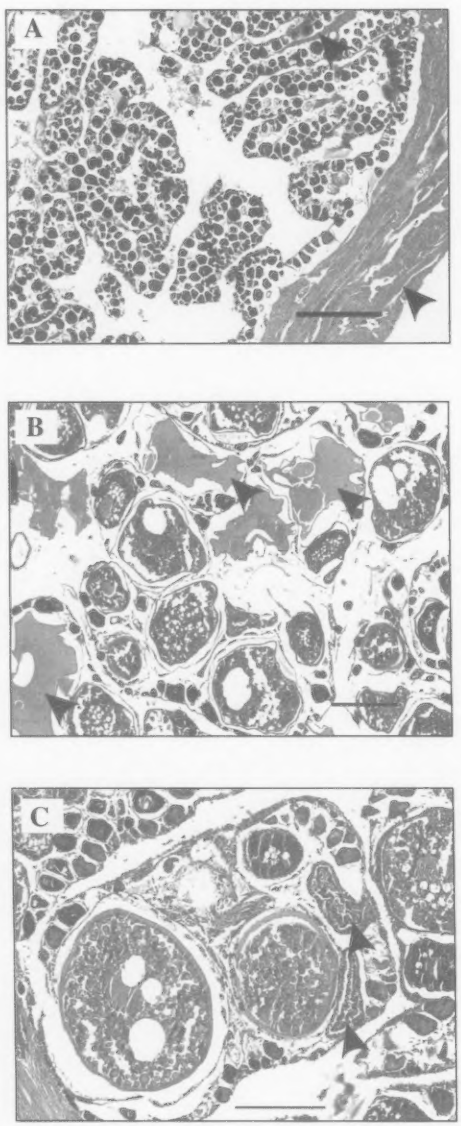

Figure 6

Transverse sections of red bream (*Beryx decadactylus*) ovarian tissue. (**A**) Ovary of resting female containing primary growth oocytes. The top arrow indicates the thickened fibromuscular cord inside long lamellae and wide spaces between lamellae; the bottom arrow indicates the thick ovary wall (bar=500 µm). (**B**) Ovary of a ripe female containing hydrated oocytes (indicated by arrows; bar=300 µm), and (**C**) ovary of a ripe female depicting 12–24 h old postovulatory follicles (indicated by arrows; bar=200 µm).

dating supported maximum ages much higher than previously reported for this species. The $\Delta^{14}C$ data also indicate that red bream in this study have been underaged by about 5 years. This is evidenced by the observed phase shift of the red bream chronology compared to the haddock reference and by the discrepancy between the two chronologies in initial and mean year of radiocarbon increase (Table 2). It is unlikely that this observed lag is due to depth-related differences in the ^{14}C signal for several reasons. First, red bream have a long pelagic juvenile stage (Mundy, 1990) which indicates that red bream and haddock experience similar environments in North Atlantic surface waters during otolith core formation. Second, the central opaque area of the first annulus in red bream otoliths is quite large and thus facilitated core extraction and reduced the likelihood that inaccurate coring was responsible for the observed phase shift. All core weights were less than the weight that was obtained for an otolith from the Azores aged to be one year old, which further indicates that coring was accurate. The bias between red bream and haddock $\Delta^{14}C$ chronologies is therefore likely due to aging error. Nevertheless, we were able to validate a minimum estimate of 49 years for red bream maximum age through bomb radiocarbon dating. In spite of the underaging indicated by the $\Delta^{14}C$ chronology shift, the bomb radiocarbon results support the annual nature of observed growth bands and, therefore, empirical age estimates of up to 69 years derived from the count of growth bands on sectioned otoliths are plausible. The positive linear relationship with a high coefficient of variation between otolith weight and estimated fish age lends additional support to maximum age estimates of 60+ years. It seems likely that red bream longevity exceeds the maximum age that can be validated with bomb radiocarbon dating. A different validation method, such as lead-radium dating which is more suitable to extremely long-lived fishes would, therefore, be more appropriate for estimating red bream lifespan (Andrews et al., 2009).

The maximum estimated age for red bream reported here is more than three times greater than previous estimates from the eastern North Atlantic (Isidro, 1996). This discrepancy could be due to underaging in previous studies, sampling bias, or it could be a reflection of a true difference in population age structure on opposite sides of the North Atlantic. Aging error is likely a contributing factor. Previous investigations of red bream age and growth from the eastern North Atlantic are based on whole otolith analysis and have not been validated. Isidro (1996) mentioned the limitations of aging larger and older red bream through whole otolith analysis and stated that his reported maximum age of 15 years should be considered a minimum estimate of longevity for this species because otoliths from larger specimens often had to be removed from the analysis due to reading difficulties. Isidro used marginal increment analysis to validate the periodicity of growth increment formation, but this method is

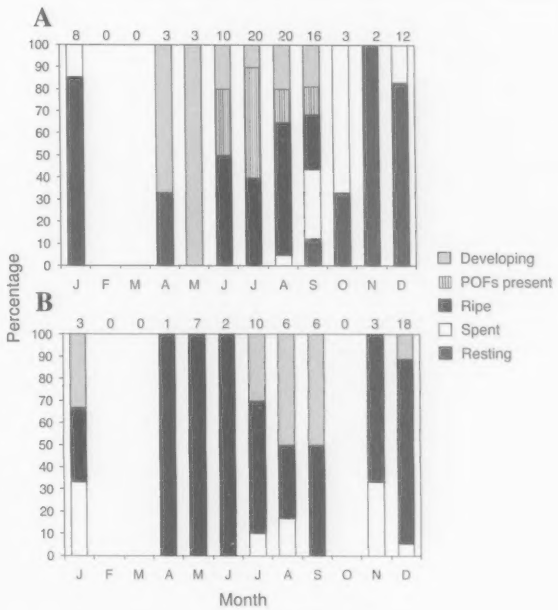

Figure 7

Percentages of reproductive stages observed for (**A**) female (n=97) and (**B**) male (n=56) red bream (*Beryx decadactylus*) collected from the commercial fishery operating around the Charleston Bump from 2003 to 2008. Sample sizes for each month are indicated above the bars. POF=postovulatory follicle.

limited to young, fast-growing fish and can lead to serious aging error if used incorrectly (Campana, 2001). Beamish (1979) showed that ages determined from the surface of otoliths tend to underestimate true ages when compared to age estimates derived from transverse sections, and there are several examples in the literature of deep-sea fishes for which ages have been severely underestimated by whole otolith analysis in the past. Orange roughy (*Hoplostethus atlanticus*) for example, was once thought to live up to 20 years, but a centenarian life span has since been validated for this species through lead-radium dating (Andrews et al., 2009). Bennett et al. (1982), also using lead-radium dating, showed that ages estimated from sectioned otoliths greatly exceeded those from whole otoliths for the rockfish genus *Sebastes*.

Although underaging of older fish was likely a factor contributing to the discrepancy in longevity estimates reported here, there was little overlap in observed fish lengths between this and previous studies, which limits our ability to make direct comparisons. Seventy-three percent of the fish sampled in this study had fork lengths of 500 mm or more, and none measured less than 410 mm FL. Conversely, fish from the Azores aged by Isidro (1996) were as small as 200 mm FL, but none reached 500 mm FL (Isidro, 1996). It is beyond the scope of this article to fully investigate the reason for this pattern in size differences, but evidence indicates that sampling bias may not be the primary explanation. In a recent study published by Menezes et al. (2009) sampling was undertaken at seamounts in the eastern North Atlantic with longlines at depths of up to 2000 m, but red bream were caught at a similar depth range to that in which the Charleston Bump fishery operates, roughly 450–600 m. The largest red bream caught in the study by Menezes measured 47 cm, which is still much less than the average length reported in our study. The observed size difference on opposite sides of the North Atlantic could thus be indicative of a true difference in population age and size structure.

The parameters of the red bream VBGF reported here for the combined sexes vary slightly from those reported by Isidro (1996) for the Azores. Isidro's L_∞ of 56 cm is 20 cm less than what was found in this study, a reflection of the smaller sizes of specimens observed in the eastern North Atlantic. Isidro estimated a k of 0.107/yr, which is slightly higher than the 0.094/yr reported here. In addition, the t_0 of –3.69 reported here is more negative than the –2.83 years reported

for Azores red bream, and this is probably due to a lack of specimens younger than 8 years in the present study, resulting in a less accurate estimation of the initial slope of the VBGF. We cannot say with certainty whether the observed differences of growth parameters are driven by differences in population dynamics or missing age groups in the analysis.

We found that male red bream were more abundant than females at smaller sizes but females predominated in the higher size classes. In previous studies on splendid alfonsino from the eastern North Atlantic, similar size distribution differences between the sexes were reported. This differential size and sex relationship was attributed to findings of slower growth in males and a distribution shift to greater depths with increasing size for this species which would result in skewed sex ratios when sampling over small depth ranges (Massey and Horn, 1990; Lehodey et al., 1994; Lehodey et al., 1997). We did not detect a difference in growth rates between male and female red bream, but the observed size frequency pattern and the lack of significance in growth rate differences from this study could be due to small sample sizes and low aging precision.

Spawning seasonality

All red bream specimens sampled from the Charleston Bump between 2003 and 2008 were sexually mature. These findings are in sharp contrast to maturity stages observed in the eastern North Atlantic, where the vast majority of specimens were immature, resting, or developing (Isidro, 1996). This is not surprising, given the observed differences in red bream size ranges between the eastern and western North Atlantic. Isidro (1996) reported a length at 50% maturity of 276 mm FL for females, which is well below the size of the smallest female observed in this study (420 mm FL). Isidro did not detect population-level spawning aggregations around the Azores and observed only very few females in spawning condition. In addition, he reported that the ovaries of the few spawning females that he observed contained only small numbers of hydrated oocytes, whereas all other oocytes were in previtellogenic condition, and therefore he concluded that only one batch of oocytes developed at a time. The ovaries of Charleston Bump females, however, contained oocytes in nearly all stages of development during the spawning season, indicating that several clutches of oocytes develop simultaneously. Male red bream on the Charleston Bump seem to be spawning year-round, but sample sizes for males were very low for some months in our study, and no data were available for February, March, or October. More samples need to be collected before any conclusive statements about the seasonality of male spawning activity on the Charleston Bump can be made.

Implications for fishery management

Red bream landings in the southeastern United States are presently not monitored, and the species is not under federal management because it is currently caught only in very small numbers as bycatch in the wreckfish fishery. In 2007, the Charleston Bump was the only area with reported wreckfish landings in the southeastern United States, and only one vessel participated in the fishery (J. McGovern, personal commun.[2]). U.S. red bream landings are so few that the population can probably be considered to be at near-virgin biomass levels. This means that natural mortality (M) can be directly estimated from Hoenig's total mortality equation and the algorithm in IGOR+, because Z approximates M in unfished populations. Natural mortality estimates are important input parameters for stock assessment models and are also commonly used in calculating reference points for fishery management, such as minimum stock size threshold (the biomass level below which a stock would be considered overfished) and proxies for fishing mortality rates that would produce maximum sustainable yield.

Underestimating the maximum age of a species, and thereby M, can bias stock assessment results and productivity estimates of a fish stock. Hoenig's estimate of natural mortality for red bream is 0.06/yr when the highest estimated age from band counts of sectioned otoliths, 69 years, is used as t_{max}. This value is in perfect agreement with the IGOR+ catch-curve–based estimate of Z. If the bomb radiocarbon-validated minimum longevity estimate of 49 years is used for t_{max}, M becomes 0.094/yr, which is still less than half the value one would obtain by using the previous t_{max} estimate of 15 years (M=0.279). Estimates of natural mortality based on life history parameters according to the equation of Pauly tended to be higher (0.097–0.124/yr) than longevity-based estimates of M but were very sensitive to the choice of mean annual temperature, which can be quite variable on bottom habitat of the Charleston Bump. It has been suggested that Pauly's equation overestimates the natural mortality of long-lived fishes because relatively few representatives with high longevity were included in the data set used by Pauly to derive the empirical equation (Newman et al., 2000). In contrast, Hoenig's data set included a wide range of long-lived species, and estimates based on Hoenig's equation have been shown to result in natural mortality rates similar to those derived from catch curves. This was indeed the case for red bream, where IGOR+ estimated the same M as Hoenig's equation based on a t_{max} of 69 years. We therefore suggest that 0.06/yr should be regarded as the current best estimate of natural mortality for the southeastern U.S. red bream population.

This study has shown that red bream are slow growing and exhibit an exceptional life-span, resulting in a very low natural mortality rate. Therefore, fisheries targeting this stock may be sustainable only at low exploitation rates. Other slow-growing, long-lived deep-water species that have been targeted by fisheries in the southeastern United States have already

[2] McGovern, Jack. 2008. NOAA Fisheries Southeast Regional Office, Saint Petersburg, FL 33701.

been showing signs of overexploitation; examples include snowy grouper (*Epinephelus niveatus*) (Wyanski et al., 2000) and blueline tilefish (*Caulolatilus microps*) (Harris et al., 2004). Even though red bream are currently not a target for commercial fisheries operating on the Charleston Bump, landings ought to be monitored closely, and red bream may need to be considered for inclusion in a fishery management plan as a stock in the fishery. Red bream that are caught are generally retained for sale, and if fishing effort increases, the stock could become subject to overfishing in the absence of management because of life history characteristics indicative of a highly vulnerable species. Management measures that would ensure the future sustainability of a fishery for red bream are likely similar to the ones that are already in place for wreckfish. They include individual transferrable quotas, closures of spawning areas, and gear restrictions.

The above comparison of life history parameters of the red bream populations from the eastern and western North Atlantic raises questions about stock structure for this species. Red bream sampled from the U.S. commercial fishery were generally larger and older than those observed in fishery-dependent and fishery-independent surveys from the Azores (Isidro, 1996; Menezes et al., 2009). Moreover, population-level spawning events have been documented in this study on the Charleston Bump, but not in the eastern North Atlantic (Isidro, 1996). These observed patterns could be due to gear selectivity and sampling bias or they could be an accurate reflection of geographic differences—perhaps even of a complex life cycle similar to that of the co-occurring wreckfish. Juvenile wreckfish are found mainly in the eastern North Atlantic, whereas spawning adults have so far been documented only on the Charleston Bump (Sedberry et al., 1999). Moreover, wreckfish have been captured off the southeastern United States with corroded hooks in their mouths that are of the same type as those used around the Azores, but not in the U.S. fishery. This finding indicates a trans-Atlantic migration of adults. In addition, population genetic analysis supports a panmictic population structure for wreckfish in the North Atlantic (Sedberry et al., 1996).

The long pelagic juvenile stage of alfonsinos would allow sufficient time for long-distance dispersal, and some authors have suggested different juvenile and adult habitat for alfonsinos in the eastern North Atlantic (Isidro, 1996; Lehodey et al., 1997). Isidro (1996) even speculated that recruitment to the Azores fishery may occur mainly through the drift of eggs and larvae from spawning areas located north or northwest of the Azores. Spawning aggregations in the Azores have since been confirmed for splendid alfonsino, but not for red bream (Menezes et al., 2009). The Charleston Bump may be an area that supplies red bream recruits to the Azores fishery by means of the Gulf Stream. Although purely speculative at this point, this hypothesis warrants further investigation. Mitochondrial DNA (mtDNA) studies to date have shown an absence of genetic structure between red bream populations from the Azores and the Charleston Bump (Friess and Sedberry, in press), but there is mtDNA evidence for localized genetically distinct populations within the eastern North Atlantic (Aboim, 2005). More extensive genetic studies that include red bream samples from throughout their range in the North Atlantic and perhaps use a different genetic marker are needed to examine red bream population structure in the North Atlantic more closely. It would be particularly important for fishery management and conservation purposes to know whether there are self-sustaining populations on individual seamounts and hard bottom habitats that serve as a source of recruits to other areas. If there was a single red bream stock in the North Atlantic, it would have to be managed carefully across international borders.

Acknowledgments

We thank B. White, J. Loefer, and M. Reichert for assisting with otolith interpretation and aging. P. Harris and A. Strand helped with data analysis. A. Williams and D. Wyanski assisted with the interpretation of reproductive stages, and A. Williams served as second reader of the histological sections. The members of the MARMAP program helped with sample collection and processing, and G. Menezes provided otoliths from eastern North Atlantic red bream. We thank S. Campana for advice on interpretation of otolith growth bands. We thank O. Hamel for providing the executable files and advice for running the deterministic models and J. Cope for advice on using IGOR+ software. We thank A. Andrews, who assisted with data analysis and interpretation, as well as K. McCarthy, and two anonymous reviewers for providing detailed suggestions that led to significant improvements at the manuscript stage. This research was supported with grants from the NOAA Fisheries Special Programs Office (NA03NMF4720321 and NA17FF2874; G. Sedberry and J. Loefer, principal investigators). Submersible observations were supported with NOAA Ocean Exploration grants NA03OAR-4600097 and NA0ROAR4600055, G. Sedberry, principal investigator. This is contribution 357 from the Grice Marine Laboratory.

Literature cited

Aboim, M. A.
2005. Population genetics and evolutionary history of some deep-sea demersal fishes from the Azores—North Atlantic. Ph.D. diss., 167 p. Univ. Southampton, Hampshire, U.K.

Adachi, K., K. Takagi, E. Tanaka, S. Yamada, and T. Kitakado.
2000. Age and growth of alfonsino *Beryx splendens* in the waters around the Izu Islands. Fish. Sci. 66:232–240.

Andrews, A., D. Tracey, and M. Dunn.
2009. Lead-radium dating of orange roughy (*Hoplostethus atlanticus*): validation of a centenarian life span. Can. J. Fish. Aquat. Sci. 66:1130–1140.

Baker, M. S., and C. A. Wilson.
2001. Use of bomb radiocarbon to validate otolith section ages of red snapper *Lutjanus campechanus* from the northern Gulf of Mexico. Limnol. Oceanogr. 46:1819–1824.

Beamish, R.
1979. Differences in the age of Pacific Hake (*Merluccius productus*) using whole otoliths and sections of otoliths. J. Fish. Res. Board Can. 36:141–151.

Bennett, J., G. W. Boehlert, and K. Turekian.
1982. Confirmation of longevity in *Sebastes diploproa* (Pisces: Scorpaenidae) from 210Pb/226Ra measurements in otoliths. Mar. Biol. 71:209–215.

Busakhin, S. V.
1982. Systematics and distribution of the family Berycidae (Osteichthyes) in the World Ocean. J. Ichthyol. 22:1–21.

Campana, S E.
1997. Use of radiocarbon from nuclear fallout as a dated marker in the otoliths of haddock *Melanogrammus aeglefinus*. Mar. Ecol. Prog. Ser. 150:49–56.

Campana, S. E.
2001. Accuracy, precision and quality control in age determination, including a review of the use and abuse of age validation methods. J. Fish Biol. 59:197–242.

Campana, S. E., M. Annand, and J. McMillan.
1995. Graphical and statistical methods for determining the consistency of age determinations. Trans. Am. Fish. Soc. 124:131–138.

Cheung, W. W. L., R. Watson, T. Morato, T. J. Pitcher, and D. Pauly.
2007. Intrinsic vulnerability in the global fish catch. Mar. Ecol. Prog. Ser. 333:1–12.

Cope, J. M., and A. E. Punt.
2007. Admitting ageing error when fitting growth curves: an example using the von Bertalanffy growth function with random effects. Can. J. Fish. Aquat. Sci. 64:205–218.

Dürr, J., and J. A. Gonzalez.
2002. Feeding habits of *Beryx splendens* and *Beryx decadactylus* (Berycidae) off the Canary Islands. Fish. Res. 54:363–374.

Filer, K. R., and G. R. Sedberry.
2008. Age, growth and reproduction of the barrelfish *Hyperoglyphe perciformes* (Mitchill) in the western North Atlantic. J. Fish Biol. 72:861–882.

Francis, M. P.
1998. Age and growth estimates for New Zealand hapuku, *Polyprion oxygeneios*. Fish. Bull. 97:227–242.

Friess, C., and G. R. Sedberry.
In press. Genetic evidence for a single stock of the deep-sea teleost red bream *Beryx decadactylus* in the North Atlantic as inferred from mtDNA control region analysis. J. Fish Biol.

Froese, R., and D. Pauly.
2008. FishBase. World Wide Web electronic publication. www.fishbase.org, version (11/2008). [Accessed 28 December 2008.]

Hamel, O., K. Piner, and J. Wallace.
2008. A robust deterministic model describing the bomb radiocarbon signal for use in fish age validation. Trans. Am. Fish. Soc. 137:852–859.

Harris, P. J., D. M. Wyanski, and P. P. Mikell.
2004. Age, growth, and reproductive biology of blueline tilefish along the southeastern coast of the United States, 1982–1999. Trans. Am. Fish. Soc. 133:1190–1204.

Hoenig, J.
1983. Empirical use of longevity data to estimate mortality rates. Fish. Bull. 81:898–903.

Isidro, E.
1996. Biology and population dynamics of selected demersal fish species of the Azores Archipelago. Ph.D. diss., 249 p. Univ. Liverpool, Isle of Man, U.K.

Kalish, J. M., J. M. Johnston, D. C. Smith, A. K. Morison, and S. G. Robertson.
1997. Use of the bomb radiocarbon chronometer for age validation in blue grenadier, *Macruronus novaezelandiae*. Mar. Biol. 128:557–563.

Kerr, L. A., A. H. Andrews, K. Munk, K. H. Coale, B. R. Frantz, G. M. Cailliet, and T. A. Brown.
2005. Age validation of quilback rockfish (*Sebastes maliger*) using bomb radiocarbon. Fish. Bull. 103:97–107.

Kimura, D.
1980. Likelihood methods for the von Bertalanffy growth curve. Fish. Bull. 77:765–776.

Koslow, J. A., G. W. Boehlert, J. D. M. Gordon, R. L. Haedrich, P. Lorance, and N. Parin.
2000. Continental slope and deep-sea fisheries: implications for a fragile ecosystem. ICES J. Mar. Sci. 57:548–557.

Large, P., C. Hammer, O. A. Bergstad, J. D. M. Gordon, and P. Lorance.
2003. Deep-water fisheries of the Northeast Atlantic: II Assessment and management approaches. J. Northwest Atl. Fish. Sci. 31:151–163.

Lehodey, P., R. Grandperrin, and P. Marchal.
1997. Reproductive biology and ecology of a deep-demersal fish, alfonsino *Beryx splendens*, over the seamounts off New Caledonia. Mar. Biol. 128:17–27.

Lehodey, P., P. Marchal, and R. Grandperrin.
1994. Modeling the distribution of alfonsino, *Beryx splendens*, over the seamounts of New Caledonia. Fish. Bull. 92:748–759.

Massey, B. R., and P. L. Horn.
1990. Growth and age structure of alfonsino (*Beryx splendens*) from the lower east coast, North Island, New Zealand. N. Z. J. Mar. Freshw. Res. 24:121–136.

Menezes, G., A. Rosa, O. Melo, and M. Pinho.
2009. Demersal fish assemblages off the Seine and Sedlo seamounts (northeast Atlantic). Deep-sea Res. II 56:2683–2704.

Merrett, N. R., and R. L. Haedrich.
1997. Deep-sea demersal fish and fisheries. Chapman & Hall, London, 296 p.

Mundy, B. C.
1990. Development of larvae and juveniles of the alfonsins, *Beryx splendens* and *B. decadactylus* (Berycidae, Beryciformes). Bull. Mar. Sci. 46:257–273.

Nelson, J. S., E. J. Crossman, H. Espinosa-Perez, L. T. Findley, C. R. Gilbert, R. N. Lea, and J. D. Willaims.
2004. Common and scientific names of fishes from the United States, Canada, and Mexico, 6th ed. Am. Fish. Soc., Spec. Pub. 29, Bethesda, MD, 386 p.

Newman, S. J., M. Cappo, and D. M. Williams.
2000. Age, growth, mortality rates and corresponding yield estimates using otoliths of the tropical red snappers, *Lutjanus erythropterus*, *L. malabaricus* and *L. sebae*, from the central Great Barrier Reef. Fish. Res. 48:1–14.

Pauly, D.
1980. On the interrelationships between natural mortality, growth parameters and mean environmental

temperature in 175 fish stocks. ICES J. Mar. Sci. 39: 175–192.

Patrick, W. S., P. Spencer, J. Link, J. Cope, J. Field, D. Kobayashi, P. Lawson, T. Gedamke, E. Cortés, O. Ormseth, K. Bigelow, W. Overholtz.
2010. Using productivity and susceptibility indices to assess the vulnerability of United States fish stocks to overfishing. Fish. Bull. 108:305–322.

Piner, K. R., O. S. Hamel, J. L. Menkel, J. R. Wallace, and C. E. Hutchinson.
2005. Age validation of canary rockfish (*Sebastes pinniger*) from off the Oregon coast (USA) using the bomb radiocarbon method. Can. J. Fish. Aquat. Sci. 62:1060–1066.

Ross, S. W.
2007. Unique deep-water ecosystems off the southeastern United States. Oceanography 20:130–139.

Sedberry, G. R., C. A. Andrade, J. L. Carlin, R. W. Chapman, B. E. Luckhurst, C. S. Manooch, G. Menezes, B. Thomsen, and G. F. Ulrich.
1999. Wreckfish *Polyprion americanus* in the North Atlantic: fisheries, biology, and management of a widely distributed and long-lived fish. Am. Fish. Soc. Symp. 23:27–50.

Sedberry, G. R., J. L. Carlin, R. W. Chapman, and B. Eleby.
1996. Population structure in the pan-oceanic wreckfish, *Polyprion americanus* (Teleostei: Polyprionidae), as indicated by mtDNA variation. J. Fish. Biol. 49:318–329.

Sedberry, G. R., J. C. McGovern, and O. Pashuk
2001. The Charleston Bump: An island of essential fish habitat in the Gulf Stream. *In* Island in the stream: oceanography and fisheries of the Charleston Bump (G. R. Sedberry, ed.), 252 p. Am. Fish. Soc., Bethesda, MD.

Solomon, C., P. Weber, J. Cech, B. Ingram, M. Conrad, M. Machavaram, A. Pogodina, and R. Franklin.
2006. Experimental determination of the sources of otolith carbon and associated isotopic fractionation Can. J. Fish. Aquat. Sci. 63:79–89.

Tomas, J., A. Geffen, I. Allen, and J. Berges.
2004. Analysis of the soluble matrix of vaterite otoliths of juvenile herring (*Clupea harengus*): do crystalline otoliths have less protein? Comp. Biochem. Physiol. Mol. Integr. Physiol. 139:301–308.

Vinnichenko, V. I.
1997. Russian investigations and deep water fishery on the Corner Rising seamount in subarea 6. NAFO Sci. Coun. Studies 30:41–49.

von Bertalanffy, L.
1938. A quantitative theory of the organic growth. II. Inquiries on growth laws. Hum. Biol. 10:181–213.

White, D. B., D. M. Wyanski, and G. R. Sedberry.
1998. Age, growth and reproductive biology of the blackbelly rosefish from the Carolinas, U.S.A. J. Fish Biol. 53:1274–1291.

Wyanski, D. M., D. B. White, and C. A. Barans.
2000. Growth, population age structure, and aspects of the reproductive biology of snowy grouper, *Epinephelus niveatus*, off North Carolina and South Carolina. Fish. Bull. 98:199–218.

Abstract—New technologies can be riddled with unforeseen sources of error, jeopardizing the validity and application of their advancement. Bioelectrical impedance analysis (BIA) is a new technology in fisheries research that is capable of estimating proximate composition, condition, and energy content in fish quickly, cheaply, and (after calibration) without the need to sacrifice fish. Before BIA can be widely accepted in fisheries science, it is necessary to identify sources of error and determine a means to minimize potential errors with this analysis. We conducted controlled laboratory experiments to identify sources of errors within BIA measurements. We concluded that electrode needle location, procedure deviations, user experience, time after death, and temperature can affect resistance and reactance measurements. Sensitivity analyses showed that errors in predictive estimates of composition can be large (>50%) when these errors are experienced. Adherence to a strict protocol can help avoid these sources of error and provide BIA estimates that are both accurate and precise in a field or laboratory setting.

Manuscript submitted 25 February 2010.
Manuscript accepted 30 September 2010.
Fish. Bull. 109:34–47 (2011).

The views and opinions expressed or implied in this article are those of the author (or authors) and do not necessarily reflect the position of the National Marine Fisheries Service, NOAA.

Measurements of resistance and reactance in fish with the use of bioelectrical impedance analysis: sources of error

M. Keith Cox (contact author)[1]
Ron Heintz[1]
Kyle Hartman[2]

Email address for contact author: Keith.Cox@noaa.gov

[1] National Marine Fisheries Service
Alaska Fisheries Science Center
Auke Bay Laboratories
11305 Glacier Hwy
Juneau, Alaska 99801

[2] West Virginia University
Davis College of Agriculture, Forestry & Consumer Sciences
1170 Agricultural Sciences Building
Morgantown, West Virginia 26506-6010

Successful application of promising new technologies is predicated on understanding and controlling sources of errors. The need to identify sources of error with the development of new fisheries technologies is documented in genetic studies (Blanca et al., 2009), in mark and recapture studies (Curtis, 2006), in the tracking of vessels with global position systems (GPS) (Palmer, 2008) and in measuring water clarity with beam transmissometers (Larson et al., 2007). To identify sources of errors for new technologies, measurements are often compared with those from established technologies (Larson et al., 2007), simulated theoretical ones (Palmer, 2008), or known measurements (Curtis, 2006). Regardless of the process, the desired end result is to identify and reduce sources of error to increase the accuracy of measurements, thereby enhancing technology to provide accurate and reliable results within the fields of fisheries research and management.

Bioelectrical impedance analysis (BIA) has the potential for wide application in fisheries as a tool to quickly and accurately perform a number of physiologically important field measurements. The BIA method is capable of estimating proximate composition, fish condition, and energy content in fish quickly, cheaply, and (after calibration) without the need to sacrifice fish (Cox and Hartman, 2005). Bioelectrical impedance analysis has been found to be accurate for measuring compositional mass (i.e., measured in grams), (Cox and Hartman, 2005), but not so accurate for measuring estimates of percentages or energy per wet weight (Pothoven et al., 2008). Bioelectrical impedance analysis involves measuring the impedance, resistance (R), and reactance (X_c) of fish tissues to an electrical current, and relating those measurements to the proximate composition, condition, or energy content of the fish. Linear models relating impedance to compositional components are highly significant ($P<0.001$) with coefficients of determination (r^2)>0.96 (Cox and Hartman, 2005). Relationships between observed and predicted values have slopes equal to one and intercepts that do not differ from zero. Estimations of body composition, condition, and energy content with BIA may be an asset to a variety of fisheries-related research and management projects by increasing the number of observations taken in the field and providing a means to take repeated measurements on individuals.

Physiological parameters are estimated from measured resistance (R) and reactance (X_c) values. Resistance

of a substance is proportional to the voltage of an applied current as it passes through a substance, or $R=V/C$, where V is applied voltage (volts), and C is current (amps). When the current is low enough, the current does not pass through the cell membrane (owing to the nonconductive lipid bilayer sandwiched between two conductive protein layers). The low current allows R to be reflective of everything extracellular. Reactance is the opposition to alternating current by a capacitor (cell membranes), and can be mathematically expressed by the following equation: $X_c=1/(2\pi fC)$, where f is frequency in Hertz, and C is capacitance in Farads (Keller et al., 1993). Higher current frequencies will cause cell membranes to become capacitive so that X_c becomes reflective of the total amount of cell membrane material within the current. Both values are thus related to the cross sectional area of the entire fish, conductor length of the organism, and the signal frequency of the current (Lukaski, 1987). The phase angle is the ratio of R to X_c of tissue and has been found to be sensitive to the health and condition of fish (Cox and Heintz, 2009). By using R and X_c, one can estimate the composition and condition of fish.

In order for BIA to be accepted in fisheries science, it is necessary first to identify sources of error, and then to use that knowledge to minimize errors. With the use of BIA in studies of human nutrition and body composition, the identification of error sources was used to establish protocols that minimized errors (Rallison et al., 1993). More specifically, predictions of proximate composition parameters with BIA were found to be accurate with established procedures, but without them, these estimates became inaccurate (Ursula et al., 2004). In previous fish research, BIA protocols were established to minimize any unforeseen sources of error (Cox and Hartman, 2005). Although protocols were established and error may have been minimized, the actual sources of error were not identified. More recently, studies with BIA methods have shown inconsonant results. For example, in a study of cobia (*Rathycentron canadum*), there was a high correlation between BIA and most cobia proximate composition values (Duncan et al., 2007); whereas in another study involving yellow perch (*Perca flavescens*), walleye (*Sander vitreus*), and lake whitefish (*Coregonus clupeaformis*), it was concluded that considerable work needs to be completed before BIA can provide reliable predictions of whole body energy and percent lipid content (Pothoven et al., 2008). Furthermore, it was indicated that there needs to be an understanding of how temperature, locations where the electrode needle is placed (possible sources of error), and lipid distribution within a fish affect BIA measures.

The objective of our study was to identify sources of error in measurements of fish with BIA and errors of R and X_c. The cumulative effects of both significant and nonsignificant errors were examined through sensitivity analysis modeling. We conclude by identifying a protocol that will minimize the sources of error and maximize the potential of BIA in providing measures of body composition and condition in the field and laboratory.

Methods

We conducted laboratory experiments to identify sources of errors within BIA measurements of R and X_c. Specifically, we considered how electrode needle location, procedure deviation, user training, time after death, temperature of the fish, and stomach fullness affected measurements of R and X_c. For a comparison, we used a reference (control) that followed the protocol outlined by Cox and Hartman (2005). For all experiments, a handheld Quantum X impedance analyzer (RJL Systems, Point Heron, MI) was used, except for temperature measurements, for which a desktop Quantum II analyzer was used. In either case, a fixed current at 800 µA, AC, and 50 kHz was used. Electrode needles were either "standard" 12 mm×28 gauge subdermal stainless steel disposable low-profile EEG needle electrodes (Grass Technologies, West Warwick, RI) as used in Cox and Hartman (2005), or "nonstandard" 38 mm×14 gauge standard hypodermic needles with a polypropylene hub. Brook trout (*Salvelinus fontinalis*) used in this study were obtained from the Bowden West Virginia State Fish Hatchery, Bowden, WV, and Chinook (*Oncorhynchus tshawytscha*), pink (*O. gorbuscha*), and coho (*O. kisutch*) salmon were obtained from the Sheldon Jackson College (SJC) salmon hatchery, Sheldon Jackson College, Sitka, AK. Approximately 100 brook trout were maintained in a living stream tank at West Virginia University at 15°C and fed standard hatchery pellets at a rate of 3% body weight per day until used in experiments. Juvenile Chinook, pink, and coho salmon used in this study were taken from the SJC hatchery round pens and adult salmon used in this study were selected from returning adults. Treatment methods are those described below for each particular experiment. Fish that were sacrificed were killed by a blow to the head. In all experiments, sample size was determined by iterative power analysis with a significance of 0.05 and a power of 0.96 (Zar, 1996). In cases where variances of sample sets were not available from previous data, sample data were collected for power analysis before testing.

Linear mixed-effects (LME) models were used to test for the effects of electrode needle location, procedure deviation, user experience, and time on R and X_c measures (Pinheiro and Bates, 2000). The effects of temperature and gut fullness were tested with regression analysis to test for differences in slopes. In each experiment, measured R and X_c values were compared between treatment and controls. Statistical tests on response measures were performed by using program R, vers, 2.4.1 (R Development Core Team, Vienna, Austria). Significance (α) was set at 0.05.

Location of the electrode needle

To determine if different electrode needle locations influence impedance, comparisions of R and X_c measurements were made between different electrode locations within an individual fish (Fig. 1A). A location refers to the simultaneous location of all four (tetrapolar) elec-

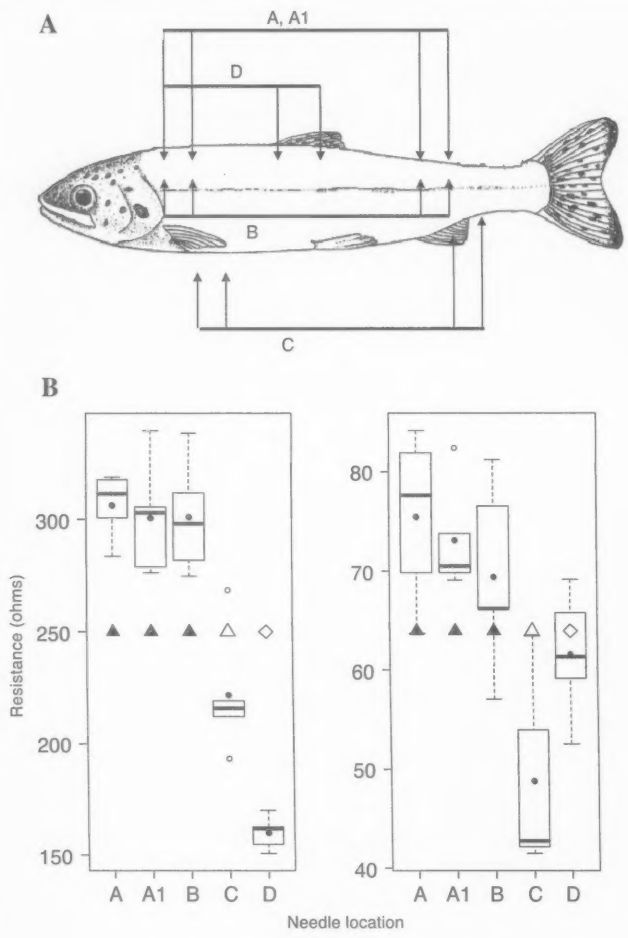

Figure 1

(**A**) Schematic diagram of needle electrode locations where resistance (R) and reactance (X_c) measurements are compared between each set of locations. Location A is the location used in Cox and Hartman (2005) with needles at a depth of 5 mm, A1 is the same location but the needles are inserted only 1 mm deep, and locations B, C, and D are different from A and have needles inserted to 5 mm. (**B**) Boxplots of mean resistance and reactance values taken from five pink salmon (*Oncorhynchus gorbuscha*) from different anatomical locations. Electrode locations are abbreviated as follows: control (A); reinserted (A1, the posterior set of electrodes were moved back to the original holes and the anterior electrodes were removed and reinserted into the exact same holes as in control); below (B, where both sets of electrodes were removed and placed approximately 1 cm below the holes in the control fish (but above the lateral line); ventral (C, where electrodes were removed and placed on the ventral portion of the fish and one set of electrodes was inserted on the anterior region one centimeter above the pelvic fin and the second set of electrodes was placed on the posterior end one centimeter above the anal fin); and half distance (D, where the posterior set of electrodes were moved forward and placed below the dorsal fin at a midpoint from the lateral line). Open circles (○) represent outliers determined by a Grubbs test. Different symbols indicate differences in means. Closed circles (●) represent mean values.

trodes. Spawning pink salmon (n=5, mean fork length=494.6 mm, standard deviation [SD]=8.9 mm) were killed, measured for fork length and weight, and placed on ice for 1 hour. A fish was randomly chosen and placed on a nonconductive board in a left-facing orientation, and measured for R and X_c for each of five electrode locations (Fig. 1A). This procedure was repeated for all five fish that were treated. Electrode locations were the following: 1) control (A, identical to measures found in Cox and Hartman, 2005); 2) reinserted (A1, both sets of electrodes were removed and reinserted into the "control" holes); 3) below (B, where both sets of electrodes were placed approximately 1 cm below the holes in the control (but above the lateral line); 4) ventral (C, where electrodes were placed on the ventral portion of the fish, and one set of electrodes was inserted on the anterior region one cm above the pelvic fin and the second set of electrodes was placed on the posterior end 1 cm above the anal fin); and 5) half distance (D, where the posterior set of electrodes was moved forward and placed below the dorsal fin at a midpoint to the lateral line). Measurements of R and X_c were recorded to the nearest 0.1 ohms (Ω).

Procedure deviations

To determine whether deviations from the procedures in Cox and Hartman (2005) would affect impedance measures, R and X_c measurements from five different treatment were compared to R and X_c measurements from the control group. Specific deviations were as follows 1) switched wires—the signal and detector leads were switched (by unplugging the leads while leaving the needle electrodes in the fish); 2) salt—two cups of seawater (31 practical salinity units) were poured under the fish; 3) conductive board—the fish was placed on a stainless steel conductive board; 4) needle size—the 28 gauge needles were replaced with larger 14 gauge hypodermic needles; and 5) needle depth—BIA electrode needles were placed in the fish in the same orientation as that in the control, except the needles were inserted to a depth of 1 mm rather than 5 mm. Spawning pink salmon (n=5, mean fork length=543.0 mm, SD=20.2) were killed, measured for length and weight, and placed on ice. Each of the five fish was randomly chosen and measured for R and X_c according to control protocols and also for each of the five treatment methods.

User experience

To determine if untrained users produce different and more variable R and X_c measurements compared to an experienced user, R and X_c measurements were compared between a user with training and four users without training. In this experiment, the single trained user had taken over 5000 BIA measurements on fish and the untrained users had no experience or previous training with BIA. Thirty juvenile coho salmon (n=30, mean weight=9.7 g, SD=2.1) were killed and randomly split into five groups of six fish, placed in plastic bags, and covered with ice. Before the experiment, four untrained users were introduced to the concepts of BIA and also to the protocols used by Cox and Hartman (2005). They were allowed to observe the trained user take R and X_c measurements on all six fish in a group. Each person was then randomly assigned a bag of fish. Immediately, each of the four inexperienced persons took R and X_c measures on all six fish within a group. During the time of taking measurements, untrained users were not allowed to ask for assistance. All fish from all groups were measured within 1 hour.

Time

We examined the effect of the time between death of the fish and BIA to determine how long dead fish can be held on ice before R and X_c measurements are compromised. Juvenile coho salmon (n=60, mean fork length=99.2 mm, SD=7.7 mm, and mean weight=10.3 g, SD=2.3 g) were killed and groups of six fish were randomly placed in plastic bags and placed on shaved ice. At 0, 3, 6, 9, 12, 24, 36, 48, 60, 72, and 96 h, a bag of fish was randomly removed and all six fish were measured for length, weight, R and X_c. It was assumed that because of the small size of the fish, the temperatures equilibrated within one hour of placement in ice and remained stable and therefore would minimize the effect of temperature on measurements. Measurements of R and X_c were taken according to the procedures found in Cox and Hartman (2005).

Temperature

The effect of temperature on R and X_c measurements was examined by taking repeated measurements on individual freshly killed fish over a range of temperatures (~0° to 12.5°C). The length of the experiment was <3 hours (the time it took the fish to freeze) and data in this study indicated that R or X_c do not change significantly within that short period and should nullify confounding effects of time on body condition after death. Regression analysis was used to test whether slopes and intercepts differed from 0 for regressions of R and X_c measurements on temperature. Adult pink salmon (n=4, mean fork length~550 mm) and juvenile (n=1, fork length~100 mm) Chinook salmon were killed and connected to a BIA Quantum-II Desktop by using standard needle electrodes and orientations as described by Cox and Hartman (2005). The Quantum-II was set to record impedance every 5 minutes for 12 hours. An ibutton thermometer (Maxim Integrated Products Inc., Sunnyvale, CA) was placed 1 cm (for juvenile) or 3 cm (for adults) inside the dorsal musculature of the fish and was set to record temperatures every 5 minutes. The juvenile fish was brought from cold (0.5°C) to warm (8.0°C) and the remaining adults were brought from warm (ambient water temperature) to cold (freezing). One adult had a starting temperature of ~12.5°C and the remaining three had a starting temperature of ~8.0°C. The automated Quantum II and the ibutton thermometers were synchronized to start recording at the same time. Each transferred fish was placed on a 4-in stand in the empty freezer compartment of a standard refrigerator. After 12 h, the fish was removed from the freezer, and R and X_c measurements and temperature logs were downloaded onto a computer. The one juvenile fish was removed from an outside cold tank, killed, and placed on a standard laboratory bench at room temperature. Initial temperature for the juvenile fish was ~0.5°C. For regression analysis, only impedance measurements taken when the fish temperature was >0°C were used. Significance tests were performed on each fish to test for slopes=0 by using a standardized major axis (SMA) test. The Bartlett-corrected likelihood ratio test (L) was used to test for differences between slopes of regression lines.

Stomach fullness and electrode location on live fish

To determine if R and X_c measurements in fish are affected by stomach fullness and electrode location, R and X_c values were taken and compared from locations on whole-body lengths and half-body lengths and with both full and empty stomachs. Measurements were taken across the length of the whole body (A1) and half its length (D) (Fig. 1A). Half- body length refers to the electrode orientation; one set of electrodes was placed toward the head region and the second was placed around midpoint of the fish (see D in Fig. 1A). Whole-body length refers to the second orientation that followed methods in Cox and Hartman (2005), where one set of electrodes was placed towards the head region and the second set was placed towards the tail region (see A in Fig. 1A). A two factor analysis of variance (ANOVA) was used to simultaneously test for differences in half-body and whole-body R and X_c measurements for brook trout with full and empty stomachs. If significance was found, a Tukey multiple comparison test was used to identify like values of R and X_c. Brook trout (n=20, length range=110–130 mm) were randomly split into four groups: A) half-body length full-stomach; B) half-body length empty-stomach; C) whole-body length full-stomach; and D) whole-body length empty-stomach (i.e., five replicates for each of the four combinations). All sets of fish were starved for three days before the experiment to ensure that the stomach was empty. Within 2 hours of the start of the experiment, the full-stomach group was fed fly larvae (*Sarcophaga bullata*) (Grubco Inc., Hamilton, OH), to satiation while those with the empty-stomach designation remained unfed. Before R and X_c measurements were taken, fish

Table 1

List of all possible bioelectrical equations that could be correlated with specific fisheries parameters (TBW=total body water, TBP=total body protein, FFM=fat-free mass, TBA=total body ash, DW=dry weight, and TBF=total body fat) or overall condition of the fish. Fisheries parameters listed here and their correlated equations are the ones presented by the authors in this article. Resistance (R) and reactance (X_c) are measured in biological tissue and the values are then inserted into each equation. In some equations, the distance between electrodes (L_d) is needed.

Obtained	Name	Equation symbol	Electrical equation	Volume symbol	Electrical volume equation	Fisheries parameter
Measured	Resistance in series	R	R	R_{sv}	L_d^2/R	TBW, TBP, FFM
Measured	Reactance in series	X_c	X_c	X_c	L_d^2/X_c	—
Derived	Resistance in parallel	R_p	$R+(X_c^2/R)$	R_{pv}	L_d^2/R_p	TBA
Derived	Reactance in parallel	X_c	$X_c+(R^2/X_c)$	X_{cv}	L_d^2/X_c	DW, TBF
Derived	Capacitance (farad)	C_{pf}	$(1{\cdot}10^{-12})/(314000{\cdot}X_c)$	C_{pfv}	L_d^2/C_{pf}	—
Derived	Impedance series	Z_s	$\sqrt{(R^2+X_c^2)}$	Z_{sv}	L_d^2/Z_s	—
Derived	Impedance parallel	Z_p	$(X_c{\cdot}R)/\sqrt{(X_c^2+R^2)}$	Z_{pv}	$L_d^2 \cdot Z_p$	—
Derived	Phase angle	phase angle	Arctan/(X_c/R)	—	—	Condition

were anesthetized in a tricane methanesulfonate (MS-222) solution of 1 g/9 L water.

Sensitivity analysis

To evaluate how sensitive models were to errors, six significant and nonsignificant errors along with six errors in distance between electrodes were incorporated into predictive models of total body water, dry weight, and phase angle (Table 1). Equations used in models were derivatives of R, X_c, and combinations of these two values which can be representative of biological tissue. Significant and nonsignificant differences (e.g., errors) from the previous experiments were converted into a percent difference from controls and used in the sensitivity analysis. The brook trout data set used in this analysis were from Cox and Hartman (2005) and the trout ranged in size from 10 to 227 g. For the predictive models used to determine total body water, dry weight, and total body fat estimates, equations including R in series (for total body fat), X_c in parallel (for dry weight and total body fat), and the electrical equation phase angle (for condition) (Table 1) were used. The significant R errors (in percentages) ranged from –58% (conductive board) to 10% (decreased needle depth) (Table 2). The significant X_c errors (in percentages) ranged from –45% (high temperature) to 47% (decreased needle depth) (Table 2). All length errors ranged from 0% to 5%. To consider how nonsignificant errors affect parameter estimates, a range of the nonsignificant R and X_c errors was inserted into each equation. The range of nonsignificant R errors (in percentages) that was inserted was –3% (full-stomach) to 3% (time=3 h). The nonsignificant X_c errors (in percentages) ranged from 1% (A1) to 9% (full-stomach) (Table 2).

For total body water, a single 6×6 matrix consisting of 36 combinations was formed from the six R and length errors. For dry weight estimates, two matrices were formed, one for R in parallel (used in the predictive model which had both R and X_c terms in it), and a second for the actual predictive model that estimated dry mass (Table 1). The data were plotted in three-dimensional matrix plots, with the x and y axes describing the range of values for either the length between detectors, R, X_c, or R in parallel, and with the z axis depicting the difference (in percentage) between predicted estimates with and without errors. In phase angle models, length between detectors is not a variable, and therefore R and X_c values were the only variables modeled. During analysis with significant errors added, phase angle values seemed to offset one another. To clarify this relationship, range of error values of –10% to 10% were added to both the R and X_c values. Three-dimensional matrices were plotted with the x and y axes representing R and X_c values and with the errors and the z axis depicting the difference between phase angle estimates with and without errors.

Results

Anatomical location of the electrode needle

The insertion of electrode needles in different locations within the fish resulted in different R and X_c mean values (Fig. 1A). Specifically, mean R and X_c values at locations C and D were significantly different from A for both R (LME $t_{16,\ 25}>8$, $P<0.001$), and X_c (LME $t_{16,\ 25}>3$, $P<0.001$). The difference in mean R values between location A (mean=306.62 Ω) and location C was –84.82 Ω (–28%), and D was –146.44 Ω (–47%). The difference in X_c means between location A (mean=75.44 Ω) and location C was –26.64 Ω (–35%), and between location A and D the difference was –13.80 Ω (–18%). There was not enough evidence to indicate that locations A1 and B were significantly different from A for either R (LME $t_{16,\ 25}<2$, $P>0.12$)

Table 2

Resistance (R) and reactance (X_c) mean values, significance levels, and percent difference for experiments to determine effects of needle location, covariates, different users, time needed for measurements, and stomach fullness on R and X_c measures. Each category has adjustments that may be a source of error when compared to a standard protocol (control) found in Cox and Hartman (2005).

		Mean		Significance		% Difference	
Category	Error source	R (Ω)	X_c (Ω)	R (Ω)	X_c (Ω)	R	X_c
Needle location	A (control)	306.62	75.44	—	—	—	—
	A1	300.80	73.12	0.58	0.54	2	1
	B	301.12	69.44	0.60	0.13	2	2
	C	221.80	48.80	<0.01	<0.01	–28	–35
	D	160.18	61.64	<0.01	<0.01	–47	–18
Covariates	Control	261.48	70.34	—	—	—	—
	Switched wires	262.38	71.02	0.87	0.81	<1	<1
	Salt	226.04	64.24	<0.01	<0.01	–14	–9
	Conductive board	108.96	56.30	<0.01	<0.01	–58	–20
	Needle size	236.38	64.04	<0.01	<0.01	–10	–9
	Needle depth	288.24	103.62	<0.01	<0.01	10	47
Different users	Control	915.35	155.73	—	—	—	—
	1	969.00	156.33	0.09	0.93	6	<1
	2	929.03	173.52	0.66	0.01	1	11
	3	857.13	142.20	0.07	0.04	–6	–8
	4	795.27	140.62	<0.01	0.02	–13	–10
Time (h)	0	896.17	166.77	—	—	—	—
	3	924.45	173.92	0.34	0.38	3	4
	6	900.85	174.62	0.87	0.34	<1	5
	9	909.87	178.03	0.64	0.17	2	7
	12	919.90	206.20	0.42	<0.01	3	24
Stomach fullness	Half-empty	321.00	89.00	0.95	0.99	–3	1
	Half-full	311.60	89.60				
	Completely empty	830.40	204.60	0.49	0.14	3	9
	Completely full	805.20	185.20				

or X_c (LME $t_{16,\ 25}<1$, $P>0.55$) (Fig. 1B). Although differences were not statistically significant, differences in mean R values between location A (mean=306.62 Ω) and locations A1 and B were –5.82 Ω (–2%) and –5.50 Ω (2%), respectively. Similarly, nonsignificant differences in X_c means between location A (mean=75.44 Ω) and locations A1 and B were –2.32 Ω (–1%) and –6.00 Ω (–2%), respectively. The anatomical locations of C and D differed the most from A, whereas locations A1 and B had the greatest similarity (Fig. 1A). Location C represented the entire length of the ventral region and D represented the forward half of the dorsal region of the fish. The location of A1 represented the same area of the fish as in A, except there was a second puncture, and location B represented an area slightly below A, but was still within the dorsal musculature (Fig. 1A).

Procedure deviations

Some procedural deviations from those outlined in Cox and Hartman (2005) significantly affected R and X_c measures. Specifically, changes in needle depth and size, and placing the fish on a conductive surface or on salt water caused significant changes in R and X_c, (LME $t_{20,30}>3$, $P<0.001$) (Table 2, Fig. 2). Ranked differences in R means and percentages from highest to lowest between the control and deviations were as follows: 1) –152.52 Ω, –58% for fish placed on a conductive board; 2) –35.44 Ω, –14% for fish placed on salt water; 3) 26.76 Ω, 10% for shallow needle depth; and 4) –25.10 Ω, –10% for the larger needle size (Table 2, Fig. 2). Ranked differences in X_c means from highest to lowest and percent differences between the control and assorted covariates were as follows: 1) 33.28 Ω, 47% for shallow needle depth; 2) –14.04 Ω, –20% for fish placed on a conductive board; 3) –6.30 Ω, –9% for the larger needle size; and 4) –6.10 Ω, –9% for fish placed on salt water (Fig. 2). Differences were not significant between the control means of R and X_c and switched wires for either R (mean R=262.38Ω, LME $t_{20,30}<0.3$, $P>0.80$), or X_c (mean X_c=71.02 Ω, LME $t_{20,30}<0.5$, $P>0.70$) (Fig. 2).

User experience

Untrained users produced different and more variable R and X_c measurements than the experienced user. Pairwise tests indicated that one untrained user obtained a significantly different mean for R (LME $t_{20,30}>3$, $P<0.009$) than the trained user (mean=915.35 Ω) with means differing by –120.08 Ω (–13%) (Fig. 3). Although differences were not significant, two of the untrained users had mean differences greater than 5% from the control. Significance was not found because of the high variance obtained from untrained users (mean deviation=46.75) and when compared to the trained user, standard deviations from untrained users were 4.6 times larger. Reactance values were significantly different for the trained user compared to those for the three untrained users (LME $t_{20,30}>2$, $P<0.04$) with differences ranging from –15.12 to 17.78 Ω (–10% to 11%). Variability of X_c standard deviations was greater (1.3×) in three of the untrained users when compared to variability in the control, but was not as great as the R variability (1.3× vs. 4.6×) (Table 2, Fig. 3).

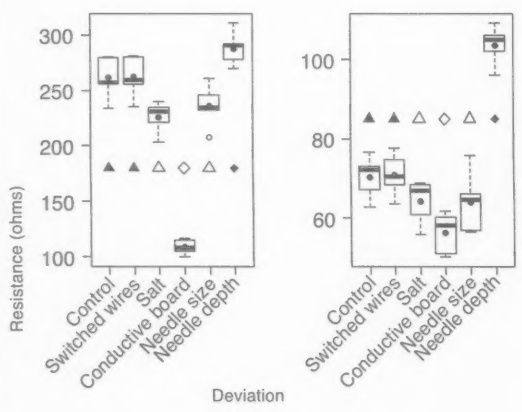

Figure 2

Boxplots of repeated resistance and reactance measurements taken from five pink salmon (*Oncorhynchus gorbuscha*) (control) and when an additional variable was added to the procedure (deviation). Specific deviations were 1) switched wires: the signal and detector leads were switched; 2) salt: two cups of seawater (31 practical salinity units) were poured under the fish; 3) conductive board: the fish was placed on a stainless steel conductive board; 4) needle size: the 28 gauge needles were replaced with larger 14 gauge hypodermic needles; and 5) needle depth: BIA electrode needles were placed in the fish in the same orientation as that used in the control, except needles were inserted to a depth of 1 mm. Open circles (○) represent outliers determined by a Grubbs test. Closed circles (●) represent mean values. Different symbols indicate differences determined by the statistical tests applied.

Time

The time period between death and BIA measurements did not affect R or X_c measures on iced fish from 0 to 72 h and from 0 to 9 h, respectively (Fig. 4, A and B). In this study, R differences between 0 and 72 h were not significant, LME ($t_{55,66}<2$, $P>0.16$) (Table 2, Fig. 4A). Although during the first 72 h, significant differences were not detected, non-\significant differences in mean R between 0 h (mean R=896.16 Ω) and subsequent times (3–60 h) ranged from to 28.28 Ω (3%) at 3 h to –41.48 Ω (–5%) at 60 h (Fig. 4A). The mean deviation of all grouped R values was 47.81. Mean values of X_c were not significantly different between 0 and 9 h (LME $t_{55,66}<2$, $P>0.17$) (Table 2, Fig. 4B). Although differences were not detected, nonsignificant differences in X_c means between 0 h and subsequent times (3, 6, and 9 h) were 7.15 Ω (4%), 7.85 Ω (5%), and 11.26 Ω (7%), respectively. Starting at 12 h, mean values of X_c were significantly different from 0 h LME ($t_{55,66}>4$, $P>0.001$) and increased from 166.76 Ω (mean at 0 h) to 206.19 Ω (24%) (mean at 12 h). The mean deviation for all grouped X_c values was 12.81.

Temperature

Temperature affected R and X_c measurements. As temperature increased, R and X_c decreased and slopes were not equal to zero (Fig. 5, A and B). Individual regressions of X_c and R with temperature were significant and all individual regressions had $r^2>0.92$. Individual slopes from each of the five R regressions were negative (–12.19, –11.64, –11.61, –10.95, and –12.01) and the mean slope was –11.65 (Fig. 5A). In the R regressions, there was no evidence of differences between slopes (L=3.82, P=0.43). In the X_c regressions, significant differences were found between slopes (L=93.65, $P<0.05$) (Fig. 5B). Slopes from the each of the five X_c regressions were negative (–4.86, –2.77, –2.87, –2.53, and –1.59). In X_c regressions, the maximum and minimum slopes were possible outliers and represented the only juvenile fish (closed circle symbol in Fig. 5B, slope=–4.86) whose temperature went in the opposite direction to that of the rest of the fish (i.e., cold to warm rather than warm to cold) and an adult fish (circle symbol in Fig. 5B, slope=–1.59) with an initial temperature 3°C higher than the others. When these two fish were removed from the regression analysis, the three remaining X_c slopes were not found to be different from each other (L=3.97 and P=0.14) (Table 2, Fig. 5B).

Stomach fullness

Stomach fullness did not affect R or X_c measures in either half- or whole-body measures (Fig. 6, A and B). Differences in R measures were not significant between fish with full or empty stomachs for half-body measurements (Tukey HSD, P=0.95) or full-body measurements (Tukey HSD, P=0.49) (Fig. 6A). Mean

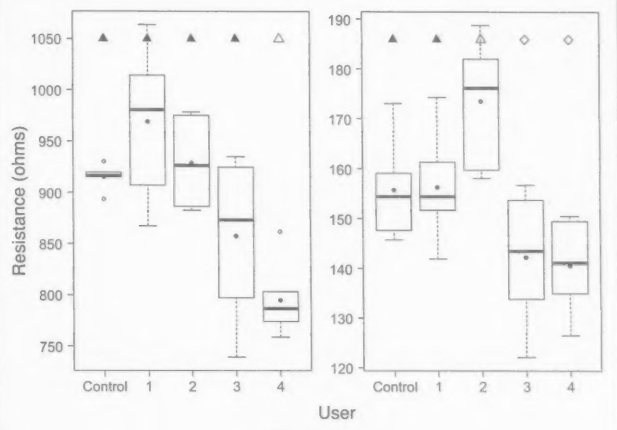

Figure 3

Boxplots of resistance and reactance measurements from five different people in a comparison of a trained user (control) with users without any training (1–4). Five coho salmon (*Oncorhynchus kisutch*) were measured by each person. Open circles (○) represent outliers determined by a Grubbs test. Closed circles (●) represent mean values. Different symbols indicate differences as determined by the statistical tests applied.

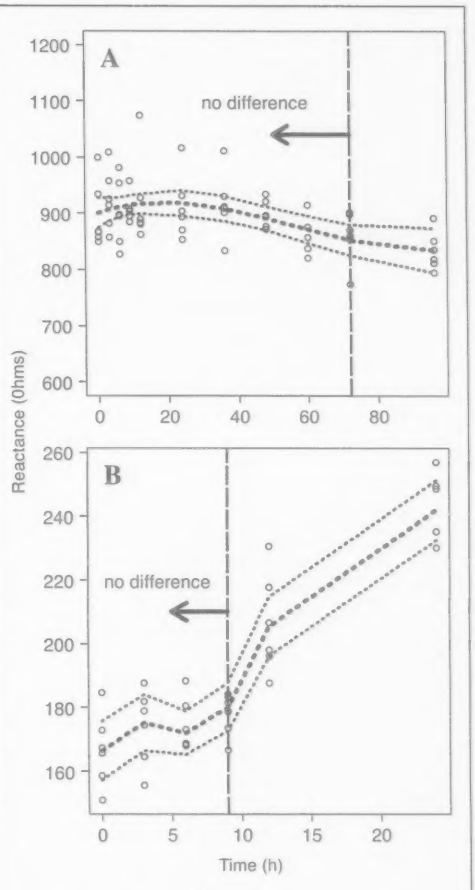

Figure 4

Resistance (**A**) and reactance (**B**) measurements taken over time on six groups of six coho salmon (*Oncorhynchus kisutch*) (n=36) that were killed and placed on ice. Open circles (○) represent outliers determined by a Grubbs test. The heavy dashed line indicates mean values and the light dashed line indicates 95% confidence intervals. The vertical dashed line and the arrow from it represent the times in which there was no difference in resistance or reactance measurements.

values of R for combinations of fish with full or empty stomachs with both half- and full-body measurements were 321, 312, 830, and 805 Ω, respectively (Fig. 6A). Although there was not a significant difference between mean values of R, nonsignificant differences in R means between full and empty stomachs for both half- and full-body measurements were –9.4 Ω (–3%) and –25.2 Ω (–3%) (Table 2). Mean X_c values were not significantly different between fish with full and empty stomachs for mid-body measurements (Tukey HSD, P=0.99) or full-body measurements (Tukey HSD, P=0.14) (Table 2, Fig. 6B). Mean values for R for fish with full or empty stomachs for both half-, and full-body measurements were 89, 89, 204, and 185 Ω, respectively (Table 2, Fig. 6B). Although there was not a significant difference between mean values of X_c, nonsignificant differences in means between fish with full or empty stomachs for both half- and full-body measurements were 0.6 Ω (<1%) and –19.4 Ω (9%). Variation of the estimations was also greater in the half-body measures in both R and X_c measures (Fig. 6, A and B).

Sensitivity analysis

Predictive models for estimating total body water were highly inaccurate when significant errors were inserted into the models and considerably more accurate when nonsignificant errors were inserted into the models (Fig. 7, A and B). Inserted significant errors (–58% to 10%) were inversely correlated with parameter estimation errors. The maximum significant negative error (–58%, conductive board) resulted in an overestimation >120% and a 10% error (decreased needle depth) resulted in an underestimation >–10% (Fig. 7A). The addition of length errors (0% to 5%) produced results that were positively correlated with parameter estimation errors and compounded the overall parameter estimation error (Fig. 7A). Inserted nonsignificant errors (–3% to 3%) were also inversely correlated to parameter estimates (Fig. 7B). The maximum nonsignificant negative error (–3%, full-stomach) resulted in an underestimation of 2.7%, and the maximum nonsignificant positive error (3%, R at 3 h) resulted in an overestimation of 2.6% (Fig. 7B). Length error alone caused overestimations to range from

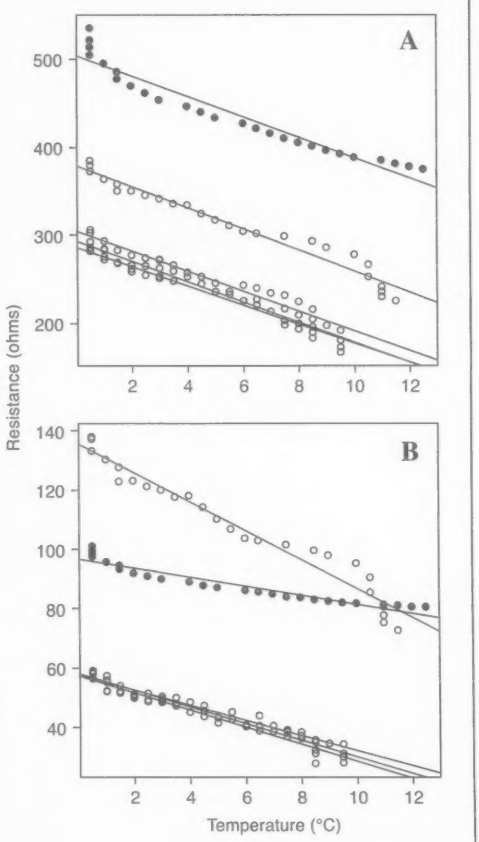

Figure 5

Influence of temperature on repeated measurements of resistance (**A**) and reactance (**B**) on dead Chinook (*Oncorhynchus tshawytscha*) (n=2) and coho salmon (*O. kisutch*) (n=3). All fish except the juvenile fish were measured from warm to cold temperatures. Solid circle=juvenile fish that was measured from cold to warm, and open circle=adult salmon that were measured from warm to cold.

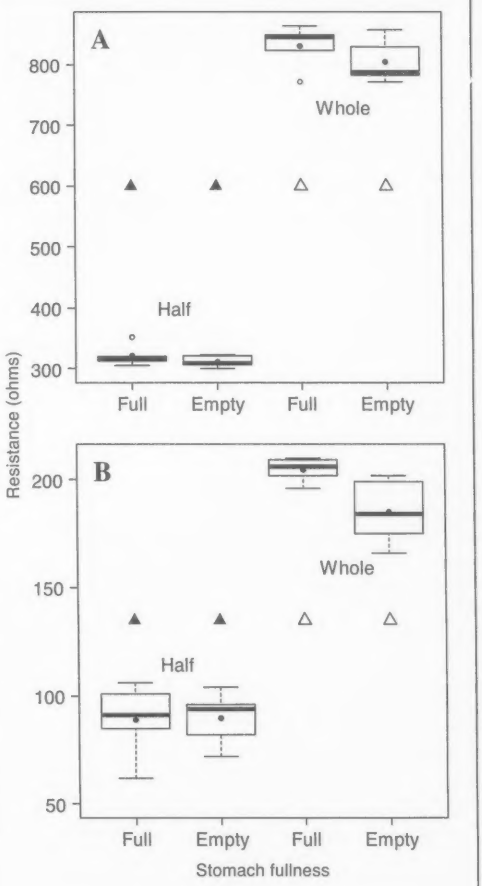

Figure 6

Boxplots describing resistance (**A**) and reactance (**B**) measurements in four groups of live brook trout (*Salvelinus fontinalis*) for different electrode locations and stomach fullness (n=5 per group), where full=full stomach, empty=empty stomach. "Whole" refers to a whole-body length (the entire length of the fish as described in Cox and Hartman [2005]). "Half "refers to a half-body length (one set of electrodes was placed towards the head region and the second being placed around mid-point [under the dorsal fin]). Open circles (○) represent outliers determined by a Grubbs test. Closed circles (●) represent mean values. Other symbols indicate differences as determined by the applied statistical tests.

0% to 9%. Compounding both maximum R (–3%) and length (5%) errors resulted in an overestimation >12%.

Both significant and nonsignificant errors inserted into the derived electrical volume equation X_c in parallel caused inaccuracies in subsequent parameter estimations of dry mass (Fig. 8, A and B). The insertion of significant errors impacted parameter estimations more substantially than nonsignificant ones. The addition of significant R errors (–58% to 10%) and X_c errors (–35% to 47%) into X_c in parallel (nonvolumetric) resulted in errors ranging from –58% to 173%. The subsequent addition of this range of errors into predictive models of DW caused estimations to be inaccurate by –45% to 349%, and length errors compounded the error (Fig. 8A). The addition of nonsignificant R errors (–3% to 3%) and X_c errors (0% to 9%) into X_c in parallel (nonvolumetric) resulted in X_c in parallel errors ranging from –11% to 4%. The subsequent addition of these errors plus the length errors (0% to 5%) into the volumetric equation to predict dry weight (DW) resulted in parameter estimations of DW that were inaccurate by

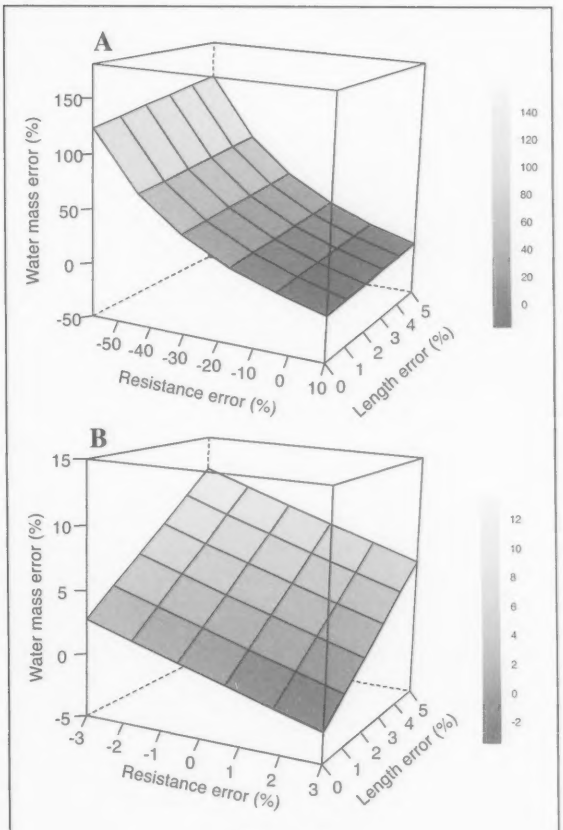

Figure 7

Comparisons of estimates of water mass parameters with resistance errors ranging from –58% to 10% (**A**) and with resistance errors ranging from –3% to 3% (**B**). The data were plotted in three-dimensional matrix plots with the x and y axes describing the range of values for either the length between detectors, R, X_c, or R in parallel, and with the z axis depicting the difference (as a percentage) between predicted estimates, with and without errors.

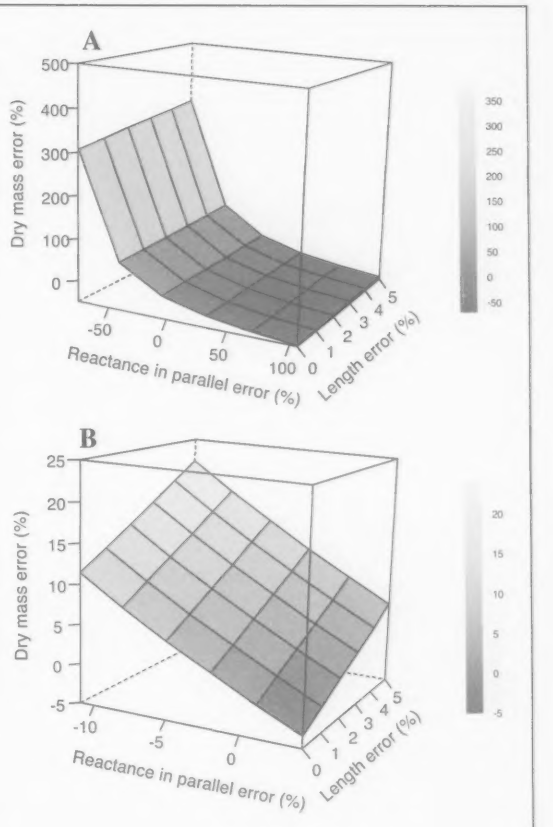

Figure 8

Comparisons of estimates of dry mass parameters with reactance in parallel $[X_c+(R^2/X_c)]$ errors ranging from –58% to 173% (**A**) and –11% to 4% (**B**), and length errors in both ranging from 0% to 5%. The data were plotted in three-dimensional matrix plots with the x and y axes describing the range of values for reactance in parallel and the length between detectors, and z axis depicts the difference (as a percentage) between predicted estimates of dry mass, with and without errors.

0% to 21% (Fig. 8B). If length errors were not included, parameter estimations of DW were inaccurate by –3% to 11%. The addition of length errors compounded the parameter estimation errors.

Individual errors of R and X_c errors affected phase angle measures, but combined errors tended to offset one another (Fig. 9, A and B). The introduction of significant errors of R and X_c (–58% to 10%, and –37% to 45%, respectively) caused phase angle measurements to vary from –60% to 129%. When inserted errors were in the same direction (i.e., both errors are either negative or non-negative numbers), they offset one another and resulting phase angle errors were closer to 0% (Fig. 9A). When inserted errors were opposite of one another (i.e., when one error was a positive number and the other negative), phase angle errors increased and decreased to their maximum values and did not offset one another, but rather increased errors. Identical errors for both R and X_c showed symmetry in that phase angle errors equaled 0% when inserted R and X_c errors were the same (Fig. 9B). Reactance errors by themselves were inversely correlated with phase angle errors and R errors were positively correlated with phase angle values.

Discussion

The ability to accurately estimate physiological parameters including proximate composition, condition, and energy content with BIA will permit increased preci-

sion in energy flow and proximate composition studies on spatial and temporal scales that were previously impractical. At the individual level, BIA will permit repeated measures on the same individual during the course of investigation, yielding better tracking of energetics components and improved precision in bioenergetic models. At the population level, BIA will permit assessment of the condition of cohorts over time and permit detailed comparisons across cohorts, and temporal and spatial scales. At the community level, BIA will permit the evaluation of growth and energy-flow dynamics across species that may elucidate community dynamics that were previously unknown, or permit correlation of condition with outbreaks of disease. This approach also has potential for the nonlethal study of threatened or endangered species by the use of models developed for closely related species. In order for the application of BIA to reach its potential, sources of error that affect R and X_c measurements need to be continually identified and analyzed.

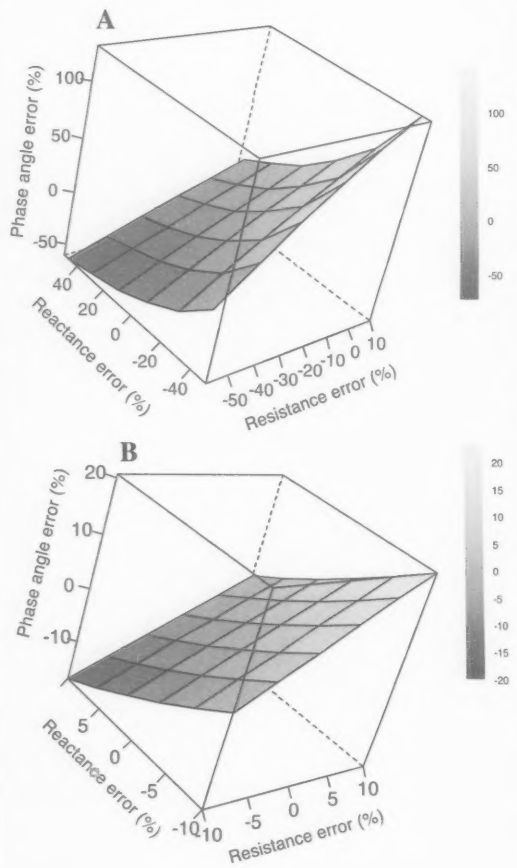

Figure 9

Comparisons of large (**A**) and small (**B**) resistance (R) and reactance (X_c) errors affecting phase angle [arctan/(X_c/R)]. Errors in resistance and reactance values are greater in A than in B. The data were plotted in three-dimensional matrix plots with the x and y axes describing the range of values for reactance and resistance, and the z axis depicting the difference (as a percentage) between phase angle, with and without errors.

Sources of error include different electrode needle locations, procedure, user experience, time periods between death and impedance measurements, and temperature. Measuring impedance in the same anatomical location of the fish is critical to obtaining accurate and reproducible impedance measurements. When electrodes are not placed in the same anatomical location of fish, incomparable and inaccurate results are obtained, but which location is best is still a question. Variability in R and X_c measurements increased with the distance of electrode placement from the control. Impedance values can change for two reasons: 1) the distance between electrodes is directly proportional to the electrical volume (e.g., R in Table 1) and consequently, halving the distance between electrodes leads to reduced values of R and X_c; and 2) when electrodes are placed in different locations on the fish, different tissue types are represented, and moving electrodes from the dorsal side of the fish to the ventral side will not only change the distance between electrodes, but it will also reflect different tissue types. The dorsal side is mainly muscle and the ventral consists of peritoneal tissue and organs. Changing the distance will change the R and X_c values, and changing the electrode location will change the tissue types that are being measured. Sensitivity to tissue types is consistent with Geddes and Baker (1967) who reported different impedance values with different tissue types (i.e., skeletal muscle, liver, and kidney tissues). Therefore, electrodes can be re-inserted into the same holes or moved slightly dorsally or ventrally as long as the same tissue type is measured and the distance stays relatively similar. Impedance measurements are dependent on the anatomical location of the needle electrodes.

Sources of error caused by procedural deviation can also be avoided by standardizing protocols. Measures of R and X_c are affected by covariates such as needle depth, needle size, and conductive surfaces where the measurements are taken. Minimizing these errors can be accomplished by inserting needles to a uniform depth, blot drying the fish before measurements are taken, taking measurements on a nonconductive board, and by using the same gauge of needle electrodes. If procedures are not standardized, R and X_c change as electrical currents are altered by procedural changes. For example, changing the needle depth or size will change the needle surface area that is in contact with the tissue. Because smaller surface areas present more resistance to the electrical current than larger ones, R and X_c values will change. Similarly, taking impedance measurements on a conductive board offers the electrical current a less resistant route. Ohm's law states that when electrical currents are offered a less

resistant route, they tend to take them, and offering the current a path through seawater or a conductive board would allow the current to take a pathway that is the least resistant and that would possibly not even include the fish. This would result in a drop in R and X_c values (which was seen in this study) that may not be representative of values for a fish. A drop in impedance values was also seen in a study by Mirtaher et al. (2005), when an electrical current was measured through increasing concentrations of NaCl. Because impedance values are used to measure the composition and condition of fish tissue, the majority of the electrical pathway needs to be within the fish. Switching the signal and detecting wire leads will not have any effect on R or X_c values, as long as the impedance analyzer unit (e.g., RJL Systems Quantum II) is internally modified to correct for this switch.

Dead fish can be held on ice for up to 9 h without compromising R or X_c. If measures of R are the only measured impedance value being used, fish may be iced up to 72 h before measurments start to change, but if R and X_c are to be used, fish need to be iced and measured within 9 h of capture. Icing fish delays postmortem rigor mortis and subsequent tissue breakdown. These processes first affect X_c, then R. This sequence is due to X_c reflecting cell membrane integrity, whereas R reflects more extracellular material. After 12 h, X_c starts to increase due to rigor mortis (muscle contraction), and upon resolution, cell membrane integrity is compromised until the cell eventually ruptures. The rupturing of cells in turn releases intracellular fluid into extracellular spaces causing decreases in R. Increasing X_c (due to muscle contractions) followed by decreasing R (due to edema) was observed in two studies. The first, a study of human health showed increases in X_c due to muscle contractions (Kashuri et al., 2007), and a second fish study showed postmortem haddock (*Melanogrammus aeglefinus*) R levels decreasing because of changes in edema (Martinsen et al., 2000). The use of ice to slow these postmortem processes is not a new technique (Orr, 1920), but it is still an important technique that can be applied to extend the time of measuring impedance in killed or dead fish,

Personnel should be trained in taking impedance measurements to increase accuracy and decrease variability of R and X_c measurements. How much training is needed cannot be answered with these data. The large variability in R and X_c values measured by untrained personnel is due to their unfamiliarity with procedures that would increase accuracy and decrease variability. Without the training of personnel, inserted electrode needles may shift during measurements, causing changes in the contact area between tissue and the needles. As the contact pressure of the needle changes, current flow is also altered and results in changes in R and X_c. Also, untrained users take more time to take measurements than do trained users and the additional time allows excess fluid buildup around the needle electrode sites that can affect current flows. Because both fluid buildup and pressure changes can cause fluctuations in impedance values, a standard procedure should be developed to minimize errors. Needles should be placed perpendicular to the fish, inserted to the appropriate depth, and held stable during measurements. Body and hand position of the user must allow the user to view the needles and measurements should be taken in a timely manner (<30 s). Likewise, procedural training can increase the proficiency in obtaining impedance measurements by decreasing variability of hand movements and increasing accuracy of the position of needle insertion. This was observed by Liddell et al. (2002) who demonstrated that formalized training for needle control and position for medical students can have lasting efficiencies on procedures involving needles. Increasing training and experience before taking BIA measures will decrease variability and increase accuracy of impedance measurements.

Temperature affects impedance measurements, but can be standardized by correcting to a set temperature. The inverse relationship between temperature and impedance is widely described in literature concerning conductive metals (Grimnes and Martinsen, 2007). Because the relationship of metals and impedance is known to be linear over a broad range of temperatures (0–1200 K), a similar relationship should exist between biological tissue and temperature. This relationship would also be more constant in cold-blooded species where temperature changes are systemic and not prone to localized temperature changes (e.g., at extremities or skin) as with warm-blooded organisms (Caton et al., 1988). In another human study, Gudivaka et al. (1996) provided a correction factor for changing skin temperatures to normalize impedance measurements by using the inverse linear relationships between impedance measurements and temperature. Because a linear relationship is shown for R in our study, it is possible to determine an empirical approximation for R at a standardized temperature which is shown to be

$$R_m - R_0 = \alpha(T_m - T_0), \quad (1)$$

where R_m = resistance measured at T_m;
R_0 = calculated resistance at T_0;
α = −6.02;
T_m = measured temperature when measured resistance was taken; and
T_0 = 0°C.

The authors would like to point out that this equation is based on five data points and the usage here is intended to show the possibility of correcting for temperature. The set point of 0°C was chosen because fish could be put either on ice or adjusted down to 0°C by using Equation 1. By icing or standardizing measurements to a set point, accuracy will increase in impedance measurements. Reactance measurements could also be standardized to a 0°C temperature by using an empirical approximation similar to R. In the X_c data presented here (with the aforementioned outliers removed), slopes between the remaining three fish are not different and

an empirical approximation for X_c at a standardized temperature (0°C) is identical to that in Equation 1, except that α=–2.8.

Stomach fullness had no effect on response measurements within the half- or whole-body groups. The stomach and alimentary canal are encased by less conductive layers of muscle than the surrounding organs located in the peritoneal cavity (Pethig, 1979). Much like an insulated wire, these less conductive muscle layers will insulate the stomach contents even if the stomach contents are more conductive than the surrounding tissue. The insulation provided by the muscle layer reduces the chance that the current pathway will include stomach contents. Decreased R values (Ω/cm) are seen in various animals in the peritoneal spleen, liver, and kidney, and relatively higher R values in nearby muscle tissue (Pethig, 1979). These insulating muscles, coupled with less resistant alternative pathways (i.e., organs), indicate that stomach fullness does not need to be accounted for in BIA measurements.

Sensitivity analyses show that significant deviations from the procedures found in Cox and Hartman (2005) can lead to unacceptable errors in predictive estimates of R and X_c, but nonsignificant deviations are more acceptable. The average of all significant errors in this study is 26% and would cause parameter estimates to be off by about 25% to 30%, which is too large for most biological studies. The nonsignificant error averages of <3% will cause parameter estimation errors to be around 2% to 4% (or about a 1:1 ratio), which may be acceptable in some studies. It should be noted that if several nonsignificant errors are encountered at the same time, they can be cumulative and result in an estimation error that is significant.

In all electrical volume equations, length between detectors (L_d) is a squared term in the numerator, making predictive estimates extremely sensitive to changes in L_d while also diluting the error effects on the denominator. Likewise, in parallel equations, the term R is either in the numerator (as in X_c in parallel, see Table 1) or in the denominator (as in R in parallel, see Table 1) and is typically a much larger number than X_c, and therefore increases the influence of errors on parallel equations, especially when R is in the numerator as in reactance in parallel (X_c). When the subsequent volume equations are used, predictive estimates are more sensitive to L_d changes. The nonsignificant errors seen and described in this study are still deviations from the standard protocol found in Cox and Hartman (2005); therefore with a standard protocol, these "nonsignificant" errors will not be reflected and any errors that are, would be from other factors not measured here (e.g., anatomy, thickness of skin and scales, condition, or biochemical composition).

In summary, sources of error have been identified and found to significantly affect parameter estimates, but small errors that are not significant may be acceptable. In particular, electrode locations with respect to anatomy can significantly affect parameter estimates, and if electrodes needles are placed in the same anatomical location on each fish, impedance measurements will reflect the same relative volumetric areas within and between fish samples. Measurements need to be taken on a nonconductive surface that is clear of salt water, on blot-dried fish, and standardized with specific needle gauges and depths. New users need to be trained and taught stable body and hand positions and positions that allow a view of the needle to ensure accurate and precise measurements. Because temperature affects R and X_c measurements, internal temperature needs to be measured to allow adjustments of R and X_c values to 0°C or fish need to be stored on ice. Time is critical in taking impedance measurements, but icing fish can add 9 h between fish death and the time of BIA measurements. Stomach fullness of fish does not affect half- or whole-body impedance measurements, and therefore does not have to be accounted for. Sensitivity analysis in our study showed that significant deviations from the procedures of Cox and Hartman (2005) can lead to unacceptable errors in predictive estimates of BIA measurements but nonsignificant deviations are more acceptable. Although adherence to these protocols can provide consistent measurements of impedance, comparability between researchers will depend on the development of training procedures, improved understanding of temperature effects, development of improved electrodes, continuous calibration with actual laboratory measurements, and unified standard protocols. It should also be noted that multifrequency impedance analyzers are available and currents at different frequencies could possibly have different measurements than those with a single frequency. The identification of sources of error illustrated here and subsequent adherence to a standardized protocol will offset the sources of error that may be present in bioelectrical impedance research and allow the technology to advance.

Acknowledgments

We acknowledge the financial support of the Alaska Fisheries Science Center, National Oceanic Atmospheric Administration, West Virginia University, U.S. Department of Agriculture, U.S. Forest Service, MeadWestvaco Corporation, West Virginia Department of Wildlife, United States Forest Service, University of Alaska, Fairbanks, and the Sitka Sound Science Center, Sitka, Alaska. We thank the many researchers and volunteers that helped collect data.

Literature cited

Blanca, L., P. Miquel, M. Soledad, P. Marina, A. P. Lucy, and H. A. Ildefonso.
2009. Sources of error and its control in studies on the diagnostic accuracy of "-omics" technologies. Proteomics Clin. Appl. 3:173–184.

Caton, J. R., P. A. Mole, W. C. Adams, and D. S. Heustis.
1988. Body composition analysis by bioelectrical imped-

ance: effect of skin temperature. Med. Sci. Sports Exerc. 20:489–491.

Cox, M. K., and K. J. Hartman.
2005. Non-lethal estimation of proximate composition in fish. Can. J. Fish. Aquat. Sci. 62:269–275.

Cox, M. K., and R. A. Heintz.
2009. Electrical phase angle as a new method to measure fish condition. Fish. Bull. 107:477–487.

Curtis, J. M. R.
2006. Visible implant elastomer color determination, tag visibility, and tag loss: potential sources of error for mark and recapture studies. N. Am. J. Fish. Manag. 26:327–337.

Duncan, M., S. R. Craig, A. N. Lunger, D. D. Kuhn, G. Salze, and E. McLean.
2007. Bioimpedance assessment of body composition in cobia *Rachycentron canadum* (L. 1766). Aquaculture 271:432–438.

Geddes, L. A., and L. E. Baker.
1967. The specific resistance fo biological material—a compendium of data for the biomedical engineer and physiologist. Med. Biol. Eng. Comput. 5:271–293.

Grimnes, S., and O. G. Martinsen.
2007. Sources of error in tetrapolar impedance measurements on biomaterials and other ionic conductors. J. Appl. Phys. 40:9–14.

Gudivaka, R., D. Schoeller, and R. F. Kushner.
1996. Effect of skin temperature on multifrequency bioelectrical impedance analysis. J. Appl. Physiol. 81:838–845.

Kashuri, H., R. Aaron, and C. A. Shiffman.
2007. Frequency dependence of forearm muscle impedance during isometric gripping contractions: 13th International conference on electrical bioimpedance and the 8th conference on electrical impedance tomography; Graz, Austria. Springer, Berlin Heidelberg. 17:651–654.

Keller, F. J., E. W. Gettys, and M. J. Skove.
1993. Physics: classical and modern, 2nd ed., 1216 p. McGraw-Hill, New York, NY.

Larson, G., R. Hoffman, B. Hargreaves, and R. Collier.
2007. Predicting Secchi disk depth from average beam attenuation in a deep, ultra-clear lake. Hydrobiologia. 574:141–148.

Liddell, M. J., S. K. Davidson, H. Taub, and L. E. Whitecross.
2002. Evaluation of procedural skills training in an undergraduate curriculum. Med. Educ. 36:1035–1041.

Lukaski, H. C.
1987. Methods for the assessment of human body composition: traditional and new. Am. J. Clin. Nutr. 46:537–556.

Martinsen, O. G., S. Grimnes, and P. Mirtaheri.
2000. Non-invasive measurements of post-mortem changes in dielectric properties of haddock muscle—a pilot study. J. Food Eng. 43:189–192.

Mirtaher, P., S. Grimnes, and O. G. Martinsen.
2005. Electrode polarization impedance in weak NaCl aqueous solultions. Trans. Bio. Eng. 52:2093–2099.

Orr, A.
1920. The retail fish market: some suggestions for equipping and conducting it. Trans. Am. Fish. Soc. 49:107–114.

Palmer, M. C.
2008. Calculation of distance traveled by fishing vessels using GPS positional data: A theoretical evaluation of the sources of error. Fish. Res. 89:57–64.

Pethig, R.
1979. Dielectric and electronic properties of biological materials, 1st ed., 390 p. John Wiley and Sons, New York.

Pinheiro, J. C., and D. M. Bates.
2000. Mixed-effects models in S and S-PLUS, 1st ed., 521 p. Springer Verlag, New York.

Pothoven, S. A., S. A. Ludsin, T. O. Hook, D. L. Fanslow, D. M. Mason, P. D. Collingsworth, and J. J. V. Tassell.
2008. Reliability of bioelectrical impedance analysis for estimating whole-fish energy density and percent lipids. Trans. Am. Fish. Soc. 137:1519–1529.

Rallison, L. R., R. F. Kushner, D. Penn, and D. A. Schoeller.
1993. Errors in estimating peritoneal fluid by bioelectrical impedance analysis and total body electrical conductivity. J. Am. Coll. Nutr. 12:66–72.

Ursula, G. K., I. Bosaeus, A. De Lorenzo, P. Deurenberg, M. Elia, J. M. Gomez, B. L. Heitmann, L. Kent-Smith, J.-C. Melchior, M. Pirlich, H. Scharfetter, A. M. W. J. Schols, and C. Pichard.
2004. Bioelectrical impedance analysis—part I: review of principles and methods. Clin. Nutr. 23:1226–1243.

Zar, J. H.
1996. Biostatistical analysis, 3rd ed., 662 p. Prentice Hall, Inc., Upper Saddle River, NJ.

An evaluation of the effects of blue crab (*Callinectes sapidus*) behavior on the efficacy of crab pots as a tool for estimating population abundance

S. Kersey Sturdivant (contact author)[1]
Kelton L. Clark[2]

Email address for contact author: kersey@vims.edu

[1] Virginia Institute of Marine Science
College of William & Mary
P.O. Box 1346
Gloucester Pt., Virginia 23062

[2] Morgan State University
Estuarine Research Center
10545 Mackall Road
St Leonard, Maryland 20685

Abstract—Crab traps have been used extensively in studies on the population dynamics of blue crabs to provide estimates of catch per unit of effort; however, these estimates have been determined without adequate consideration of escape rates. We examined the ability of the blue crab (*Callinectes sapidus*) to escape crab pots and the possibility that intraspecific crab interactions have an effect on catch rates. Approximately 85% of crabs that entered a pot escaped, and 83% of crabs escaped from the bait chamber (kitchen). Blue crabs exhibited few aggressive behavioral interactions in and around the crab pot and were documented to move freely in and out of the pot. Both the mean number and size of crabs caught were significantly smaller at deeper depths. Results from this study show that current estimates of catch per unit of effort may be biased given the high escape rate of blue crabs documented in this study. The results of this paper provide a mechanistic view of trap efficacy, and reveal crab behavior in and around commercial crab pots.

Manuscript submitted 15 December 2009.
Manuscript accepted 18 October 2010.
Fish. Bull. 109:48–55 (2011).

The views and opinions expressed or implied in this article are those of the author (or authors) and do not necessarily reflect the position of the National Marine Fisheries Service, NOAA.

Population dynamics of blue crabs (*Callinectes sapidus*) can be studied by using a variety of fishery dependent and independent methods, such as the use of crab pots (Abbe and Stagg, 1996), bottom trawl data, and commercial fisheries landing statistics (Lipcius and Van Engel, 1990). Commercial fisheries data sets provide extensive information on blue crab landings which are related to population dynamics (Lipcius and Van Engel, 1990), but pots and trawl information are also used because of the need for independent assessments of population dynamics. Pots are viewed as an important method for assessing blue crab abundance through estimates of catch per unit of effort (CPUE) (Abbe and Stagg, 1996) because CPUE is generally assumed to be proportional to total abundance (Harley et al., 2001). However, previous studies have indicated that CPUE may not accurately correlate with changes in abundance (Harley et al., 2001). Factors that have been shown to bias CPUE for crustaceans include soak-time (Miller, 1974; Smith and Jamieson, 1989a), freshness of bait (Smith and Jamieson, 1989b), temperature (Sharov et al., 2003), and pot design (Miller, 1974; Smith and Jamieson, 1989b). The usefulness of surveys for population assessment depends on accurate methods to identify and control for these biases.

Behavioral factors, such as intraspecific interactions, affect crustacean catch rates and can lead to biased CPUE estimates. Studies have shown that interactions among conspecifics negatively affect portunid crabs and American lobster (*Homarus americanus*) catch rates (Williams and Hill, 1982; Jury et al., 2001), and Miller (1974) showed that catch rates of Dungeness crab (*Cancer magister*) decreased with increasing pot density. Jury et al. (2001) observed with the use of underwater videotape recordings that the aggressive behavior of American lobsters played a vital role in overall American lobster catch rates. What is not clear is whether there is a consistent relationship between aggressive species and pot catch rates.

The blue crab is an economically and ecologically important species to Chesapeake Bay (Van Engel, 1958) and has well documented intraspecific (Jachowski, 1974; Clark et al., 2000) and interspecific (deRivera et al., 2005) agonistic behavior. It is possible that blue crab behavior in and around crab pots may have a significant role on pot catch rate. To address this notion, we developed techniques to observe crab behavior in and around a crab pot.

Since the 1950s underwater video monitoring has been used in marine science to observe the behavior of fish and invertebrates (Barnes, 1963;

Myrberg, 1973). Early underwater video recording techniques, which are still in use, include towed video sleds (Chapman, 1979), hand-held video cameras (Potts et al., 1987), and remotely operated vehicles (ROVs) (Spanier et al., 1994). Although *in situ* video recording is ideal, high turbidity (as in Chesapeake Bay) can prevent the use of this technique. In the absence of *in situ* video surveillance, mesocosm studies are very effective because the environment can be manipulated to allow for accurate observation in representative constructions of the natural setting.

By combining *in situ* experimentation with mesocosm observation, we attempted to assess whether blue crab behavior affected crab pot efficacy. The specific objectives of this study were 1) to determine whether intraspecific interactions affect catch and escape rates with respect to crab size and abundance; 2) to determine if catch or escape rates are influenced by abiotic factors such as depth or the submersion time of pots; and 3) to assess the effects of blue crab behavior on crab pot efficacy.

Materials and methods

Study site

The study took place during July and August of 2003 at the Smithsonian Environmental Research Center (SERC), in Edgewater, Maryland. Field experiments were conducted at Canning House Bay (CHB), a half-moon–shaped embayment of Chesapeake Bay in the Rhode River. CHB is characterized by sandy beaches intermingled with coarse woody debris, marsh plants, and ever-encroaching populations of common reed (*Phragmites* spp.). The Rhode River is a subestuary that connects to the mesohaline central Chesapeake Bay. Water temperatures in the Rhode River peaks in July, with an average of 27–28°C, and summer temperatures can exceed 30°C along the shore. Salinity varies seasonally in the river from 3 to 17 ppt. Mean tidal amplitude in the river is 0.3 m, and mean low tide level is 0.2 m above mean lower low water. Daily tidal action in the Rhode River is highly influenced by winds, and tidal fluxes greater than predicted can occur. Turbidity in the Rhode River is often high in summer, with Secchi depths <0.5 m (Everett and Ruiz, 1993).

Crab pots

We employed commercial crab pots used by waterman in Chesapeake Bay (Van Engel, 1962) to test crab-pot catch rates. The pots are square wire-mesh (3.8 cm) cubes 55.9×61.0×55.9 cm, with an upper and lower section. The lower section is called the kitchen or bait chamber, and the upper section is called the parlor or trap chamber. There is an entrance on each of the four sides of the kitchen, and a conical bait well is situated in the center. The kitchen and parlor are separated by a wire-mesh panel, raised in the middle to form an inverted V. There are two openings along the apex of the V that lead into the parlor. The parlor contains two circular escape holes (cull rings) on either side to provide an exit for sublegal-size crabs (smaller than 127 mm). Pots were attached to floats with a 2.5-m line for retrieval.

Field experiment

Field experiments were conducted to assess the effects of blue crab size and water depth on catch and escape rates. Before the pots were set, test crabs were placed to seed (placing crabs in pots before experimental run) the pots in an attempt to initiate behavioral interactions amongst crabs to determine if the presence and size of a crab in a pot affected catch rates. Three water depths were examined: shallow (1 m); medium (2 m); and deep (3 m); the maximum depth of the study site was 5 m. These depths were chosen on basis of previous work at this site by Ruiz et al. (1993) who showed a difference in the abundance and size of crabs with depth. The pots were placed on a muddy substrate free of vegetation or other structured habitat. Test crab sizes were classified as large, small, and control. Large crabs were defined as greater than 155 mm carapace width (CW), small crabs were 127–130 mm CW, and a control of no crabs was also used. The crab size of 127 mm CW was the minimum size for legal catches in Maryland during 2003, and is the minimum size of crabs that cannot fit through the escape ring on the pot. This limit was set because of our interest in blue crabs that are considered legal catch. There were three sampling areas within Canning House Bay, and three pots were placed in each area. Areas were evenly spaced within CHB, and each area contained a deep, medium, and shallow water depth (1-, 2-, and 3-m depths). The pots and depths were distributed in a full 3×3 factorial design. Test crabs used for this experiment were collected predominantly by trawling, and occasionally in pot catches, both of which were undertaken separately from the experiment. To reduce behavioral variance, test crabs had all appendages and were males in molt stage C, an intermolt stage when crabs are presumed to exhibit standard behavior.

During an experimental run, a single test crab was measured, numbered, and placed in the kitchen of each pot before initial deployment. Test crabs were held in deck tanks until needed, and were fed chopped pieces of partially frozen alewife (*Alosa pseudoharengus*) until 24 hours before being placed in the experiment. Pots deployed in the field experiment were also baited with chopped pieces of partially frozen alewife. The bait was chopped, frozen, and then placed in the bait wells of pots before deployment. Catch rates of pots can vary with fresh and frozen bait; however, owing to logistics, frozen bait was used for this experiment. However, because of the summer heat, the bait became partially unfrozen by the time the sampling area was reached and pots were deployed. Pots were placed at depths of 1, 2, and 3 meters in each area of CHB for 48 hours. A single experimental run was 48 h, divided into two 24-h periods. After the first 24 hours, pots were

checked, and the presence or absence and location of the original test crabs were noted. The size, sex, and molt stage of the additional captured crabs were recorded, and any unusual occurrences were documented. Captured crabs were numbered and placed back in their original locations (parlor or kitchen) in the pot. Pots were rebaited and set out for another 24-h period to assess escape rates from baited pots, to determine whether pots would reach some saturation point, and to establish the theoretical density when a pot cannot catch anymore crabs. After the second 24-h period, pots were retrieved, and similar information was recorded. It was noted whether crabs from the first 24-h period had escaped or were still present. Size, sex, molt stage, and location in the pot were recorded for newly captured crabs. After all information was documented, all crabs were released. This experiment was repeated four times, for a total of five trials. Both the size and number of crabs caught were analyzed with a 2-factor analysis of variance (ANOVA) with the factors of depth and test crab size. Additionally, Tukey's honestly significant difference test was used for multiple mean comparisons. All statistical tests were conducted with SAS® software (SAS, vers. 9.0.0, SAS Institute, Inc., Cary, NC).

Crab-trap video (CTV) system

The crab-trap video (CTV) was modeled after the lobster-trap video presented in Jury et al. (2001). It is a low cost tool for observing interactions between crabs in and around pots in a mesocosm. Although it was not used for *in situ* observations in our experiment CTV could be easily modified for *in situ* observations. CTV consists of a standard commercial crab pot matching the specifications described above with video camera equipment attached for observation. A low-light, black-and-white, Sony time-lapse video recorder, model EVT-820, was used to record images every minute for 24 hours. The camera was set 38 cm above the pot on a support system of four 93.9-cm long PVC pipes connected by four shorter PVC pipes 55.9 cm in length (Fig. 1). This configuration allowed the entire pot to be observed, as well as a few centimeters on each side of the pot. For nighttime recording, a red light, undetectable by crabs (A. Hines, personal commun.[1]), was affixed to one of the PVC legs and used to light the area. All images were recorded on Hi-8 tapes in an adjacent building connected to the mesocosm camera by cables. Connection cables were placed approximately 40 cm above the surface of the water surface in the mesocosm experiment. The system was capable of collecting data for at least 24 hours; therefore it continuously captured all crab interactions within the field of view for the experimental time-frame. The system also recorded crab approaches, entries into the kitchen and parlor, and escapes of crabs.

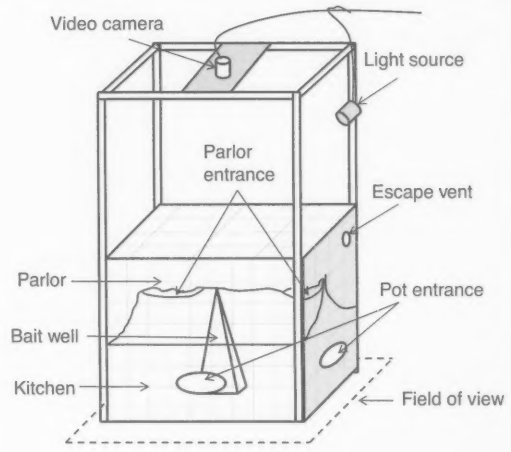

Figure 1

Diagram of the crab trap video (CTV) system. CTV is a time-lapse video recording system affixed to a standard commercial crab pot. The design allows the movements of crabs in and around the pot to be recorded during the day and night. Image not drawn to scale. Field of view=field of view from the camera lens.

Mesocosm experiment

A mesocosm experiment was conducted to determine the influence of crab behavior on pot catch. A large above-ground circular mesocosm (4.8 m×1.06 m, 18.6 m^3) set on preleveled ground was used for this experiment. A mesocosm was used because the high turbidity of the Rhode River made *in situ* observations impractical. Ambient water from the Rhode River was transferred into the mesocosm and filtered for two days to increase water clarity. Water was constantly filtered when experiments were not running, and filter bags were changed daily. During experimental runs, filters were turned off and removed from the mesocosm. Fine-grain sand was used to cover the bottom of the mesocosm in an attempt to mimic the muddy-sandy substrate of the Rhode River. Mummichogs (*Fundulus heteroclitus*) were placed inside the mesocosm to help control mosquito larvae populations and other insects but were removed before each testing to limit nonsubstantial variables. As with the field experiment, crabs were held in deck tanks and were fed chopped alewife until 24 hours before use in an experiment.

For each experiment, 16 male blue crabs (6 large [155 mm CW or greater], and 10 smaller [127–150 mm CW]) were used. Test crabs had all appendages, and only male crabs of molt stage C were used to reduce any behavioral variance. The number of crabs per unit of area

[1] Hines, Anson. 2003. Smithsonian Environmental Research Center, 647 Contees Wharf Road Edgewater, Maryland 21037.

was chosen to simulate high density conditions (Clark et al., 1999). Crabs were placed in the mesocosm an hour before the start of the experiment and allowed to acclimate. An hour after acclimation, the CTV camera system was inserted into the center of the mesocosm.

At the end of the 24-h experiment, the CTV camera was removed, and the number of crabs caught was recorded. A new set of 6 large and 10 smaller male blue crabs were obtained for the next trial, and the procedure was repeated. All video recordings from the experiments were analyzed at SERC. The number of approaches, entries, escapes, and catch rates were recorded, as well as behavioral interactions between crabs. Crab behaviors were classified into three qualitative categories: aggressive, agonistic, or neutral. Aggressive interactions were characterized by the extension of both chelipeds, and cheliped embracing or grasping. Neutral interactions were defined as those where the chelipeds were in a resting position while the crabs passed within 3.8 cm (the diameter of a mesh ring) of each other (Jachowski, 1974). Agonistic interactions comprised any other interactions that occurred, such as shielding (using the cheliped as a shield), fending off predators, poking, leaning backward, or leaning to the side (Jachowski, 1974). Only one crab needed to exhibit an aggressive or agonistic act for the interaction to be recorded as such. If an aggressive and agonistic act co-occurred, the interaction was defined as aggressive.

Results

Field experiment

A total of 119 crabs were caught in 45 experimental runs for an average catch rate of 2.7 crabs per deployment. Crabs ranged in size from 81 to 179 mm CW (mean of 142 mm [SE ±1.8]). Size of test crabs had no significant effect on the size of crabs caught, nor was there a significant size by depth interaction (ANOVA, $P>0.05$, $F=0.63$, df=4). There was a significant effect of depth (Fig. 2A) on the size of crabs caught. Crabs caught at the 3-m depth were significantly smaller then crabs caught at 1 and 2 m (Tukey, $P=0.03$, $F=3.72$, df=4).

The size of test crabs had no significant effect on the number of crabs caught nor was there a significant depth-by-size interaction (ANOVA, $P>0.05$, $F=0.11$ df=4). There was a significant effect of depth on the quantity of crabs caught (Fig. 2B). At the 1-m and 2-m depths, the number of crabs caught did not significantly differ. The number of crabs caught at 3 m was significantly less than at the 1-m and 2-m depths (Tukey, $P=0.04$, $F=3.60$, df=4).

It is possible that the experimental design impacted the effect of the test crabs in our field experiment. In the field study, the test crabs were not tethered to the pot, therefore the possibility of escape existed. However, although the majority of experiments retained their test crab (~70%), if a test crab escaped from the pot before interacting with a conspecific, the pot essentially became a control pot. The opposite held true for control pots. Once a crab entered a control pot, the control pot basically became a test pot because it then harbored a single crab.

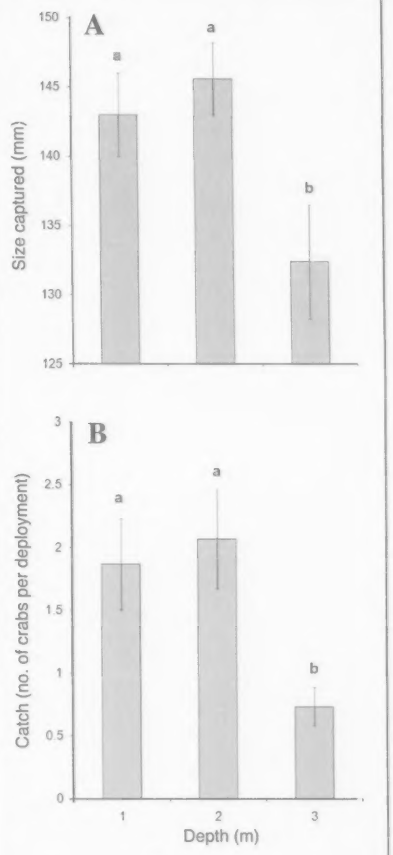

Figure 2

(**A**) Mean size (±1 standard error [SE]) of crabs caught in relation to depth. Depth had a significant effect on size of crabs caught ($P=0.03$, $F=3.72$, df=4). Pots at the 3-m depth caught significantly smaller crabs than pots at the 1- and 2-m depths. (**B**) Mean abundance (±1 SE) of crabs caught in relation to depth. Depth had a significant effect on the number of crabs caught ($P=0.04$, $F=3.60$, df=4). Pots at the 3-m depth caught significantly fewer crabs than pots at the 1- and 2-m depths. Different letters denote significance. $n=15$ for each of the three depth treatments. Results were based on an analysis of 119 crabs.

Of the crabs caught in the first 24 hours of the field experiment, 41% escaped before the end of the second

Table 1

Summary of data documented with crab trap video (CTV), used to observe behavior of male blue crabs (*Callinectes sapidus*) in and around crab pots. The observation time, number of approaches, entries, escapes, and captures are shown for each mesocosm video trial. These data were used to create the conceptual diagram of crab trap dynamics seen in Figure 3. Kitchen= the kitchen section of a crab pot; parlor=the parlor section of a crab pot.

Date	Observation period (h)	No. of crab approaches	No. of crab entries	No. of escapes (from the kitchen)	No. of escapes (from the parlor)	No. of crabs caught
07 Aug 03	17	232	58	51	2	4
12 Aug 03	25	146	8	5	0	3
14 Aug 03	23	158	22	17	1	5
15 Aug 03	16	113	37	29	0	8
16 Aug 03	23	179	43	37	0	6
Total	104	828	168	139	3	26

24 hours; and 10% of those that escaped were from sublegal-size crabs. There was no sign of cannibalism in any of the pots. Neither depth (ANOVA, $P>0.05$, $F=0.92$, df=2) nor test crab (ANOVA, $P>0.05$, $F=1.44$, df=2) had a significant effect on escape rate, nor was there a significant size-by-depth interaction on escape rate (ANOVA, $P>0.05$, $F=1.97$, df=4).

There was no significant difference between the number and size of crabs caught in the first 24 hours and the second 24 hours; this finding indicated that in our experiment, the pot submersion time did not appear to affect catch rate (*t*-test, $P>0.05$).

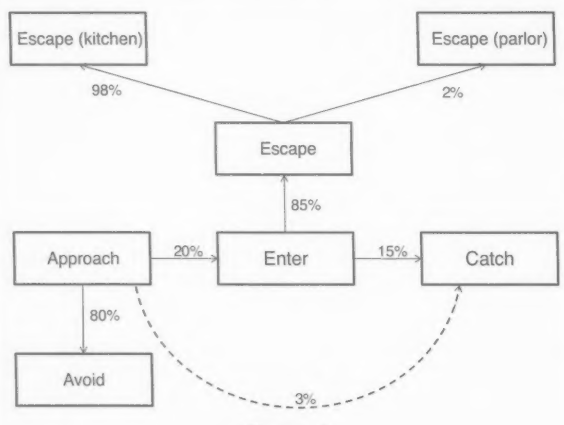

Figure 3

Conceptual diagram of trap dynamics as observed with a crab trap video (CTV) camera system. Percentage values are means of data from Table 1. Of the blue crabs (*Callinectes sapidus*) that approached the pots, 80% avoided them and 20% entered them. Of the 20% that entered the pots, 85% escaped and 15% were caught. Of the 85% that escaped, 98% of the escapes occurred for blue crabs that entered the kitchen section only and 2% of the escapes were for blue crabs that entered the parlor. Overall, pots retained only 3% of all crabs that approached and entered the pots; the dashed curve line shows the final catch for those crabs that approached the pots.

Mesocosm experiment

For the duration of each deployment, the approaches, entries, escapes, and catches of crabs were observed (Table 1). These data were then used to develop a model of trap dynamics (Fig. 3). In our analysis, the number of pots that were approached far exceeded those that were entered; only 20% of crab approaches resulted in an entry. The cause of pot avoidance in nearly 80% of approaches is unknown, but was not caused by conspecifics (discussed below). An interesting observation was the relative ease with which the crabs entered and exited the pots. During the duration of the mesocosm experiments, a total of 168 entries into the pots and 142 escapes from the pots were observed. The 85% escape rate in our mesocosm experiment consisted of 139 escapes from the kitchen, and three escapes from the parlor. The ability of crabs to exit the pot is clearly related to the section of the pot where the crab is located. Of the total escapes, 98% occurred from the kitchen and only 2% from the parlor.

A total of 286 intraspecific interactions were observed, and during 133 of these, crabs physically touched each other. Of all 286 interactions, the majority (178) took place in the kitchen, 12 in the entrance, 78 in the parlor, and 18 outside the pot. Approximately 10% of all observed interactions were aggressive, 42% were agonistic, and 48% neutral. Twelve interactions were observed at one of the four entrances. Of the 12 interactions, 1 was aggressive, 4 were agonistic, and 7 were neutral. In 4 of the 12 entryway interactions there was physical contact between crabs; all 4 of these interactions were agonistic. There were no interactions at the pot entrances that affected entry or exit of the pot.

Discussion

Intraspecific blue crab interactions did not affect crab trap efficacy, and although 52% of the observed interactions between crabs were aggressive or agonistic, none prevented entry or resulted in an exit from the pots. *In situ*, the presence of crabs in pots did not affect the catch rate. These findings are contrary to those from other studies where the relationship between crustacean behavior and catch rates was observed (Jury et al., 2001; Barber and Cobb, 2009). Jury et al. (2001) observed large American lobsters actively defending and preventing conspecifics from entering pots and accessing the bait, and Barber and Cobb (2009) observed Dungeness crabs guarding the entrance to pots and restricting entrance to conspecifics. Clark et al. (2000) showed that at high blue crab density, foraging success is hampered by intraspecific aggression; however, the caveat from our study is that feeding does not occur in crab pots. In American lobster pots the bait hangs down between the entrances to the pot. American lobsters can enter the pot only by coming in close proximity to a lobster feeding on the bait. Observations from work by Jury et al. (2001) described lobsters wielding the bait and fending off interested conspecifics. In standard commercial crab pots, unlike lobster traps, the bait is placed in a wire cage inside the pot and is inaccessible. The unattainable bait may change the nature of the intraspecific behavioral dynamics of crabs in the presence of food. In other studies showing that aggressive behavior impacts catch rate, the aggressive behavior may have been related to the defense of a habitat or territory. Barber and Cobb (2009) observed Dungeness crabs guarding the entrance to pots and not the bait. We found no evidence in the literature that blue crabs guard specific habitats or exhibit spatial fidelity. Male crabs, in tagging experiments where a similar size and molt stage were used, ranged widely, meandering on scales of 50 to 100 meters for several hours to days, but sometimes moving on a fairly constant course at rates exceeding 300 m/h (Wolcott and Hines, 1996).

Blue crabs may have been using the pots as a refuge from predators rather than entering them to feed. Blue crabs have been found in higher abundance in structured, woody debris (Everett and Ruiz, 1993) and sea grass (Eggleston et al., 1998) than in unstructured habitat. The design of the experiment is such that pots were a structured habitat relative to the surrounding environment. The crabs may have entered the pots in response to their value as structure. As further evidence that blue crabs may use pots for the structure that they provide, crabs have been found in unbaited pots (Guillory, 1993). These results may indicate a pot design by species interaction is important in the efficacy of pots.

Although intraspecific interactions were not observed or quantified to have an effect on catch or escape rates, there was a significant effect of depth on catch rate in our field experiments. Blue crabs caught at the 3 m depth were significantly smaller and less abundant than crabs caught at the 1 and 2 m depths. Studies have shown the importance of shallow water as refuge habitat for juvenile fishes and crustaceans in this system (Ruiz et al., 1993). The shallow waters are associated with increased abundance and decreased risk of predation for smaller organisms (Ruiz et al., 1993; Clark et al., 2000). In our study, the increased catch rate of smaller crabs at deeper "riskier" depths may be a function of an increased risk of predation; the smaller crabs used the pots as a refuge, which allowed them to exploit deeper depths. Significantly fewer blue crabs were caught at the 3-m depth than at the 1- and 2-m depths. It is possible that the benthic secondary-production of the 1- and 2-m depths in CHB exceeds that of the 3-m depth enough to attract higher numbers of and larger crabs.

In our field and mesocosm experiments blue crabs escaped at high percentages of 41% and 85%, respectively. The field observations may actually underestimate and the mesocosm experiment may overestimate escape percentages. The percentage of crabs that escaped in the field experiment was calculated from tagged crabs placed in the pots. These point observations do not account for blue crabs that entered and exited before the pot was sampled. In the mesocosm study, we were unsuccessful in our attempts to individually identify crabs. We had no method of determining the number of times an individual crab entered and exited the pot, and this may have artificially inflated our observed escape rate. We observed crabs entering and exiting the kitchen section of the pot with relative ease. Most crabs only needed a few minutes to find the exit, and some swam in through one side and directly out another opening. It is important to note that once crabs entered the parlor, the rate of escape decreased dramatically; crab escape from the parlor was only 2%. Most crabs that entered the parlor explored for a few minutes before becoming inactive. However, one particularly determined crab crawled around the parlor for several hours before escaping into the kitchen. It is possible that blue crab population estimates that use pots should only rely on parlor captures as an accurate measure of relative crab abundance. The escape rate from the parlor was almost zero, but the ease and high escape rate from the kitchen will undeniably bias CPUE results if included in population estimates.

The escape rate of crustaceans from pots is a recognized factor in the trap fishery (Bennet, 1974). Traditionally, escape rates for blue crabs have focused on mechanisms for excluding sublegal crabs from the catch and on inferences from the impacts of derelict pots (Guillory, 1993; 1998). Jury et al. (2001) found that American lobster traps retained only 6% of their potential catch. In previous studies, the range of escape rate for lobsters and crabs was approximately 60–70% (Muir et al., 1984; Karnofsky and Price, 1989). High and Worlund (1979) found that an average of 80% of tagged king crabs (*Paralithodes camtschaticus*) escaped from pots. They identified a number of factors that impacted escape rate, such as presence of bait, soak time,

and crab size. Guillory (1993), one of few to evaluate blue crab escape from derelict pots, found an average of 45% of crabs that entered pots escaped. This number mirrors the 41% escape rate determined in our field study, and Guillory acknowledges that his 45% escape rate is likely an underestimate because of the number of crabs that enter and exit pots during the intermission between pot sampling.

Our mesocosm observations clearly showed the ability of blue crabs to freely enter and exit commercial crab pots. Crab behavior does not appear to play a substantial role in commercial crab trap efficacy, and it appears that behavioral dynamics of blue crabs, in relation to conspecifics, are different when food is accessible and inaccessible (Clark et al., 1999). This study is limited to adult blue crabs at molt stage C. A number of factors impact blue crab behavior and catch. The observed behavioral patterns exhibited in this study might have been different if female crabs or crabs in a different molt stage had been used. For example watermen in the Chesapeake Bay use male crabs as bait in pots to attract peeler females ("peeler" is a term applied to shedding crabs caught by soft-shell fishermen) .

Blue crab behavior effects crab pot catch and escape rates. Eighty-five percent of blue crabs that entered pots were shown to escape, and escape rates may have something to do with the accessibility of food in crab pots. However, the behavioral interactions between blue crabs were not observed or quantified as impacting catch or escape rates. Blue crabs in this study exhibited few quantifiable aggressive interactions, which is atypical of their documented aggressive nature (Clark et al. 1999; deRivera et al., 2005). The escape rates documented in this study may impact blue crab population dynamics based on CPUE and should be further investigated. We also demonstrate that in population studies, two species with similar agonistic behavior characteristics (such as the American lobster and blue crab) can behave differently under similar conditions and therefore require species-specific assessments. Moreover, we caution against broad generalizations about species with perceived similarities in their behavioral characteristics.

Acknowledgments

This work was supported in part by the National Science Foundation funded LSAMP grant to K. Clark, and by the Smithsonian Environmental Research Center for providing research facilities. We also thank G. Abbe for a helpful critique and critical discussions. This is contribution number 3118 from the Virginia Institute of Marine Science.

Literature cited

Abbe, G. R., and C. Stagg.
1996. Trends in blue crab (*Callinectes sapidus* Rathbun) catches near Calvert Cliffs, Maryland, from 1968 to 1995 and their relationship to the Maryland commercial fishery. J. Shellfish Res. 15:751–758.

Barber, J. S., and J. S. Cobb.
2009. Qualitative observations of Dungeness crabs, *Cancer magister*, in and around traps: evidence of resource guarding and clustering. Mar. Freshw. Behav. Physiol. 42:135–146.

Barnes, H.
1963. Underwater television. Oceanogr. Mar. Biol. Annu. Rev. 1:115–128.

Bennet, D. B.
1974. The effects of pot immersion time on catches of crabs, *Cancer pagurus* L. and lobsters *Homarus gammarus* (L.). J. Const. Int. Explor. Mer 35:332–336.

Clark, M. E., T. G. Wolcott, D. L. Wolcott, and A. H. Hines.
1999. Intraspecific interference among foraging blue crabs *Callinectes sapidus*: interactive effects of predator density and prey patch distribution. Mar. Ecol. Prog. Ser. 178:69–78.
2000. Foraging behavior of an estuarine predator, the blue crab *Callinectes sapidus* in a patch environment. Ecography 23:21–31.

Chapman, C. J.
1979. Some observations on populations of Norway lobster, *Nephrops norvegicus* (L.), using diving, television and photography. J. Const. Int. Explor. Mer 175:127–133.

deRivera, C. E., G. M. Ruiz, A. H. Hines, and P. Jivoff.
2005. Biotic resistance to invasion: native predator limits abundance and distribution of an introduced crab. Ecology 86:3364–3376.

Eggleston, D. B., L. L. Etherington, and W. E. Elis.
1998. Organism response to habitat patchiness: Species and habitat-dependent recruitment of decapods crustaceans. J. Exp. Mar. Biol. Ecol. 223:111–132.

Everett, R. A., and G. M. Ruiz.
1993. Coarse woody debris as a refuge from predation in aquatic communities: an experimental test. Oecologia 93:475–486.

Guillory, V.
1993. Ghost fishing by blue crab traps. N. Am. J. Fish. Manag. 13:457–466.
1998. Blue crab, *Callinectes sapidus*, retention rates in different trap meshes. Mar. Fish. Rev. 60:35–37.

Harley, S. J., R. A. Myers, and A. Dunn.
2001. Is catch-per-unit-effort proportional to abundance? Can. J. Fish. Aquat. Sci. 58:1760–1772.

High, W. L., and D. D. Worlund.
1979. Escape of king crab, *Paralithodes camtschatica*, from derelict pots. NOAA Tech. Rep. NMFS SSRF-734, 11 p.

Jachowski, R. L.
1974. Agonistic behavior of the blue crab, *Callinectes sapidus* Rathbun. Behavior 50:232–253.

Jury, S. H., H. Howell, D. F. O'Grady, and W. H. Watson III.
2001. Lobster trap video: *in situ* video surveillance of the behavior of *Homarus americanus* in and around traps. Mar. Freshw. Res. 52:1125–1132.

Karnofsky, E. B., and H. J. Price.
1989. Behavioural response of the lobster *Homarus americanus* to traps. Can. J. Fish. Aquat. Sci. 46:1625–1632.

Lipcius, R. N., and W. A. Van Engel.
1990. Blue crab population dynamics in Chesapeake Bay: Variation in abundance (York River 1972–1988) and stock-recruit functions. Bull. Mar. Sci. 46: 180–194.

Miller, R. J.
1974. Saturation of crab traps: reduced entry and escapement. J. Cons. Int. Explor. Mer 38:338–345.
Myrberg, A. A., Jr.
1973. Underwater television- a tool for the marine biologist. Bull. Mar. Sci. 23:824–836.
Muir, W. D., J. T. Durkin, T. C. Coley, and G. T. McCabe Jr.
1984. Escape of captured Dungeness crabs from commercial crab pots in the Columbia River Estuary. N. Am. J. Fish. Manag. 4:552–555.
Potts, G. W., J. W. Wood, and J. M. Edwards.
1987. Scuba diver operated low-light level video system for use in underwater research and survey. J. Mar. Biol. Assoc. U.K. 67:299–306
Ruiz, G. M., A. H. Hines, and M. H. Posey.
1993. Shallow water as a refuge habitat for fish and crustaceans in non-vegetated estuaries: an example from Chesapeake Bay. Mar. Ecol. Prog. Ser. 99:1–16.
Sharov, A. F., J. H. Vølstad, G. R. Davis, B. K. Davis, R. N. Lipcius, and M. M. Montane.
2003. Abundance and exploitation rate of the blue crab (*Callinectes sapidus*) in Chesapeake Bay. Bull. Mar. Sci. 72:543–565.
Smith, B. D., and G. S. Jamieson.
1989a. A model for standardizing Dungeness crab (*Cancer magister*) catch rates among traps which experienced different soak times. Can. J. Fish. Aquat. Sci. 46:1600–1608.
1989b. Exploitation and mortality of male Dungeness crabs (*Cancer magister*) near Tofino, British Columbia. Can. J. Fish. Aquat. Sci. 46: 1609–1614.
Spanier, E., J. S. Cobb, and M. Clancy.
1994. Impacts of remotely operated vehicles (ROVs) on the behavior of marine animals: an example using American lobsters. Mar. Ecol. Prog. Ser. 104:257–266.
Williams, M. J., and B. J. Hill.
1982. Factors influencing pot catches and population estimates of the portunid crab *Scylla serrata*. Mar. Biol. 71:187–192.
Wolcott, T. G., and A. H. Hines
1996. Advances in ultrasonic biotelemetry for animal movement and behavior: The blue crab case study. *In* Methods and techniques of underwater research: proceedings of the American Academy of Underwater Sciences scientific diving symposium; October 12–13, 1996 (M. A. Lang, and C. C. Baldwin, eds.), p. 229–236. Smithsonian Institution, Washington, D.C.
Van Engel, W. A.
1958. The blue crab and its fishery in Chesapeake Bay. reproduction, early development, growth, and migration. Comm. Fish. Rev. 20:6–17.
1962. The blue crab and its fishery in Chesapeake Bay. Types of gear for hard crab fishing. Comm. Fish. Rev. 24:1–10.

BotCam: a baited camera system for nonextractive monitoring of bottomfish species

Daniel Merritt (contact author)[1]
Mary K. Donovan[1]
Christopher Kelley[2]
Lynn Waterhouse[2]
Michael Parke[3]
Kevin Wong[3]
Jeffrey C. Drazen[4]

Email address for contact author: Daniel.Merritt@noaa.gov

[1] Joint Institute for Marine and Atmospheric Research
University of Hawai`i, and
NOAA Pacific Islands Fisheries Science Center
Coral Reef Ecosystem Division
1000 Pope Rd., MSB 312
Honolulu, Hawaii 96822

[2] Hawaii Undersea Research Laboratory (HURL)
1000 Pope Rd., MSB 303
Honolulu, Hawaii 96822

[3] NOAA Pacific Islands Fisheries Science Center
Coral Reef Ecosystem Division
2570 Dole St.
Honolulu, Hawaii 96822

[4] Department of Oceanography,
University of Hawai`i
1000 Pope Rd., MSB
Honolulu, Hawaii 96822

Abstract—A stereo-video baited camera system (BotCam) has been developed as a fishery-independent tool to monitor and study deepwater fish species and their habitat. During testing, BotCam was deployed primarily in water depths between 100 and 300 m for an assessment of its use in monitoring and studying Hawaiian bottomfish species. Details of the video analyses and data from the pilot study with BotCam in Hawai`i are presented. Multibeam bathymetry and backscatter data were used to delineate bottomfish habitat strata, and a stratified random sampling design was used for BotCam deployment locations. Video data were analyzed to assess relative fish abundance and to measure fish size composition. Results corroborate published depth ranges and zones of the target species, as well as their habitat preferences. The results indicate that BotCam is a promising tool for monitoring and studying demersal fish populations associated with deepwater habitats to a depth of 300 m, at mesohabitat scales. BotCam is a flexible, nonextractive, and economical means to better understand deepwater ecosystems and improve science-based ecosystem approaches to management.

Manuscript submitted 19 March 2010.
Manuscript accepted 25 October 2010.
Fish. Bull. 109:56–67 (2011).

The views and opinions expressed or implied in this article are those of the author (or authors) and do not necessarily reflect the position of the National Marine Fisheries Service, NOAA.

The ability to monitor stocks targeted by a fishery in order to understand the effects of regulatory measures, such as spatial or temporal fishing closures, is important to stakeholders. An understanding of species composition, age- and size-class distributions, habitat use, and other population parameters is critical for developing resource management programs and for monitoring their effectiveness (Jennings, 2001). However, acquisition of data for stock assessments within, and adjacent to, marine protected areas (MPAs) may be compromised by restrictions on extractive sampling or fishery-dependent data. Further, monitoring deepwater species is challenging because of limitations (both logistical and regulatory) on diving in deep water; catch-and-release, or other nonlethal techniques typically are used in shallow water. Because deepwater fisheries have developed rapidly over the last few years, it is important to develop reliable, nonextractive, and fisheries-independent methods for stock assessment and monitoring that will enable managers to assess fishery impacts, evaluate MPAs, and implement ecosystem-based management (Roberts, 2002).

Camera systems provide a fisheries-independent and nonextractive tool for monitoring fish stocks, associated communities, and habitat preferences. Baited camera systems have been used in a number of fisheries habitat studies (Ellis and DeMartini, 1995; Gledhill et al., 1996; Priede and Merrett, 1996; Francour et al., 1999; Willis et al., 2000; Cappo et al., 2003). Most of these studies involved deepwater deployments (>1500 m) for the study of deep-sea scavengers or they involved deployments in relatively shallow waters (<100 m) as a supplement to scuba surveys (Willis et al., 2000; Watson et al., 2007). Currently, there is a need to develop systems for use at intermediate depths.

In Hawai'i, the bottomfish fishery targets snappers, groupers, and jacks that inhabit waters down to 400 m around the archipelago. The most important commercial species live below 100 m and are often referred to as the "deep 7" (WPRFMC, 2007). Six of these are snappers that include *Etelis coruscans* (flame snapper, onaga), *Etelis carbunculus* (ruby snapper, ehu), *Pristipomoides zonatus* (oblique-banded snapper, gindai), *Pristipomoides sieboldii* (lavender snapper, kalekale), *Pristipomoides filamentosus* (pink snapper, opakapaka), and *Aphareus rutilans* (silvermouth snapper, lehi). The seventh species is an endemic grouper called *Epinephelus quernus* (Hawaiian grouper, hapu`upu`u)

(Randall, 2007). Most of these species are long-lived, slow-growing, and are assumed to have a low annual natural mortality rate and limited reproductive capacity (Haight et al., 1993a). These characteristics make these bottomfish stocks especially susceptible to overfishing and habitat destruction (Ralston et al.[1]).

The Hawaiian bottomfish fishing is primarily conducted by jigging hooks and lines on motorized reels. All of the deep 7 species eat a variety of fish and invertebrate species opportunistically. For example, *E. coruscans* are known to feed on species within the water column near the bottom, whereas *E. carbunculus* targets species on the bottom. All target species are caught by using both fish, such as mackerel (*Decapterus* spp.) and invertebrates (such as squid) as bait. Fishing vessels that anchor will often use a *palu* bag containing a mixture of baits.

Although the entire range of depths used by the Hawai`i deepwater bottomfish assemblage has not been determined, the Western Pacific Regional Fishery Management Council (WPRFMC) has defined the deepwater bottomfish essential fish habitat as all depths between 100 and 400 m, and adult habitat areas of particular concern as slopes and escarpments between 40 and 280 m depth (WPRFMC, 1998). Low light levels at these depths complicate the use of cameras. However, surveys with submersibles and remotely operated vehicles (ROVs) indicate that ambient lighting is preferable to artificial area lights or strobes because the artificial lights may repel or attract target species (Ralston et al., 1986; Ryer et al., 2009).

To address the need for a nonextractive, fishery-independent method for monitoring Hawaiian bottomfish stocks, a baited stereo-video camera system (BotCam) has been developed by the National Oceanic and Atmospheric Administration's Pacific Islands Fisheries Science Center (PIFSC) in collaboration with the Hawai`i Undersea Research Laboratory. BotCam is designed to survey the distribution, relative abundance, and size composition of bottomfish, and associated biological and physical characteristics of their habitat.

A pilot study was designed to test BotCam as a tool in making stock assessments. The main purpose of the study was to determine whether, from an operational perspective, BotCam can consistently and reliably collect the same types of data collected by other baited stereo-video camera systems, as reported in the literature, on the commercially important Hawaiian bottomfishes. More specifically, we asked if the system could obtain a metric of relative abundance, accurate information on habitat associations, and a length-frequency distribution for fish of a given fishery.

[1] Ralston, S., S. Cox, M. Labelle, and C. Mees. 2004. Western Pacific Regional Fishery Management Council bottomfish stock assessment workshop final panel report; January 13–16, 20 p. [Available from Western Pacific Fishery Management Council, 11643 Bishop Street, Suite 1400, Honolulu, HI 96813.]

Materials and methods

Baited stereo-video camera system

BotCam was designed as a fully autonomous baited stereo-video camera system (Merritt, 2005). Most of the components are housed in an aluminum frame (1.2 m wide×0.5 m deep×0.45 m tall) designed to protect the cameras and maintain fixed camera positions to one another for accurate length measurements (Fig. 1). The system consists of two ultralow-light video cameras (Monochrome Navigator, Remote Ocean Systems, San Diego, CA), the video capture electronics and system controller (Viperfish Deep, Deep Development Corporation, Sumas, WA), a temperature and pressure recorder (SBE 39TP, Seabird Electronics Inc., Bellvue, WA), a custom-built battery pack and relay used to trigger a delayed bait release-system (BWR, Sexton Photographics LLC, Salem, OR), and syntactic foam blocks for positive buoyancy (Flotation Technologies, Biddeford, ME). The frame also allows for the attachment of oceanographic instruments such as current meters, temperature and depth recorders, and hydrophones. The system is moored to the bottom by anchor weights attached to an anchor line and is designed to float above the bottom and to record video by pointing horizontally down-current with a nominal downward angle of 15°. This orientation improves the view of the benthic habitat without sacrificing the field of view. Each camera provides an 80° diagonal field of view in water. Because of the depth of targeted deployments, motions of the floating system are not affected by surface waves and the platform moves only by means of the currents, which are generally driven by tides, and are therefore stable on the order of several minutes. BotCam does often rotate and change the field of view relative to the substratum over the duration of a deployment. This floating design was chosen to address a couple of concerns. First, the target species are known to school in the water column several meters above the bottom. Second, the habitat of these target species is found on extremely steep and rocky slopes and setting a system directly on the bottom would be problematic for both the deployment and recovery of the system. An extension arm attached to the frame can carry both a stereo-video synchronizing (SVS) device and a bait canister or bag in view of the cameras (Fig. 1). The SVS, a grid of lights that flash in rapid succession, was custom made by Sexton Photographics LLC (similar to a system used by Harvey and Shortis (1996)) and allows two video streams to be synchronized by time for accurate stereo-video measurements. The lights flash at 30 Hz for 1 second every minute and no reaction to the lights has been observed by any of the target species. The first of two baiting modes involves simply attaching a bait bag or trap feeder to the extension arm. The second method involves the use of a 1.7-L Niskin bottle to hold bait sealed inside; at a predetermined time the bottle opens, exposing the bait.

An acoustic release (AR701, Ixsea, Boston, MA) was placed between the bottom of the frame and a set of two

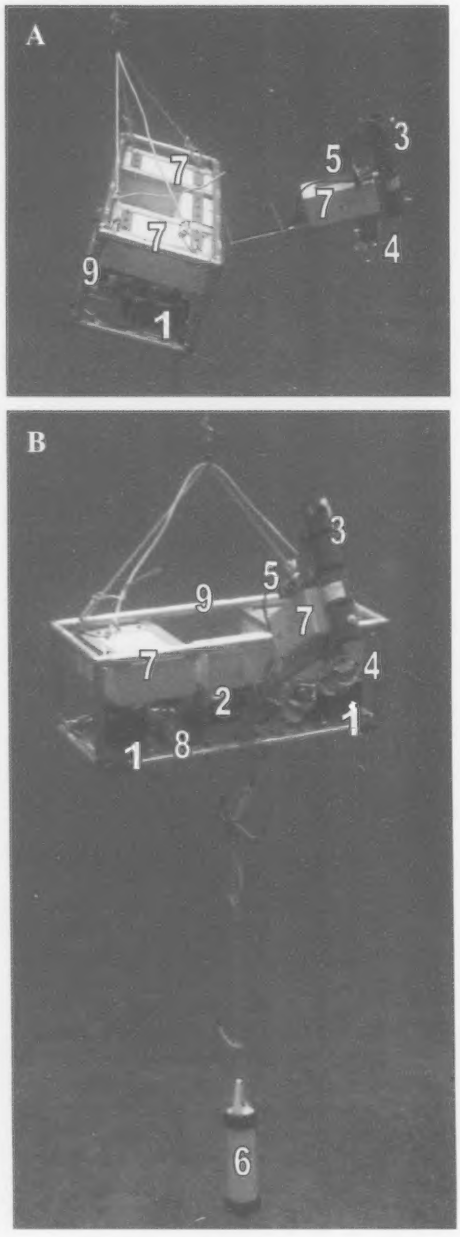

Figure 1

(**A**) side view and (**B**) front view of stereo-video baited camera system (BotCam). Components include (1) ultralow-light video camera, (2) controller-power supply-video capture device, (3) bait container, (4) stereo-video synchronization device, (5) bait release system, (6) acoustic release, (7) syntactic foam flotation, (8) pressure and temperature sensor, (9) aluminum frame. Not shown below the acoustic release is the anchor (concrete blocks).

or three concrete blocks that served as the sacrificial anchor. Concrete was used because it is environmentally benign, inexpensive, and readily available. BotCam was set to float 3 m above the seafloor, thus allowing deployments along steep, rocky slopes without risking entanglement of the instrument on the bottom. It was recovered when it floated to the surface after the acoustic release was triggered to separate the sacrificial anchor from the buoyant instrument frame. The instrument can also be tethered to a surface buoy to allow recovery by a line haul.

The complete system, as used during the pilot study, cost approximately $40,000; however, the systems being used presently with very similar capabilities are about $25,000 per unit. The largest single expense is the pair of ultra-lowlight cameras. In addition, charter time for an appropriate survey vessel in Hawaii runs about $1000 per day.

Study design

During its development, BotCam was tested in approximately 50 deployments around Hawai`i, Wake Atoll, Guam, and the Commonwealth of the Northern Mariana Islands at depths down to 400 m. It was determined that 300 m was the maximum reliable deployment depth under ambient light conditions that would allow accurate species identification and sizing. Further, it was determined that by using a 30- to 60-minute recording time, a single BotCam unit could be deployed, recovered, and ready for redeployment in 90 minutes (Merritt, 2005). Ten- to 60-minute deployments are also consistent with other shallow baited camera studies (Ellis and DeMartini, 1995; Willis et al., 2003).

Given these constraints and a limited number of available charter vessel days, a study site was selected relatively close to Honolulu, home port for the charter vessel and the Pacific Islands Fisheries Science Center. The site was centered on bottomfish habitat located along the west side of Penguin Bank, between the Hawaiian Islands of Oahu and Molokai. Penguin Bank has historically been a productive bottomfish area and its proximity to the highly populated island of Oahu has resulted in high fishing pressure on both the east and west sides of the bank (Haight et al., 1993b).

Previous studies with submersibles and anecdotal evidence from bottomfish fishermen have indicated that the deep 7 bottomfish species generally prefer high-slope, hard-bottom habitats (Kelley et al., 2006; Parke, 2007), which are present at Penguin Bank. Twenty-meter resolution bathymetry and backscatter data derived from multibeam sonar were available for the entire study area and were incorporated into a geographic information system in order to derive intersections of depth, slope, and substratum hardness (i.e., backscatter). The upper and lower depth boundaries for BotCam deployments were 100 and 300 m, respectively, set by the biological and logistical constraints given above, with a resulting sampling area of 24.9 km^2. Within this depth range, four habitat types

were defined on the basis of intersecting substratum (bottom) hardness and slope: 1) hard bottom–high slope (HB–HS); 2) hard bottom–low slope (HB–LS); 3) soft bottom–high slope (SB–HS); and 4) soft bottom–low slope (SB–LS). High slope values were considered to be 20 degrees or greater and hard substrata had backscatter values equal to or greater than 41 on a scale of 0–100 (actual maximum measurement was 92). The sampling locations were randomly selected within these four habitat types and weighted towards the preferred bottomfish habitat. A total of 38 sites were sampled on HB–HS, 14 on HB–LS, 17 on SB–HS, and 13 on SB–LS. In this way greater replication was performed where fish densities were expected to be higher and replication was lower where few or no fish were expected to be found. Adjacent sampling locations were no closer than 200 m and to avoid cross influence of the bait, no two adjacent sites were sampled on the same day.

The BotCam system was set to begin recording after its release from the boat but before its arrival on the bottom. For each deployment, the recording period was between 45 and 60 minutes. The bait consisted of equal parts of ground squid and mackerel, and the volume of bait used for each deployment was standardized to approximately 1 liter. This mixture was designed 1) to be similar to what bottomfish fishermen typically use on their rigs; 2) to provide multiple types of scent; and 3) to provide food similar to the natural diets of the "deep 7" which include both fish and cephalopods (Haight et al., 1993b).

The bait was placed in a simple plastic mesh container that allowed the bait scent to disperse as soon as the system was placed in the water. The bait station was considered to have started when BotCam arrived at the seafloor, as determined from the video recording. From that point, the cameras were allowed to record for a minimum of 30 minutes before BotCam was recovered.

Data analysis

Each video stream from the two cameras was viewed independently. Each video was viewed in 3-minute intervals to allow for flexibility in analyzing the data. The data from the 10 intervals per 30-minute station could be combined into larger intervals or a subset could be randomly selected for statistical comparison with data from other bait stations. The maximum number (MaxNo) of each species seen in any one frame within the time interval (Ellis and DeMartini, 1995) and the exact time from the start of the deployment to the time of first arrival (TFA) of each species seen over the entire 30 minutes were recorded. Further, the largest MaxNo from all the increments was noted as the MaxNo for the deployment for each species observed.

For the purposes of this study, enumeration and measurements were performed only for the two primary bottomfish species of interest, *P. filamentosus* and *E. coruscans*, which were also the two most frequently observed of the "deep 7" species and represent the majority of the bottomfish catch in the Hawaiian Islands (Haight et al., 1993a; Parke, 2007).

Bottomfish fork-length measurements were made from the video recordings by using a software package called Visual Measurement System (SVS) (Geomsoft, Victoria, Australia). With this software, the video streams were synchronized by time by using the SVS device, and then viewed simultaneously frame by frame. Measurements of lengths for *E. coruscans* and *P. filamentosus* were conducted by using the MaxNo video frame and adjacent frames to avoid repeat measurement of individual fish congregating around the bait. Each individual fish was measured six times from different video frames to evaluate the consistency of the measurement technique. This method of only measuring at MaxNo may bias the data by possibly selecting for smaller schooling fish (Willis et al., 2003).

To specifically test the precision and accuracy of the stereo-photogrammetric method of fish measurement, a separate experiment was performed in shallow water. BotCam video was used to measure four different fish models (foam cutouts shaped like fish) of varying length (469.9 mm, 581.0 mm, 628.7 mm, and 997.0 mm) and body depth. The models were filmed at various locations in the field of view at distances of 3 m and 6 m from the cameras. The BotCam was rotated by a diver so that the fish traversed the field of view to simulate swimming. The models were moved vertically to obtain coverage of the models throughout the fields of view of the cameras and the models were measured at haphazard angles. Length measurements on each fish were made by three scientists using stereophotometric software.

The relative distributions of each species across substratum and slope categories described above were evaluated within the framework of a generalized linear model based on a Poisson distribution and log-link function. The model development for predictor variables was based on likelihood ratio tests with a comparison of the full and reduced models. A Pearson chi-square goodness-of-fit test was used to evaluate the appropriateness of the model fits (Kutner et al., 2005). Model fitting included habitat and depth categories and their two-way interaction.

Results

Thirty-three sampling trips were conducted between June 2006 and February 2007, on which a total of 102 BotCam deployments were completed. The fabrication of a second BotCam system toward the end of the study increased the average number of deployments per boat trip to 5.5. Six to eight drops could easily be conducted per day depending on travel time from port to the deployment sites. Of the 102 BotCam deployments, 82 were successful and were distributed amongst habitat and depth categories as outlined above (Table 1). Of the 20 that failed, four landed below 300 m so their recording was too dark; four landed above 100 m outside the

Table 1

Number of baited stereo-video camera (BotCam) deployments that fell within the 100-m to 300-m depth contours and recorded video at Penguin Banks, Hawai'i, between June 2006 and February 2007. Deployments are separated by habitat classification (substratum and slope), depth by 50-m bin, and time period, and the average maximum number (AveMaxNo) and standard error (SE) of counts of *Etelis coruscans* and *Pristipomoides filamentosus* by habitat type and depth. na=not available.

Multibeam habitat classification	Depth (m)	Sample size						*Etelis coruscans*		*Pristipomoides filamentosus*	
		Total	Jun 6	Jul 6	Aug 6	Dec 6	Feb 7	AveMaxNo	SE	AveMaxNo	SE
Hard bottom–high slope	100–150	3	0	0	3	0	0	0.0	na	1.3	1.3
	150–200	9	1	6	2	0	0	0.0	na	3.0	1.5
	200–250	16	1	10	5	0	0	1.9	1.0	1.5	0.6
	250–300	10	1	4	5	0	0	6.1	3.0	0.0	na
Soft bottom–high slope	100–150	1	0	0	0	0	1	0.0	na	1.0	na
	150–200	2	1	1	0	0	0	1.0	1.0	4.5	0.5
	200–250	5	0	1	0	2	2	0.0	na	1.8	1.2
	250–300	6	1	1	1	1	2	0.2	0.2	0.0	na
Hard bottom–low slope	100–150	1	0	0	0	0	1	0.0	na	4.0	na
	150–200	6	0	4	1	0	1	0.3	0.2	5.5	4.3
	200–250	6	0	2	1	1	2	1.7	1.6	1.4	0.5
	250–300	4	2	1	1	0	0	4.3	4.3	0.0	na
Soft bottom–low slope	100–150	2	0	2	0	0	0	0.0	na	0.0	na
	150–200	1	0	0	0	1	0	0.0	na	5.0	na
	200–250	6	0	0	0	6	0	0.7	0.7	1.0	0.8
	250–300	4	0	2	0	1	1	0.8	0.8	0.0	na

Hawaiian bottomfish essential fish habitat; nine did not record because of technical failures; and three failed as a result of human errors. No equipment was lost during the study.

All of Hawaii's "deep 7" bottomfish species were recorded on videotape (Fig. 2). Other species of note observed included goldflag snapper (*Pristipomoides auricilla*), greater amberjack (*Seriola dumerili*), large-head scorpionfish (*Pontinus macrocephalus*), dawn boarfish (*Antigonia eos*) (Randall, 2007), shortspine spurdog (*Squalus mitsukurii*), and numerous carcharhinid sharks. The appearances of each species under ambient light conditions were noted, and a photo library of BotCam videotapes was developed for species identification.

MaxNo values for *E. coruscans* and *P. filamentosus* recorded by BotCam varied between 0 and 29. MaxNo distributions for the two species across the study area are shown in Figure 3, A and B, respectively. *Etelis coruscans* was recorded at 21 locations and *P. filamentosus* at 30 locations and both species were present throughout the study area. No linear relationship between MaxNo and TFA was detected, although the apparent pattern for both species was similar (Fig. 4). For both species, most TFAs were less than 200 seconds (3.3 minutes) and all MaxNos higher than five were reached within the first 200 seconds.

Depth and the interaction of depth and habitat significantly affected *E. coruscans* MaxNo ($P<0.05$). The greatest MaxNo of *E. coruscans* was reached at depths between 250 and 300 m ($P<0.01$, Fig. 5A). Within this depth category, greater mean MaxNo for *E. coruscans* were found in habitats with a slope greater than 20 degrees with either hard or soft bottom substratums ($P<0.05$, Fig. 5A). *Pristipomoides filamentosus* was more widely distributed than *E. coruscans* across the sampled depth range and substratum types. Habitat, depth, and their interaction significantly affected the MaxNo for *P. filamentosus* ($P<0.05$). The interaction of depth and slope significantly affected the MaxNo for *P. filamentosus* with the highest MaxNo observed between 150 and 200 m regardless of habitat type ($P<0.01$, Fig. 5B). No significant relationships were found between temperature and the MaxNo for either species ($r^2<0.10$, $P>0.05$).

In the experiment where model fish were measured, the average residual measurement error (the difference between the actual measurement and the measurement estimated from the photos) of the stereo-photogrammetric analysis was –3.1 mm (percent error of 0.5%) when the models were a distance of 3 m from the camera, and –8.8 mm (percent error of –1.3%) when models were 6 m from the camera. However, the percent error does not appear to be a function of fish size within the range of models measured; therefore, the residual error appears to be a more relevant statistic to use when assessing variance (Table 2).

In the video analysis from the actual survey, it was possible to measure 56 individual *E. coruscans* out of

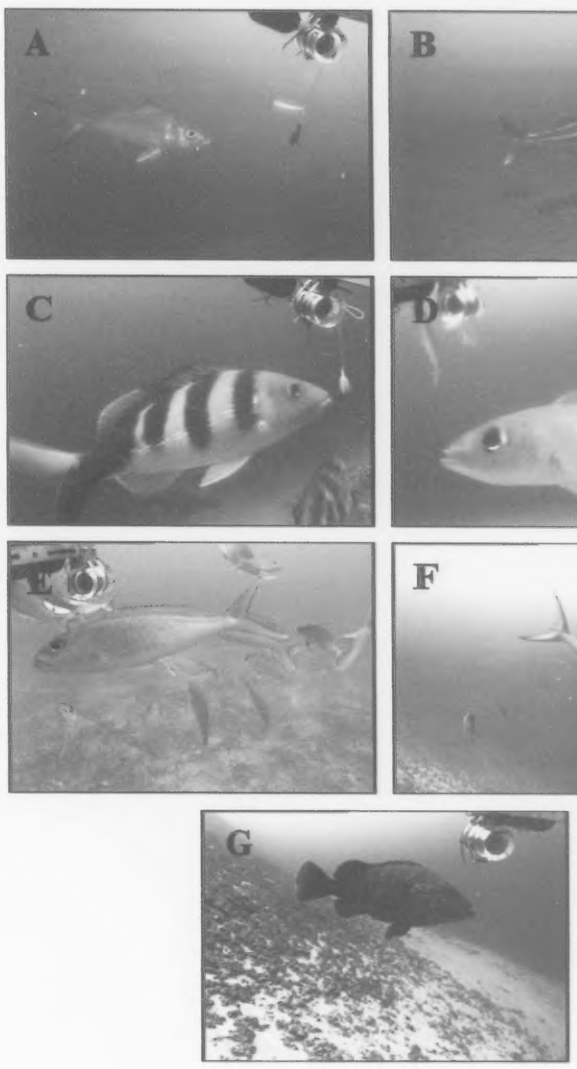

Figure 2

Hawaiian deepwater bottomfish fishery target species referred to as the "deep 7" as recorded by BotCam in Hawaiian waters from depths between 100 m and 300 m. (**A**) *Etelis coruscans* (longtailed red snapper or onaga), (**B**) *Etelis carbunculus* (red snapper or ehu), (**C**) *Pristipomoides zonatus* (Brigham's snapper or gindai), (**D**) *Pristipomoides sieboldii* (von Siebold's snapper or kalekale), (**E**) *Pristipomoides filamentosus* (pink snapper or opakapaka), (**F**) *Aphareus rutilans* (ironjaw snapper or lehi), and (**G**) *Epinephelus quernus* (Hawaiian grouper or hapu`upu`u).

129 counted at the time of MaxNo (43%), and to measure 78 *P. filamentosus* out of the 134 counted (58%). The ability to measure a fish was constrained by the angle of orientation of the fish to the camera, distance from the camera, amount of overlap with other fish, and video clarity. *Etelis coruscans* fork lengths ranged between 432 and 833 mm (mean ±standard deviation [SD] = 605.7 ±26.8 mm, Fig. 6A), and *P. filamentosus* fork lengths ranged between 344 and 660 mm (mean ±SD = 518.0 ±10.9 mm, Fig. 6B).

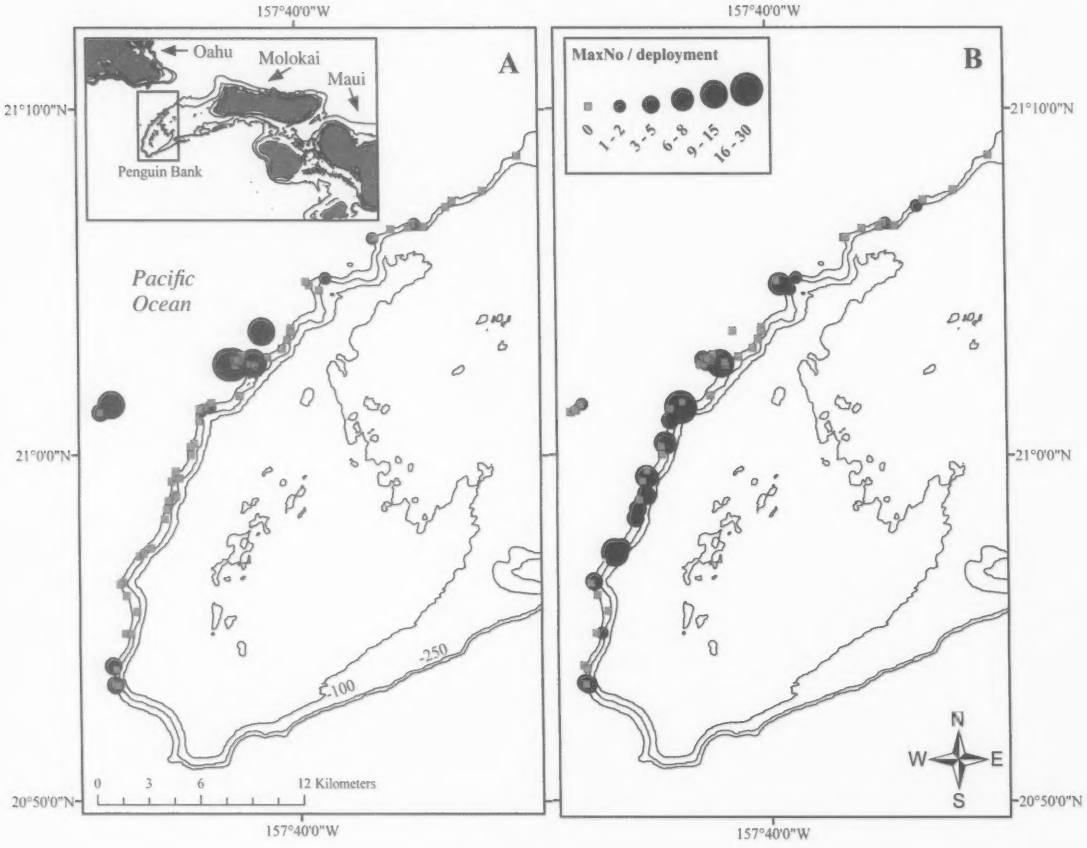

Figure 3

Distribution of (**A**) *Etelis coruscans* and (**B**) *Pristipomoides filamentosus* seen on the BotCam video at Penguin Banks, Hawai`i, between June 2006 and February 2007. Shown is the MaxNo (maximum number in a single frame) of each species seen at each camera deployment site, and the location of all 82 successful deployments.

Table 2

Measurement statistics for testing the precision and accuracy of the stereo-video camera system. A BotCam video camera was used to measure four different models of fish of varying length (469.9 mm, 581.0 mm, 628.7 mm, and 997.0 mm) and body depth. The fish models were filmed in approximately 10 m of water off the South Shore of Oahu, Hawai'i, at distances of 3 m and 6 m from the cameras. The BotCam was rotated by a diver so that the fish traversed the field of view to simulate swimming. The models were moved vertically to obtain coverage throughout the fields of view of the two cameras and were measured at haphazard angles. Length measurements on each fish were made by three scientists (user 1, 2, and 3) using Vision Measurement Software (Geomsoft, Victoria, Australia). Error is defined by the following: Error = actual fork length–fork length measured by stereo-video (also called residual).

	User 1		User 2		User 3		Total	
	3 m	6 m	3 m	6 m	3 m	6 m	3 m	6 m
Number of measurements	193	113	192	134	249	0	634	247
Average error (mm)	–2.3	–6.2	–0.8	–17.0	–7.5	na	–3.1	–8.8
Standard deviation of average error (mm)	22.2	50.8	25.6	42.0	30.8	na	27.7	51.6
Percent error (%)	–0.3	–1.2	0.0	–2.2	–1.1	na	–0.5	–1.3

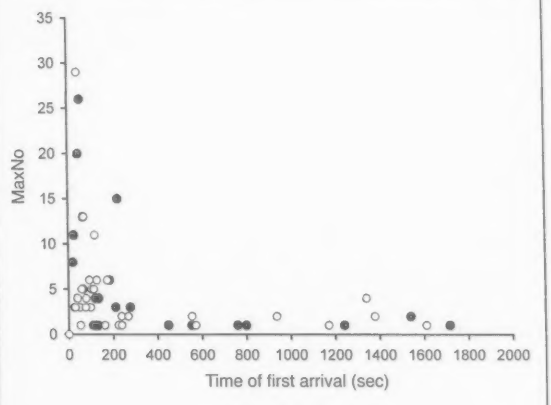

Figure 4

MaxNo (maximum number in a single frame) as a function of TFA (time of first arrival) for *Etelis coruscans* (●) and *Pristipomoides filamentosus* (○) recorded from BotCam deployments at Penguin Banks, Hawai'i, between June 2006 and February 2007.

Discussion

The primary objective of this research was to investigate whether, from an operational perspective, BotCam can provide reliable fishery-independent data on Hawaiian deepwater bottomfish populations that are of similar quality to data obtained from camera systems placed in shallower waters. The results indicate that BotCam can be a useful tool and furthermore illustrate the different types of data it is capable of collecting. Of particular importance, 80% of the deployments were successful in hitting their target sites and recording for the planned time interval. All of the "deep 7" species were attracted to BotCam and were recorded on videotape during the study. Thus from an operational standpoint, BotCam has the potential to collect data useful for assessment of bottomfish populations. Studies are underway to compare results of the pilot study with those from subsequent deployments to determine whether the method can lead to a greater understanding of the temporal and spatial dynamics of bottomfish populations.

As with data collected with other methods, fish count data collected with underwater video systems are confounded by a number of factors, especially when a baited design is used. One factor that affects variance is the inconsistent size of the sampling area due to an unknown size of the bait-plume. One of the outstanding questions about baited camera stations is how extensive is the area of influence of the bait (Priede and Merrett, 1996; Willis et al., 2000). Initial attempts to measure bait dispersal with the stereo-video system proved inadequate; however, measurements of current speeds were promising (Merritt, 2005). Watson et al. (2005) compared baited and unbaited stereo-video surveys with

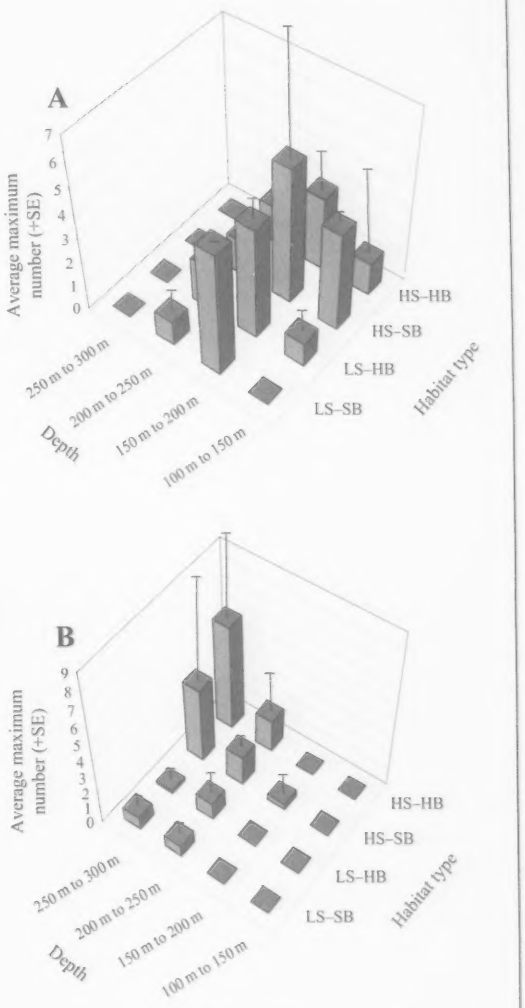

Figure 5

Average MaxNo (maximum number of individuals in a single frame) and standard error (SE) of (**A**) *Etelis coruscans* and (**B**) *Pristipomoides filamentosus* at Penguin Banks, Hawai'i, between June 2006 and February 2007. Depth bins and bottom or substratum types (defined by bottom slope and hardness) were derived from multibeam data during deployment planning. Error bars indicate standard error. HS: high slope, LS: low slope, HB: hard bottom, SB: soft bottom.

underwater visual surveys in a shallow-water environment and found that the baited stereo-video system was the best technique for obtaining consistent fish counts with the least sampling effort, and that unbaited techniques would require a high level of replication to yield similar results (see Harvey et al., 2007). Heagney et al. (2007), working in the open-water column, found

that an area-based bait plume model worked well to explain variation in their count data but were unable to determine if the correlation between counts and current was a result of the bait plume size or an indication of the preferred habitat of the fishes. Further work with BotCam is necessary to evaluate the area of influence of the bait, but the skewed relationship between MaxNo and TFA (Fig. 4) indicates that attraction to the bait is rapid and, therefore, local in its effect.

Another confounding factor is the visual attraction of fish to the camera system itself. Watson (2005) refer to this as the "curiosity" effect and although it is a difficult value to quantify, it is clear from the video recordings that fish do react to the camera system. Unbaited deployments need to be carried out to better understand the magnitude of this effect.

Baited camera systems have historically been used to determine either TFA or MaxNo to estimate relative density of the attracted fishes (Bailey et al., 2007). In many studies, TFA has been used in an inverse-square model as a metric of abundance (Priede et al., 1994). It is assumed with the use of TFA that individuals are uniformly distributed in space, act independently of each other (i.e., there is no schooling behavior), all fishes that contact the odor plume swim up current to the camera, and the effect of the bait plume on fish counts is linear and dependent on local current speed. Thus, short TFAs imply greater densities than long TFAs. In more recent statistical models, the arrival rate instead of the TFA has been used, which allows an estimate of a confidence interval (Farnsworth et al., 2007), but both measures are based on the same basic assumptions. These metrics have been applied primarily to deep sea fishes (>1000 m) inhabiting low-energy, bathymetrically monotonous environments (Priede and Merrett, 1996). They are also hypersensitive at rapid TFAs (<~5 min) and insensitive at long TFAs (>~120 min; King et al., 2006; Yeh and Drazen, 2009). Shallower water environments, such as those surveyed in the current study, are more dynamic ecologically and physically than in the deep sea and therefore fishes tend to be less evenly distributed in space.

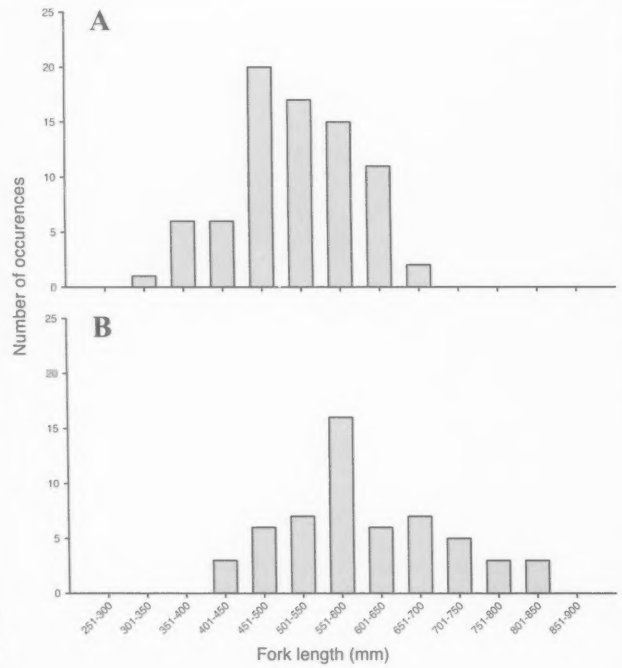

Figure 6

Length-frequency distribution of (**A**) *Etelis coruscans* and (**B**) *Pristipomoides filamentosus* from BotCam deployments at Penguin Banks, Hawai'i, between June 2006 and February 2007 as measured by stereo-video software Vision Measurement System (Geomsoft, Victoria, Australia). Only fish identified at the time of MaxNo (maximum number of individuals in a single frame) were measured. Each fish seen around the time of MaxNo was measured six times (from six different frames of the video) in order to tease out errors due to fish motions and human error. The average fork lengths are binned in 50-mm intervals.

The assumptions about the uniform distribution of the target fishes or linearity of responses to the odor plume required by TFA models often cannot be met. As a result, studies examining shallow-water fishes (Ellis and DeMartini, 1995; Willis et al., 2000; Watson et al., 2005; Kelley and Ikehara, 2006; Stoner et al., 2008) have used MaxNo as an index of relative density which avoids the potential for recounts of the same fish as they exit and reenter the field of view during the survey period. Ellis and DeMartini (1995) found that MaxNo is positively correlated to catch per unit of effort (CPUE) and concluded that it is a useful index of abundance. Likewise, Stoner et al. (2008) concluded that MaxNo was the optimal measure because it is correlated with seine hauls and is consistent across habitat types. Willis et al. (2000) compared a baited camera system with visual surveys and angling surveys and also concluded that video survey techniques with MaxNo provided reliable estimates of relative density. In the present study, TFAs were very short (Fig. 4) and could produce highly variable and spuriously high estimates of abundance (King et al., 2006). This is associated with the lack of sensitivity of TFA to small densities where arrival time is dependent on the position and response to bait of the closest fish. We assumed that the bait plume was not uniform because of the variability in conditions (i.e., currents) and rugged bathymetry. Furthermore, it is well known that some species of bottomfish school, whereas others associate only with

hard substrate; therefore in any sampling there will be an aggregated distribution rather than a random or uniform one (Haight et al., 1993a; Kelley and Ikehara, 2006). Indeed, the present results show that MaxNo, similar to many other types of count data, were not normally distributed; many camera deployments resulted in zero fish and others with up to 29 fish (Fig. 4). MaxNo appears to be a more appropriate metric than TFA for estimating relative abundance in this case, but will likely require analysis with statistical models that are designed for nonuniform dispersion patterns.

Knowledge of the distribution of fishes among habitats is of importance to fisheries management, and such information can readily be obtained with the BotCam system. The distributions of *E. coruscans* and *P. filamentosus* among depth bins and habitat substrata types in our study (Fig. 5) indicate that *E. coruscans* on Penguin Bank prefer high slopes and deeper water, whereas *P. filamentosus* do not have a strong preference for a particular bottom type but are found in the shallowest three quarters of the depth range sampled. Modeling the distribution of both species across depth, slope, and substrate type indicated that these factors were important in understanding the association of these species with their habitat. Currently, the essential fish habitat for these species is simply defined as all waters between 100 and 400 m deep. Although beyond the scope of this study, the results show that additional work with BotCam would enable fisheries scientists to more accurately define essential fish habitats and habitat areas of particular concern on a species-by-species basis. Combined with direct observation of habitat, BotCam is also a tool that will allow for a much finer resolution of habitat classification (i.e., bedrock versus boulders versus cobbles) and enable species preferences to be discerned (see Stoner et al., 2008). Parrish et al. (1997) applied this technique to investigate habitat affinity of juvenile *P. filamentosus* and identified premium habitat by using direct observations from video cameras.

One objective of this study was to evaluate the precision and accuracy of the stereo-photogrammetric technique for obtaining accurate size measurements of bottomfishes. After analyzing repeated measurements of *E. coruscans* and *P. filamentosus*, a discrepancy was apparent between the species. The smaller number of *E. coruscans* measured and the larger standard deviation of the measurements relative to *P. filamentosus* were likely the result of *E. coruscans* being found in deeper water, where visibility and image quality decrease, making video measurement more difficult. Nonetheless, valuable information about the size distribution of these fishes was collected (Fig. 6), indicating that BotCam could be useful as a nonextractive tool for sampling size distributions for stock assessment. Additional experience in both calibrating the camera system and in using the stereo-video software will improve the precision and accuracy of size measurements as evidenced by previous studies where a similar system and software were used (Harvey et al., 2003). Harvey et al. (2002) compared fish length estimates from stereo-video and scuba divers and found video to provide consistently more accurate and precise data. Additionally, Harvey et al. (2010) conducted a similar study on the accuracy and precision of stereo video camera system and found that the length of the object measured was a major factor in reducing variance during measuring. In contrast to this finding, we suggest that size was not a factor, although our study supports the finding that precision degrades with distance away from the camera.

The size distributions of *P. filamentosus* and *E. coruscans* estimated in our study were consistent with published data for both species. Haight et al. (1993a) estimated the length at maturity of *P. filamentosus* to be 430 mm, and maximum length to be 780 mm. Our estimates for *P. filamentosus* ranged from 344 mm to 660 mm, normally distributed throughout the reported size range (Fig. 6). Everson et al. (1989) estimated the length at maturity of *E. coruscans* to be 663 mm, and maximum length to be 925 mm. Our estimates for *E. coruscans* ranged from 432 mm to 832 mm, again normally distributed across the reported size range (Fig. 6). These results indicate that BotCam can estimate relative size frequencies, both pre- and post-sexual maturity and therefore could be used for monitoring recruitment and changes in spawning potential ratios. In neither species was a fish measured near its reported maximum size. The reasons for this could be low sampling effort, size-related differences in behavior or habitat use, bias caused by measuring only at MaxNo, or simply that individuals of such large size were absent from the sampled area. Juveniles of these species were also absent from the video recordings, possibly because they remained close to the bottom near cavities because of their vulnerability to predation, as typical of other bottom associated fishes. Juveniles could have been in the vicinity of BotCam, but because of the presence of larger fish, such as *S. dumerili*, were possibly unwilling to come up to the cameras.

Monitoring deepwater fishes and their habitat is a difficult and costly undertaking. We tested the effectiveness of a new baited stereo-video camera system (BotCam) and found it an efficient tool in places where diver surveys are impossible and ROV or submersible surveys are cost prohibitive or provide data of uncertain quality (Kelley et al., 2006; Stoner et al., 2008). The success rate of data collected per deployment in this study supports the use of BotCam for studying biologic assemblages at depths ranging from 0 to 300 meters. As a nonextractive method, BotCam could prove particularly valuable in marine protected areas, where restrictions on fish removal may limit the usefulness of traditional sampling methods (Willis et al., 2003; Denny et al., 2004; Willis and Millar, 2005). Future work must include careful calibration of BotCam data with traditional population assessment data, including measures of relative abundance based on fisheries-dependent data such as CPUE. In addition, calibration with other nonextractive methods, such as acoustic surveys, is needed.

In future studies with the BotCam system, current meters should be used to model bait dispersal and its effects on fish counts and other measurements. The development of a diverse suite of methods for assessing fish stocks, including baited camera systems such as BotCam, strengthens the scientist's toolkit and allows for more reliable stock assessments and cross-validation of these assessments.

Acknowledgments

The authors thank personnel from the NOAA Coral Reef Conservation Program and the Western Pacific Regional Fishery Management Council members for supporting this research and development effort. We especially thank T. Hourigan of NOAA's Office of Habitat Conservation for initially proposing this work and for his continued advice and encouragement throughout the project. Much appreciation goes to V. Moriwake and B. Alexander for their many hours of field work and video analysis. The authors would also like to acknowledge the crew and officers of the NOAA Ship RV *Oscar Elton Sette* and the Cates International Inc. MV *Wailoa* for their important contributions to the success of this project.

Literature cited

Bailey, D. M., N. J. King, and I. G. Priede.
2007. Cameras and carcasses: historical and current methods for using artificial food falls to study deep-water animals. Mar. Ecol. Prog. Ser. 350:179–191.

Cappo, M. C., E. S. Harvey, H. A Malcolm, and P. J. Speare.
2003. Potential of video techniques to design and monitor diversity, abundance and size of fish in studies of Marine Protected Areas. *In* Aquatic protected areas—what works best and how do we know? (Beumer, J. P., A. Grant, and D. C. Smith, eds.); world congress on aquatic protected areas proceedings; Cairns, Australia, August 2002, p. 455–464. Australian Soc. Fish Biology, Cairns, QLD, Australia.

Denny, C. M., T. J. Willis, R. C. Babcock.
2004. Rapid recolonisation of snapper *Pagrus auratus*: Sparidae within an offshore island marine reserve after implementation of no-take status. Mar. Ecol. Prog. Ser. 272:183–190.

Ellis, D. M., and E. E. DeMartini.
1995. Evaluation of a video camera technique for indexing abundances of juvenile pink snapper, *Pristipomoides filamentosus*, and other Hawaiian insular shelf fishes. Fish. Bull. 93:67–77.

Everson, A. R., H. A. Williams, and B. M. Ito.
1989. Maturation and reproduction in two Hawaiian eteline snappers, uku, *Aprion virescens*, and onaga, *Etelis coruscans*. Fish. Bull. 87:877–888.

Farnsworth, K. D., U. H. Thygesen, S. Ditlevsen, and N. J. King.
2007. How to estimate scavenger fish abundance using baited camera data. Mar. Ecol. Prog. Ser. 350:223–244.

Francour, P., C. Liret, and E. Harvey.
1999. Comparison of fish abundance estimates made by remote underwater video and visual census. Naturalista sicil. 23:155–168.

Gledhill, C., J. Lyczkowski-Shultz, K. Rademacher, E. Kargard, G. Crist, and M. A. Grace.
1996. Evaluation of video and acoustic index methods for assessing reef-fish populations. ICES J. Mar. Sci. 53(2):483–485.

Haight, W. R., D. R. Kobayashi, and K. E. Kawamoto.
1993a. Biology and management of deepwater snappers of the Hawaiian Archipelago. Mar. Fish. Rev. 52(2):20–27.

Haight W. R, J. D. Parrish, T. A. Hayes.
1993b. Feeding ecology of deepwater lutjanid snappers at Penguin Bank, Hawaii. Trans. Am. Fish. Soc. 122: 328–347.

Harvey, E. S., M. Cappo, J. J. Butler, N. Hall, and G. A. Kendrick.
2007. Bait attraction affects the performance of remote underwater video stations in assessment of demersal fish community structure. Mar. Ecol. Prog. Ser. 350: 245–254.

Harvey, E., M. Cappo, M. Shortis, S. Robson, J. Buchanan, and P. Speare.
2003. The accuracy and precision of underwater measurements of length and maximum body depth of southern bluefin tuna (*Thunnus maccoyii*) with a stereo-video camera system. Fish. Res. 63:315–326.

Harvey, E., D. Fletcher, and M. Shortis.
2002. Estimation of reef fish length by divers and by stereo-video: A first comparison of the accuracy and precision in the field on living fish under operational conditions. Fish. Res. 57:255–265.

Harvey, E. S., J. Goetze, B. McLaren, T. Langlois, M. R. Shortis.
2010. Influence of range, angle view, image resolution and image compression on underwater stereo-video measurements: high definition and broadcast video cameras compared. Mar. Technol. Soc. J. 44(1):1–17.

Harvey, E., and M. Shortis.
1996. A system for stereo-video measurement of subtidal organisms. Mar. Technol. Soc. J. 29(4):10–22.

Heagney, E. C., T. P. Lynch, R. C. Babcock, and I. M. Suthers.
2007. Pelagic fish assemblages assessed using mid-water baited video: standardizing fish counts using plume size. Mar. Ecol. Prog. Ser. 350:255–266.

Jennings, S., M. J. Kaiser, and J. D. Reynolds.
2001. Marine fisheries ecology, 347 p. Blackwell Publ., Oxford, UK.

Kelley, C., and W. Ikehara.
2006. The impacts of bottomfishing on Raita and West St. Rogatien Banks in the Northwestern Hawaiian Islands. Atoll Res. Bull. 543:305–318.

Kelley, C., R. Moffitt, and J. R. Smith.
2006. Mega- to micro-scale classification and description of bottomfish essential fish habitat on four banks in the Northwestern Hawaiian Islands. Atoll Res. Bull. 543:319–332.

King, N. J., P. M. Bagley, and I. G. Priede.
2006. Depth zonation and latitudinal distribution of deep-sea scavenging demersal fishes of the Mid-Atlantic Ridge. Mar. Ecol. Prog. Ser. 319:263–274.

Kutner, M. H., C. J. Nachtsheim, J. Neter, and W. Li.
2005. Applied linear statistical models, 5th ed., 580 p. McGraw-Hill Publ., Boston, MA.

Merritt, D. W.
2005. BotCam: Design, testing and development of a fully automated stereo-video bottom camera bait station for ecosystem monitoring of bottom fish species. M.S. thesis, 174 p. Univ. Hawaii, Honolulu.

Parke, M.
2007. Linking Hawaii fisherman reported commercial

bottomfish catch data to potential bottomfish habitat and proposed restricted fishing areas using GIS and spatial analysis. NOAA Tech. Memo. NOAA-TM-NMFS-PIFSC-11, 37 p.

Parrish, F. A., E. E. DeMartini, and D. M. Ellis.
1997. Nursery habitat in relation to production of juvenile pink snapper, *Pristipomoides filamentosus*, in the Hawaiian Archipelago. Fish. Bull. 95:137–148.

Priede, I. G., P. M. Bagley, and K. L. Smith Jr.
1994. Seasonal change in activity of abyssal demersal scavenging grenadiers *Coryphaenoides* (*Nematonurus*) *armatus* in the eastern North Pacific Ocean. Limnol. Oceanogr. 39:279–285.

Priede, I. G., and N. R. Merrett.
1996. Estimation of abundance of abyssal demersal fishes; a comparison of data from trawls and baited cameras. J. Fish. Biol. 49 (suppl. A):207–216.

Ralston, S., R. M. Gooding, and G. M. Ludwig.
1986. An ecological survey and comparison of bottomfish resource assessments (submersible versus handline fishing) at Johnston Atoll. Fish. Bull. 84:141–55.

Randall, J. E.
2007. Reef and shore fishes of the Hawaiian Islands. Sea Grant College Program, Univ. Hawaii, Honolulu.

Ryer, C. H., A. W. Stoner, P. J. Iseri, and M. L. Spencer.
2009. Effects of simulated underwater vehicle lighting on fish behavior. Mar. Ecol. Prog. Ser. 391:97–106.

Roberts, C.M.
2002. Deep impact: the rise of fishing in the deep sea. Trends Ecol. Evol. 17:242–245.

Stoner, A.W., B. J. Laurel, and T. P. Hurst.
2008. Using a baited camera to assess relative abundance of juvenile Pacific cod: field and laboratory trials. J. Exp. Mar. Biol. 354: 202–211.

Watson, D. L., E. S. Harvey, M. J. Anderson, and G. A. Kendrick.
2005. A comparison of temperate reef fish assemblages recorded by three underwater stereo-video techniques. Mar. Biol. 148:1432–1793.

Watson, D. L., E. S. Harvey, G. A. Kendrick, G. A. Nardi, and M. J. Anderson.
2007. Protection from fishing alters the species composition of fish assemblages in a temperate-tropical transition zone. Mar. Biol. 152:1197–1206.

WPRFMC (Western Pacific Regional Fishery Management Council).
1998. Magnuson-Stevens Act definitions and required provisions. WPRFMC, Honolulu, Hawaii. [Available at http://www.wpcouncil.org/documents/magnuson.pdf, Accessed October 2010.]
2007. Amendment 14 to the Fishery Management Plan for Bottomfish and Seamount Groundfish Fisheries of the Western Pacific Region. [Available at http://www.wpcouncil.org/bottomfish/Documents/FMP/Bottomfish%20A14.pdf, accessed October 2010.]

Willis, T. J., R. B. Millar, and R. C. Babcock.
2000. Detection of spatial variability in relative density of fishes: comparison of visual census, angling, and baited underwater video. Mar. Ecol. Prog. Ser. 198:249–260.

Willis, T. J., R. B. Millar, and R. C. Babcock.
2003. Protection of exploited fish in temperate regions: high density and biomass of snapper *Pagrus auratus* (Sparidae) in northern New Zealand marine reserves. 40:214–227.

Willis, T. J., R. B. Millar.
2005. Using marine reserves to estimate fishing mortality. Ecol. Letters. 8: 47–52.

Yeh, J., and J.C. Drazen.
2009. Depth zonation and bathymetric trends of deep-sea megafaunal scavengers of the Hawaiian Islands. Deep-Sea Res. Pt. I. 56:251–266.

Larval abundance of summer flounder (*Paralichthys dentatus*) as a measure of recruitment and stock status

Kenneth W. Able (contact author)[1]

Mark C. Sullivan[2]

Jonathan A. Hare[3]

Gretchen Bath-Martin[4]

J. Christopher Taylor[5]

Roland Hagan[1]

Email address for contact author: able@marine.rutgers.edu

[1] Marine Field Station
Institute of Marine and Coastal Sciences
Rutgers University
800 c/o 132 Great Bay Boulevard
Tuckerton, New Jersey 08087

[2] School of Natural Sciences and Mathematics
The Richard Stockton College of New Jersey
PO Box 195, Jimmie Leeds Road
Pomona, New Jersey 08240

[3] Narragansett Laboratory
Northeast Fisheries Science Center
National Marine Fisheries Service, NOAA
28 Tarzwell Drive
Narragansett, Rhode Island 02882

[4] Beaufort Laboratory
Southeast Fisheries Science Center
National Marine Fisheries Service, NOAA
101 Pivers Island Rd
Beaufort, North Carolina 28516

[5] Center for Coastal Fisheries and Habitat Research
National Centers for Coastal Ocean Science
National Ocean Service, NOAA
101 Pivers Island Rd
Beaufort, North Carolina 28516

Abstract—Summer flounder (*Paralichthys dentatus*) is one of the most economically and ecologically important estuarine-dependent species in the northeastern United States. The status of the population is currently a topic of controversy. Our goal was to assess the potential of using larval abundance at ingress as another fishery independent measure of spawning stock biomass or recruitment. Weekly long-term ichthyoplankton time series were analyzed from Little Egg Inlet, New Jersey (1989–2006) and Beaufort Inlet, North Carolina (1986–2004). Mean size-at-ingress and stage were similar between sites, whereas timing of ingress and abundance at ingress were not similar. Ingress primarily occurred during the fall at Little Egg Inlet and the winter at Beaufort Inlet. These findings agree with those from earlier studies in which at least two stocks (one north and one south of Cape Hatteras) were identified with different spawning periods. Larval abundance at Little Egg Inlet has increased since the late 1990s and most individuals now enter the estuary earlier during the season of ingress. Abundance at Little Egg Inlet was correlated with an increase in spawning stock biomass, presumably because spawning by larger, more abundant fish during the late 1990s and early 2000s provided increased larval supply, at least in some years. Larval abundance at ingress at Beaufort Inlet was not correlated with spawning stock biomass or with larval abundance at ingress at Little Egg Inlet, further supporting the hypothesis of at least two stocks. Larval abundance at Little Egg Inlet could be used as a fishery-independent index of spawning stock size north of Cape Hatteras in future stock assessments. Larval occurrence at Beaufort Inlet may provide information on the abundance of the stock south of Cape Hatteras, but additional stock assessment work is required.

Manuscript submitted 1 October 2009.
Manuscript accepted 5 October 2010.
Fish. Bull. 109:68–78 (2011).

The views and opinions expressed or implied in this article are those of the author (or authors) and do not necessarily reflect the position of the National Marine Fisheries Service, NOAA.

Summer flounder (*Paralichthys dentatus*) is one of the most economically important species in the northeastern United States because of the central role it plays in both commercial and recreational fisheries (Collette and Klein-McPhee, 2002). There was considerable concern over this species in the late 1980s when landings and spawning stock biomass declined precipitously (Kraus and Musick, 2001; Terceiro, 2002). In recent years, summer flounder has started to recover, but there is continued controversy over the rate of recovery relative to established benchmarks and recruitment success based on recent stock assessments (NRC, 2000; NEFSC[1]).

Two major issues contribute to this controversy. First, there are differing opinions as to the number of stocks present off of the U.S. east coast. Summer flounder is managed as a unit from the southern border of North Carolina to the U.S.-Canada border (Terceiro, 2002) based on stock-definition research (Wilk et al., 1980) and a population genetics study (Jones and Quattro, 1999). The assessment unit, from which catch and survey data are obtained, however, is an area from Cape Hatteras, North Carolina, to the U.S.-Canada border, consistent with a recent review of stock definition (Kraus and Musick, 2001). A coastal North Carolina stock (extending from Cape Hatteras southward) has been hypothesized (Burke et al., 2000; Kraus and Musick, 2001), but this unit is not subject to a separate assessment (Terceiro, 2002). Second, recruitment processes in summer flounder are unclear, particularly the relationship between spawning stock

[1] NEFSC(Northeast Fisheries Science Center). 2008. 47th northeast regional stock assessment workshop (47th SAW) assessment report. NMFS NEFSC Ref. Doc. 08–12a, 335 p. NEFSC, Woods Hole, MA

size and larval and juvenile abundance. Brodziak and O'Brien (2005) found that summer flounder recruitment lagged after the North Atlantic Oscillation (NAO) index by two years (i.e., recruitment in 1990 was related to the NAO in 1988). Analyses conducted during a recent stock assessment confirmed this relationship (NEFSC[1]), but a mechanistic recruitment hypothesis has yet to be developed. Recruitment is the result of the integration of survival from spawning through the juvenile stage, whereas the stage at which recruitment is determined can be inferred by examining the abundance indices at successive life stages (Nash and Dickey-Collas, 2005).

In an attempt to resolve these issues, we examined the relationship between two long-term time series of summer flounder larval abundance at ingress, recruitment, and spawning stock biomass over the period of presumed stock recovery. We evaluated whether these data sets 1) contribute to an improved understanding of stock identification; and 2) result in indices that correlate with patterns of abundance relative to spawning-stock biomass and recruitment. In prior studies of the abundance of larval summer flounder at ingress, the timing, size, and developmental stage of inlet samples at the New Jersey (Able et al., 1990; Szedlmayer et al., 1992; Keefe and Able, 1993, 1994) and North Carolina (Williams and Deubler, 1968; Burke et al., 2000; Taylor et al., 2009) sites were determined from a shorter time series. A combined analysis has not been attempted until now.

Materials and methods

General life history of summer flounder and study sites

Summer flounder spawn during an offshore migration from estuaries and bays to the outer continental shelf. This spawning event occurs during fall and early winter and the larvae are transported inshore from where they enter estuaries, settle to the bottom, and grow quickly. Most fish are sexually mature by age 2 and it is about this time that they begin to be caught in the commercial fishery.

The locations of data collections were Little Egg Inlet (New Jersey) and Beaufort Inlet (North Carolina) from the northeast and southeast United States continental shelf ecosystems, respectively (Fig. 1). Little Egg Inlet is the primary source of Atlantic Ocean water that enters the Great Bay–Little Egg Harbor estuarine system, which is polyhaline and shallow (average water depth 1.7 m). The system is composed of a drowned river valley (Mullica River), an embayment (Great Bay), and an adjacent barrier beach estuary (Little Egg Harbor). This estuary has a broad, seasonal temperature range (–2° to 28° C) and a moderate tidal range (~1 m; Kennish, 2004). Sampling was conducted from a bridge over Little Sheepshead Creek (water depth ~3 m), a thoroughfare connecting Great Bay and Little Egg Harbor, located 3 rkm from the creek mouth and 2.5 km from Little Egg Inlet. Atlantic Ocean water flows into the estuary through Little Egg Inlet during flood tides, and portions are diverted into the mouth of Little Sheepshead Creek (Charlesworth, 1968; Chant et al., 2000). Recent work has shown that ichthyoplankton samples collected from this location are representative of dynamics occurring in the estuary proper (e.g., Witting et al., 1999; Chant et al., 2000; Neuman et al., 2002; Able and Fahay, 2010).

Beaufort Inlet connects several estuarine systems and two sounds, Back Sound and Bogue Sound, to the Atlantic Ocean (Churchill et al., 1999). The area around the inlet shares many characteristics with other estuarine systems in the southeast United States. Seasonal temperature variation (8° to 30°C) is more moderate than that at Little Egg Inlet, whereas tidal range is similar (~1 m). Sampling is performed from a bridge (~1.5 km inside of Beaufort Inlet) that spans a 40-m wide channel between Radio Island and Pivers Island (water depth ~4 m). Atlantic Ocean water flows into the estuary through Beaufort Inlet and approximately 10% moves up the channel that provides water to the Radio Island–Pivers Island channel (Churchill et al., 1999). Species composition and abundance of samples taken from Beaufort Inlet are also characteristic of collections from surrounding sounds and have potential value as predictive measures of year-class strength of estuarine-dependent fishes (Lewis and Mann, 1971; Hettler et al., 1997; Hettler and Hare, 1998; Forward et al., 1999; Rice et al., 1999; Taylor et al., 2009).

Sampling of larvae at ingress

At Little Egg Inlet, larvae entering the estuary were collected with a 1-m diameter, circular plankton net (1-mm mesh) fitted with a flow meter. From August 1991 to 2006, three replicate 30-min sets were made weekly with the net deployed to a depth of 1.5 m during nighttime flood tides. From February 1989 to May 1990 (the first year of sampling), five 30-min sets of two concurrent plankton nets (one at the surface and one at the bottom) were made for a total of 10 sets per sampling date. From May 1990 to July 1991, three 30-min sets of two concurrent plankton nets (one at the surface and one at the bottom) were conducted. Weekly surface and bottom data from February 1989 to July 1991 were averaged and combined with weekly mid-water data from August 1991 to 2006 to develop a full time series of larval collections (Able and Fahay, 1998, 2010; Witting et al., 1999).

At Beaufort Inlet, larvae were collected with a 2-m^2 rectangular plankton net (1-mm mesh) fitted with a flow meter. The net was deployed during nighttime flood tides and larvae were sampled at the surface (0–1 m depth). Four replicate sets were made weekly from November to April, 1985–2001. Before 1998, tow duration was nearly constant (~5 min), resulting in a variable volume being filtered. Since 1998, tow volume has been standardized (~100 m^3) with the use of an electronic flow meter.

The differences in sampling designs between locations resulted from the logistics of net deployment from the bridges and the abundance of fishes in the water col-

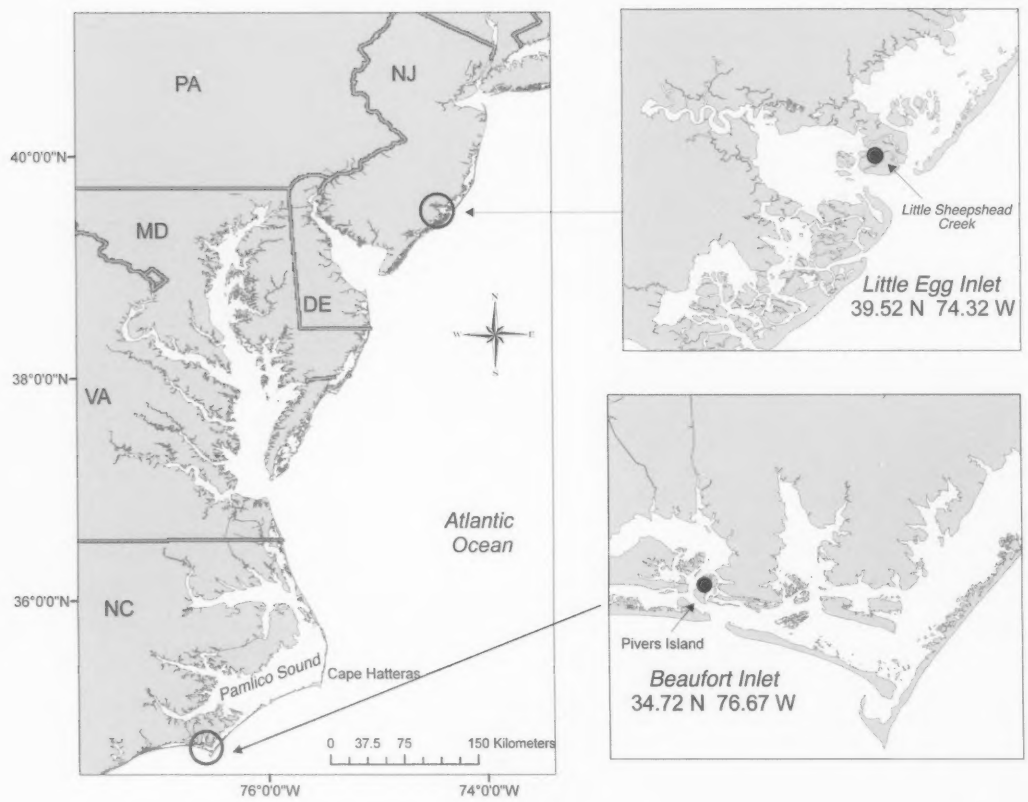

Figure 1

Location of larval summer flounder (*Paralichthys dentatus*) monitoring sites in the northeast and southeast United States shelf ecosystems during 1989–2006 (Little Egg Inlet) and 1986–2004 (Beaufort Inlet).

umn (Sullivan et al., 2006). Characteristics of the two sites and gears implied that the sampling programs were comparable: the environmental setting was similar (salinity ranges, proximity to respective inlets, presence of a well-mixed water column), and mesh-size (1 mm), and sampling time (nighttime and incoming flood tide) were identical.

Larval abundance at both collecting sites was standardized as the number of individuals per 1000 m^3 of water that was filtered. Mean abundance for the replicate net sets on a given night was used as the estimate of summer flounder abundance at ingress during the flood tide. A maximum of 20 larvae per tow were preserved in 95% ethanol and then measured for standard length per tow and for developmental stage determination (after Keefe and Able, 1993).

Spawning stock biomass and recruitment data

Spawning stock biomass and recruitment data for summer flounder were obtained from the most recent stock assessment conducted by the Northeast Fisheries Science Center (NEFSC[1]). In this assessment, indices of spawning stock biomass and recruitment data were derived from the following surveys: Northeast Fisheries Science Center winter, spring, and autumn survey; Massachusetts spring and autumn survey: Rhode Island annual survey: Connecticut spring and autumn survey; New Jersey annual survey; and Delaware annual trawl survey. Recruitment indices were also developed from young-of-the-year surveys conducted by the states of North Carolina, Virginia, and Maryland. These indices were combined with catch-at-age information to estimate recruitment and spawning stock biomass by using the statistical catch at age model implemented in the Age Structured Assessment Program (NEFSC).

Statistical analysis

The following null hypotheses were examined with respect to the two overlapping time series: 1) there is no synchrony between inlets in annual abundance of summer flounder larvae and 2) there is no synchrony between annual abundance at each inlet, spawning stock biomass (SSB), and recruitment (REC). Using the overlapping time periods from each inlet, we determined syn-

chrony in magnitude of abundance of ingressing summer flounder larvae between Little Egg and Beaufort inlets (and their respective relationship with SSB and REC) using two methods: 1) average cross-correlations of series values (r); and 2) measures based strictly on change (Buonaccorsi et al., 2001). For the latter method, the data consisted of n series, measured at T points in time, where x_{it} is the larval concentration at a given inlet, SSB, or REC. The relative direction of change was calculated as A_{ij}, where A_{ij}=(number of times series i and j move in same direction)/ (T–1). This expression was then modified into a correlative measure by using $\tau_{ij}=2A_{ij}-1$ (Buonaccorsi et al., 2001). For both methods, a large, positive value of r or τ signals strong synchrony in magnitude of abundance between populations (reject H_0), a value near zero corresponds with weak synchrony in magnitude of abundance (accept H_0), whereas a value below zero is indicative of populations consistently out of phase (accept H_0; Jones et al., 2003). In all cases, data were lagged to relate spawning stock biomass to subsequent larval abundance at ingress and recruitment. Spawning stock biomass in year y was related to larval abundance at ingress during the fall–winter of year y and the winter–spring of year y+1 and to recruitment in year y+1. All time series data on abundance were natural log transformed (ln).

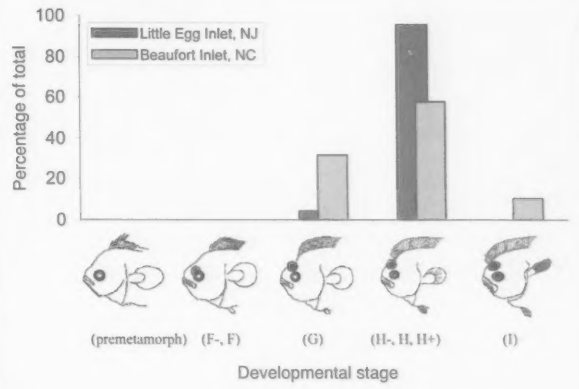

Figure 2

Frequency of developmental stages for summer flounder (*Paralichthys dentatus*) at ingress from Little Egg Inlet, New Jersey, and Beaufort Inlet, North Carolina. Stage notation refers to the scheme of Keefe and Able (1993) as depicted in the head views. The right and left eyes are bilateral and symmetrical in premetamorphs. At the first stage of metamorphosis, F-, the eyes are bilateral but asymmetrical and the right eye is just dorsal to the left eye. By stage F, the asymmetry due to the movement of the right eye is most evident. At stage G, the right eye has reached the dorsal midline and is visible from the left side of the fish. Stage H- differs from G in that the cornea of the eye is visible from the left side of the fish. At stage H, the right eye has migrated halfway and is midline at the dorsal edge of the head. By stage H+, the right eye has reached the left surface but has not yet reached its final resting place. At stage I, the eye is set in the socket and the dorsal canal has closed.

Results

Patterns of larval ingress

At both Little Egg Inlet and Beaufort Inlet, the larvae captured at ingress were in similar stages of development, i.e., transitional stages (stages F–I, based on Keefe and Able, 1993) nearing the completion of eye migration (Fig. 2). These same individuals had overlapping sizes from 10 to 17 mm standard length (SL) and most (90%) were between 12 and 15 mm SL in both inlets, but with slightly larger individuals at Beaufort Inlet (Fig. 3). Summer flounder larvae were consistently more abundant at Beaufort Inlet than Little Egg Inlet (average for all positive months, 8.18/1000 m^3 compared to 4.95/1000 m^3, respectively, Fig. 4).

The timing of ingress differed within and between inlets (Figs. 4 and 5). In the year-round collections at Little Egg Inlet, larvae were found from October through June over the study period (1989–2006). Before 1998, larvae were more abundant in the late winter and spring (January–March). The inconsistently late occurrence of the peak in 1993 is an artifact due to missed collections during the peak period of ingress. From 1998 onwards, larvae were typically more abundant in the fall and early winter (October–December; Fig. 5). From 1989 through 1998 fall and early winter larvae averaged 1.66/1000 m^3, whereas from 1999 through 2006 they averaged 9.08/1000 m^3. At Beaufort Inlet, larvae occurred from December through the end of the sampling period in April or May, but individuals were most abundant from February through April. It is possible that larvae continued ingress but were undetected because sampling typically ended at the end of April or May (Fig. 4). Abundance at Beaufort Inlet varied annually, but seasonal patterns of ingress did not vary over the time series as strikingly as at Little Egg Inlet (Fig. 5). From 1989 through 1998, the late winter and spring larval abundance average (6.62/1000 m^3) was similar for those from 1999 through 2006 (7.76/1000 m^3).

Relationships between larval abundance at ingress, spawning stock biomass, and recruitment

Estimated spawning stock biomass of summer flounder has increased since the late 1990s and reached the highest values during 2000–06 (Fig. 6A). Estimated recruitment has been variable over the same period (Fig 6B). A Beverton-Holt model has been used to describe the stock-recruitment relationship, but this model essentially predicts constant recruitment over the range of observed spawning stock biomass (NEFSC[1]). Trends in larval abundance at Little Egg Inlet are similar to

trends in spawning stock biomass, with the highest values in the series occurring in 2003 and 2004 (Fig. 6C). Larval abundance at ingress into Little Egg Inlet and spawning stock biomass were significantly correlated (Fig. 7A, Table 1). This pattern was not evident at Beaufort Inlet where ingress values varied and had no long-term pattern (Fig. 6D), resulting in no significant correlation with spawning stock biomass (Fig. 7B, Table 1). Recruitment and larval abundance at ingress were not correlated (Fig. 7, A and B, Table 1). Abundance at ingress at the two sites did show a tendency to move in the same direction from year to year but were not correlated with overall abundance (Table 1).

Table 1

Pearson correlations r (right) and Kendall's tau (T, top) values for summer spawning stock biomass (SSB), recruitment (REC), larval abundance at Little Egg Inlet, NJ, and larval abundance of summer flounder at Beaufort Inlet, NC.

Magnitude of change (r)	Direction of change (T)			
	SSB	REC	NJ	NC
SSB	—	-0.20^{ns}	-0.18^{ns}	0.18^{ns}
REC	0.01^{ns}	—	0.06^{ns}	0.06^{ns}
NJ	0.49*	0.12^{ns}	—	0.47*
NC	0.33^{ns}	0.19^{ns}	0.29^{ns}	—

*P <0.05; ns=not significant.

Discussion

Stock identification

Annual patterns of summer flounder larval ingress (timing, abundance) between Little Egg Inlet, New Jersey, and Beaufort Inlet, North Carolina, were not synchronous. The strong differences in timing of ingress between the two inlets could be the result of different spawning times north and south of Cape Hatteras, North Carolina (Burke et al., 2000; Rogers and Van Den Avyle[2]). North of Cape Hatteras, spawning peaks in October–November based on gonad maturation (Morse, 1981; Wilk et al., 1990). A large peak in egg production is evident in October and November and a second, smaller peak occurs in April and May in the southern portion of the Bight. South of Cape Hatteras, a peak in summer flounder gonad development occurs during December and January (Powell, 1974). Other data on summer flounder eggs and larvae south of Cape Hatteras are relatively scarce, partly because identification has been complicated by the presence of other species of *Paralichthys* (Deubler, 1958; Williams and Deubler, 1968; Powles and Stender, 1976; Weinstein, 1979). Two separate spawning periods are also indicated by the occurrence of larvae just north of Cape Hatteras during the fall and again in the spring (Able and Kaiser, 1994; Burke et al., 2000), presumably representing contributions from spawning both from the north and south.

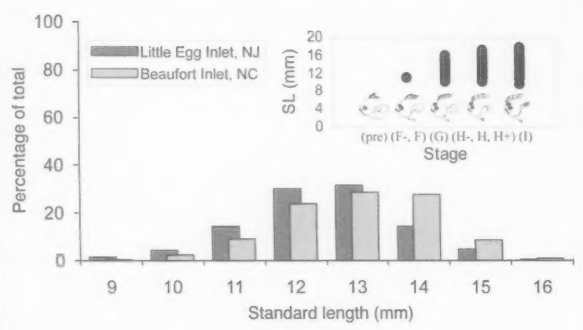

Figure 3

Frequency of standard lengths for summer flounder (*Paralichthys dentatus*) documented at ingress from Little Egg Inlet, New Jersey and Beaufort Inlet, North Carolina. Inset: relationship between standard length (SL) and developmental stages of summer flounder (after Keefe and Able, 1993). The right and left eyes are bilateral and symmetrical in premetamorphs. At the first stage of metamorphosis, F-, the eyes are bilateral but asymmetrical and the right eye is just dorsal to the left eye. By stage F, the asymmetry due to the movement of the right eye is most evident. At stage G, the right eye has reached the dorsal midline and is visible from the left side of the fish. Stage H- differs from stage G in that the cornea of the eye is visible from the left side of the fish. At stage H, the right eye has migrated halfway and is midline at the dorsal edge of the head. By stage H+, the right eye has reach the left surface but has not yet reached its final resting place. At stage I, the eye is set in the socket and the dorsal canal has closed.

The two-stock hypothesis is supported by differences in timing of ingress at Little Egg Inlet and at Beaufort Inlet. Multiple studies indicate that summer flounder spawning (and subsequent ingress) throughout the area north of Cape Hatteras is most common in the fall (Able et al., 1990; Berrien and Sibunka, 1999; Burke et al., 2000). Similar trends in the timing of ingress are evident at other sites north of Cape Hatteras, including Chesapeake Bay, Virginia (Hare et al., 2005), and at Oregon Inlet, North Carolina (Hettler and Barker, 1993; Burke et al., 2000). For the area south of Cape Hatteras, winter spawning results in larval ingress in the late winter and early

[2] Rogers, S. G., and M. J. Van Den Avyle. 1983. Species profiles: life histories and environmental requirements of coastal fishes and invertebrates (South Atlantic): summer flounder, 14 p. U.S. Fish Wild. Serv. Biol. Serv. Prog. FWS/OBS 82(11.15).

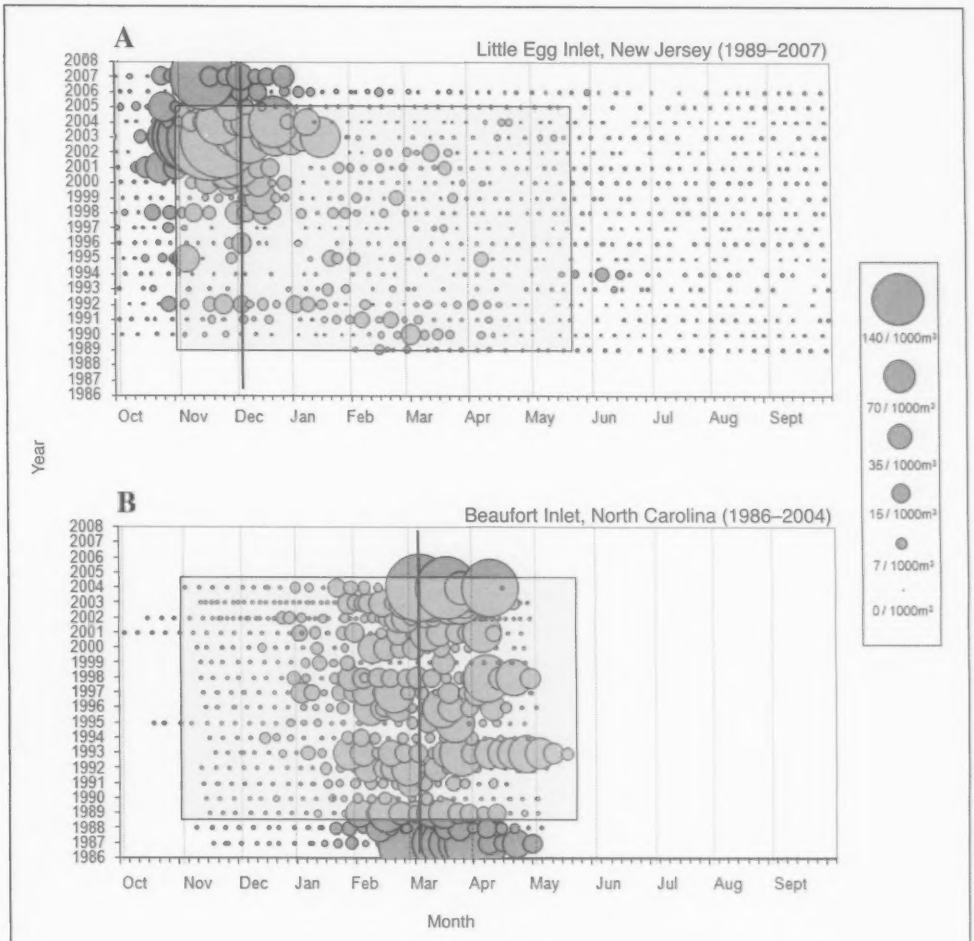

Figure 4

Mean weekly abundance of summer flounder (*Paralichthys dentatus*) larvae ingressing into (**A**) Little Egg Inlet, New Jersey, and (**B**) Beaufort Inlet, North Carolina. Data for overlapping years and months are denoted by the gray rectangles. Summer flounder abundance is proportional to the size of the circle area. Small open circles indicate a sample was taken, but no larvae were caught. The bold vertical line indicates average date of 50% ingress for each series. Data for a given year class began in October of the previous year.

spring only (Smith, 1973; Weinstein, 1979; Bozeman and Dean, 1980; Hettler and Chester, 1990; Burke et al., 2000; this study).

Although there are clear differences between Little Egg Inlet and Beaufort Inlet with respect to timing and abundance at ingress, size and developmental stage at ingress are similar (Keefe and Able, 1993; Forward et al., 1999; this study). The present analysis indicates that these trends are consistent over time and space and likely occur at other inlets along the east coast of the United States (e.g., Hare et al., 2005). These findings do not counter the multiple stock hypothesis, rather they suggest a narrow biological window (optimal length and stage) exists for successful entry of summer flounder larvae into estuarine nursery habitats.

The possible existence of multiple summer flounder stocks is not new and has been frequently discussed and debated in the literature (see Burke et al., 2000; Kraus and Musick, 2001; Terceiro, 2002; Collette and Klein-McPhee, 2002, for reviews). The Beaufort Inlet site likely represents a winter spawning "southern stock" (or stocks)—also termed a coastal North Carolina stock. The Little Egg Inlet site likely represents a fall spawning "northern stock"—also termed a Mid-Atlantic stock. This interpretation is consistent with the stock hypothesis of Burke et al. (2000) and Kraus and Musick

(2001). Further, the examination of larval ingress immediately north (Oregon Inlet) and south (Beaufort Inlet) of Cape Hatteras indicates that this change occurs as a distinct step and not a smooth gradient (Burke et al., 2000).

To further resolve the identification of summer flounder stocks, it is necessary to understand population connectivity (e.g., larval dispersal, juvenile and adult movements) and associated vital rates (e.g., growth, mortality, recruitment) throughout their distribution range (Begg and Waldman, 1999; Hare, 2005). To complicate matters, Nye et al. (2009) documented changes in the latitude and depth of adult summer flounder from the late-1960s to the present, and these changes raise the possibility that stock boundaries are shifting over time. Identifying stocks and understanding their dynamic distribution remains a major issue for the management of U.S. east coast fisheries.

The ability to define the relationship between larval supply at ingress relative to spawning stock biomass and recruitment may be influenced by the scale of the different measures. Larval supply at ingress is measured at local inlets and it is assumed that they are representative of the separate stocks north and south of Cape Hatteras. This interpretation is supported by the available literature. The measures of spawning stock biomass and recruitment used here were calculated for the portion of the population north of Cape Hatteras.

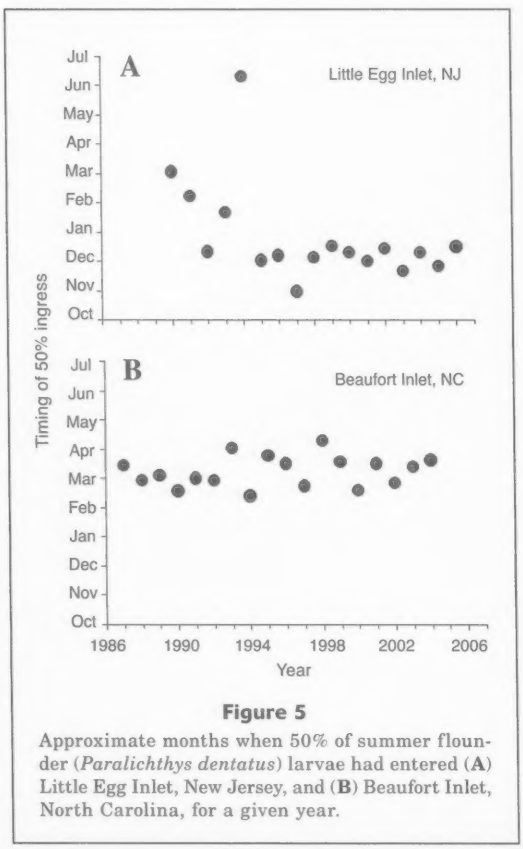

Figure 5

Approximate months when 50% of summer flounder (*Paralichthys dentatus*) larvae had entered (**A**) Little Egg Inlet, New Jersey, and (**B**) Beaufort Inlet, North Carolina, for a given year.

Larval abundance at ingress and spawning stock biomass

The long-term patterns of larval abundance at Little Egg Inlet and spawning stock biomass north of Cape Hatteras indicate that spawning and larval abundance at ingress are linked, presumably because increased spawning by larger, more abundant fish during the late 1990s and early 2000s resulted in increased larval abundance and survival and ultimately increased larval supply. Although the positive correlation may be biased by a few high values, we hypothesize that high spawning stock biomass is responsible for this increase in larval abundance at ingress. If a mechanistic link exists between these two data sets, data at ingress from Little Egg Inlet can be used as a fishery-independent index of spawning stock biomass for the "northern stock" of summer flounder. The lack of a relationship between spawning stock biomass and Beaufort Inlet larval abundance at ingress is not surprising because larvae entering Beaufort Inlet may be the result of a spawning event from a separate stock (see previous discussion). In a recent multispecies analysis of the Beaufort Inlet ichthyoplankton community, Taylor et al. (2009) concluded that the larval ingress from species spawning predominantly north of Cape Hatteras, including summer flounder, was not related to juvenile abundance in the Pamlico Sound system, but that ingress and juvenile abundance were related for species spawning predominantly south of Cape Hatteras. They proposed that larval supply to Pamlico Sound by northern spawning species is predominantly through inlets north of Cape Hatteras. The Beaufort Inlet site is south of Cape Hatteras.

One alternative explanation for the relationship between spawning stock biomass and larval ingress is that general warming trends in the Mid-Atlantic Bight region (Nye et al., 2009) may be contributing to an increased availability of summer flounder larvae to Little Egg Inlet. Hare and Able (2007) suggested for another common estuarine dependent species (Atlantic croaker [*Micropogonias undulatus*]) that warmer water temperatures are allowing juveniles to survive critical developmental periods. Thus, there are multiple hypotheses to explain the concomitant increase in spawning stock biomass and abundance at ingress into Little Egg Inlet and these hypotheses should be explored. In the meantime, abundance at ingress into Little Egg Inlet can be used as a fishery-independent index of spawning stock biomass.

Recruitment

Many studies have shown that larval fish supply influences subsequent recruitment to adult populations (Powell and Steele, 1995; Myers and Barrowman, 1996; Hamer and Jenkins, 1996; Leggett and Frank, 1997;

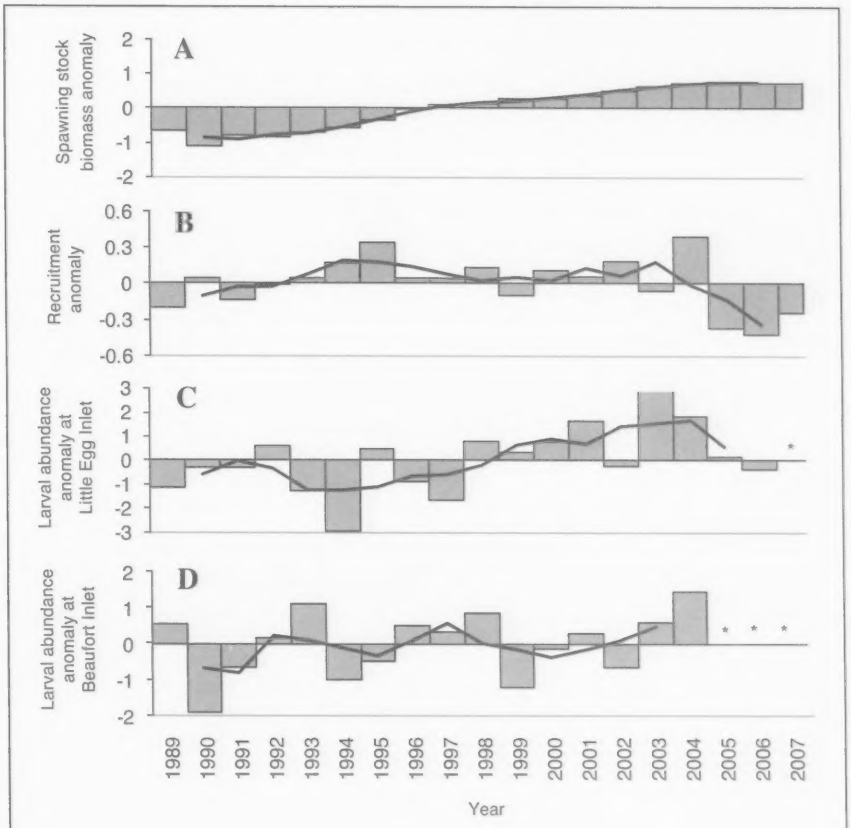

Figure 6

(**A**) Anomalies of spawning stock biomass for summer flounder (*Paralichthys dentatus*). (**B**) Recruitment anomalies. (**C**) Larval abundance anomalies for Little Egg Inlet, New Jersey. (**D**) Larval abundance anomalies for Beaufort Inlet, North Carolina. Anomalies were calculated as [ln(*variable*) for a given year – average ln(*variable*) over entire series]. Black lines denote the three-year moving averages. *=data were not available.

Jenkins et al., 1998; Chapin et al., 2000). Thus, estimates of larval abundance at ingress could contribute to an improved understanding of the relationship between stock size and larval supply, and larval supply and recruitment (e.g., Quinlan and Crowder, 1999). For summer flounder there appears to be no direct relationship between larval supply and recruitment at Beaufort Inlet or Little Egg Inlet (Taylor et al., 2009; this study). This finding implies that recruitment strength may be determined by factors later in the life cycle, likely during the estuarine juvenile stage.

The complexity of habitats occupied by the early life history stages of fishes may be especially problematic for temperate species that encounter extended periods of low temperatures after ingress, which consequently result in suboptimal growth and potentially death, (Hurst, 2007; Able and Fahay, 2010). Slow growth may extend the period during which individuals are susceptible to abiotic and biotic size-dependent selection pressures (see Houde, 1987). The above scenario applies to summer flounder, which shows reduced growth and increased mortality at low temperatures (Malloy and Targett, 1991; Szedlmayer et al., 1992; Keefe and Able, 1994; Able and Fahay, 1998). Temperature effects may be most pronounced for those larvae that enter northern estuaries during the fall and are subsequently exposed to low winter temperatures, as is the case for summer flounder at Little Egg Inlet (Keefe and Able [1994] report 4°C as the lower lethal limit for summer flounder). In addition, during ingress and subsequent settlement, slow growing larvae may be more susceptible to predation by common invertebrate predators such as blue crabs (*Callinectes sapidus*) and the seven-spine bay shrimp (*Crangon septemspinosa*) (Witting and Able, 1995; Barbeau, 2000). If cold winters, combined with increased predation pressure, are relevant factors,

juvenile abundance would be reduced. At Little Egg Inlet, colder winters have become less frequent since the late 1990s (Able and Fahay, 2010), perhaps resulting in the release of early stage flounder from various sources of temperature-induced mortality. A similar hypothesis was proposed for Atlantic croaker (i.e., Hare and Able, 2007).

An improved understanding of the factors affecting the relationship between spawning stock biomass and larval supply, and larval supply and recruitment during the juvenile stage is likely to be critical to an improved management of year-class strength for summer flounder and other estuarine-dependent fishes (Myers and Barrowman, 1996). From a management standpoint, the continuation of larval collections at time of ingress into Little Egg Inlet would provide a fishery independent index for tracking spawning stock biomass for the stock north of Cape Hatteras, as well as data for continuing to explore the links between spawning, larval abundance at ingress, juvenile survival, and recruitment. Additionally, monitoring of larvae at ingress at Beaufort Inlet may provide an index of spawning stock biomass of the coastal North Carolina or "southern stock." The continuation and initiation of similar larval fish sampling programs at other estuarine inlets should provide an improved measure of stock status as well as help disentangle the complex relationships between biological and environmental factors affecting survival and ultimately recruitment for a number of species along the east coast of the United States.

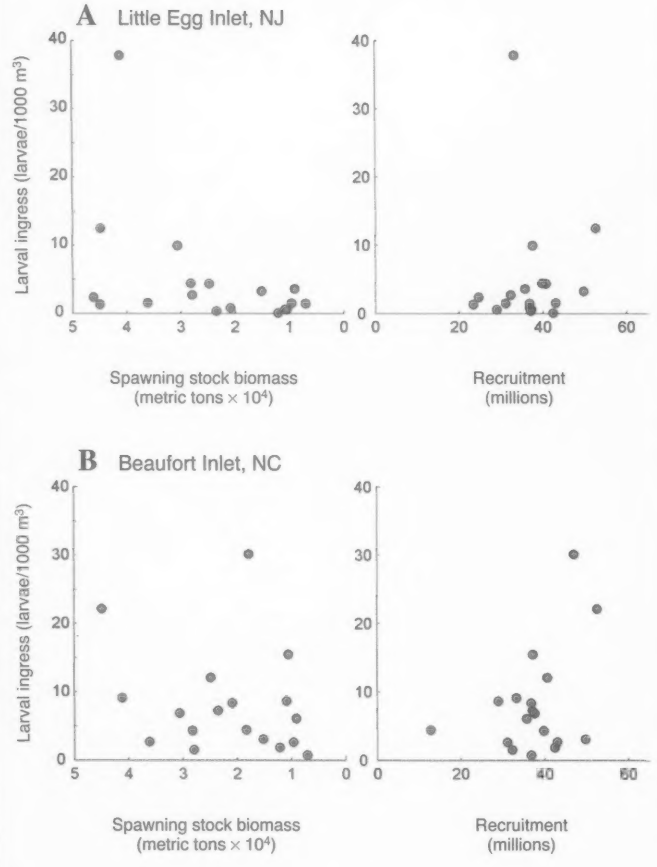
A Little Egg Inlet, NJ
Larval ingress (larvae/1000 m³)
Spawning stock biomass (metric tons × 10⁴)
Recruitment (millions)
B Beaufort Inlet, NC
Larval ingress (larvae/1000 m³)
Spawning stock biomass (metric tons × 10⁴)
Recruitment (millions)

Figure 7

Partial Paulik diagrams for summer flounder (*Paralichthys dentatus*) showing the relationships between spawning stock biomass and larval abundance at ingress, and between larval abundance at ingress and recruitment at (**A**) Little Egg Inlet, New Jersey, and (**B**) Beaufort Inlet, North Carolina. See Table 1 for correlation statistics.

Acknowledgments

Funding for this analysis was provided by the Rutgers University Marine Field Station, the National Ocean Service Center for Coastal Fisheries and Habitat Research and the NMFS Fisheries and Environment Program. We acknowledge the numerous individuals at the Rutgers University Marine Field Station in New Jersey and the Center for Coastal Fisheries and Habitat Research in North Carolina who have worked hard to keep these time series going (in particular, H. Walsh, S. Warlen, and D. Hoss). The staff of the Zaklad Sortowania i Oznaczania Planktonu Szczecin Poland processed the Beaufort Inlet samples. We thank M. Terceiro, D. Ahrenholz, J. Govoni, and P. Marraro for their reviews of an earlier draft. Our acknowledgement of individuals or institutions does not imply that they agree with the content of this manuscript. This article is contribution 2010-6 from Rutgers University Institute of Marine and Coastal Sciences.

Literature cited

Able, K. W., and M. P. Fahay.
1998. The first year in the life of estuarine fishes in the Middle Atlantic Bight, 342 p. Rutgers Univ. Press, Piscataway, NJ.
2010. Ecology of estuarine fishes: temperate waters of the western North Atlantic. Johns Hopkins Univ. Press, Baltimore, MD.

Able, K. W., and S. C. Kaiser.
1994. Synthesis of summer flounder habi-

tat parameters. 68 p. NOAA Coastal Ocean Program Decision Analysis Series No. 1.

Able, K. W., R. E. Matheson, W. W. Morse, M. P. Fahay, and G. Shepherd.
1990. Patterns of summer flounder *Paralichthys dentatus* early life history in the Mid-Atlantic Bight and New Jersey estuaries. Fish. Bull. 88:1–12.

Barbeau, S.
2000. The influence of temperature-dependent growth of summer flounder, *Paralichthys dentatus*, on their period of vulnerability to two invertebrate predators. M.S. thesis, 70 p. Rutgers Univ., New Brunswick, NJ.

Begg, G. A., and J. R. Waldman.
1999. A holistic approach to fish stock identification. Fish. Res. 43:35–44.

Berrian, P., and J. Sibunka.
1999. Distribution patterns of fish eggs in the U.S. Northeast continental shelf ecosystem, 1977–1987. NOAA Tech. Rep. NMFS-145, 310 p.

Bozeman, E. L., Jr., and J. M. Dean.
1980. The abundance of estuarine larval and juvenile fish in a South Carolina intertidal creek. Estuaries 3:89–97.

Brodziak, J., and L. O'Brien.
2005. Do environmental factors affect recruits per spawner anomalies of New England groundfish? ICES J. Mar. Sci. 62:1394–1407.

Buonaccorsi, J. P., J. S. Elkinton, S. R. Evans, and A. M. Leibhold.
2001. Measuring and testing for spatial synchrony. Ecology 82:1668–1679.

Burke, J. S., J. P. Monaghan Jr., and S. Yokoyama.
2000. Efforts to understand stock structure of summer flounder (*Paralichthys dentatus*) in North Carolina, USA. J. Sea Res. 44:111–122.

Chant, R. J., M. C. Curran, K. W. Able, and S. M. Glenn.
2000. Delivery of winter flounder (*Pseudopleuronectes americanus*) larvae to settlement habitats in coves near tidal inlets. Estuar. Coast. Shelf Sci. 51:529–541.

Chapin, S. F., D. A. McGuire, J. Randerson, R. Pielke, D. Baldocchi, E. S. Hobbie, N. Roulet, W. Eugster, E. Kasischke, B. E. Rastetter, A. S. Zimov, and W. S. Running.
2000. Arctic and boreal ecosystems of western North America as components of the climate system. Glob. Change Biol. 6:211–223.

Charlesworth, L. J.
1968. Study of bay, inlet, and nearshore marine sedimentation: Beach Haven—Little Egg Inlet region, New Jersey. Ph.D. diss., 474 p. Univ. Michigan, Ann Arbor, MI.

Churchill, J. H., J. L. Hench, R. A. Luettich Jr., J. O. Blanton, and F. E. Werner.
1999. Flood tide circulation near Beaufort Inlet, North Carolina: implications for larval recruitment. Estuaries 22:1057–1070.

Collette, B. B., and G. Klein-MacPhee [eds].
2002. Bigelow and Schroeder's fishes of the Gulf of Maine. 3rd ed., 748 p. Smithsonian Institution Press, Washington, D.C.

Deubler, E. E., Jr.
1958. A comparative study of the postlarvae of three flounders (*Paralichthys*) in North Carolina. Copeia 1958(2):112–116.

Forward, R. B., Jr., K. A. Reinsel, D. S. Peters, R. A. Tankersley, J. H. Churchill, L. B. Crowder, W. F. Hettler, S. M. Warlen, and M. D. Greene.
1999. Transport of fish larvae through a tidal inlet. Fish. Oceanogr. 8:153–172.

Hamer, P. A., and G. P. Jenkins.
1996. Larval supply and short-term recruitment of a temperate demersal fish, the King George whiting, *Sillaginodes punctata* Cuvier and Valenciennes, to an embayment in south-eastern Australia. J. Exp. Mar. Biol. Ecol. 208:197–214.

Hare, J. A.
2005. The use of early life stages in stock identification studies. *In* Stock identification methods (S. Cardin, K. Friedland, and J. Waldman, eds.), p. 89–117. Academic Press, San Diego, CA.

Hare, J. A., and K. W. Able.
2007. Mechanistic links between climate and fisheries along the east coast of the United States: explaining population outbursts of Atlantic croaker (*Micropogonias undulatus*). Fish. Oceanogr. 16:31–45.

Hare, J. A., S. Thorrold, H. Walsh, C. Reiss, A. Valle-Levinson, and C. Jones.
2005. Biophysical mechanisms of larval fish ingress into Chesapeake Bay. Mar. Ecol. Prog. Ser. 303:295–210.

Hettler, W. F., Jr., and D. L. Barker.
1993. Distribution and abundance of larval fishes at two North Carolina inlets. Estuar. Coast. Shelf Sci. 37:161–179.

Hettler, W. F., Jr., and A. J. Chester.
1990. Temporal distribution of ichthyoplankton near Beaufort Inlet, North Carolina. Mar. Ecol. Prog. Ser. 68:157–168.

Hettler, W. F. Jr., and J. A. Hare.
1998. Abundance and size of larval fishes outside the entrance to Beaufort Inlet, North Carolina. Estuaries 21:476–499.

Hettler, W. F., Jr., D. S. Peters, D. R. Colby, and E. H. Laban.
1997. Daily variability in abundance of larval fishes inside Beaufort Inlet. Fish. Bull. 95:477–493.

Houde, E. D.
1987. Fish early life dynamics and recruitment variability. Am. Fish. Soc. Symp. 2:17–29.

Hurst, T. P.
2007. Causes and consequence of winter mortality in fishes. J. Fish Biol. 71:315–345.

Jenkins, G. P., M. J. Keough, and P. A. Hamer.
1998. The contributions of habitat structure and larval supply to broad-scale recruitment variability in a temperate zone, seagrass-associated fish. J. Exp. Mar. Biol. Ecol. 226:259–278.

Jones, J., P. J. Doran, and R. T. Holmes.
2003. Climate and food synchronize regional bird abundances. Ecology 84:3024–3032.

Jones, W. J., and J. M. Quattro.
1999. Genetic structure of summer flounder (*Paralichthys dentatus*) populations north and south of Cape Hatteras. Mar. Biol. 133:129–135.

Keefe, M., and K. W. Able.
1993. Patterns of metamorphosis in summer flounder, *Paralichthys dentatus*. J. Fish Biol. 42:713–728.
1994. Contributions of abiotic and biotic factors to settlement in summer flounder, *Paralichthys dentatus*. Copeia 1994:458–465.

Kennish, M. J.
2004. Jacques Cousteau National Estuarine Research Reserve. *In* Estuarine research, monitoring and resource protection (M. J. Kennish, ed.), p. 59–115. CRC Press, Boca Raton, FL.

Kraus, R. T., and J. A. Musick.
2001. A brief interpretation of summer flounder, *Para-*

lichthys dentatus, movements and stock structure with new tagging data on juveniles. Mar. Fish. Rev. 63(3):1–6.

Leggett, W. C., and K. T. Frank.
1997. A comparative analysis of recruitment variability in North Atlantic flatfishes: Testing the species range hypothesis. J. Sea Res. 37:281–299.

Lewis, R. M., and W. C. Mann.
1971. Occurrence and abundance of larval Atlantic menhaden, *Brevoortia tyrannus*, at two North Carolina inlets with notes on associated species. Trans. Am. Fish. Soc. 100:296–301.

Malloy, K. D., and T. E. Targett.
1991. Feeding, growth and survival of juvenile summer flounder *Paralichthys dentatus*: experimental analysis of the effects of temperature and salinity. Mar. Ecol. Prog. Ser. 72:213–223.

Morse, W. W.
1981. Reproduction of the summer flounder, *Paralichthys dentatus* (L.). J. Fish Biol. 19:189–203.

Myers, R. A., and N. J. Barrowman.
1996. Is fish recruitment related to spawner abundance? Fish. Bull. 94:707–724.

Nash, R. D. M., and M. Dickey-Collas.
2005. The influence of life history dynamics and environment on the determination of year class strength in North Sea herring (*Clupea harengus* L.). Fish. Oceanogr. 14:279–291.

(NRC) National Research Council.
2000. Improving the collection, management, and use of marine fisheries data, 222 p. Ocean Studies Board, Commission on Geosciences, Environment, and Resources. National Academy Press, Washington, D.C.

Neuman, M. J., K. W. Able, and S. M. Glenn.
2002. The effects of upwelling on larval fish occurrence and abundance in the Jacques Cousteau National Estuarine Research Reserve at Mullica River—Great Bay (JCNERR). Jacques Cousteau Technical Report 100-17, 48 p. Institute of Marine and Coastal Sciences, Rutgers Univ., New Brunswick, NJ.

Nye, J. A., J. S. Link, J. A. Hare, and W. J. Overholtz.
2009. Changing spatial distribution of fish stocks in relation to climate and stock size within the Northeast US continental shelf. Mar. Ecol. Prog. Ser. 393:111–129.

Powell, A. B.
1974. Biology of the summer flounder, *Paralichthys dentatus*, in Pamlico Sound and adjacent waters, with comments on *P. lethostigma* and *P. albigutta*. M.S. thesis, 145 p. Univ. North Carolina, Chapel Hill, NC.

Powell, T. M., and J. H. Steele.
1995. Ecological time series. Chapman & Hall, New York.

Powles, H., and W. Stender.
1976. Observations on composition, seasonality and distribution of ichthyoplankton from MARMAP cruises in the South Atlantic Bight in 1973. Technical Report 11, 46 p. South Carolina Marine Resources Center, Charleston, SC.

Quinlan, J. A., and L. B. Crowder.
1999. Searching for sensitivity in the life history of Atlantic menhaden: inferences from a matrix model. Fish. Oceanogr. 8:124–133.

Rice, J. A., J. A. Quinlan, S. W. Nixon, W. F. Hettler Jr., S. M. Warlen, and P. M. Stegmann.
1999. Spawning and transport dynamics of Atlantic menhaden: inferences from characteristics of immigrating larvae and predictions of a hydrodynamic model. Fish. Oceanogr. 8:93–110.

Smith, W. G.
1973. The distribution of summer flounder, *Paralichthys dentatus*, eggs and larvae on the continental shelf between Cape Cod and Cape Lookout, 1965–66. Fish. Bull. 71:527–548.

Sullivan, M. C., K. W. Able, J. A. Hare, and H. J. Walsh.
2006. *Anguilla rostrata* glass eel ingress into two U.S. east coast estuaries: patterns, processes and implications for adult abundance. J. Fish Biol. 69:1081–1101.

Szedlmayer, S. T., K. W. Able, and R. A. Rountree.
1992. Growth and temperature-induced mortality of young of the year summer flounder (*Paralichthys dentatus*) in southern New Jersey. Copeia 1992(1):120–128.

Taylor, J. C., W. A. Mitchell, J. A. Buckel, H. J. Walsh, K. W. Shertzer, G. B. Martin, and J. A. Hare.
2009. Relationships between larval and juvenile abundance of winter-spawned fishes in North Carolina, USA. Mar. Coastal Fish.: Dynamics, Manag., Eco. Sci. 1:12–21.

Terceiro, M.
2002. The summer flounder chronicles: science, politics, and litigation, 1975–2000. Rev. Fish Biol. Fish. 11:125–168.

Weinstein, M. P.
1979. Shallow marsh habitats as primary nurseries for fishes and shellfishes, Cape Fear River, North Carolina. Fish. Bull. 77:339–357.

Wilk, S. J., W. W. Morse, and L. L. Stehlik.
1990. Annual cycles of gonad-somatic indices as indicators of spawning activity for selected species of finfish collected from the New York Bight. Fish. Bull. 88:775–786.

Wilk, S. J., W. G. Smith, D. E. Ralph, and J. Sibunka.
1980. Population structure of summer flounder between New York and Florida based on linear discriminant analysis. Trans. Am. Fish. Soc. 109:265–271.

Williams, A. B., and E. E. Deubler Jr.
1968. A ten year study of macroplankton in North Carolina estuaries: Assessment of environmental factors and sampling success among bothid flounders and penaeid shrimps. Chesapeake Sci. 9:27–41.

Witting, D. A., and K. W. Able.
1995. Predation by sevenspine bay shrimp *Crangon septemspinosa* on winter flounder *Pleuronectes americanus* during settlement: laboratory observations. Mar. Ecol. Prog. Ser. 123:23–31.

Witting, D. A., K. W. Able, and M. P. Fahay.
1999. Larval fishes of a Middle Atlantic Bight estuary: assemblage structure and temporal stability. Can. J. Fish. Aquat. Sci. 56:222–230.

The effect of temperature on the duration of spawning markers—migratory-nucleus and hydrated oocytes and postovulatory follicles—in the multiple-batch spawner Japanese flounder (*Paralichthys olivaceus*)

Yutaka Kurita (contact author)[1]
Yuichiro Fujinami[2]
Masafumi Amano[3]

E-mail address for contact author: kurita@affrc.go.jp

[1] Tohoku National Fisheries Research Institute
Fisheries Research Agency
Shinhama 3-27-5
Shiogama, Miyagi 985-0001, Japan.

[2] Miyako National Center for Stock Enhancement
Fisheries Research Agency
Sakiyama, Miyako, Iwate 027-0097, Japan.

[3] School of Marine Biosciences
Kitasato University
Ofunato, Iwate 022-0101, Japan.

Abstract—The duration of spawning markers (e.g. signs of previous or imminent spawnings) is essential information for estimating spawning frequency of fish. In this study, the effect of temperature on the duration of spawning markers (i.e., oocytes at early migratory nucleus, late migratory nucleus, and hydrated stages, as well as new postovulatory follicles) of an indeterminate multiple-batch spawner, Japanese flounder (*Paralichthys olivaceus*), was evaluated. Cannulation was performed to remove samples of oocytes, eggs, and postovulatory follicles in individual females at 2–4 hour intervals over 27–48 hours. The duration of spawning markers was successfully evaluated in 14 trials ranging between 9.2° and 22.6°C for six females (total length 484–730 mm). The durations of spawning markers decreased exponentially with temperature and were seen to decrease by a factor of 0.16, 0.36, 0.30, and 0.31 as temperature increased by 10°C for oocytes at early migratory nucleus, late migratory nucleus, and hydrated stages, and new postovulatory follicles, respectively. Thus, temperature should be considered when estimating spawning frequency from these spawning markers, especially for those fish that do not spawn synchronously in the population.

Manuscript submitted 7 May 2010.
Manuscript accepted 27 October 2010.
Fish. Bull. 109:79–89 (2011).

The views and opinions expressed or implied in this article are those of the author (or authors) and do not necessarily reflect the position of the National Marine Fisheries Service, NOAA.

Production of eggs in fish populations varies spatially and temporally during a single spawning season (Scott et al., 2006; Allain et al., 2007) and interannually (Kjesbu et al., 1998). These variations can be caused by changes in temperature, food supply (Somarakis et al., 2004, 2006), fish size composition, and nutritional condition of spawners (Motos, 1996; Marteinsdottir and Begg, 2002; Scott et al., 2006). Spatial and temporal variations in egg production probably affect reproductive success (Kjesbu et al., 1996b; Wright and Gibb, 2005; Secor, 2007; Nishimura et al., 2007; Wright and Trippel, 2009). Therefore, it is necessary to understand the mechanism of spatiotemporal variation in egg production at the population level. Based on the above cited information, the variations in egg production of multiple-batch spawners can be evaluated by using accurate estimates of batch fecundity and spawning frequency in relation to age, size, and condition.

Quantification of population egg production per day is also essential for estimating population size (spawning stock biomass [SSB]) when using the daily egg production method (DEPM; Parker, 1980; Lasker, 1985). DEPM has so far been applied mainly to some clupeid fish populations and is expected to be applied to other fish species including demersal fish (Stratoudakis et al., 2006). Accurate estimation of spawning frequency is important because the largest source of error in the estimation of SSB with DEPM is believed to be associated with spawning frequency (Stratoudakis et al., 2006).

Spawning frequency (S) is expressed as the average number of spawnings per individual per day or as spawning interval (day) (in this study, the former definition is adopted). In both cases, it is estimated from the fraction (F) of mature fish that have a trait (spawning marker) related to imminent or recent spawning, e.g., oocytes at migratory nucleus (MN) or hydrated (HD) stages indicating imminent spawning, and postovulatory follicles (POFs) indicating recent spawning (Hunter and Goldberg, 1980; Hunter and Macewicz, 1985). In the case of some clupeid fish populations, it is sufficient to have a rough estimate of the duration of a spawning marker, e.g., day-0 POF, day-1 POF, etc., because these populations spawn synchronously during

a restricted period of a few hours in the early night, and sampling time is restricted to just after spawning (Hunter and Goldberg, 1980; Hunter and Macewicz, 1985; Funamoto and Aoki, 2002). However, for many other species, spawning time is not synchronized at the population level (i.e., egg release by the population is not restricted to a few hours of the day) or the sampling period for these species is broader. In this case, spawning frequency (S: 1/day) is corrected by the duration (t_i) of a spawning marker i as follows:

$$S = F \times (24 / t_i) \quad (1)$$

(Priede and Watson, 1993; Murua et al., 2003).

Many multiple-batch spawning fish have a long spawning season, and as a consequence, they spawn at a wide range of water temperatures. Therefore, the information on the duration of spawning markers in relation to ambient water temperature is critical for estimating spawning frequency accurately. So far, the duration of a stage of POF has been reported to vary depending on the ambient temperature (Fitzhugh and Hettler, 1995; Ganias et al., 2007). However, to our knowledge, temperature effects on the duration of oocytes at MN and HD stages have not been reported.

In many previous studies, the duration of spawning markers at a given temperature were evaluated by the observation of ovaries which were dissected out of periodically sampled females taken from a spawning population in the field or laboratory (Hunter and Goldberg, 1980; Hunter and Macewicz, 1985; Matsuyama et al., 1988, 2002; Shiraishi et al., 2005). This type of sampling schedule is valid when spawning occurs synchronously or over a short period (h) in the day. However, many fish species, e.g., European plaice (*Pleuronectes platessa*) and Atlantic mackerel (*Scomber scombrus*) have a relatively long spawning-time distribution (in hours per day) at the population level (Ferraro, 1980; Nichols, 1989; Walsh and Johnstone, 1992; Nichols and Warnes, 1993; Scott et al., 1993), and consequently, it is not possible to accurately estimate the duration of spawning markers by fish-group-based studies. For these fish, periodical observations of the presence of spawning markers should be taken from the same fish for a period of 24 hours. Periodic sampling of oocytes and POFs from individual captive fish by cannulation (e.g., Kjesbu et al., 1996a; Kennedy et al., 2008; Withames et al., 2010), is a promising method for estimating the duration of spawning markers.

In this study, we used Japanese flounder (*Paralichthys olivaceus*) (also called the "bastard halibut") as a model species. The flounder is a commercially important bottom fish that inhabits coastal areas <150 m in depth. This species is a multiple-batch spawner and the most active fish spawn every day (Hirano and Yamamoto, 1992). A batch of advanced oocytes among vitellogenic oocytes (ca. 300–600 µm) enters the final oocyte maturation process and is ovulated (Kurita and Kjesbu, 2009). This species is also a typical indeterminate spawner that continues to produce vitellogenic oocytes during the spawning season (Murua and Saborido-Rey, 2003). Each individual female typically spawns over a period of three months (Hirano and Yamamoto, 1992), and the spawning season of the population lasts 4–5 months (Takeno et al., 1999). Japanese flounder experience temperatures of 7–19°C during their spawning season (Y. Kurita, unpubl. data). Spawning occurs throughout 24-h periods at the population level (Y. Kurita, unpubl. data). Thus, the duration of spawning markers during final maturation in relation to temperature is crucial information for accurately estimating spawning frequency.

The objective of this study is to evaluate the effects of temperature on the duration of spawning markers (i.e., oocytes at the MN and HD stages, and POFs) of Japanese flounder by successive sampling of ovarian tissue from individuals with a catheter over a range of ambient temperatures typically encountered during the spawning season.

Materials and methods

Experiments

To evaluate the duration of spawning markers over a range of temperatures, oocyte developmental stages relating to final maturation, and as well as POF degeneration stages (Table 1) of individual captive females were documented periodically. Two kinds of analyses were conducted: 1) an approximate evaluation of the duration for those markers; and 2) a fine-scale evaluation of the duration of hydrated oocytes.

Spawning females were held separately with two males each in cylindrical tanks with a diameter of 2.5 m and a water depth of 1 m (ca. 5 m^3 in volume) during the period covering the spawning season. A constant flow of seawater at ambient temperature was provided. Ovary samples of 1–1.5 mL were taken from each individual every 2–4 hours through 27–48 h with a thin (inner diameter; 2 mm) soft catheter (Pipelle de Cornier, Laboratoire C.C.D., France). At each catheterization, fish were weakly anesthetized with 0.08% 2-phenoxyethanol sea water for 30–120 seconds until fish did not beat their tails when they were turned over in the water. Samples were fixed in 3.6% phosphate buffered formaldehyde and subjected to the following analyses.

Samplings were conducted for 27–48 hours for a total of 14 trials (four trials for 27 hours and 10 trials for 48 hours) for six females (total length [TL] 484–730 mm) and with ambient temperature ranging from 9.2° to 22.6°C (Table 2). Out of 14 trials, the duration of all stages of oocytes during final maturation, i.e., early migratory nucleus (MN[E]), late migratory nucleus (MN[L]), and HD stages, and new postovulatory follicles (POF[new]) (Table 1) were monitored for five trials (three females; TL 605–710 mm); MN(E), MN(L), and POF(new) for one trial (one female; TL 605 mm); and MN(L) and HD for another trial (one female; TL 730 mm). Moreover, the duration and growth rate of only

Table 1

Criteria for each developmental stage of oocyte, ovulated egg, and postovulatory follicle of Japanese flounder (*Paralichthys olivaceus*).

Developmental stage	Abbreviation	Description	
		Histology	Whole mount appearance with transmitted light
Yolk granule	YG	Yolk granules present. Many small oil droplets are distributed around the nucleus which is located in the center (Fig. 1A).	Oocytes are slightly dark and oil droplets, which are located around the nucleus, look like a dark shadow (Fig. 1B).
Early migratory nucleus	MN(E)	Yolk granules are larger. Oil droplets fuse and are distributed unevenly to one side (within 180° from the center of nucleus) beside the nucleus (Fig. 1C).	Uneven distribution of oil droplets can be recognized as dark shadow. Difficult to distinguish from YG (Fig. 1D).
Late migratory nucleus	MN(L)	Oil droplets fuse into 1–3 big droplets (Fig. 1E).	Yellowish oil droplets can be easily recognized (Fig. 1F) and usually distinguishable from MN(E) and YG.
Hydrated	HD	In the earlier phase, yolk granules fuse progressively and start to become irregularly shaped (Fig. 1G). In the later phase, all yolk glanules fuse into a uniform yolk mass that occupies the inside of the oocyte (Fig. 1I). Oocyte is still surrounded by the follicle layer.	In the earlier phase, the whole mount appearance turns opaque and dark (Fig. 1H). In the later phase the whole mount appearance turns translucent and a big yellowish oil droplet is prominent (Fig. 1J). Oocytes at this stage are easily distinguished from other stages of oocytes.
New ovulated egg	OV	A uniform yolk mass occupies the inside of the egg. Egg is free from follicle layer. Egg coexists with POF(new).	Appearance is similar to the oocyte at the late HD stage.
New postovulatory follicle	POF(new)	Granulosa cells are clearly recognized. Cell membrane and nucleus of granulosa cells are intact (Fig. 1K).	

HD-stage oocytes were monitored for seven other trials (four females; 484–710 mm TL). The former seven trials where the duration was monitored for more than two spawning markers, conducted between 9.2° and 22.6°C, were used for analyses of the approximate evaluation of the duration of spawning markers and the size range of hydrated oocytes, the latter of which is the range between the maximum and the minimum diameters of hydrated oocytes through the final maturation process at each temperature of the experiment). In total, 20 events of hydration from 13 trials conducted between 9.2° and 19.7°C were used for analyses of growth rate and the duration of HD-stage oocytes.

Histological and whole mount examination for evaluation of the duration of the spawning marker

Approximate evaluation of the duration for spawning markers was conducted as follows. A part of each cannulated sample was dehydrated and embedded in resin (Historesin), sectioned at 4 µm thickness, and stained with 2% toluidine blue and 1% borax. The occurrence of oocytes at the yolk granule (YG; Table 1), MN(E), MN(L), and HD stages, and POF(new) were recorded by a combination of histological examination under a light microscope and whole mount examination under a binocular microscope (Fig. 1). The start time of the duration of each stage was estimated as the mid-point of the two consecutive sampling times when the developmental stage was not observed and then observed. Similarly, the end time was the mid-point of the two consecutive sampling times when the developmental stage was observed and not observed. The duration of oocytes at the MN(E) and MN(L) stages, and POF(new) were estimated at each trial, and the relationships with temperature were analyzed as the exponential formulae.

Measurement of oocyte diameter for evaluation of duration of the HD stage

The duration of HD stage was estimated more precisely as the range of hydrated oocyte diameter divided by the

Table 2

Experimental data obtained from ovarian tissue from Japanese flounder (*Paralichthys olivaceus*). Ovarian tissue was examined every two to four hours over a 27- or 48-hour sampling period. MN(E)=oocyte at early migratory nucleus stage; MN(L)=at late migratory nucleus stage; HD=at hydrated stage; POF(new)=new postovulatory follicles.

Fish number	Total length (mm)	Experiment period	Duration of experiment (hour)	Temperature (°C)	Spawning markers used for evaluating marker duration or estimating hydrated oocyte growth rate[1]			
					MN(E)	MN(L)	HD[2]	POF(new)
1	605	7–9 June 2004	48	14.1	Y	Y	Y(2)	Y
1		12–14 July 2004	48	16.7	Y	Y	Y(1)	Y
1		9–11 Aug 2004	48	22.6	Y	Y		Y
2	710	30 May–1 June 2005	48	11.3(11.9)[3]	Y	Y	Y(2)	Y
2		30–31 June 2005	27	13.7			Y(2)	
2		20–22 July 2005	48	16.7			Y(2)	
3	707	30 May–1 June 2005	48	11.2(11.9)[3]			Y(2)	
3		30–31 June 2005	27	14.1			Y(2)	
3		20–22 July 2005	48	16.9	Y	Y	Y(2)	Y
3		11–13 Aug 2005	48	19.7	Y	Y	Y(1)	Y
4	484	12–14 July 2004	48	16.8			Y(1)	
5	545	30 May–1 June 2005	48	11.2			Y(1)	
5		30–31 June 2005	27	13.7			Y(1)	
6	730	23–24 May 2006	27	9.2		Y	Y(1)	
				Total	6	7	20	6

[1] "Y" indicates that data were obtained.

[2] Figures in parentheses show the number of hydration events used for calculation of the growth rate of hydrated oocytes.

[3] Figures in parentheses show the temperature at the second hydration event.

growth rate of hydrated oocytes. Changes in those two variables were evaluated in relation to temperature as follows. For the measurements of oocyte diameter, the width of follicle layer was not included.

First, the growth rate of hydrated oocytes was examined. For each cannulated sample, the diameters of 30 hydrated oocytes were measured manually in a whole mount (dispersed sample observed under a binocular microscope) with image-analysis software (Image Pro PLUS, Media Cybernetics, Inc., Bethesda, MD). Growth rate of hydrated oocytes (μm/h) was calculated as the slope of the regression line between the average hydrated oocyte diameter and sampling time. The relationship between the growth rate of hydrated oocytes and temperature was established as the exponential formula.

Next, to estimate the size range of diameters of hydrated oocytes at each temperature unit of the experiment, ovulated egg diameter and the maximum MN(L)-stage oocyte diameter through 48 hours of sampling were measured as the substitution for the maximum and the minimum hydrated oocyte diameters, respectively.

The diameter of 30 newly ovulated eggs (Table 1) that remained in the ovarian cavity from each cannulated sample were measured manually with image-analysis software and averaged. Ovulated eggs were distinguished from large hydrated oocytes by histological examination; i.e., ovulated eggs did not have follicle layers around them and coexisted with new postovulatory follicles. Diameters of ovulated eggs were measured for the two consecutive samples after the samples in which the largest hydrated oocytes in each hydration process were observed.

The diameters of an additional 200–300 fixed, whole-mount oocytes at the YG, MN(E), and MN(L) stages from each cannulated sample were also measured with image analysis software. Average diameters of oocytes at the MN(L) stage were calculated for each sample. When the MN(L) stage oocytes were distinguishable in whole-mount samples (Table 1), the diameters of these oocytes were measured and averaged. However, in some cases, the MN(L)-stage oocytes were difficult to distinguish from the MN(E)-stage oocytes in the whole-mount samples by diameter and appearance. In those cases, the proportion of the number of MN(L)-stage oocytes to the number of the developing oocytes (oocytes at the YG, MN(E), MN(L), and HD stages) was set as the same proportion of the number of HD-stage oocytes to the developing oocytes (Fig. 2). For the example in Figure 2, the proportion of MN(L)-stage oocytes to the developing oocytes was

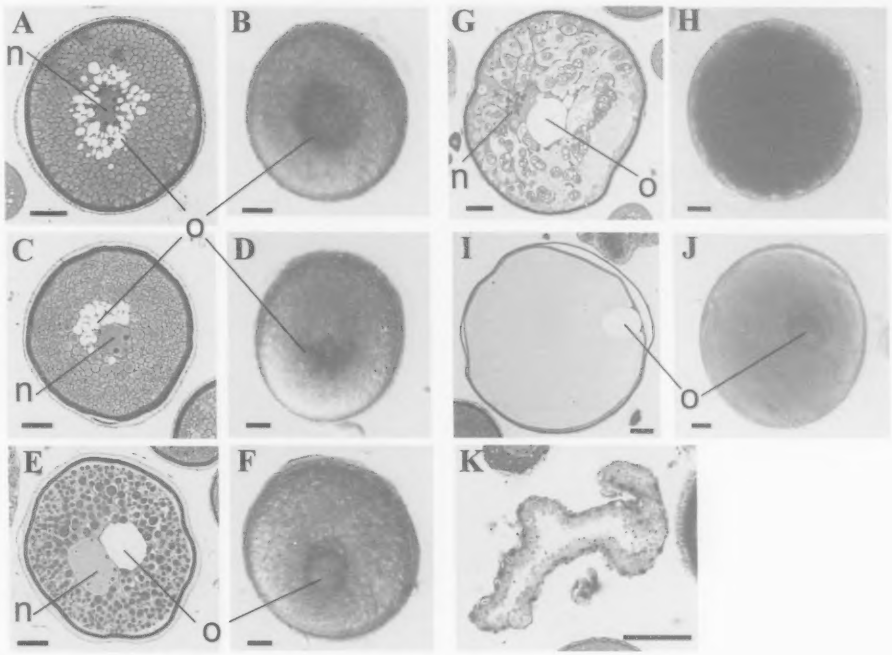

Figure 1

Histological and whole mount images of oocytes and postovulatory follicles (POFs) of Japanese flounder (*Paralichthys olivaceus*). (**A**, **B**) Oocyte at yolk granule stage; diameter ca. 500 µm. (**C**, **D**) Early migratory nucleus stage; diameter ca. 600 µm. (**E**, **F**) Late migratory nucleus stage; diameter ca. 650 µm. (**G**, **H**) Early hydrated stage; diameter ca. 720 µm. (**I**, **J**) Late hydrated stage; diameter ca. 900 µm. (**K**) New POF. Scale bars=100 µm. See Table 1 for detailed definitions. o=oil droplet; n=nucleus.

set at 4.5% which was the same proportion as that for the HD-stage oocytes.

The lower size limit of hydrated oocytes at a given temperature was considered equal to the maximum average size of MN(L)-stage oocytes among the successive 48-h samplings (Table 2) at that temperature because the growth rate of MN(L)-stage oocytes was very slow and the maximum average size of MN(L)-stage oocytes can be considered as the smallest diameter for the hydrated oocytes (see Fig. 3). The average egg diameter was considered as the maximum diameter for the hydrated oocytes. The lower and upper limits of hydrated oocyte diameters were obtained from six (9.2–19.7°C) and seven (9.2–22.6°C) time series samples, respectively. Changes in those diameters were analyzed in relation to temperature.

Average diameters of oocytes at the MN(E) stage and the leading cohort of oocytes at the yolk granule stage (YG[LC]) were also calculated for each sample. The proportions of the number of oocytes at the MN(E) and the YG(LC) stages to the developing oocytes were determined in the same manner as that for MN(L) stage (Fig. 2). The leading cohort of YG-stage oocytes is usually defined as the largest 10% of YG-stage oocytes (Kjesbu, 1994) to specify the maturity phase. In this study, however, the proportion of YG(LC)-stage oocytes to the developing oocytes was set at the same proportion of HD-stage oocytes (e.g., 4.5 % in Fig. 2) to correspond to the expected batch of oocytes.

Body size and individual effects on the growth rate of hydrated oocytes

To evaluate size effect on the growth rate of hydrated oocytes, multiple regression analysis was conducted for 20 data sets of log-transformed growth rates of hydrated oocytes (dependent variable), temperature, and total length (independent variables). In addition, to evaluate the individual effect on the growth rate of hydrated oocytes, the relationship between the log-transformed growth rate of hydrated oocytes and temperature (T) was compared for two females (fish no. 2; TL 710 mm, $11.3 \leq T \leq 16.7$°C, $n=6$: fish no. 3; TL 707

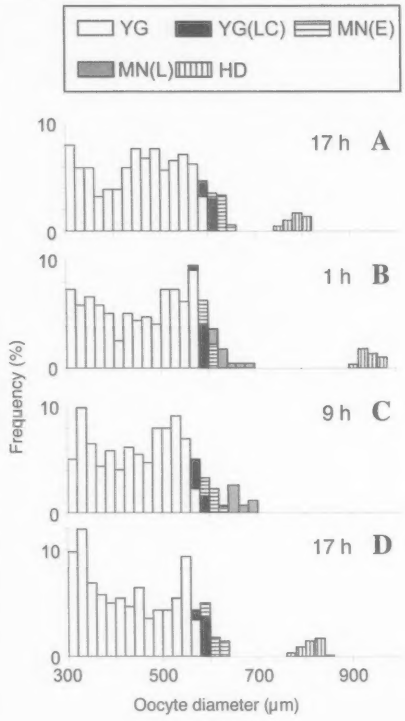

Figure 2

Temporal changes in the frequency distribution of oocyte diameter at different developmental stages of Japanese flounder (*Paralichthys olivaceus*). Data are from successive samples of oocytes from fish no. 2, 30 May-1 June 2005 (see Table 2 and Fig. 3**A**). (**A**) on 30 May, and (**B**–**D**) on 31 May. HD=oocyte at hydrated stage; MN(L)=at late migratory nucleus stage; MN(E)=at early migratory nucleus stage; YG(LC)=the leading cohort of oocytes at yolk granule stage; and YG=yolk granule stage.

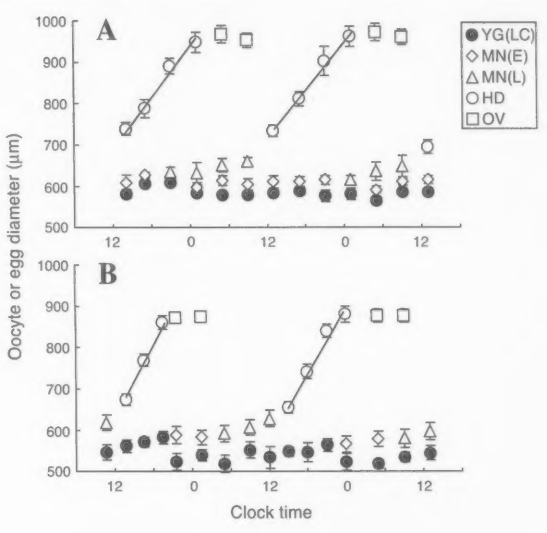

Figure 3

Diurnal changes in oocyte diameters at each developmental stage for individual Japanese flounder (*Paralichthys olivaceus*). (**A**) Experiment for fish no. 2, conducted between 30 May and 1 June in 2005 at 11.3°C. (**B**) Experiment for fish no. 3, conducted between 20 and 22 July in 2005 at 16.9°C. Bars indicate standard deviation. The slopes of regression lines for HD-stage oocytes represent the growth rate of hydrated oocytes. OV=ovulated egg; HD=oocyte at hydrated stage; MN(L)=at late migratory nucleus stage; MN(E)=at early migratory nucleus stage; and YG(LC)=the leading cohort of oocytes at yolk granule stage.

mm, 11.2≤T≤16.9°C, n=6: Table 2) by ANCOVA. We could not examine the effect of other females because the overlap of temperature was narrow.

Results

Experiments

The growth rates of oocytes at MN(L), MN(E), and YG(LC) stages were slow, whereas the growth rate of HD-stage oocytes was rapid (Fig. 3). At the lower temperature, HD- and MN-stage oocytes, or MN(L)- and MN(E)-stage oocytes coexisted, indicating that the two batches of oocytes entered the final maturation process at the same time (Figs. 2 and 3).

In five out of ten 48-h experiments, final maturation processes were observed twice at about 24-h interval (Figs. 2 and 3). In the other five 48-h experiments, the final maturation process occurred only once on the first day of each experiment. Once a batch of oocytes entered the final maturation process, these oocytes completed final maturation to be ovulated.

Although females spawned naturally in the tank for their spawning periods of 2–3 months, they could not spawn naturally during the 48-h experiments. They could only ovulate oocytes into their ovarian cavity.

Duration of each spawning marker

The duration of each spawning marker changed considerably with temperature. The durations of oocytes at the MN(E) and MN(L) stages, and POF(new) decreased exponentially from 24 to 3 h, 16 to 4 h, and 16 to 4 h, respectively, for the established temperature ranges (9.2° or 11.3° to 22.6°C; Fig. 4). Duration of these markers decreased by a factor of 0.16, 0.36, 0.31, respectively, as temperature increased by 10°C (Table 3).

The growth rate of hydrated oocyte diameter (G_{HD}, in µm/h) increased exponentially as temperature (T) increased (Fig. 5) as follows:

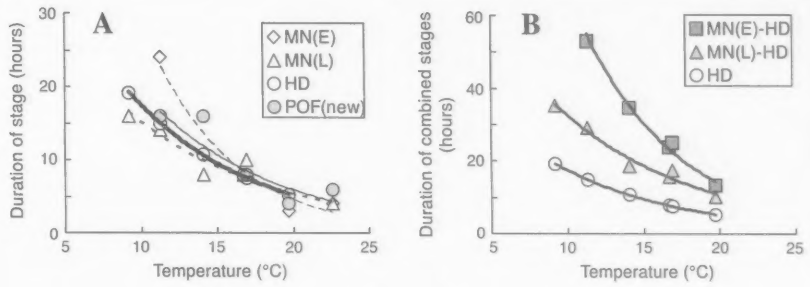

Figure 4

(**A**) Duration of oocytes at each developmental stage and new postovulatory follicles and (**B**) combined developmental stages in relation to temperature for Japanese flounder (*Paralichthys olivaceus*). MN(E)=oocyte at early migratory nucleus stage; MN(L)=at late migratory nucleus stage; HD=at hydrated stage; POF(new)=new postovulatory follicles; MN(E)-HD=combined stages of MN(E), MN(L), and HD; MN(L)-HD=combined stages of MN(L) and HD. Statistics for regression lines are shown in Table 3.

$$G_{HD} = 8.66\ e^{0.0799T},$$
$$(9.2 \leq T \leq 19.6°C,\ n=20,\ r^2=0.937,\ P<0.001). \quad (2)$$

Thus, growth rate increased by a factor of 2.2 as temperature increased by 10°C. Body size and individual effects on the relationship between the growth rate of hydrated oocytes and temperature were not observed (body size effect; multiple regression analysis, $P=0.12$: individual effect; ANCOVA, slope, $P=0.29$; intercept, $P=0.75$).

Ovulated egg diameters (*ED*, µm), as a substitution for the maximum hydrated oocyte diameter, decreased from 980 to 830 µm as temperature increased (Fig. 6) as follows:

$$ED = -11.8T + 1099,$$
$$(9.2 \leq T \leq 22.6°C,\ n=7,\ r^2=0.975,\ P<0.001). \quad (3)$$

The largest diameter of oocytes at the MN(L) stage, as a substitution for the minimum hydrated oocyte diameter, did not decrease significantly with temperature ($9.2 \leq T \leq 19.6°C$, $n=6$) and averaged 645 µm. Thus, the ranges of hydrated oocyte diameter also decreased linearly from 345 to 220 µm as temperature increased from 9.2° to 19.7°C (Fig. 6). As a result, the duration of the HD stage, i.e., the range of hydrated oocyte diameter divided by the growth rate of hydrated oocytes, also decreased exponentially from 19.1 to 5.3 h as temperature increased from 9.2° to 19.7°C (Fig. 4, Table 3). Duration of this stage decreased by a factor of 0.30 as temperature increased by 10°C.

The duration of combined spawning markers, i.e., MN(L) + HD stages and MN(E) + MN(L) + HD stages, also decreased exponentially from 35.1 to 10.3 h (9.2–19.7°C) and 53.0 to 13.3 h (11.3–19.7°C), respectively (Fig. 4, Table 3).

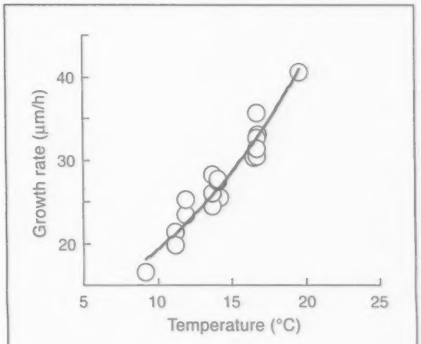

Figure 5

Relationship between growth rate of oocyte diameter during hydration and temperature for Japanese flounder (*Paralichthys olivaceus*). Each data point represents one hydration event. See Equation 2 in the main text.

Discussion

In this study, we clearly show that duration of spawning markers, i.e., oocytes at the MN(E), MN(L), and HD stages, and the POF(new) stage, largely varied because of water temperature. The duration of a marker affects estimates of spawning frequency according to Equation 1 and can have large effects if fixed spawning markers are used for a range of ambient temperatures. The duration of spawning markers decreased exponentially as temperature increased. Thus, estimates of spawning frequency per day in colder and warmer waters tend to be overestimated and underestimated, respectively, if the effect of temperature on marker duration is not

considered and if a constant estimate of duration is used. In the case of Japanese flounder, the duration of the HD stage decreased from 19.1 to 5.3 h between 9.2° and 19.7°C. If an HD-stage oocyte is used as a spawning marker and 2 out of 10 sampled females have HD-stage oocytes in their ovaries, the estimated spawning frequency by Equation 1 will be very different, i.e., 0.25 at 9.2°C and 0.91 at 19.7°C, leading to answers that differ by a factor of 3.6 (=[0.2×24/5.3]/[0.2×24/19.1]).

Each spawning marker has advantages and disadvantages for estimating spawning frequency. The merit of using POFs as spawning markers is that females with day-1 or day-2 old POFs are usually found away from spawning aggregations and estimates of spawning frequency are therefore less biased (Hunter and Goldberg, 1980; Picquelle and Stauffer, 1985; Ganias et al., 2003). However, aging or staging is difficult because the process of degeneration is continuous (Ganias et al., 2003). On the other hand, the merit of using oocytes at the MN and HD stages as spawning markers is that aging or staging is easy. However, in some cases estimates of spawning frequency with the MN- or HD-stage oocytes provide biased estimates because of the nonuniformity of their distribution, i.e., during spawning aggregations. Therefore, in cases where fish populations spawn within a restricted period of a few hours, as occurs with some clupeid fish populations (Stratoudakis et al., 2006) and sampling is also conducted within a restricted time period, the POF is an appropriate spawning marker because staging is easier as the age of POF appears intermittently (Hunter and Goldberg, 1980; Hunter and Macewicz, 1985). But when fish spawn over a prolonged period (over many hours in a day) at the population level, or when sampling time is not restricted to a short period, oocyte at the MN or HD stage is appropriate spawning marker because aging or staging is much easier than POFs, and the use of Equation 1 is recommended. Even in species that form spawning aggregations around spawning events, a MN-stage oocyte may be a useful spawning marker because oocytes at the MN stage appear several hours before spawning and the duration of the MN stage is relatively long. In any case, precise evaluation of the duration of a marker and its changes due to ambient temperature is essential, especially for species that spawn over long time periods within a day.

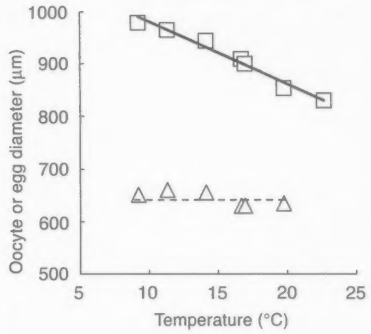

Figure 6

Changes in the range (from the minimum to the maximum) of sizes of oocytes at the hydrated stage (HD) as a function of temperature (T) for Japanese flounder (*Paralichthys olivaceus*). The minimum and maximum sizes of oocytes at the HD stage were replaced with the maximum size of oocytes at the late migratory nucleus stage (△), and with the average diameter of ovulated eggs (□), respectively, in a 48-h experiment at each temperature. The broken line shows the average diameter of the maximum sizes of oocytes at the late migratory nucleus stage (645 μm) and the solid line shows the regression line for the diameter of ovulated eggs. See Equation 3 in the main text.

Table 3

Parameters of equations used to determine stage duration (D) at temperature (T); $D=a\times e^{-bT)}$ for Japanese flounder (*Paralichthys olivaceus*) with statistics (n=number of data points; r^2=coefficient of determination; P=probability of error in the regressions). The reduction rate of D for an increase in temperature of 10°C ($D_{(T+10)}/D_T$) is also shown. MN(E)=at early migratory nucleus stage; MN(L)=at late migratory nucleus stage; HD=at hydrated stage; POF(new)=new postovulatory follicle.

Stages	a	b	$D_{(T+10)}/D_T$	n	r^2	P
MN(E)	186	0.186	0.16	6	0.88	0.006
MN(L)	42.4	0.103	0.36	7	0.90	0.001
HD(calculated)[1]	59.4	0.122	0.30	6	1.00	<0.001
POF(new)	62.9	0.118	0.31	6	0.74	0.028
MN(L) + HD	98.4	0.111	0.33	6	0.96	<0.001
MN(E) + MN(L) + HD	332	0.159	0.20	5	0.98	0.001

[1] Stage duration at each temperature was calculated with the size range and the growth rate of HD-stage oocytes (Eq. 2).

To our knowledge, this is the first report to clearly illustrate the duration and growth rate of oocytes during final maturation, on an individual-fish basis, in relation to ambient water temperature. Final maturation, in this study, is considered to have progressed normally for the following three reasons, although successive sampling in general would produce strong stress on animals. First, past *in vitro* incubation experiments of Japanese flounder at 15°C have shown that the duration of the HD stage is 12 hours and the duration of the final maturation process is about 33 hours (Matsubara et al., 1995). These results are comparable to ours, namely that the estimated duration of the HD stage is 10 hours and the duration of final maturation (MN[E], MN[L], and HD stages) is 30 hours at 15°C. Second, other studies also have reported the negative relationship between the duration of final maturation (from injection of pituitary extracts or gonadotropin-releasing hormone [GnRH] to ovulation) and ambient water temperature (common carp [*Cyprinus carpio*], Drori et al., 1994; streaked prochilod [*Prochilodus platensis*], Fortuny et al., 1988) as seen in this study. Third, hydration is driven by the osmotic gradient caused by protein hydrolysis of yolk and ion accumulation through many enzyme catalyses (Cerdà et al., 2007). The rate of enzyme catalysis increases as temperature increases, within a range of appropriate temperatures. Therefore, it is reasonable that the growth rate of hydrated oocytes increases, or in other words, duration of this stage decreases as ambient water temperature increases.

In some trials, females did not produce a new batch of oocytes that entered the final maturation process during the 48-h experiment period, probably because of the stress experienced during the sampling procedure. However, once a batch of oocytes entered the MN stage, those oocytes completed final maturation and proceeded to ovulation, even when under the stressful conditions of the experiments. This finding indicates that GnRH or gonadotropin secretion, which induce a batch of oocytes to proceed to final maturation, is likely susceptible to stress, but the process of the final maturation of oocytes is less susceptible, at least for Japanese flounder. In addition, fish could ovulate oocytes but could not spawn them during the 48-h experiment period. Spawning behaviour or the endocrine control of spawning, or both, are also likely susceptible to stress.

Successive sampling of oocytes from individual females with a catheter is a useful method for clarifying the diurnal rhythm of the final maturation of fish species, especially those with a long spawning time distribution within a day at the population level. However, careful consideration should be paid for reducing stress to fish during the sampling procedure. Anesthetizing and handling seem to be the main sources of stress. In this study, we tried to reduce stress by weakly anesthetizing fish for a short duration. We also did not use a scoop net to pick up fish because the fish would move around in the tank to escape the net and struggle in the net, both of which would cause undue stress and physical injury to the fish, e.g., injuries to their body surface and internal bleeding. Instead, we lowered the water level of the tank, gently picked up the fish, placing both hands under its body, put it into a crate made of styrene foam, which floated on the surface of water, carried the crate with the fish and placed the fish in a bath filled with 0.08% 2-phenoxyethanol sea water without touching the fish. During this procedure, the fish did not struggle much and seemed to be less stressed. We also experimented with taking ovary samples by cannulation without anaesthesia; i.e., we picked up the fish with both hands placed under its body, put it on a board floating on the surface of water, and then took samples of oocytes. These operations took 10–20 seconds and females stayed still on the board. The latter method seemed to be a better procedure to reduce stress.

Spawning frequency is, in general, estimated by using the fraction of fish with a spawning marker and the duration of the marker as seen in Equation 1 (Priede and Watson, 1993; Murua et al., 2003). Duration of oocytes at the MN and HD stages, in addition to POFs (Fitzhugh and Hettler, 1995; Ganias et al., 2007), changes as temperature changes. Thus, accurate estimates of the duration of a marker in relation to temperature are essential for estimating spawning frequency accurately, especially for those fish species that have long spawning-time distribution within a day at the population level and experience a wide range of ambient water temperatures during their long spawning season.

Acknowledgments

We thank the staff at Miyako National Center for Stock Enhancement for their help with the experiments. We are grateful to K. X. Pham for his assistance in the experiments. We are also grateful to T. Matsubara and M. Matsuyama for providing valuable information and to four anonymous referees for their valuable reviews of an earlier version of the manuscript. This work was supported by a grant-in-aid from the Fisheries Research Agency of Japan. This contribution is catalogued as B127 by the Tohoku National Fisheries Research Institute.

Literature cited

Allain, G., P. Petitgas, and P. Lazure.
2007. The influence of environment and spawning distribution on the survival of anchovy (*Engraulis encrasicolus*) larvae in the Bay of Biscay (NE Atlantic) investigated by biophysical simulations. Fish. Oceanogr. 16:506–514.

Cerdà, J., M. Fabra, and D. Raldúa.
2007. Physiological and molecular basis of fish oocyte hydration. *In* The fish oocyte: from basic studies to biotechnological applications (P. J. Babin, J. Cerdà, and E. Lubzens, eds.), p. 349–396. Springer-Verlag, Dordrecht, The Netherlands.

Drori, S., M. Ofie, B. Levavi-Sivan, and Z. Yaron.
1994. Spawning induction in common carp (*Cyprinus carpio*) using pituitary extract or GnRH superactive analogue combined with metoclopramide: analysis of hormone profile, progress of oocyte maturation and dependence on temperature. Aquaculture 119:393–407.

Ferraro, S. P.
1980. Daily time of spawning of 12 fishes in the Peconic Bays, New York. Fish. Bull. 78:455–464.

Fitzhugh, G. R., and W. F. Hettler.
1995. Temperature influence on postovulatory follicle degeneration in Atlantic menhaden, *Brevoortia tyrannus*. Fish. Bull. 96:568–572.

Fortuny, A., A. Espinach Ros, and V. G. Amutio.
1988. Hormonal induction of final maturation and ovulation in the Sábalo, *Prochilodus platensis* Holmberg: treatments, latency and incubation times and viability of ovules retained in the ovary after ovulation. Aquaculture 73:373–381.

Funamoto, T., and I. Aoki.
2002. Reproductive ecology of Japanese anchovy off the Pacific coast of eastern Honshu, Japan. J. Fish Biol. 60:154–169.

Ganias, K., C. Nunes, and Y. Stratoudakis.
2007. Degeneration of postovulatory follicles in the Iberian sardine *Sardina pilchardus*: structural changes and factors affecting resorption. Fish. Bull. 105:131–139.

Ganias, K., S. Somarakis, A. Machias, and A. J. Theodorou.
2003. Evaluation of spawning frequency in a Mediterranean sardine population (*Sardina pilchardus sardina*). Mar. Biol. 142:1169–1179.

Hirano, R., and E. Yamamoto.
1992. Spawning rhythm and egg number at the individual female spawning experiment in the hirame flounder, *Paralichthys olivaceus*. Bull. Tottori Pref. Fish. Exp. Stn. 33:18–28.

Hunter, J. R., and S. R. Goldberg.
1980. Spawning incidence and batch fecundity in northern anchovy, *Engraulis mordax*. Fish. Bull. 77:641–652.

Hunter, J. R., and B. J. Macewicz.
1985. Measurement of spawning frequency in multiple spawning fishes. *In* An egg production method for estimating spawning biomass of pelagic fish: application to the northern anchovy, *Engraulis mordax* (R. Lasker, ed.), p. 79–94. NOAA Tech. Rep. NMFS 36.

Kennedy, J., P. R. Witthames, R. D. M. Nash, and C. J. Fox.
2008. Is fecundity in plaice (*Pleuronectes platessa* L.) down-regulated in response to reduced food intake during autumn? J. Fish Biol. 72:78–92.

Kjesbu, O. S.
1994. Time of start of spawning in Atlantic cod (*Gadus morhua*) females in relation to vitellogenic oocyte diameter, temperature, fish length and condition. J. Fish Biol. 45:719–735.

Kjesbu, O. S., H. Kryvi, and B. Norberg.
1996a. Oocyte size and structure in relation to blood plasma steroid hormones in individually monitored, spawning Atlantic cod. J. Fish Biol. 49:1197–1215.

Kjesbu, O. S., P. Solemdal, P. Bratland, and M. Fonn.
1996b. Variation in annual egg production in individual captive Atlantic cod (*Gadus morhua*). Can. J. Fish. Aquat. Sci., 53:610–620.

Kjesbu, O. S., P. R. Witthames, P. Solemdal, and M. Greer Walker.
1998. Temporal variations in the fecundity of Arcto-Norwegian cod (*Gadus morhua*) in response to natural changes in food and temperature. J. Sea Res. 40:303–321.

Kurita, Y., and O. S. Kjesbu.
2009. Fecundity estimation by oocyte packing density formulae in determinate and indeterminate spawners: theoretical considerations and applications. J. Sea Res. 61:188–196.

Lasker, R.
1985. Introduction: an egg production method for anchovy biomass assessment. *In* An egg production method for estimating spawning biomass of pelagic fish: application to the northern anchovy, *Engraulis mordax* (R. Lasker, ed.), p. 1–4. NOAA Tech. Rep. NMFS 36.

Marteinsdottir, G., and G. A. Begg.
2002. Essential relationships incorporating the influence of age, size and condition on variables required for estimation of reproductive potential in Atlantic cod *Gadus morhua*. Mar. Ecol. Prog. Ser. 235:235–256.

Matsubara, T., S. Adachi, S. Ijiri, and K. Yamauchi.
1995. Changes of lipovitellin during *in vitro* oocytes maturation in Japanese flounder *Paralichthys olivaceus*. Fish. Sci. 61:478–481.

Matsuyama, M., S. Adachi, Y. Nagahama, and S. Matsuura.
1988. Diurnal rhythm of oocyte development and plasma steroid hormone levels in the female red sea bream, *Pagrus major*, during the spawning season. Aquaculture 73:357–372.

Matsuyama, M., S. Onozato, and M. Kashiwagi.
2002. Endocrine control of diurnal oocyte maturation in the kyusen wrasse, *Halichoeres poecilopterus*. Zool. Sci. 19:1045–1053.

Motos, L.
1996. Reproductive biology and fecundity of the Bay of Biscay anchovy population (*Engraulis encrasicolus* L.). Sci. Mar. 60 (suppl. 2):195–207.

Murua, H., G. Kraus, F. Saborido-Rey, P. R. Witthames, A. Thorsen, and S. Junquera.
2003. Procedures to estimate fecundity of marine fish species in relation to their reproductive strategy. J. Northw. Atl. Fish. Sci. 33:33–54.

Murua, H., and F. Saborido-Rey.
2003. Female reproductive strategies of marine fish species of the North Atlantic. J. Northw. Atl. Fish. Sci. 33:23–31.

Nichols, J. H.
1989. The diurnal rhythm in spawning of plaice (*Pleuronectes platessa* L.) in the southern North Sea. J. Cons. Int. Explor. Mer 45:277–283.

Nichols, J. H., and S. Warnes.
1993. Field observations of the daily pattern of spawning in the western stock of mackerel (*Scomber scombrus* L.). ICES J. Mar. Sci. 50:219–225.

Nishimura, A., T. Hamatsu, O. Shida, I. Mihara, and T. Mutoh.
2007. Interannual variability in hatching period and early growth of juvenile walleye pollock, *Theragra chalcogramma*, in the Pacific coastal area of Hokkaido. 2007. Fish. Oceanogr. 16:229–239.

Parker, K.
1980. A direct method for estimating northern anchovy, *Engraulis mordax*, spawning biomass. Fish. Bull. 78:541–544.

Picquelle, S., and G. Stauffer.
1985. Parameter estimation for an egg production method of northern anchovy biomass assessment. *In* An egg production method for estimating spawning biomass of pelagic fish: application to the northern anchovy,

Engraulis mordax (R. Lasker, ed.), p. 7–15. NOAA Tech. Rep. NMFS 36.

Priede, I. G., and J. J. Watson.
1993. An evaluation of the daily egg production method for estimating biomass of Atlantic mackerel (*Scomber scombrus*). Bull. Mar. Sci. 53:891–911.

Scott, B. E., G. Marteinsdottir, G. A. Begg, P. J. Wright, and O. S. Kjesbu.
2006. Effects of population size/age structure, condition and temporal dynamics of spawning on reproductive output in Atlantic cod (*Gadus morhua*). Ecol. Model. 191:383–415.

Scott, S. G., J. R. Zeldis, and N. W. Pankhurst.
1993. Evidence of daily spawning in natural populations of the New Zealand snapper *Pagrus auratus* (Sparidae). Environ. Biol. Fish. 36:149–156.

Secor, D. H.
2007. The year-class phenomenon and the storage effect in marine fishes. J. Sea Res. 57:91–103.

Shiraishi, T., K. Ohta, A. Yamaguchi, M. Yoda, H. Chuda, and M. Matsuyama.
2005. Reproductive parameters of the chub mackerel *Scomber japonicus* estimated from human chorionic gonadotropin-induced final oocyte maturation and ovulation in captivity. Fish. Sci. 71:531–542.

Somarakis, S., K. Ganias, A. Siapatis, C. Koutsikopoulos, A. Machias, and C. Papaconstantinou.
2006. Spawning habitat and daily egg production of sardine (*Sardina pilchardus*) in the eastern Mediterranean. Fish. Oceanogr. 15:281–292.

Somarakis, S., I. Palomera, A. Garcia, L. Quintanilla, C. Koutsikopoulos, A. Uriarte, and L. Motos.
2004. Daily egg production of anchovy in European waters. ICES J. Mar. Sci. 61:944–958.

Stratoudakis, Y., M. Bernal, K. Ganias, and A. Uriarte.
2006. The daily egg production method: recent advances, current applications and future challenges. Fish Fish. 7:35–57.

Takeno, K., Y. Hamanaka, I. Kinoshita, and T. Miyajima.
1999. Maturity of the Japanese flounder *Paralichthys olivaceus* in western Wakasa Bay, the Japan Sea. Nippon Suisan Gakkaishi 65:1023–1029.

Walsh, M, and A. D. F. Johnstone.
1992. Spawning behaviour and diel periodicity of egg production in captive Atlantic mackerel, *Scomber scombrus* L. J. Fish Biol. 40:939–950.

Witthames, P. R., A. Thorsen, and O. S. Kjesbu.
2010. The fate of vitellogenic follicles in experimentally monitored Atlantic cod *Gadus morhua* (L.): application to stock assessment. Fish. Res. 104:27–37.

Wright, P. J., and F. M. Gibb.
2005. Selection for birth date in North Sea haddock and its relation to maternal age. J. Anim. Ecol. 74:303–312.

Wright, P. J., and E. A. Trippel.
2009. Fishery-induced demographic changes in the timing of spawning: consequences for reproductive success. Fish Fish. 10:283–304.

Integrating methods for determining length-at-age to improve growth estimates for two large scombrids

Aaron C. Ballagh (contact author)[1,*]
David Welch[1,2]
Ashley J. Williams[1,3]
Amos Mapleston[1]
Andrew Tobin[1]
Nicholas Marton[4]

Email address for contact author: aaron.ballagh@jcu.edu.au

[1] Fishing and Fisheries Research Centre
School of Earth and Environmental Sciences
James Cook University
Townsville, Queensland 4811, Australia
*Present address for contact author: Research Services
James Cook University
Townsville, Queensland 4811 Australia

[2] Queensland Primary Industries and Fisheries
Department of Employment, Economic Development and Innovation
P.O. Box 1085
Oonoonba, Queensland 4811, Australia

[3] Oceanic Fisheries Programme
Secretariat of the Pacific Community BP D5
98848 Noumea CEDEX, New Caledonia

[4] Australian Bureau of Agricultural and Resource Economics–Bureau of Rural Sciences
Department of Agriculture, Fisheries and Forestry
GPO Box 1563
Canberra, Australian Capital Territory 2601, Australia

Abstract—Fish growth is commonly estimated from length-at-age data obtained from otoliths. There are several techniques for estimating length-at-age from otoliths including 1) direct observed counts of annual increments; 2) age adjustment based on a categorization of otolith margins; 3) age adjustment based on known periods of spawning and annuli formation; 4) back-calculation to all annuli, and 5) back-calculation to the last annulus only. In this study we compared growth estimates (von Bertalanffy growth functions) obtained from the above five methods for estimating length-at-age from otoliths for two large scombrids: narrow-barred Spanish mackerel (*Scomberomorus commerson*) and broad-barred king mackerel (*Scomberomorus semifasciatus*). Likelihood ratio tests revealed that the largest differences in growth occurred between the back-calculation methods and the observed and adjusted methods for both species of mackerel. The pattern, however, was more pronounced for *S. commerson* than for *S. semifasciatus*, because of the pronounced effect of gear selectivity demonstrated for *S. commerson*. We propose a method of substituting length-at-age data from observed or adjusted methods with back-calculated length-at-age data to provide more appropriate estimates of population growth than those obtained with the individual methods alone, particularly when faster growing young fish are disproportionately selected for. Substitution of observed or adjusted length-at-age data with back-calculated length-at-age data provided more realistic estimates of length for younger ages than observed or adjusted methods as well as more realistic estimates of mean maximum length than those derived from back-calculation methods alone.

Manuscript submitted 6 January 2010.
Manuscript accepted 25 October 2010.
Fish. Bull. 109:90–100 (2011).

The views and opinions expressed or implied in this article are those of the author (or authors) and do not necessarily reflect the position of the National Marine Fisheries Service, NOAA.

Growth is perhaps the most studied of all parameters used to describe the life history of exploited fish. Growth is usually expressed as a mathematical equation describing the mean growth of a population and relating size to age (Katsanevakis and Maravelias, 2008). An understanding of growth is fundamental for population modeling, stock assessments, and managing exploited species (Gulland, 1988). The methods used to estimate growth in fish vary significantly with the type of data being used. The most commonly used data for estimating fish growth is length-at-age data, although length-frequency data and mark recapture data are also used (Francis, 1988; Labelle et al., 1993). Counts of periodic growth increments observed in otoliths or other hard parts are predominantly used to estimate fish age (Begg et al., 2005; Campana, 2005), and a range of growth models have been developed to be fitted to length-at-age data (e.g., Ricker, 1979; Schnute, 1981). However, length-at-age estimates are not always collected or treated in the same way, either because of sampling bias or differences in aging protocols, and it is often unknown to what degree differences in length-at-age estimation methods affect parameter estimates from growth models.

Obtaining length-at-age data from otoliths is not always as simple as counting the number of growth increments (Francis et al., 1992; Campana, 2001), and many methods have been used to obtain length-at-age data such as image analysis (e.g., Fablet, 2006), back-calculation (e.g., Campana, 1990; Secor and Dean, 1992), otolith weight and morphometric relationships (e.g., Lou et al., 2005; Steward et al., 2009), length-mediation (e.g., Francis et al., 2005), and age adjustment (e.g., DeVries and Grimes, 1997; Williams et al., 2005; Williams et al., 2008). A combination of methods have been used in studies to estimate growth, where methods such as

back-calculation allow the estimation of lengths-at-ages that are rarely observed, particularly in the absence of a representative sample because of gear selectivity (Lopez-Abellan et al., 2008), or to increase the amount of length-at-age data to be used in fitting a growth curve (e.g., Shafi and Jasim, 1982; Grudtsev and Korolevich, 1986).

Temporal and spatial variation in growth can have significant implications for the assessment and management of exploited populations (Rahikainen and Stephenson, 2004). However, variation in growth from estimation error is also likely to have significant implications for stock assessment, and accounting for bias in growth estimation is not always feasible (Gwinn et al., 2010). Substantial differences in growth estimates have previously been demonstrated from different methods for determining length-at-age from otoliths and other hard parts (e.g., Lucena and O'Brien, 2001; Ballagh et al., 2006). We examine the effects of several different methods for determining length-at-age from otoliths.

Here we compared estimates of growth derived from several commonly used methods for obtaining length-at-age data from otoliths. We applied this approach to the otoliths of two large scombrids, narrow-barred Spanish mackerel (*Scomberomorus commerson*) and broad-barred king mackerel (*Scomberomorus semifasciatus*), to test for differences in growth attributable to the methods used, and to make inferences about which method(s) provides the most appropriate estimate of length-at-age for growth estimation. *Scomberomorus commerson* and *S. semifasciatus* are fast growing species and it was expected that differences in growth estimates from different length-at-age data would be clearer than those for slower growing species. We also examined the effects on growth estimates when length-at-age data from different methods are combined, such as when back-calculated and observed length-at-age data are combined (e.g., Lopez-Abellan et al., 2008).

Materials and methods

Samples of *S. commerson* were collected from several locations along the east coast of Queensland from commercial and recreational fishermen using various hook-and-line gears, and *S. semifasciatus* samples were collected from the east coast of Queensland, Gulf of Carpentaria, and the Northern Territory from commercial fishermen using gillnets of various mesh sizes. A small number of juveniles of each species were collected by beam trawl from the east coast of Queensland.

Length-at-age and growth

For each mackerel species five methods of determining length-at-age from otoliths were investigated: observed (Obsv); category-adjusted (Adj-cat); formula-adjusted (Adj-frm); back-calculation to all annuli (BC-all); and back-calculation to the last annulus only (BC-last).

Table 1

Description of otolith margin categories used in age adjustment of *Scomberomorus commerson* and *S. semifasciatus*.

Margin category	Description
0	Complete and continuous opaque band formed around edge of otolith, and no translucent material beyond the last opaque band
I	Translucent band laid onto the outer edge comprising 1/4–1/3 the width of the previous translucent band
II	Translucent band laid onto outer edge comprising roughly ½ the width of the previous translucent band
III	Opaque band present on edge; however, is not continuous or complete

Otoliths were aged, measured, and back-calculation of previous length-at-age for both species was done by using identical methods (Ballagh et al., 2006; Tobin and Mapleston[1]; Welch et al.[2]). Observed length-at-age was defined as the agreed upon count of complete opaque increments (annuli) from multiple readings (up to three) of each otolith, coupled with the fork length of the fish at capture. Back-calculation of previous length-at-age was done by using the body proportional hypothesis described by Francis (1990) with the parameters from linear geometric mean regression of otolith radius on fork length (e.g., Ballagh et al., 2006).

Two methods for age adjustment were investigated in this study: category adjustment, and formula adjustment. Category adjustment was based on simple criteria whereby the observed age of each otolith was adjusted for the marginal increment at the outer edge of the otolith, which was categorized according to a system (margin category, Table 1, Fig. 1). Otoliths for which there was agreement in the annuli count were assigned a final margin category if any two of the margin categories from multiple readings for a single otolith were the same. For final margin categories of 0 or I, no age adjustment was deemed necessary and the agreed upon count of annuli was accepted as the

[1] Tobin, A. J., and A. Mapleston. 2004. Exploitation dynamics and biological characteristics of the Queensland East Coast Spanish mackerel (*Scomberomrous commerson*) fishery. CRC Reef Research Centre Technical Report No 51, 61 p. CRC Reef Research Centre, Townsville, Australia.

[2] Welch, D. J., R. C. Buckworth, J. R. Ovenden, S. J. Newman, D. Broderick, R. J. G. Lester, A. C. Ballagh, J. M. Stapley, R. A. Charters, and N. A. Gribble. 2009. Determination of management units for grey mackerel fisheries in northern Australia. Final Report, Fisheries Research and Development Corporation Project 2005/010. Fishing and Fisheries Research Centre Technical Report No. 4, 158 p. Fishing and Fisheries Research Centre, James Cook University, Townsville, Australia.

final age because marginal increment growth beyond a complete annulus, and thus a whole year, was considered to be negligible. Final margin categories of II were considered to be closer to half a complete annulus, and thus the equivalent of growth for half a year, and therefore the age was adjusted by adding 0.5 to the count of annuli to give the final age. For otoliths with a final margin category of III, the marginal increment was considered to be close to a whole annulus and therefore the age was adjusted by adding one to the agreed upon count of annuli. For otoliths with margin categories that were not the same, the higher of the category estimates was accepted as the final margin category and age was adjusted accordingly.

For otoliths with no agreed upon age, it was still possible to assign an adjusted age in some cases on the basis of the margin increment category and the age estimates. If multiple age estimates were no more than one year apart, the margin category of the higher age was 0 or I, and the margin category for the lower age estimate was III, the adjusted age was accepted as the higher of the two age estimates. If there was still no agreement between readings on ages and margin categories, the otolith was rejected for age adjustment. Less than 0.5% of all otoliths were rejected for age adjustment.

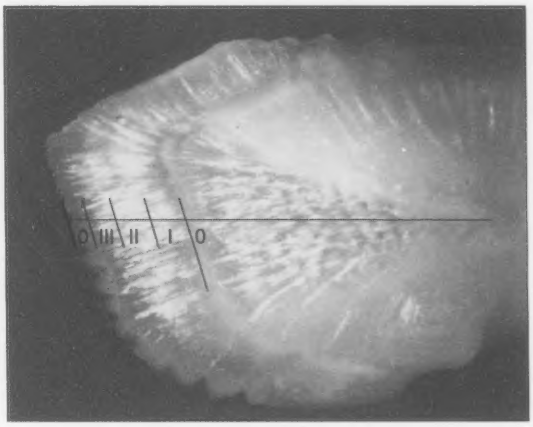

Figure 1

Otolith of narrow-barred Spanish mackerel (*Scomberomorus commerson*), showing the margin categories used in age adjustment (see Table 1). In this example a complete opaque band (annulus) is visible at the otolith margin (margin category=0, adjusted age=2).

Formula adjustment was based on a modification of the age adjustment algorithms used in Williams et al. (2008). The age adjustment formula corrected for the collection of samples across different months of the year by adjusting observed-age estimates to account for the period of annuli formation, spawning period (birth date), and the date of capture. The following algorithms were used to adjust age estimates:

$$\text{If } N = 0,\ age_m = m_c, \tag{1}$$

$$\text{If } N > 0,\ age_m = \left((N-1)\times 12\right) + m_b + m_c, \tag{2}$$

where N = number of complete annuli;
age_m = age in months;
m_b = number of months from the assigned birth date to the assigned date of annuli formation; and
m_c = number of months from the assigned date of annuli formation to the date of capture.

It was inferred from previous studies that the period of annuli formation coincides with the spawning period for both species (McPherson, 1992, 1993; Tobin and Mapleston[1]; Welch et al.[2]; Cameron and Begg[3]). The birth date and date of annulus completion was assigned as 1 November, which represents the mid spawning period for both species (McPherson, 1993; Welch et al.[2]; Cameron and Begg[3]). As a result, the time between spawning (birth date) and the timing of annuli formation (m_b) was assigned as 12 months.

All analyses were done separately for females and males as previous studies have shown both species have sexually dimorphic growth (McPherson, 1992; Ballagh et al., 2006; Welch et al.[2]; Cameron and Begg[3]). The von Bertalanffy growth function (VBGF, Beverton and Holt, 1957) was used to describe the growth of both species for all length-at-age data and is described by the following equation:

$$L_t = L_\infty\left(1 - e^{(-K(t-t_0))}\right), \tag{3}$$

where L_t = length at age t;
L_∞ = theoretical maximum length;
K = growth coefficient or the rate at which L_∞ is asymptotically reached; and
t_0 = theoretical age where length is equal to zero.

VBGF curves were fitted to length-at-age data by nonlinear regression. Likelihood ratio tests (Kimura, 1980) were used to test for differences in growth among the different methods for estimating length-at-age for both species. Likelihood ratio tests were used to test for overall differences in growth (all parameters assumed equal), as well as differences in individual parameters of the VBGF. Data were truncated for all likelihood ratio tests so that equivalent age ranges were compared (Haddon, 2001). Where differences were found, multiple comparisons were performed by using likelihood

[3] Cameron, D., and G. Begg. 2002. Fisheries biology and interaction in the northern Australian small mackerel fishery. Final report to the Fisheries Research and Development Corporation, projects 92/144 and 92/144.02, 236 p. Department of Primary Industries, Brisbane, Queensland, Australia.

ratio tests on pairs of individual methods. A Bonferroni adjustment was used for the multiple comparisons to account for inflation in the probability of a type-I error by adjusting the significance level:

$$\alpha_{adj} = \frac{\alpha}{n}, \quad (4)$$

where α = significance level;
α_{Adj} = adjusted significance level; and
n = number of multiple comparisons.

Selectivity effects

Mean back-calculated length-at-age from all annuli was compared to mean back-calculated length-at-age from the last annulus to infer if there were any selectivity effects that had biased the sample of each species, or if Lee's phenomenon (Ricker, 1969) was present. Lee's phenomenon, whereby lengths at early ages back-calculated from younger fish are greater than lengths at the same age estimated from older fish, has been shown to bias estimates of growth based on back-calculation of length-at-age by using all annuli (Vaughan and Burton, 1994). This bias can be a result of large otoliths in slow growing fish confounding the relationship between length and otolith size and resulting in relatively small back-calculated length-at-age for younger ages (Campana, 1990). However, it can also result from selectivity bias in the sample whereby the faster younger fish are disproportionately selected for by the fishing gears (Lucena and O'Brien, 2001; Ballagh et al., 2006) or where size-selective mortality has removed fast growing individuals from older age classes, thereby biasing the population demographics (Fossen et al., 1999). Differences in the mean back-calculated lengths-at-age from all annuli and the last annulus can therefore be used to infer any biases such as selectivity on sampling (Vaughan and Burton, 1994). Analysis of variance (ANOVA) and Student's t-test were used to compare mean back-calculated length-at-age from all annuli to mean back-calculated length-at-age from the last annulus only.

Substitution of data

Back-calculated lengths-at-age from all annuli were compared to observed lengths-at-age by using ANOVA and t-tests. Comparisons were made to determine the ages for which there were no differences between back-calculated and observed length-at-age to test the hypothesis that supplementing back-calculated length-at-age with observed or adjusted length-at-age can provide estimates of growth parameters that are more appropriate representations of the population (Ballagh et al., 2006). Observed and adjusted length-at-age data were substituted with back-calculated length-at-age data (BC-all and BC-last) for the first few consecutive ages that were significantly different from observed length-at-age. This procedure resulted in several combinations of data from different methods for determining length-at-age (back-calculated, observed, and adjusted), and is hereafter referred to as substitution.

VBGF curves were fitted to the substituted length-at-age data sets by using nonlinear regression. Likelihood ratio tests were performed to test for differences in growth among the different substituted combinations of length-at-age data. Where differences were found, multiple comparisons by using likelihood ratio tests with Bonferroni adjustments (Eq. 4) were performed on pairs of substituted data combinations.

Results

Growth

A high degree of variability was observed among the VBGF parameter estimates from the different methods for estimating length-at-age for both species and sexes (Table 2). The two back-calculation methods consistently yielded lower estimates of L_∞ and higher estimates of K and t_0 than the observed and adjusted methods. Less error was also observed in the estimates of L_∞ and t_0 for the back-calculated methods than for the observed and adjusted methods.

Comparison of the VBGF growth estimates by using overall likelihood ratio tests revealed significant differences in growth estimates among the methods for both species and sexes (*S. commerson* females: χ^2=678.9, df=12, P<0.0001, males: χ^2=704.4, df=12, P<0.0001; *S. semifasciatus* females: χ^2=849.4, df=12, P<0.0001, males: χ^2=913.1, df =12, P<0.0001). Multiple comparisons revealed some consistent patterns in growth estimates among methods (Table 3). Significant differences were observed between the back-calculation methods (BC-all, BC-last) and the adjusted and observed methods (Adj-cat, Adj-frm, Obsv), and no significant differences were found between the two back-calculation methods for both species. There were no significant differences between the two adjusted methods for both sexes of *S. commerson* and female *S. semifasciatus*, whereas the two adjusted methods differed significantly for male *S. semifasciatus*. No significant differences were found between the adjusted and observed methods for both species, with the exception of the formula adjusted and observed methods for female *S. commerson*.

Comparison of VBGF parameter estimates by using likelihood ratio tests revealed further differences (P<0.05, df=1) between the methods that differed in the overall likelihood ratio test comparisons. For *S. commerson*, all VBGF parameters differed significantly between individual methods with the exception of the formula adjusted and observed methods for females, for which none of the VBGF parameters differed significantly. For *S. semifasciatus*, significant differences were observed for all VBGF parameters in comparisons between the back-calculation methods and the adjusted and observed methods. No significant difference was observed between any of the VBGF parameter estimates for comparisons between observed and formula-

Table 2

Estimates for von Bertalanffy growth function parameters: growth coefficient (K), theoretical maximum length (L_∞), and theoretical age where length is equal to zero (t_0) (± standard error), sample numbers (n), age ranges, and adjusted R^2 values from different methods (observed [Obsv], category-adjusted [Adj-cat], formula adjusted [Adj-frm], back-calculation to all annuli [BC-all], and back-calculation to the last annulus only [BC-last]) for estimating length-at-age for *Scomberomorus commerson* and *S. semifasciatus*.

Species	Sex	Method	K	L_∞ (mm)	t_0 (years)	n	Min age	Max age	R^2_{adj}
S. commerson	Female	Obsv	0.16 (0.03)	1508 (153)	−4.55 (1.02)	288	1	15	0.7592
		Adj-cat	0.11 (0.03)	1725 (173)	−5.56 (1.08)	247	1	11	0.7806
		Adj-frm	0.10 (0.03)	1735 (186)	−5.86 (1.18)	239	1	11.9	0.7821
		BC-all	0.51 (0.03)	1248 (13)	−0.39 (1.06)	811	1	10	0.8473
		BC-last	0.45 (0.05)	1273 (25)	−0.68 (0.15)	216	1	10	0.8603
	Males	Obsv	0.21 (0.06)	1186 (109)	−5.77 (2.64)	213	1	11	0.8396
		Adj-cat	0.20 (0.06)	1202 (55)	−5.25 (1.58)	187	0.5	11	0.5715
		Adj-frm	0.21 (0.06)	1186 (47)	−5.18 (1.52)	187	0.8	11	0.586
		BC-all	0.75 (0.05)	1047 (9)	−0.18 (0.07)	601	1	9	0.588
		BC-last	0.74 (0.09)	1063 (15)	−0.27 (0.15)	157	1	9	0.8168
S. semifasciatus	Female	Obsv	0.29 (0.06)	896 (22)	−4.08 (0.78)	306	0	9	0.555
		Adj-cat	0.23 (0.06)	938 (38)	−4.64 (1.13)	310	1	9	0.5371
		Adj-frm	0.20 (0.06)	929 (41)	−5.40 (1.44)	306	0.6	9	0.4937
		BC-all	1.04 (0.05)	827 (6)	0.19 (0.04)	923	1	9	0.8243
		BC-last	0.99 (0.07)	834 (8)	0.15 (0.07)	289	1	9	0.797
	Males	Obsv	0.31 (0.04)	840 (13)	−3.87 (0.43)	323	0	10	0.7049
		Adj-cat	0.34 (0.04)	845 (14)	−2.86 (0.43)	325	0.5	10	0.6822
		Adj-frm	0.28 (0.04)	847 (16)	−3.77 (0.54)	323	0.5	10.6	0.661
		BC-all	1.04 (0.05)	781 (5)	0.14 (0.04)	974	1	10	0.8262
		BC-lLast	0.98 (0.07)	785 (6)	0.08 (0.07)	300	1	10	0.8268

Table 3

Chi-squared values for the overall likelihood ratio test between growth estimates from different methods (category adjusted [Adj-cat], formula adjusted [Adj-frm], back-calculation to all annuli [BC-all], back-calculation to the last annulus only [BC-lLast], and observed [Obsv]) for estimating length-at-age for *Scomberomorus commerson* and *S. semifasciatus* (* indicates significant difference at $P<0.005$, Bonfferoni-adjusted α for multiple comparisons, df=3).

Species	Sex	Method	Adj-frm χ^2	BC-all χ^2	BC-lLast χ^2	Obsv χ^2
S. commerson	Female	Adj-cat	1.2	197.1*	114.9*	9.2
		Adj-frm		162.6*	101.0*	13.6*
		BC-all			10.4	464.9*
		BC-last				229.9*
	Male	Adj-cat	0.575	158.3*	80.8*	5.4
		Adj-frm		161.6*	86.0*	8.1
		BC-all			12.0	496.7*
		BC-last				240.6*
S. semifasciatus	Female	Adj-cat	7.7	172.9*	167.3*	16.3*
		Adj-frm		139.8*	147.7*	23.7*
		BC-all			0.546	524.8*
		BC-last				350.9*
	Male	Adj-cat	16.6*	169.2*	174.4*	55.8*
		Adj-frm		102.9*	136.8*	43.6*
		BC-all			0.37	561.7*
		BC-last				434.0*

adjusted methods for both sexes and the observed and category-adjusted methods for female *S. semifasciatus*. Significant differences in the estimates of K and t_0 were observed between the observed and category-adjusted methods, and no significant difference was observed between any of the VBGF parameters for the two adjusted methods for male *S. semifasciatus*.

Selectivity effects

Comparison of length-at-age between the two back-calculation methods using ANOVA revealed significant differences in mean length-at-age existed for female *S. commerson* only ($F_{1,7}$=2.13, P=0.039). Multiple t-tests revealed differences in mean back-calculated length for age-1 female (t_{245}=3.94, P<0.001), and age-1 (t_{184}=2.68, P=0.008), and age-2 (t_{129}=2.38, P<0.019) male *S. commerson*.

Substitution of data

Comparison of length-at-age between the back-calculation to all annuli and observed methods with ANOVA revealed significant differences in mean length-at-age for both species and sexes (*S. commerson* females: $F_{1,9}$=32.3, P<0.001, males: $F_{1,8}$=37.8, P<0.001; *S. semifasciatus* females: $F_{1,8}$=52.5, P<0.001, males: $F_{1,9}$=53.9, P<0.001). For *S. commerson*, t-tests revealed differences in mean length between back-calculated and observed methods for the first four consecutive ages for both sexes (females age 1: t_{332}=20.39, P<0.001, age 2: t_{218}=5.44, P<0.001, age 3: t_{132}=2.14, P=0.034, age 4: t_{140}=3.54, P<0.001; males age 1: t_{242}=17.72, P<0.001, age 2: t_{172}=8.61, P<0.001, age 3: t_{104}=3.64, P<0.001, age 4: t_{103}=3.94, P<0.001), as well as age 6 for males (t_{47}=2.68, P=0.01). For *S. semifasciatus*, differences in mean length between back-calculated and observed methods were observed for the first three consecutive ages for females (age 1: t_{353}=16.61, P<0.001, age 2: t_{329}=6.00, P<0.001, age 3: t_{250}=3.37, P<0.001), and the first two consecutive ages for males (age 1: t_{332}=16.5, P<0.001, age 2: t_{332}=5.43, P<0.001). Consequently, substitution of observed and adjusted length-at-age with back-calculated length-at-age was done for the first four ages for male and female *S. commerson*, the first three ages for female *S. semifasciatus*, and the first two ages for male *S. semifasciatus*. Von Bertalanffy growth functions were then fitted to the combined data sets (Table 4, Fig. 2).

Growth estimates from substitution displayed a general pattern of higher estimates of K and lower estimates of L_∞ than the respective observed or adjusted methods alone, and higher estimates of L_∞ than the respective back-calculated methods alone (Table 4). All observed length-at-age data beyond age 8 for *S. semifasciatus*, and male *S. commerson*, and age 9 for female *S. commerson*, had a greater length than the back-calculated and substituted VBGF estimates (Fig. 2). Comparison of the different combinations of substituted methods revealed no significant differences for *S. semifasciatus* (Table 5). However, there were significant differences between some combinations for *S. commerson*, mostly for females (Table 5). Notably, all the significant differences occurred between combinations with BC-last and BC-all substituted data, with the combination of BC-last and observed data differing to all combinations with BC-all data for female *S. commerson*.

Discussion

Alternative methods for estimating length-at-age from otoliths resulted in significant differences in estimates of growth. A clear pattern emerged that revealed large differences between the back-calculation (BC-all, BC-last) methods and the observed and adjusted methods (Obsv, Adj-cat, Adj-frm) for both species of mackerel. However, the pattern was more pronounced for *S. commerson* than for *S. semifasciatus*, most likely because of the more pronounced effects of selectivity on *S. commerson* length-at-age data. The method of substituting length-at-age data obtained from observed or adjusted methods with back-calculated length-at-age produced different estimates of growth to the individual methods. This technique proved valuable for providing estimates of population growth, which are likely to be more accurate than those provided with the individual methods alone, particularly in the presence of selectivity biases; the technique also improved estimates of length for younger ages over observed or adjusted methods and provided more realistic estimates of mean maximum length than estimates from back-calculation methods alone.

A significant difference in growth between back-calculated length-at-age to all annuli and the last annulus was observed for *S. commerson* if the result of the overall likelihood ratio test is taken in isolation of the multiple comparisons with other methods (i.e., P<0.05), indicating that selectivity bias was inherent in *S. commerson* samples. Comparison of the two back-calculation methods for *S. commerson* indicated that fish are fully recruited to the fishery at approximately 900 mm fork length, above which no difference in length-at-age was observed between the back-calculation methods. No significant difference was observed between the two back-calculation methods for *S. semifasciatus* and therefore indicated that selectivity was not biasing length-at-age data.

In choosing which method(s) to use in determining length-at-age for growth estimation, careful consideration should be given to the growth characteristics of a species. We examined relatively fast growing species with similar growth characteristics in this study, and thus some of our conclusions may not be applicable or practical when applied to other species with different growth characteristics. Each method for determining length-at-age has its pros and cons, which differ depending on the growth characteristics of the species in consideration.

Table 4

Von Bertalanffy growth function parameter estimates (growth coefficient [K], theoretical maximum length [L_∞], and theoretical age where length is equal to zero [t_0], ± standard error), sample numbers (n), age ranges, and adjusted R^2 values from different combinations of substituted methods (observed [Obsv], category adjusted [Adj-cat], formula adjusted [Adj-frm], back-calculation to all annuli [BC-all], and back-calculation to the last annulus only [BC-last]) for estimating length-at-age for *Scomberomorus commerson* and *S. semifasciatus*.

Species	Sex	BC data	Method	K	L_∞ (mm)	t_0 (years)	n	Min age	Max age	R^2_{adj}
S. commerson	Female	BC-all	Obsv	0.41 (0.02)	1319 (17)	−0.60 (0.07)	741	1	15.0	0.84
		BC-all	Adj-cat	0.43 (0.02)	1304 (16)	−0.55 (0.07)	747	1	11.0	0.84
		BC-all	Adj-frm	0.44 (0.02)	1295 (15)	−0.53 (0.07)	750	1	11.9	0.84
		BC-last	Obsv	0.29 (0.03)	1411 (33)	−1.30 (0.19)	263	1	15.0	0.87
		BC-last	Adj-cat	0.31 (0.03)	1383 (29)	−1.18 (0.17)	268	1	11.0	0.87
		BC-last	Adj-frm	0.32 (0.03)	1366 (26)	−1.14 (0.17)	271	1	11.9	0.87
	Male	BC-all	Obsv	0.60 (0.04)	1092 (12)	−0.39 (0.08)	562	1	11.0	0.81
		BC-all	Adj-cat	0.63 (0.04)	1084 (12)	−0.35 (0.08)	561	1	11.0	0.81
		BC-all	Adj-frm	0.64 (0.04)	1081 (11)	−0.34 (0.07)	573	1	11.0	0.82
		BC-last	Obsv	0.54 (0.06)	1118 (15)	−0.62 (0.17)	191	1	11.0	0.84
		BC-Last	Adj-cat	0.58 (0.06)	1108 (14)	−0.55 (0.16)	190	1	11.0	0.84
		BC-Last	Adj-frm	0.57 (0.06)	1103 (13)	−0.57 (0.15)	202	1	11.0	0.84
S. semifasciatus	Female	BC-All	Obsv	1.02 (0.06)	830 (7)	0.18 (0.04)	828	1	9.0	0.81
		BC-All	Adj-cat	1.02 (0.05)	830 (7)	0.18 (0.04)	846	1	9.0	0.82
		BC-All	Adj-frm	1.08 (0.06)	821 (6)	0.21 (0.04)	894	1	9.0	0.82
		BC-Last	Obsv	0.95 (0.07)	841 (8)	0.12 (0.07)	295	1	9.0	0.80
		BC-Last	Adj-cat	0.95 (0.07)	840 (7)	0.12 (0.07)	312	1	9.0	0.80
		BC-Last	Adj-frm	1.02 (0.07)	828 (6)	0.17 (0.06)	359	1	9.0	0.79
	Male	BC-All	Obsv	1.03 (0.06)	790 (7)	0.14 (0.04)	748	1	10.0	0.80
		BC-All	Adj-cat	1.04 (0.06)	787 (7)	0.15 (0.04)	774	1	10.0	0.80
		BC-All	Adj-frm	1.13 (0.06)	771 (6)	0.18 (0.04)	825	1	10.6	0.79
		BC-Last	Obsv	0.96 (0.06)	794 (6)	0.08 (0.06)	306	1	10.0	0.83
		BC-Last	Adj-cat	0.96 (0.06)	791 (6)	0.07 (0.06)	332	1	10.0	0.83
		BC-Last	Adj-frm	1.00 (0.06)	776 (5)	0.07 (0.06)	383	1	10.6	0.78

Observed length-at-age, although being relatively easy to obtain compared to other data, can have the most aging error given that any growth beyond a whole year is not accounted for. The magnitude and frequency of aging error has been shown to be uniform across all ages for *S. semifasciatus* (Marriott et al., 2010). However, given the rapid growth of such species in the first few years, aging error for younger ages will have more influence on growth estimates than aging error in older ages. Although this problem can be exacerbated for fast growing species such as *S. commerson* and *S. semifasciatus*, uniform aging error across age classes may be a lesser issue for growth estimation of long-lived, slow growing fish, and observed length-at-age could be more accurate if samples are collected after the period of annuli formation and the opaque increment at the edge is included in age estimates.

Adjustment methods for determining length-at-age theoretically provide a more accurate estimate of age than observed length-at-age by accounting for growth on a finer temporal scale, especially if the spawning period and period of annuli formation is discrete (e.g., DeVries and Grimes, 1997). The formula-adjustment method, however, is useful only if population-specific spawning and annuli formation periods are known for a given species, and it is less useful if the species has a protracted spawning period or if the timing of annuli formation varies (e.g., Williams et al., 2005). The category-adjustment method is useful for assigning ages to cohorts for use in assessment models (Begg et al.[4]) as well as for estimating growth (Shepard et al., 2010).

Back-calculation is useful for estimating selectivity effects (Campana, 1990; Lucena and O'Brien, 2001; Ballagh et al., 2006), providing length-at-age estimates for younger fish that may not be seen in fishery-dependent samples (Campana, 2001; Lopez-Abellan et al., 2008), providing comparisons between different populations (Johnson et al., 1983; Fable et al., 1987; Ballagh et al., 2006), and assessing individual growth variability (Fossen et al., 1999; Pilling et al., 2002).

[4] Begg, G. A., C. C.-M. Chen, M. F. O'Neill, and D. B. Rose. 2006. Stock assessment of the Torres Strait Spanish mackerel fishery. CRC Reef Research Centre Technical Report No 66, 81 p. CRC Reef Research Centre, Townsville, Australia.

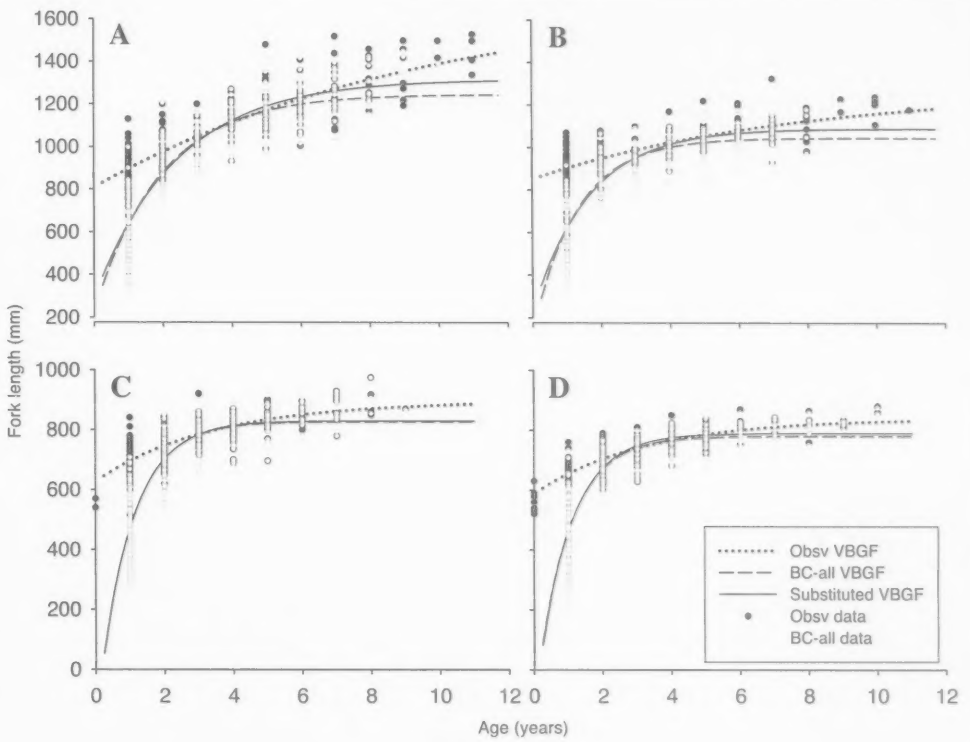

Figure 2

Von Bertalanffy growth functions (VBGF) fitted to observed (Obsv), back-calculated to all annuli (BC-all), and substituted (Obsv and BC-all) length-at-age data for (**A**) female, and (**B**) male *Scomberomorus commerson*, and (**C**) female, and (**D**) male *Scomberomorus semifasciatus*.

However, this method can be influenced by statistical dependency whereby estimated lengths at younger ages are dependent on lengths from older ages through the back-calculation process and are therefore susceptible to bias in the presence of size-selective mortality (Vaughan and Burton, 1994; Pilling et al., 2002). Other drawbacks of back-calculation include the specialized equipment and software needed and the significant time required to obtain data.

We demonstrated that although back-calculation was effective for estimating length-at-age for younger ages in the presence of selectivity within a fishery that selects for the faster growing younger fish, it appears to underestimate mean maximum length (L_∞). This finding is shown by observed length-at-age data being consistently higher than the back-calculated VBGF for older age classes and is subject to the assumption that there is little or no selectivity acting on older fish. The underestimation of back-calculated mean maximum length is likely due to three effects: smaller length-at-age for younger fish; weighting of data in younger ages; and the negative correlation between the VBGF parameters of L_∞ and K. Back-calculating to all annuli results in a disproportionate amount of data for young ages which, depending on the growth estimation method used, gives more weight to younger ages when fitting a VBGF. Because the VBGF parameters L_∞ and K have been shown to be negatively correlated (Pilling et al., 2002), increasing the estimate of K through smaller length-at-age for younger ages, or a weighting of data in younger ages, will inevitably reduce the estimate of L_∞, and thus underestimate average maximum length. One option for overcoming this problem could be to constrain L_∞ to the largest observed length, although some prior knowledge of the size-selectivity pattern of sampling gears is required to make an informed decision to constrain parameters (Gwinn et al., 2010),

Fishery-independent sampling can improve estimates of growth through the collection of small, slower growing young fish not fully represented in fishery-dependent samples. However, fishery-independent sampling is typically expensive and not always possible or practical. Methods have been developed to correct bias in length-at-age data; however, these require previous knowledge of selectivity patterns, mark-recapture data or intensive sampling over several consecutive

Table 5

Chi-squared values for overall likelihood ratio tests between growth estimates from different combinations of substituted methods (observed [Obsv], category adjusted [Adj-cat], formula adjusted [Adj-frm], back-calculation to all annuli [BC-all], and back-calculation to the last annulus only [BC-last]) of estimating length-at-age for *Scomberomorus commerson* and *S. semifasciatus* (* indicates significant difference at $P<0.0033$, α was Bonfferoni adjusted for multiple comparisons, df=3).

Species	Sex	Methods	BC-all–Adj-cat χ^2	BC-all–Adj-frm χ^2	BC-last–Obsv χ^2	BC-last–Adj-cat χ^2	BC-last–Adj-frm χ^2
S. commerson	Female	BC-all–Obsv	0.087	0.434	13.8*	13.0	12.6
		BC-all–Adj-cat		0.138	15.3*	14.4*	13.7
		BC-all–Adj-frm			16.5 *	15.4*	14.3*
		BC-last–Obsv				0.073	0.680
		BC-last–Adj-cat					0.349
	Male	BC-all–Obsv	0.193	0.428	11.2	10.4	9.6
		BC-all–Adj-cat		0.050	12.7	11.6	10.5
		BC-all–Adj-frm			14.0*	12.6	11.3
		BC-last–Obsv				0.203	0.719
		BC-last–Adj-cat					0.220
S. semifasciatus	Female	BC-all–Obsv	0.001	0.709	0.957	0.853	0.103
		BC-all–Adj-cat		0.802	0.992	0.879	0.110
		BC-all–Adj-frm			3.6	3.5	0.538
		BC-last–Obsv				0.020	1.8
		BC-last–Adj-cat					1.6
	Male	BC-all–Obsv	0.199	5.5	0.529	1.346	8.8
		BC-all–Adj-cat		3.9	0.581	0.934	6.7
		BC-all–Adj-frm			6.2	4.9	1.9
		BC-last–Obsv				0.374	9.0
		BC-last–Adj-cat					6.3

years (Gwinn et al., 2010). Recently, several different methods for reducing bias in growth estimates from length-at-age data from size-selective samples have been proposed, including multinomial estimation models (Taylor et al., 2005), multigrowth model inference (Thorson and Simpfendorfer, 2009) and biologically based von Bertalanffy fitting procedures (Gwinn et al., 2010).

Substitution was shown to be a potentially useful method for providing more accurate estimates of population growth than the individual methods alone in the presence of selectivity pressure for faster growing young fish. Given that a significant difference in growth was observed between data substituted with the two different back-calculation methods for *S. commerson*, it is presumed that back-calculating data to all annuli would be the most appropriate back-calculation method to use in substitution in this instance given the selectivity bias observed in the young age classes. We therefore recommend that back-calculated length-at-age data from all annuli for young age classes be combined with observed or adjusted length-at-age data from older age classes to estimate population growth in the presence of selectivity favoring faster growing younger fish. Further studies should be undertaken to investigate the appropriateness of different methods for length-at-age determination and the effectiveness of substitution for species with different growth characteristics and under different selectivity regimes of fisheries.

Acknowledgments

The authors would like to thank members of the Fishing and Fisheries Research Centre for their support. The Fisheries Research and Development Corporation (projects 2001/019 and 2005/010), the School of Earth and Environmental Sciences of James Cook University, and the CRC Reef Research Centre provided funding and support for this study. This manuscript was greatly improved by thorough reviews from anonymous reviewers.

Literature cited

Ballagh, A. C., G. A. Begg, A. Mapleston, and A. Tobin.
2006. Growth trends of Queensland east coast Spanish mackerel (*Scomberomorus commerson*) from otolith back-calculations. Mar. Freshw. Res. 57:383–393.

Begg, G. A., S. E. Campana, A. J. Fowler, and I. M. Suthers.
2005. Otolith research and application: current directions in innovation and implementation. Mar. Freshw. Res. 56:477–483.

Beverton, R. J. H., and S. J. Holt.
1957. On the dynamics of exploited fish populations, 533 p. Ministry of Agriculture, Fisheries and Food, London.
Campana, S. E.
1990. How reliable are growth back-calculations based on otoliths? Can. J. Fish. Aquat. Sci. 47:2219–2227.
2001. Accuracy, precision and quality control in age determination, including a review of the use and abuse of age validation methods. J. Fish Biol. 59:197–242.
2005. Otolith science entering the 21st century. Mar. Freshw. Res. 56:485–495.
DeVries, D. A., and C. B. Grimes.
1997. Spatial and temporal variation in age and growth of king mackerel, *Scomberomorus cavalla*, 1977–1992. Fish. Bull. 95:694–708.
Fable, W. A. J., A. G. Johnson, and L. E. Barger.
1987. Age and growth of Spanish mackerel, *Scomberomorus maculatus*, from Florida and the Gulf of Mexico. Fish. Bull. 85:777–783.
Fablet, R.
2006. Semi-local extraction of ring structures in images of biological hard tissues: application to the Bayesian interpretation of fish otoliths for age and growth estimation. Can. J. Fish. Aquat. Sci. 63:1414–1428.
Fossen, I., O. T. Albert, and E. M. Nilssen.
1999. Back-calculated individual growth of long rough dab (*Hippoglossoides platessoides*) in the Barents Sea. ICES J. Mar. Sci. 56:689–696.
Francis, R. I. C. C.
1988. Are growth parameters estimated from tagging and age-length data comparable? Can. J. Fish. Aquat. Sci. 45:936–942.
1990. Back-calculation of fish length: a critical review. J. Fish Biol. 36:883–902.
Francis, R. I. C. C., S. J. Harley, S. E. Campana, and P. Doering-Arjes.
2005. Use of otolith weight in length-mediated estimation of proportions at age. Mar. Freshw. Res. 56:735–743.
Francis, R. I. C. C., L. J. Paul, and K. P. Mulligan.
1992. Aging of adult snapper (*Pagrus auratus*) from otolith annual ring counts: validation by tagging and oxytetracycline injection. Mar. Freshw. Res. 43:1069–1089.
Grudtsev, M. E., and L. I. Korolevich.
1986. Studies of frigate tuna *Auxis thazard* (Lacepede) age and growth in the eastern part of the equatorial Atlantic. Coll. Vol. Sci. Pap. ICCAT 25:269–274.
Gulland, J. A.
1988. Fish population dynamics: the implications for management, 422 p. John Wiley and Sons Ltd., New York.
Gwinn, D. C., M. S. Allen, and M. W. Rogers.
2010. Evaluation of procedures to reduce bias in fish growth parameter estimates resulting from size-selective sampling. Fish. Res. 105:75–79.
Haddon, M.
2001. Modelling and quantitative methods in fisheries, 406 p. Chapman and Hall/CRC Press, Boca Raton, FL.
Johnson, A. G., W. A. J. Fable, M. L. Williams, and L. E. Barger.
1983. Age, growth and mortality of King mackerel, *Scomberomorus cavalla*, from the southeastern United States. Fish. Bull. 81:97–106.
Katsanevakis, S., and C. D. Maravelias.
2008. Modelling fish growth: multi-model inference as a better alternative to *a priori* using von Bertalanffy equation. Fish Fish. 9:178–187.
Kimura, D. K.
1980. Likelihood methods for the von Bertalanffy growth curve. Fish. Bull. 77:765–776.
Labelle, M., J. Hampton, K. Bailey, T. Murray, D. A. Fournier, and J. R. Sibert.
1993. Determination of age and growth of South Pacific albacore (*Thunnus alalunga*) using three methodologies. Fish. Bull. 91:649–663.
Lopez-Abellan, L. J., M. T. G. Santamaria, and J. F. Gonzalez.
2008. Approach to aging and growth back-calculation based on the otolith of the southern boarfish Pseudopentaceros richardsoni (Smith, 1844) from the south-west Indian Ocean seamounts. Mar. Freshw. Res. 59:269–278.
Lou, D. C., B. D. Mapstone, G. R. Russ, C. R. Davies, and G. A. Begg.
2005. Using otolith weight-age relationships to predict age-based metrics of coral reef fish populations at different spatial scales. Fish. Res. 71:279–294.
Lucena, F. M., and C. M. O'Brien.
2001. Effects of gear selectivity and different calculation methods on estimating growth parameters of bluefish, *Pomatomus saltatrix* (Pisces: Pomatomidae), from southern Brazil. Fish. Bull. 99:432–442.
Marriott, R., B. D. Mapstone, A. C. Ballagh, L. M. Currey, A. Penny, A. J. Williams, G. Jackson, D. Lou, A. J. Mapleston, N. D. C. Jarvis, I. S. Keay, and S. J. Newman.
2010. Accepting final counts from repeat readings of otoliths: should a common criterion apply to the age estimation of fish? Mar. Freshw. Res. 61:1171–1196.
McPherson, G. R.
1992. Age and growth of the narrow-barred Spanish mackerel (*Scomberomorus commerson* Lacepede, 1800) in north-eastern Queensland waters. Mar. Freshw. Res. 43:1269–1282.
1993. Reproductive biology of the narrow barred Spanish mackerel (*Scomberomorus commerson* Lacepede, 1800) in Queensland waters. Asian Fish. Sci. 6:169–182.
Pilling, G. M., G. P. Kirkwood, and S. G. Walker.
2002. An improved method for estimating individual growth variability in fish, and the correlation between von Bertalanffy growth parameters. Can. J. Fish. Aquat. Sci. 59:424–432.
Rahikainen, M., and R. L. Stephenson.
2004. Consequences of growth variation in northern Baltic herring for assessment and management. ICES J. Mar. Sci. 61:338–350.
Ricker, W. E.
1969. Effects of size-selective mortality and sampling bias on estimates of growth, mortality, production and yield. J. Fish. Res. Board Can. 26:479–541.
1979. Growth rates and models. *In* Fish physiology (W. S. Hoar, D. J. Randall, and J. R. Brett, eds.), p. 677–743. Academic Press, Orlando, Fla.
Schnute, J.
1981. A versatile growth model with statistically stable parameters. Can. J. Fish. Aquat. Sci. 38:1128–1140.
Secor, D. H., and J. M. Dean.
1992. Comparison of otolith-based back-calculation methods to determine individual growth histories of larval striped bass, *Morone saxatilis*. Can. J. Fish. Aquat. Sci. 49:1439–1454.
Shafi, M., and B. M. Jasim.
1982. Some aspects of the biology of a cyprinid, *Aspius vorax* Heckel. J. Fish Biol. 20:271–278.

Shepard, K. E., W. F. Patterson, D. A. Devries, and M. Ortiz.
2010. Contemporary versus historical estimates of king mackerel (*Scomberomorus cavalla*) age and growth in the U.S. Atlantic Ocean and Gulf of Mexico. Bull. Mar. Sci. 86:515–532.

Steward, C. A., K. D. DeMaria, and J. M. Shenker.
2009. Using otolith morphometrics to quickly and inexpensively predict age in the gray angelfish (*Pomacanthus arcuatus*). Fish. Res. 99:123–129.

Taylor, N. G., C. J. Walters, and S. J. D. Martell.
2005. A new likelihood for simultaneously estimating von Bertalanffy growth parameters, gear selectivity, and natural and fishing mortality. Can. J. Fish. Aquat. Sci. 62:215–223.

Thorson, J. T., and C. A. Simpfendorfer.
2009. Gear selectivity and sample size effects on growth curve selection in shark age and growth studies. Fish. Res. 98:75–84.

Vaughan, D. S., and M. L. Burton.
1994. Estimation of Von Bertalanffy growth parameters in the presence of size-selective mortality: a simulated example with red grouper. Trans. Am. Fish. Soc. 123:1–8.

Williams, A. J., L. M. Currey, G. A. Begg, C. D. Murchie, and A. C. Ballagh.
2008. Population biology of coral trout species in eastern Torres Strait: Implications for fishery management. Cont. Shelf Res. 28:2129–2142.

Williams, A. J., C. R. Davies, and B. D. Mapstone.
2005. Variation in the periodicity and timing of increment formation in red throat emperor (*Lethrinus miniatus*) otoliths. Mar. Freshw. Res. 56:529–538.

Age validation, growth, mortality, and demographic modeling of spotted gully shark (*Triakis megalopterus*) from the southeast coast of South Africa

Anthony J. Booth (contact author)[1]
Alan J. Foulis[1]
Malcolm J. Smale[2]

Email address for contact author: t.booth@ru.ac.za

[1] Department of Ichthyology and Fisheries Science
Rhodes University
P.O. Box 94
Grahamstown, 6140, South Africa

[2] Port Elizabeth Museum
P.O. Box 13147
Humewood, 6013, South Africa

and

Department of Zoology
Nelson Mandela Metropolitan University
P.O. Box 77000
Port Elizabeth, 6013, South Africa

Abstract—This study documents validation of vertebral band-pair formation in spotted gully shark (*Triakis megalopterus*) with the use of fluorochrome injection and tagging of captive and wild sharks over a 21-year period. Growth and mortality rates of *T. megalopterus* were also estimated and a demographic analysis of the species was conducted. Of the 23 OTC (oxytetracycline)-marked vertebrae examined (12 from captive and 11 from wild sharks), seven vertebrae (three from captive and four from wild sharks) exhibited chelation of the OTC and fluoresced under ultraviolet light. It was concluded that a single opaque and translucent band pair was deposited annually up to at least 25 years of age, the maximum age recorded. Reader precision was assessed by using an index of average percent error calculated at 5%. No significant differences were found between male and female growth patterns ($P>0.05$), and von Bertalanffy growth model parameters for combined sexes were estimated to be L_∞=1711.07 mm TL, k=0.11/yr and t_0= −2.43 yr (n=86). Natural mortality was estimated at 0.17/yr. Age at maturity was estimated at 11 years for males and 15 years for females. Results of the demographic analysis showed that the population, in the absence of fishing mortality, was stable and not significantly different from zero and particularly sensitive to overfishing. At the current age at first capture and natural mortality rate, the fishing mortality rate required to result in negative population growth was low at $F>0.004$/yr. Elasticity analysis revealed that juvenile survival was the principal factor in explaining variability in population growth rate.

Manuscript submitted 14 May 2010.
Manuscript accepted 3 November 2010.
Fish. Bull. 109:101–112 (2011).

The views and opinions expressed or implied in this article are those of the author (or authors) and do not necessarily reflect the position of the National Marine Fisheries Service, NOAA.

Spotted gully shark (*Triakis megalopterus*, Smith, 1839), is one of five *Triakis* species and is endemic to southern Africa (Compagno, 1988). Its distribution range extends from northern Namibia (although anecdotal information indicates that it is caught as far north as Angola) southward around the coast to Coffee Bay in the Eastern Cape Province, South Africa (Compagno, 1988; Compagno et al., 2005). It is a shallow water (<50 m) (Compagno et al., 1989; Smale and Goosen, 1999), demersal species that is recreationally important to shore and ski-boat anglers. With the exception of some information pertaining to its reproductive and feeding biology (Smale and Goosen, 1999) there is little information available to guide its management. Given its narrow distribution range and small population size, it could be vulnerable to overexploitation in a manner similar to its congener, *T. semifasciata*, that has declined in abundance and is now carefully managed (Smith and Abramson, 1990; Cailliet, 1992). An equivalent analysis is required for *T. megalopterus* to assess its vulnerability to fishing pressure.

Demographic modeling has been conducted on many elasmobranch populations when there are insufficient catch, effort, and abundance data available to conduct a full stock assessment (Simpfendorfer, 1998; Romine et al., 2009). Demographic modeling is a popular approach because it provides the best available description of the population being studied given several life history parameters. Demographic modeling therefore provides a compromise between simple life history tables and more detailed stock assessment models. Demographic models became popular in the 1990s and are now the most widely used population models used to assess shark populations (Simpfendorfer, 2005). A fundamental requirement for the application of age-structured demographic models is that ages of sharks are available.

Correctly determining the age of fish, particularly elasmobranchs, is crucial if (unbiased) time-based life history rates such as growth, maturity, and mortality are to be estimated. Although numerous fish age and growth studies have been undertaken, remarkably few have included

validation (Campana, 2001; Cailliet and Goldman, 2004). Campana (2001) defines validation as either the validation of the periodicity of growth increments, or as the validation of the age estimate made by reader(s). In a recent review, Campana (2001) noted that of the 372 papers in which age validation was reported, only 15% of the papers actually incorporated validation of the absolute age of wild fish. Therefore, when conducting an age and growth study it is necessary to specify whether one or both validation goals are met and which validation method is used.

Three methods of validation are typically used. These are edge analysis (also known as marginal increment or zone analysis), carbon dating, and mark-recapture of tagged fish injected with a calcium-chelating fluorescing chemical such as the antibiotic, oxytetracycline hydrochloride (OTC). All of these methods have been used to validate elasmobranch ages (Campana et al., 2002; Smith et al., 2003; Cailliet and Goldman, 2004; Ardizzone et al., 2006; Chen et al., 2007). The most commonly used and most reliable validation method is tagging with OTC (Campana, 2001).

In studies of elasmobranchs by OTC-injection, sharks are measured, injected with OTC, tagged, and released. The date of release is then noted. Once the shark is recaptured, the number of vertebral band pairs distal to the fluorescent mark is compared with the time between release and recapture of the shark. This experimental approach can be problematic if recapture rates are low. Validating elasmobranch age estimates can be time consuming because recapture rates are generally low and there is a long period of time between collecting a sufficient number of samples and analyzing the vertebrae.

We developed a Leslie matrix-based demographic model to evaluate the ability of *T. megalopterus* to sustain increased levels and patterns of fishing pressure. We also validated the age of *T. megalopterus* using oxytetracycline to estimate growth and mortality rates, important demographic model parameters.

Materials and methods

General overview

In 1994, a tagging program incorporating researchers and trained volunteer fishermen was initiated at the Port Elizabeth Museum in order to obtain age validation, movement studies, and population dynamics of the spotted gully shark. A total of 402 wild sharks (113 male, 230 female, and 59 of undetermined sex) were tagged, injected with OTC at a dosage of 50 mg/kg (Tanaka, 1990), and released. A total of 53 sharks were recaptured once, and one shark twice. The date for the first recaptured fish was unfortunately unrecorded, but it was evident that it had been re-injected with OTC from the presence of an additional fluorescing mark in its vertebrae. An additional 12 display sharks were held in the Bayworld Aquarium in Port Elizabeth and injected with OTC. All 12 display sharks and 11 tagged wild sharks were sacrificed for vertebral analysis.

In addition, a total of 129 spotted gully sharks were collected opportunistically from ski-boat fishermen, fishing competitions, and research cruises over a 21-year period (1984–2009) between Cape St Francis and Coffee Bay, South Africa. Vertebrae were collected from a subsample of 96 sharks. Total length (TL) and sex were recorded for all these sharks.

Age determination

Between five and eight vertebrae were removed from the trunk region in the vicinity of the first dorsal fin, soaked in 4.5% sodium hypochlorite for 15–45 minutes to remove excess connective tissue, and were either stored in 70–80% ethyl alcohol or frozen (Yudin and Cailliet, 1990). Cleaned vertebrae were embedded in polyester casting resin and sectioned with a diamond-bladed saw along the sagittal plane to a thickness of 0.6 mm (Natanson et al., 2006; Rizzo et al.[1]), and mounted on glass slides with DPX mountant (Lasec, South Africa).

Band pairs, defined as one optically opaque and one optically translucent band were counted by using a dissecting microscope with transmitted white light (460–490 nm). OTC-injected specimens were also viewed with an Olympus BX60 microscope (Olympus, Johannesburg, South Africa) under ultraviolet transmitted light (510–550 nm). Each specimen was aged twice, three weeks apart by a single reader, without prior knowledge of the length or sex of the specimen. Counts were accepted only if both counts were in agreement. If the estimated number of bands differed by two or less, the specimen was recounted and the final count was accepted as the agreed upon number; if not, the specimen was discarded. If the third count did not concur with one of the previous two counts, the sample was rejected.

An age-bias plot was used to graphically assess the readings and their associated agreement (Campana, 2001; Natanson et al., 2006). A t-test was conducted on the slope of the age-bias plot (the linear regression of the second against the first age readings) to test the null hypothesis that the slope was equal to one. Comparisons of reader accuracy for each age were made by using a paired t-test, and a χ^2-test of symmetry was used to test for systematic bias in the determination of age (Hoenig et al., 1995).

The variability of the within-reader age estimates was estimated with an index of average percent error

[1] Rizzo, P., S. Gancitano, C. Badalucco, S. Enajjar, C. Mancusi, A. Mosteiro Cabañelas, B. Saidi, and L. Sion. 2004. Contribution to guidelines for age determination of chondrichthyes fish from the Mediterranean Sea (application to selected species). Report of the MedSudMed training course on age determination of selacean fish; 22 November–01 December 2004, Mazara del Vallo, Italy, 22 p. [Available from FAO-MedSudMed Project ,Mazara del Vallo, Italy

(IAPE) (Beamish and Fournier, 1981) with the following equation:

$$IAPE(\%) = \frac{100}{N}\sum_{i=1}^{N}\left[\frac{1}{R}\sum_{j=1}^{R}\frac{\left|X_{ij}-X_i\right|}{X_i}\right],$$

where N = the number of fish aged;
R = the number of readings;
X_{ij} = j^{th} vertebral count of the i^{th} fish; and
X_i = the final agreed age of fish i.

As with Goosen and Smale (1997), an IAPE calculated to be less than 10% was considered acceptable.

Growth was modeled with the Schnute (1981) growth model. This four-parameter model is general and allows for the estimation of various nested models. The length of a shark at age a, L_a , is modeled as

$$L_a = L_1^{\beta} + \left(L_2^{\beta} - L_1^{\beta}\right)\left[\frac{1-e^{-\alpha(a-t_1)}}{1-e^{-\alpha(t_2-t_1)}}\right]^{1/\beta},$$

where t_1 = the youngest fish in the sample;
t_2 = the oldest fish in the sample;
L_1 = the estimated length of a fish at age t_1;
L_2 = the estimated length of fish at age t_2; and
α and β are the curvature parameters.

By setting the parameter β to either 1 or –1, the model reduces to either the von Bertalanffy or logistic growth model. Both of these nested models have three estimated parameters. The von Bertalanffy and logistic models are expressed as

$$L_a = L_\infty\left(1-e^{-k(a-t_0)}\right) \text{ and } L_a = \frac{L_\infty}{\left(1-e^{-k(a-t_0)}\right)},$$

where L_∞ = the theoretical maximum size;
k = the growth coefficient; and
t_0 = the theoretical age at zero length.

The von Bertalanffy (β=1) and logistic (β=–1) parameters were calculated with the following equations:

$$L_\infty = \left(\frac{e^{\alpha t_2}L_2^{\beta} - e^{\alpha t_1}L_1^{\beta}}{e^{\alpha t_2} - e^{\alpha t_1}}\right)^{1/\beta},$$

$$t_0 = t_1 + t_2 - \frac{1}{\alpha}\ln\left(\frac{\beta\left(e^{\alpha t_2}L_2^{\beta} - e^{\alpha t_1}L_1^{\beta}\right)}{L_2^{\beta} - L_1^{\beta}}\right), \text{ and } K = \alpha.$$

The Schnute growth model was fitted to the combined-sex data and the parameters were estimated by nonlinear minimization of a negated normal log-likelihood function of the form

$$-\ln L = \frac{n}{2}\ln\hat{\sigma}^2,$$

where $\hat{\sigma}^2 = \frac{1}{n}\sum_{i=1}^{n}\left(L_{ia} - \hat{L}_{ia}\right)^2$ is the maximum likelihood estimate of the model variance;
L_{ia} and $\hat{L}_{ia}$ are the observed and model predicted lengths of fish i at age a; and
n is the number of observed data.

The most parsimonious model was selected with the lowest Akaike information criterion (Akaike, 1973) of the form

$$AIC = 2(-\ln L + p),$$

where p = the number of model parameters.

A likelihood ratio test was used to test the null hypotheses that there is no difference in growth parameters between males and females (Simpfendorfer et al., 2000; Neer et al., 2005; Natanson et al., 2006). Parameter variability was estimated by using parametric bootstrapping with 1000 iterations and the 95% confidence intervals were estimated from the bootstrap results by using the percentile method (Buckland, 1984).

Age at maturity

Age at maturity, t_m, was estimated directly from the von Bertalanffy growth model as

$$t_m = t_0 - \frac{1}{k}\ln\left(1-\frac{l_{50}^{w}}{L_\infty}\right),$$

where l_{50}^{w} = the length at maturity obtained from Smale and Goosen (1999); and
L_∞, k and t_0 are the von Bertalanffy growth model parameters.

Natural mortality

Natural mortality was estimated from the median of Pauly's (1980), Hoenig's (1983) and Jensen's (1996) empirical models of the form

$$M_{\text{Pauly}} = \exp\left(-0.0152 - 0.279\ln L_\infty + 0.6543\ln k + 0.463\ln T\right)$$

$$M_{Hoenig} = \exp\left(1.44 - 0.982\ln t_{\max}\right)$$

$$M_{Jensen} = 1.6k,$$

where L_∞ and k are the Von Bertalanffy growth model parameters;
T = the mean water temperature (estimated to be 16°C); and
t_{max} = the age of the oldest fish sampled (Hoenig, 1983).

Demographic modeling

The demographics of female *T. megalopterus* was modeled with an age-structured matrix model (Caswell, 2001) of the form $\mathbf{n}_{t+1}=\mathbf{A}\times\mathbf{n}_t$, where $\mathbf{n}_t$ is a vector of numbers at age at time t and $\mathbf{A}$ is the Leslie projection matrix. In matrix formulation the model is expressed as

$$\begin{pmatrix} N_{1,t+1} \\ N_{2,t+1} \\ N_{3,t+1} \\ \vdots \\ N_{t_{max},t+1} \end{pmatrix} = \begin{pmatrix} \phi_1 & \phi_2 & \phi_3 & \cdots & \phi_{t_{max}} \\ S_1 & 0 & 0 & 0 & 0 \\ 0 & S_2 & 0 & 0 & 0 \\ 0 & 0 & \ddots & 0 & 0 \\ 0 & 0 & 0 & S_{t_{max}-1} & 0 \end{pmatrix} \times \begin{pmatrix} N_{1,t} \\ N_{2,t} \\ N_{3,t} \\ \vdots \\ N_{t_{max},t} \end{pmatrix},$$

where S_a and ϕ_a = age-dependent survivals and fecundities, respectively; and
t_{max} = the maximum age considered in the analysis.

The annual population growth rate (λ), stable age distribution ($\mathbf{w}$), and age-specific reproductive value ($\mathbf{v}$) vectors were obtained by solving the equations $\mathbf{Aw}=\lambda\mathbf{w}$ and $\mathbf{v}^*\mathbf{A}=\lambda\mathbf{w}$, where * is the complex conjugate transpose function. In the solutions, λ is the common dominant eigenvalue and $\mathbf{w}$ and $\mathbf{v}$ are the corresponding right and left eigenvectors. The reproductive value vector was normalized in relation to the age-1 value.

The conditional intrinsic rate of increase (Gedamke et al., 2007) was calculated as $r=\ln\lambda$, the average age of mothers of newborn individuals in a population with a stable age distribution as $\overline{T}=\langle\mathbf{w},\mathbf{v}\rangle=\mathbf{w}'\mathbf{v}$, and the average number of female offspring per female during her lifespan as $R_0=\exp(r\overline{T})$.

The sensitivity of λ to changes in the demographic parameters provides an indication of which parameter has the largest impact on the population growth rate. Sensitivity can be measured in either relative (as "sensitivity") or absolute terms (as "elasticity"). Both forms of sensitivity were calculated from the individual values of the Leslie matrix, $a_{i,j}$, the population growth rate, and the left-right eigenvectors as

$$s_{i,j}=\frac{\partial\lambda}{\partial a_{i,j}}=\frac{v_i w_j}{\langle\mathbf{w},\mathbf{v}\rangle}=\frac{\mathbf{vw}'}{\langle\mathbf{w},\mathbf{v}\rangle}.$$

Elasticities, or

$$\frac{\partial\ln\lambda}{\partial\ln a_{i,j}}$$

were calculated as

$$e_{i,j}=\frac{a_{i,j}}{\lambda}s_{i,j}$$

such that

$$\sum_i\sum_j e_{i,j}=1.$$

Elasticities were summarized by age

$$E_j=\sum_i e_{i,j},$$

fertilities

$$E_1=\sum_{i=1}^{t_{max}} e_{0,j},$$

juvenile survival

$$E_2=\sum_{i=2}^{t_{max}}\sum_{j=1}^{a_{50}} e_{i,j}$$

and adult survival

$$E_2=\sum_{i=2}^{t_{max}}\sum_{j=a_{50}}^{t_{max}} e_{i,j}$$

(Mollet and Cailliet, 2002).

Model implementation

Age-dependent survival was estimated as a function of both age-independent instantaneous natural mortality (M), age-dependent selectivity (ξ_a), and fully recruited fishing mortality (F), such that $S_a=\exp(-M-\xi_a F)$. A maximum age of $t_{max}=26$ was used in the analysis. All parameters used in the analysis are summarized in Table 1.

Age-dependent fertility was estimated as the number of embryos surviving to age-1 per female in a calendar year, E_a, and was weighted by the proportion of females that were mature at age a, ψ_a, such that $\phi_a=S_0\psi_a E_a$.

Because maturity, selectivity, and number of embryos are length- rather than age-dependent, all age-dependent values were calculated from the corresponding lengths predicted from the von Bertalanffy growth model for combined sexes.

Both maturity-at-length, ψ_l, and selection-at-length, ξ_l, were modeled as logistic ogives as

$$\psi_l=\left(1+\exp\left(-\left(l-l_{50}^{\psi}\right)/\delta^{\psi}\right)\right)^{-1}$$

and

$$\xi_l=\left(1+\exp\left(-\left(l-l_{50}^{\xi}\right)/\delta^{\xi}\right)\right)^{-1},$$

respectively, where l_{50}^{ψ} and l_{50}^{ξ} are the lengths at which shark were 50% mature or at which 50% of sharks were selected by the fishery. The inverse rates of maturation and selection are denoted as $\delta^{\psi}$and δ^{ξ}, respectively. Because these rates were not available from the literature, they were assumed to be 2% of their corresponding 50% values. These rates were considered reasonable given other maturity and selectivity studies (Booth, unpubl. data). Length at 50% selectivity was estimated as 1326 mm TL, which is the mean length of sharks (n=252) measured from recreational anglers (Smale, unpubl. tag and release data). The number of female embryos per adult female at length l in a calendar year, given a gestational period of 20 months and a sex ratio of 1:1, was calculated as

Table 1

Fixed parameter values estimated during this study or obtained from Smale and Goosen's study (1999) that were used in the demographic analysis of *Triakis megalopterus*. TL=total length.

Parameter	Description	Value	Source
L_∞	Theoretical maximum size	1711.07 mm TL	This study
k	Growth coefficient	0.11 /yr	This study
t_0	Theoretical age at zero length	–2.43 yr	This study
M	Natural mortality rate	0.14 /yr	This study
F	Fishing mortality rate	0.yr^{-1}	This study
l_{50}^{ψ}	Length at 50% maturity	1450 mm TL	Smale and Goosen (1999)
l_{50}^{ε}	Length at 50% selectivity	1326 mm TL	This study
δ^{ψ}	Inverse rate of maturity	29 mm TL	This study
δ^{ε}	Inverse rate of selectivity	26 mm TL	This study
t_{max}	Maximum age	26 years	This study
E_l	Number of female embryos per adult female at length l in a calendar year given a gestational period of 20 months and a sex ratio of 1:1	$0.5\times\frac{20}{12}\times(0.2l-21.74)$	Smale and Goosen (1999)

$$E_l = 0.5\times\frac{20}{12}\times(0.2l - 21.74)$$

(Smale and Goosen, 1999).

Uncertainty in the model outputs was estimated with Monte-Carlo simulation (Cortés, 2002). For each simulation, i, random lengths were drawn around the predicted von Bertalanffy growth model with an estimated growth model standard deviation of 110 such that $L_a^i = L_a + \varepsilon_p$, and $\varepsilon_p \sim N(0,110^2)$. These length estimates were used to draw random variable for the length-at-maturity as $l_{50}^{i,\psi} = l_{50}^{\psi} + e_{\psi}$ and $\varepsilon_{\psi} \sim N(0,16^2)$. The standard deviation corresponded to that required to obtain the 1st and 99th percentiles at 1391 mm TL and 1500 mm TL, the lengths at first and 100% maturity reported by Smale and Goosen (1999). Natural mortality was assumed to be log-normally distributed with a coefficient of variation of 20%, such that $M_i = M_i \exp(\varepsilon_M)$, and $\varepsilon_M \sim N(0,0.2^2)$. No adjustments were made for log-normal bias. A total of 1000 simulations were conducted, and standard error and 95% confidence intervals were calculated for λ, ρ, $\overline{T}$, R_0, E_a, E_1, E_2, and E_3 by using the percentile method (Buckland, 1984).

Three-dimensional isopleth plots were constructed to assess the response of the conditional intrinsic rate of population increase parameter, r, to different inputted combinations of fishing mortality and the age at which 50% of sharks were selected.

Results

All aquarium specimens were either moribund or had died in the aquarium and had decreased in length by the end of the study. These sharks were not included in the estimation of the growth parameters but were included in the validation aspect of the analysis. The vertebrae from 25 male (1123.2 ±404 mm TL) and 71 female (1258.0 ±397 mm TL) sharks were processed for age estimation. Vertebrae were interpreted without difficulty up to the margin of the corpus calcareum where magnification needed to be increased to accurately interpret the remaining band pairs (Fig. 1). No distinctive features were identified in reading the vertebrae of *T. megalopterus*.

Of the 96 vertebrae examined, 86 were considered suitable for aging. Age estimates ranged from 0+ to 25 years. Of the 15 OTC-injected specimens examined, only seven fluoresced (three captive and four wild specimens) under ultraviolet light and confirmed that one vertebral band pair was deposited annually (Table 2; Fig. 1). The maximum validated age was from a shark that was 25 years old. An age-length key is presented in Table 3.

There was no significant difference in the accuracy of age assessments between readings (paired t-test; $P>0.05$). There was a 45% agreement on all age assessments, 80% agreement between age readings within 1 year, and 94% agreement between readings within 2 years. There was a strong positive correlation between the first and second readings ($r^2=0.97$) that was not statistically different from unity (t-test on slopes; $P>0.05$) (Fig. 2). There was no evidence for systematic age bias between readings (χ^2-test; $P>0.05$). Band pair counts were considered to be reasonably precise with an estimated IAPE of 5.02%.

Of the three models assessed, the von Bertalanffy was considered to be the most parsimonious (Schnute:

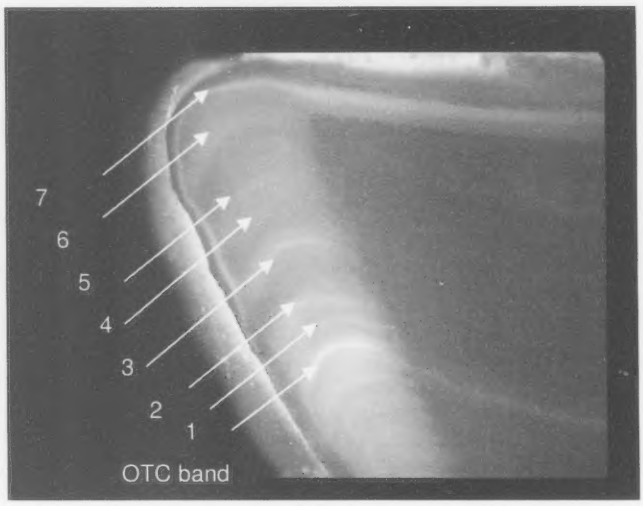

Figure 1

A sectioned vertebra of a 14-year-old wild spotted gully shark (*Triakis megalopterus*) tagged and injected with oxytetracycline hydrochloride seven years before recapture.

Table 2

Sex, capture locations and dates, total lengths (TL), and estimated ages of specimens of *Triakis megalopterus* tagged and injected with oxytetracycline hydrochloride (OTC) that exhibited fluorescing zones on vertebrae. All specimens were sampled off the southeast coast of South Africa. "Zones distal to OTC"=zones that fluoresced and that were distal to the site of the OTC injection.

Gender	Capture → recapture locations	Tagging date	Recapture date	Years at liberty	Tagging length (mm TL)	Recapture length (mm TL)	Zones distal to OTC	Total age
Female	Bayworld aquarium	Feb 1999	Dec 2000	1.8	1700	1580	1	20
Female	Bayworld aquarium	Nov 2001	Jan 2003	1.2	1660	1600	1	25
Male	Bayworld aquarium	Apr 2002	Dec 2002	0.7	1560	1428	1	11
Female	De Hoop → De Hoop	Feb 1996	Feb 1998	2.0	1111	1140	2	12
Male	De Hoop → De Hoop	Sep 1996	May 2003	6.7	1530	1550	7	14
Female	Algoa Bay → Knysna	Mar 1998	Mar 2005	7.0	950	1250	7	14
Undetermined	De Hoop → De Hoop	Sep 2000	May 2003	2.7	1020	1140	3	10

p=4, AIC=906.47; von Bertalanffy: p=3, AIC=904.56; logistic: p=3, AIC=912.89). The logistic model provided the worst fit of all three models considered. Although wild female sharks tended to grow larger and slower than males (Table 4, Fig. 3), there were no significant differences among any of the growth parameters (likelihood ratio test, P>0.05). Overall, the growth trajectories of the tagged and recaptured sharks were consistent with the predicted von Bertalanffy growth model for combined sexes (Fig. 4).

Age at maturity was calculated to be 10.9 years for males and 15.3 for females from the estimates of size of maturity for males (1320 mm TL) and females (1450 mm TL) (Smale and Goosen, 1999). Natural mortality was estimated at 0.15/yr, the median of 0.10/yr, 0.16/yr and 0.17/yr, from the Pauly (1980), Hoenig (1983), and Jensen (1996) models, respectively.

Under the assumption of zero fishing mortality, the conditional intrinsic rate of increase parameter, r, was estimated at 0.00%/yr and was not significantly different from zero based on the 95% confidence interval (P>0.05) (Table 5). The average age of mothers of newborn individuals in the stable-age population was estimated at 18.76 years, and the average number of

Table 3

Age-length key showing the number of fish aged within different length classes for *Triakis megalopterus* sampled on the southeast coast of South Africa. TL=total length. Sexes were combined.

Length class (mm TL)	Age																								
	0	1	2	3	4	5	6	7	8	9	10	11	12	13	14	15	16	17	18	19	20	21	22	23	24	25
200–399	6																									
400–599	5																									
600–799			3	2			1																			
800–999				1	3	1	2	1																		
1000–1199					1	1	1	1	3	1			2		1											
1200–1399								1	1	2	1		2		2	1					1					
1400–1599												1	2	2	3	4	5	4	2	1	1	1		2		1
1600–1799											1							1	2		4			1	1	

Table 4

Estimates for von Bertalanffy growth model parameters (and their associated variability and correlation matrices) for male, female, and combined-sexes of *Triakis megalopterus* sampled on the southeast coast of South Africa. L_∞=theoretical maximum size, k=growth coefficient, t_0=theoretical age at zero length, SE=standard error, CV=coefficient of variation, 95% CI=95% confidence intervals, TL=total length.

Parameter	Estimate	SE	CV	95% CI	k	t_0
Males (n=26)						
L_∞ (mm TL)	1667.89	103.35	6.1%	(1517.25 to 1909.17)	−0.95	−0.63
k (/yr)	0.12	0.02	17.4%	(0.09 to 0.17)		0.79
t_0 (yrs)	−2.15	0.42	19.4%	(−3.07 to −1.39)		
Females (n=60)						
L_∞ (mm TL)	1738.93	90.60	5.2%	(1618.95 to 1969.19)	−0.95	−0.70
k (/yr)	0.10	0.02	16.2%	(0.07 to 0.14)		0.85
t_0 (yrs)	−2.67	0.59	21.4%	(−4.02 to −1.75)		
Combined (n=86)						
L_∞ (mm TL)	1711.07	56.42	3.3%	(1615.79 to 1844.95)	—0.93	−0.65
k (/yr)	0.11	0.01	10.7%	(0.09 to 0.13)		0.82
t_0 (yrs)	−2.43	0.35	14.2%	(−3.18 to −1.80)		

female offspring per female during her lifespan was estimated at 1.00 (Table 5).

Over half (50.6%) of the female stable-age distribution of this population was accounted for by sharks less than four years of age. Age-1 sharks contributed 16% of the female stable-age distribution, and only 8% of the female stable-age distribution was mature (≥15 years of age).

The elasticity of λ, the annual population growth rate, was relatively low for both fertility (5.5%) and adult survival (14.4%) and the highest for juvenile survival (80.2%) (Table 5).

The conditional intrinsic rate of increase parameter, r, exhibited a nonlinear response when calculated for a variety of combinations of fishing mortality and age-at-capture scenarios (Fig. 5). In general, the conditional intrinsic rate of increase declined as fishing mortality increased and the rate of decline was inversely proportional to age at first capture. When the conditional intrinsic rate of increase was modeled as a function of fishing mortality at the current natural mortality rate and age at 50% selectivity, a zero rate of increase was observed at F=0.04/yr.

Discussion

In this study, *T. megalopterus* exhibited annular growth zone ftormation, depositing one band pair per year, as was also found in *T. semifasciata* (Smith, 1984; Kusher et al., 1992). The ratio of the number of sharks that exhibited fluorescence in their vertebrae (n=7) to the number of sharks injected (n=23) was unfortunately low and may (see Smith, 1984) or may

Table 5

Summary of demographic parameters and elasticities estimated during this study for *Triakis megalopterus* and four other triakid shark species from Cortés (2002). Values in parenthesis denote lower and upper 95% confidence intervals calculated from 1000 Monte-Carlo simulations. λ=annual population growth rate, r=conditional intrinsic rate of increase (calculated as r=lnλ), $\overline{T}$ = average age of mothers of newborn individuals in a population with a stable age distribution, R_0=average number of female offspring per female during her lifespan (calculated as $R_0 = \exp(r\overline{T})$).

					Elasticity (%)		
Species	λ	r	$\overline{T}$	R_0	Fecundity	Juvenile survival	Adult survival
Triakis megalopterus	1.000 (0.976–1.041)	0.000 (−0.024–0.040)	18.76 (14.44–19.86)	1.00 (0.63–1.83)	5.4	78.3	16.4
Mustelus californicus	1.132	0.124	4.6	1.77	18.5	34.7	46.8
Mustelus manazo	1.096	0.092	6.6	1.83	13.3	52.4	34.3
Mustelus antarcticus	1.082	0.079	11.5	2.48	8.0	50.6	41.3
Triakis semifasciata	1.016	0.016	18.5	1.34	5.1	63.9	31.0

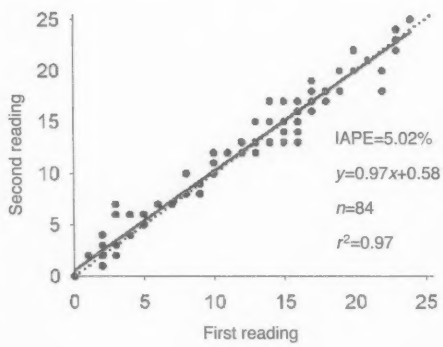

Figure 2

Age-bias plot of estimated ages from *Triakis megalopterus* vertebrae. Sharks were sampled on the southeast coast of South Africa. The age-bias plot regresses the age estimates from a second reading against the age estimates from the first reading. IAPE=index of average percent error.

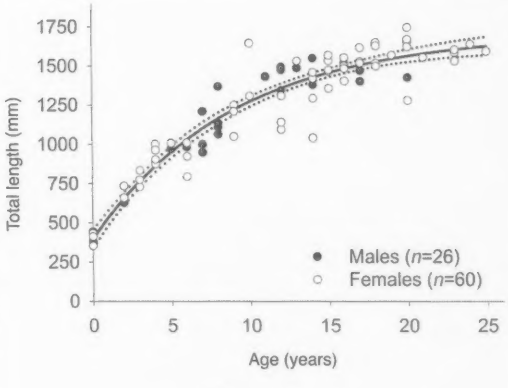

Figure 3

Observed total lengths of male and female *Triakis megalopterus* sampled from the southeast coast of South Africa. Length data were overlaid with the predicted von Bertalanffy growth model (solid line) and its 95% confidence intervals (dotted lines) estimated by using parametric bootstrapping.

not (see McFarlane and King, 2009) be related to the slow growth and low levels of calcification of the vertebrae of these long lived sharks. Absolute age was validated up to 25 years. Oxytetracycline was shown to be an effective growth marker for *T. megalopterus*, which, like its congener *T. semifasciata*, exhibits slow growth and a maximum age of at least 25 years (Smith, 1984; Smith et al., 2003).

Female *T. megalopterus* were found to grow larger than males—a finding similar to that of Kusher et al. (1992) for *T. semifasciata*. In both studies, males grew to a similar size but female *T. megalopterus* were considerably larger. Kusher et al. (1992) found that their growth coefficient estimates of 0.07/yr for females, 0.09/yr for males, and 0.08/yr for both sexes combined were lower than what would be predicted from Holden's (1974) method of estimation with the ratios of length at birth to maximum observed length (range=0.1–0.2/yr). Using a birth size of 435 mm and a female maximum observed length of 2075 mm TL together with a gestation period of 1.7 years (Smale and Goosen, 1999), Holden's (1974) estimated the growth coefficient at 0.12/yr, which corresponds well with the growth curve estimate.

Our estimate of age at maturity for *T. megalopterus* exceeds that of *T. semifasciata* (7 years for males, 10

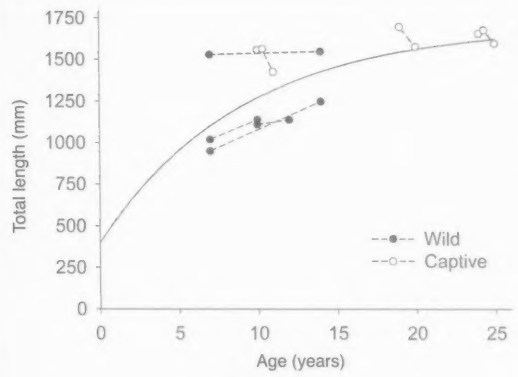

Figure 4

Observed length at age (dots) and von Bertalanffy predicted growth (line) of captive and wild *Triakis megalopterus* (sexes combined) sampled from the southeast coast of South Africa. The dotted lines between the dots represent the growth in length between successive ages after validation with oxytetracycline hydrochloride.

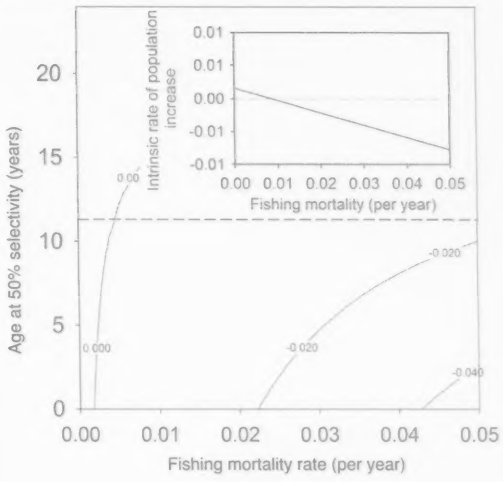
Age at 50% selectivity (years)
Fishing mortality rate (per year)
Intrinsic rate of population increase
Fishing mortality (per year)

Figure 5

Isopleth of the conditional intrinsic rate of population increase (r) for *Triakis megalopterus* at different combinations of age at 50% selectivity and fishing-induced mortality rate. The dashed line illustrates the current age at 50% selectivity of 11.13 years. The inset figure illustrates the conditional intrinsic rate of population increase as a function of fishing mortality at the current age at 50% selectivity.

years for females) estimated by Kusher et al. (1992). In *T. megalopterus*, sexual maturation occurs at approximately 79% and 83% of asymptotic length for males and females, respectively. In terms of maximum observed length, sexual maturation occurs at 86% and 70% of asymptotic length. These ratios were higher than those of *T. semifasciata*, which are 63% and 72% for males and females, respectively (Kusher et al., 1992). Although our estimates are high, and could possibly be improved with larger sample sizes, they indicate that *T. megalopterus* is vulnerable to overexploitation and that management measures (particularly exemption of this species from commercial exploitation in South Africa) need to be rigorously enforced to protect this endemic species (Compagno et al., 1989).

Unfortunately all captive specimens examined in this study exhibited retarded growth. In some teleosts, this has been attributed to an effect of OTC (Monaghan, 1993). In both Japanese wobbegong (*Orectolobus japonicas*) and nurse sharks (*Ginglymostoma cirratum*), Tanaka (1990) and Gelsleichter et al. (1998) showed that OTC, at concentrations ranging from 20 to 80 mg/kg, had little adverse effects on growth or health. It is therefore unlikely that OTC, administered at 50 mg/kg, would have caused growth retardation, and there appears to be an alternative explanation for the negative growth observed —one that may be related to temperature stress.

Sustained water temperature, if beyond the optimal range of the species, can have an adverse affect on growth. Selong et al. (2001) showed that if an upper temperature threshold is exceeded, the result is inhibited feeding and later, death. Summer temperatures in the Bayworld Aquarium exceeded the upper threshold of the natural temperature range tolerated by spotted gully sharks in their natural habitat—occasionally spiking at 27°C—whereas the normal temperature range off the Eastern Cape coast is approximately 12°C to 21°C in waters of <20 m. All the captive sharks were observed to reduce their food consumption and were noticeably thinner during summer than in winter, indicating that the summer elevated temperatures were exerting physiological stress on these display specimens. Whereas wild sharks are able to respond to high temperatures by swimming to deeper or cooler waters, this option is not available to captive individuals and they may not be able to avoid temperature stress. The aquarium animals used in this study were removed from display and were euthanized when they began to show signs of lethargy and exhibited marked weight loss and heat stress. It should be noted that some individuals of this species were able to cope with the high temperatures and survived multiple years, indicating that there is individual variation in susceptibility to heat stress.

The growth of the specimens over a seven-year period followed the growth curve and supports the robustness of the von Bertalanffy growth model for this species. Meaningful estimates of length between capture and recapture events in slow growing, long-lived species can only be attained if the time interval between the two events is large. If the time interval is too small, measurement error would be high in relation to the

gain in growth, particularly when measuring a robust, lively shark. The impact of this error would therefore be reduced when sampling intervals are years apart and more growth has occurred. Where growth is modest and measuring error occurs, the scope for inaccurate size estimates is greater. For this reason, size estimates of sharks from aquaria may be less reliable because of the relatively short time between measurements. However, this study would best be repeated in aquaria without unseasonably high summer temperatures.

The results from the demographic model indicate that *T. megalopterus* can sustain very limited fishing pressure, and therefore these results reinforce the biological interpretation of its life history parameters. It has been shown that species that are long lived, have a low rate of natural mortality, and produce few offspring per year cannot sustain high levels of fishing pressure (Holden, 1974; Cailliet, 1992; Simpfendorfer, 2005; Dulvey and Forrest, 2010). Even small increases in fishing-induced mortality, particularly at the current size of selection will negatively impact the population. At 11 years, sharks are harvested 4 years before the onset of sexual maturity. This age is of concern because the model predicts that an average age of a female shark is around 19 years and it will produce only a single female offspring over her lifetime. Any additional increase in fishing mortality would further decrease the number of adults and possibly contribute to recruitment overfishing. There are numerous examples in the literature of overexploitation and even extirpation of populations of chondrichthyans because their life history parameters are not understood and/or taken into consideration in management scenarios (Dulvey and Forrest, 2010).

The life history parameters of *Triakis megalopterus* were similar to those of its congener, *T. semifasciata*. Both sharks live to about 25 years of age, have similar natural mortality rates, and produce similar numbers of embryos per annum. As a result, it is not surprising that the demographic model applied to both species shows similar trends. Cailliet (1992) recommended that fishing mortality be reduced to $0.5M$, and that the size at capture be increased to prevent a decline in abundance. We determined in this study that, at current selection levels, the fishing mortality rate required for a stable population size would be $0.02M$. Even if the age at 50% capture were increased significantly to 20 years, *T. megalopterus* would not be able to sustain even moderate levels of fishing mortality. Any possible increases in fishing mortality should, therefore, be closely monitored.

Triakis megalopterus is legislated as a noncommercial species with zero commercial harvest. This species is, however, targeted by recreational anglers. From personal observations, there has been a steady increase in recreational anglers targeting elasmobranchs because of a reduction in the availability of other favoured teleost species. Increased targeted fishing of this shark species could possibly result in higher levels of postrelease mortality from hooking and handling. Despite its noncommercial status, *T. megalopterus* is unfortunately mistaken as *Mustelus mustelus* in a small, yet developing, inshore shark longline fishery. Even if bycatch rates were to remain constant, the increased catches in this developing fishery would result in obvious increases in mortality from commercial fishing.

Of the triakids that have been demographically modeled (Table 5), the *Mustelus* species appear to be the most resilient to harvesting pressure and have been shown to support sustainable fisheries (Walker, 1992; Chiaramonte, 1998; Francis and Shallard, 1999). The two reef-associated *Triakis* species have less habitat available and correspondingly smaller population sizes. Given their reduced habitat and life history characteristics, it is not surprising that their populations will decrease with commercial harvesting.

Acknowledgments

This study would not have been possible without the assistance of numerous anglers, and in particular M. Spies, who assisted with tagging with A. Goosen, who initiated the growth study with MJS. C. Attwood and his tagging team are acknowledged for their assistance at De Hoop, and for supplying data and material used in this study. Work at Bird Island was initiated under research permits from the Eastern Cape Department of Economic Affairs, Environment and Tourism, and South African National Parks. Financial support from the National Research Foundation and administration by Bayworld Centre for Research and Education are gratefully acknowledged. K. Goldman and two anonymous reviewers are thanked for their helpful comments.

Literature cited

Akaike, H.
1973. Information theory as an extension of the maximum likelihood principle. *In* Second international symposium on information theory (B. N. Petrov and F. Csaki, eds.), p. 267–281. Akademiai Kiado, Budapest.

Ardizzone, D., G. M. Cailliet, L. J. Natanson, A. H. Andrews, L. A. Kerr, and T. A. Brown.
2006. Application of bomb radiocarbon chronologies to shortfin mako (*Isurus oxyrinchus*) age validation. Environ. Biol. Fish. 77:355–366.

Beamish, R. J., and D. A. Fournier.
1981. A method for comparing the precision of a set of age determinations. Can. J. Fish. Aquat. Sci. 38:982–983.

Buckland, S. T.
1984. Monte-carlo confidence intervals. Biometrics 40:811–817.

Cailliet, G. M.
1992. Demography of the central California population of the leopard shark (*Triakis semifasciatus*). Aust. J. Mar Freshw. Res. 43:183–193.

Cailliet, G. M., and K. J. Goldman.
2004. Age determination and validation in chondrichthyan fishes. *In* Biology of sharks and their relatives (J. C. Carrier, J. A. Musick, and M. R. Heithaus, eds.), p. 399–447. CRC Mar. Biol. Ser., London.

Campana, S. E.
2001. Accuracy, precision and quality control in age determination, including a review of the use and abuse of age validation methods. J. Fish Biol. 59:197–242.
Campana, S. E., L. J. Natanson, and S. Myklevoll.
2002. Bomb dating and age determination of large pelagic sharks. Can. J. Fish. Aquat. Sci. 59:450–455.
Caswell, H.
2001. Matrix population models: construction, analysis, and interpretation, 722 p. Sinauer, MA.
Chiaramonte, G. E.
1998. Shark fisheries in Argentina. Mar. Freshw. Res. 49:601–609.
Chen, W. K., P. C. Chen, K. M. Liu, and S. B. Wang.
2007. Age and growth estimates of the whitespotted bamboo shark, *Chiloscyllium plagiosum*, in the northern waters of Taiwan. Zool. Stud. 46:92–102.
Compagno, L. J. V.
1988. Sharks of the order Carcharhiniformes, 485 p. Princeton Univ. Press, Princeton, NJ.
Compagno, L. J. V., M. Dando, and S. Fowler.
2005. A field guide to the sharks of the world, 386 p. Collins, London.
Compagno, L. J. V., D. A. Ebert, and M. J. Smale.
1989. Guide to the sharks and rays of southern Africa, 58 p. Struik Publishers, Cape Town.
Cortés, E.
2002. Incorporating uncertainty into demographic modeling: application to shark populations and their conservation. Cons. Biol. 16:1048–1062.
Dulvey, N. K., and R. E. Forrest.
2010. Life histories, population dynamics, and extinction risks in Chondrichthyans. *In* Sharks and their relatives: biodiversity, adaptive physiology and conservation (J. C. Carrier, J. A. Musick, and M. R. Heithaus, eds.), p. 639–679. CRC Press, London.
Francis, M. P., and B. Shallard.
1999. New Zealand shark fishery management. *In* Case studies of management of elasmobranch fisheries (R. Shotton, ed.) p. 515–579. FAO Fisheries Technical Paper no. 378. FAO, Rome.
Gedamke, T., Hoenig, J., Musick, J. A., and W. D. DuPaul.
2007. Using demographic models to determine intrinsic rate of increase and sustainable fishing for elasmobranchs: pitfalls, advances, and applications. N. Am. J. Fish. Manage. 27:605–618.
Gelsleichter, J., E. Cortes, C. A. Manire, R. E. Heuter, and J. A. Musick.
1998. Evaluation of oxytetracycline on growth of captive nurse sharks, *Gingymostoma cirratum*. Fish. Bull. 96:624–627.
Goosen, A. J, and M. J. Smale.
1997. A preliminary study of age and growth of the smoothhound shark *Mustelus mustelus* (Triakidae). S. Afr. J. Mar. Sci. 18:85–91.
Hoenig, J. M.
1983. Empirical use of longevity data to estimate mortality rates. Fish. Bull. 82: 898–903.
Hoenig, J. M., M. Morgan, and C. A. Brown.
1995. Analyzing differences between two age determination methods by tests of symmetry. Can. J. Fish. Aquat. Sci. 52:364–368.
Holden, M. J.
1974. Problems in the rational exploitation of elasmobranch populations and some suggested solutions. *In* Sea fisheries research (F. R. Harden Jones, ed.) p 117–137. Elek Science, London.
Jensen, A. L.
1996. Beverton and Holt life history invariants result from optimal trade-off of reproduction and survival. Can. J. Fish. Aquat. Sci. 53:820–822.
Kusher, D. I., S. E. Smith, and G. M. Cailliet.
1992. Validated age and growth of the leopard shark, *Triakis semifasciata*, from central California. Environ. Biol. Fish. 35:187–203.
McFarlane, G. A., and J. R. King.
2009. Re-evaluating the age determination of spiny dogfish using oxytetracycline and fish at liberty up to 20 years. *In* Biology and management of dogfish sharks (V. F. Gallucci, G. A. McFarlane, and G. G. Bargmann, eds), p. 153–160. Am. Fish. Soc., Bethesda, MD.
Mollet, H. F., and G. M. Cailliet.
2002. Comparative population demography of elasmobranches using life history tables, Leslie matrices and stage-based matrix model. Mar. Freshw. Res. 53:503–516.
Monaghan, J. P.
1993. Comparison of calcein and tetracycline as chemical markers in summer flounder. Trans. Am. Fish. Soc. 122:298–301.
Natanson, L. J., N. E. Kohler, D. Ardizzone, G. M. Cailliet, S. P. Wintner, and H. F. Mollet.
2006. Validated age and growth estimates for the shortfin mako, *Isurus oxyrinchus*, in the North Atlantic Ocean. Environ. Biol. Fish. 77:367–383.
Neer, J. A., B. A. Thompson, and J. K. Carlson.
2005. Age and growth of *Carcharhinus leucas* in the northern Gulf of Mexico: incorporating variability in size at birth. J. Fish Biol. 67:370–383.
Pauly, D.
1980. On the interrelationships between natural mortality, growth parameters and mean environmental temperature in 175 fish stocks. J. Cons. Int. L'Expl. Mer 39:175–192.
Romine, J. G., Musick, J. A. and G. H. Burgess.
2009. Demographic analyses of the dusky shark, *Carcharhinus obscurus*, in the Northwest Atlantic incorporating hooking mortality estimates and revised reproductive parameters. Environ. Biol. Fish. 84:277–289.
Selong, J. H., T. E. McMahon, A. V. Zale, and F. T. Barrows.
2001. Effect of temperature on growth and survival of bull trout, with application of an improved method for determining thermal tolerance in fishes. Trans. Am. Fish. Soc. 130:1026–1037.
Schnute, J.
1981. A versatile growth model with statistically stable parameters. Can. J. Fish. Aquat. Sci. 38:1128–1140.
Simpfendorfer, C. A.
1998. Mortality estimates and demographic analysis for the Australian sharpnose shark, Rhizoprionodon taylori, from northern Australia. Fish Bull. 97:978–986.
2005. Demographic models: life tables, matrix models and rebound potential. *In* Management techniques for elasmobranch fisheries (J. A. Musick and R. Bonfil, eds), p. 143–153. FAO Fisheries Technical Paper No. 474, Rome.
Simpfendorfer, C. A., J. Chidlow, R. McAuley, and P. Unsworth.
2000. Age and growth of the whiskery shark, *Furgaleus macki*, from southwestern Australia. Environ. Biol. Fish. 58:335–343.

Smale, M. J., and A. J. Goosen.
1999. Reproduction and feeding of the spotted gully shark , *Triakis megalopterus,* off the Eastern Cape, South Africa. Fish. Bull. 97:987–998.

Smith, S. E.
1984. Timing of vertebral-band deposition in tetracycline-injected leopard sharks. Trans. Am. Fish. Soc. 113:308–313.

Smith, S. E., and N. J. Abramson.
1990. Leopard shark *Triakis semifasciata* distribution, mortality rate, yield, and stock replenishment estimates based on a tagging study in San Francisco Bay. Fish. Bull. 88:371–381.

Smith, S. E., R. A. Mitchell, and D. Fuller.
2003. Age-validation of a leopard shark (*Triakis semifasciata*) recaptured after 20 years. Fish. Bull. 101:194–198.

Tanaka, S.
1990. Age and growth studies on the calcified structures of newborn sharks in the laboratory aquaria using tetracycline. *In* Elasmobranchs as living resources: advances in the biology, ecology, systematics, and the status of the fisheries (H. L. Pratt, S. H. Gruber, and T. Taniuch, eds.), p. 189–202. U.S. Dep. Commer. NOAA Tech. Rep. 90.

Walker, T. I.
1992. Fishery simulation model for sharks applied to the gummy shark, *Mustelus antarcticus* Günther, from southern Australian waters. Aust. J. Freshw. Res. 43:195–212.

Yudin, K. G., and G. M. Cailliet.
1990. Age and growth of the gray smoothhound, *Mustelus californicus*, and the brown smoothhound, *M. henlei*, sharks from central California. Copeia 1990:191–204.

Ontogenetic and temporal variability in the fat content and fatty acid composition of Atlantic herring (*Clupea harengus*) from the Bay of Fundy, Canada

Hillary A. Lane (contact author)[1,2*]
Andrew J. Westgate[1,2]
Heather N. Koopman[1,2]

Email address for contact author: hillaryannelane@gmail.com

[1] Department of Biology and Marine Biology
University of North Carolina Wilmington
601 South College Road
Wilmington, North Carolina 28403
* Present address for contact author: University of Maryland
Department of Biology
College Park, Maryland 20742

[2] Grand Manan Whale and Seabird Research Station
24 Route 776
Grand Manan, New Brunswick, E5G 1A1, Canada.

Abstract—Atlantic herring (*Clupea harengus*) is an ecologically and economically valuable species in many food webs, yet surprisingly little is known about the variation in the nutritional quality of these fish. Atlantic herring collected from 2005 through 2008 from the Bay of Fundy, Canada, were examined for variability in their nutritional quality by using total lipid content (n=889) and fatty acid composition (n=551) as proxies for nutritional value. A significant positive relationship was found between fish length and total lipid content. Atlantic herring also had significantly different fatty acid signatures by age. Fish from 2005 had significantly lower total lipid content than fish from 2006 through 2008, and all years had significantly different fatty acid signatures. Summer fish were significantly fatter than winter fish and had significantly different fatty acid signatures. For all comparisons (ontogenetic, annual, and seasonal) percent concentrations of omega-3, -6, and long-chain monounsaturated fatty acids were the most important for distinguishing between the fatty acid signatures of fish. This study underscores the importance of quantifying variation in prey quality synoptically with prey quantity in food webs over ontogenetic and temporal scales when evaluating the effect of prey nutritional quality on predators and on modeling trophic dynamics.

Manuscript submitted 11 May 2010.
Manuscript accepted 9 November 2010.
Fish. Bull. 109:113–122 (2011).

The views and opinions expressed or implied in this article are those of the author (or authors) and do not necessarily reflect the position of the National Marine Fisheries Service, NOAA.

Variation in prey abundance has been documented in a wide range of food webs (e.g., Colwell and Landrum, 1993; Forsman and Lindell, 1997; Greenstreet et al., 1998; Melvin and Stephenson, 2007); however, variation in the nutritional quality of those prey has not been well investigated. In most studies to date, the nutritional quality of prey is assumed to be constant over space and time (e.g., Chase, 2002; Krebs et al., 2003, Womble and Sigler, 2006; Woo et al., 2008), despite the fact that species can exhibit considerable variation in their value as prey items (e.g., Iverson et al., 2002; Diamond and Devlin, 2003; Jensen et al., 2007; Huynh and Kitts, 2009). Despite the ecological and economic importance of Atlantic herring (*Clupea harengus*), robust temporal and ontogenetic data quantifying the variation in the nutritional value of these fish do not exist. Here we show, using Atlantic herring as a model prey species, that considerable temporal and ontogenetic variation does exist in the nutritional value of a given prey item, underscoring the importance of collecting data on both the quantity and quality of prey when evaluating its impact on an ecosystem level.

Atlantic herring are a major portion of the diet of many upper trophic level predators in the western North Atlantic (wNA), such as seals, porpoises, dolphins, whales, predatory fish, sharks, and seabirds (Katona et al., 1993, and are also the target of several major fisheries (purse seine, weir) for human consumption. Herring feed mainly on zooplankton (De Silva, 1973) and thus serve as an important connection between lower and upper trophic levels in food webs and can be considered a keystone prey species in this ecosystem (Overholtz and Link, 2007). Herring in the wNA generally spawn in the fall (Boyar et al., 1973; Colton et al., 1979), eggs incubate for about 15 days (Messieh et al., 1985) and then enter a six-month pelagic larval phase (Sinclair and Tremblay, 1984). Rapid juvenile growth is observed for 1–2 years (Anthony, 1972), and maturity occurs at around age 3 (O'Brien et al., 1993). Historically the biomass of these stocks has undergone fluctuations in the wNA (Anthony and Waring, 1980; Overholtz and Friedland, 2002), but little is known about changes in Atlantic herring nutritional quality.

The substantial effort required to collect robust spatial and temporal data has created prey quality data sets that do not adequately capture the variability present in the prey

field that was sampled. For example, the few studies that exist to date on the nutritional value of Atlantic herring have been conducted with limited types of analyses or comprise small temporal and spatial ranges (e.g., Torcher et al., 1985; Bradford, 1993; Budge et al., 2002). Jensen et al. (2007) demonstrated that Baltic herring do exhibit significant variation in their fatty acid composition; however, comparable data are not available through most of the range of these fish. In fact, the most recent comprehensive examination of the lipid profiles of herring from the Bay of Fundy was conducted by Stoddard[1] over 40 years ago. Considering the ecological importance of herring in the Bay of Fundy, it is surprising that so little is currently known about the nutritional value of this species.

The high abundance of herring in the Bay of Fundy system combined with the role of this species as a main prey item creates a perfect model in which to evaluate variation in prey quality. We used total lipid content and lipid composition (specifically, fatty acid profiles) as indices of prey quality for two reasons: 1) the lipids of a fish can be used as indicators of its nutritional value and overall body condition (Sargent et al., 1988); and 2) lipids provide twice the energy per unit of mass when metabolized than do proteins and carbohydrates (Hadley, 1985) and therefore are the main determinants of the caloric value of lipid-rich fish such as Atlantic herring. Documenting the individual fatty acid components that comprise Atlantic herring lipids also has the potential to provide information about the nutritional value of a given fish because certain fatty acids have important and specific physiological (e.g., the familiar omega-3 and omega-6 molecules; Pond, 1998, Szlinder-Richert et al., 2010.) and energetic (long-chain saturates; Hadley, 1985) roles. Fatty acid (chemical profile) data can also be used as trophic markers to indicate shifts in diet (Bishop et al., 1983; Budge et al., 2002; Dalsgaard et al., 2003; Budge et al., 2006), however these types of trophic studies require an extensive library of data on the fatty acid composition of all members of an ecosystem, which is not currently available for the Bay of Fundy. This study is a first step in creating such a prey library because the main objective is to determine the total lipid content and fatty acid composition of different sizes of Atlantic herring collected between 2005 and 2008 across ontogenetic, annual, and seasonal scales.

Materials and methods

Sample collection

Atlantic herring samples were provided by local fishermen from stationary weirs or purse-seine nets in the Bay of Fundy, New Brunswick, Canada, from 2005 through 2008. During summer (June–September), fish were collected weekly, whereas during winter (October–May) fish were collected more opportunistically. Owing to sampling constraints, fish from only a single winter season were sampled (2006–07). Spring and fall fish were not collected because the largest differences in nutritional value were expected to occur between the seasons that were the most different in regards to climate and ocean productivity (summer and winter). All fish from each sampling period (typically 10–30 fish) were weighed to the nearest milligram, and their fork length was recorded to the nearest millimeter. After the initial measurements, 10 fish from each sample were selected to encompass the entire size range of the individuals collected in each sampling period, and each fish was individually homogenized in a food processor (KitchenAid®, St. Joseph, MI). Generally, the fish that were collected were sexually immature although sexually mature individuals were processed when available. Subsamples of the homogenate from each fish were sealed in cryovials under nitrogen gas and frozen at –20°C. Vials were kept extremely full to limit risk of oxidation, and all samples were processed within six months of collection (Budge et al., 2002; 2006).

Analysis of total lipid content and fatty acid composition

Total lipids were extracted from Atlantic herring samples using a modified Folch et al. (1957) chloroform/methanol extraction as described in Budge et al. (2002) and Koopman (2007) and are reported as a percentage of wet tissue weight. For gas chromatography (GC) analysis, fatty acid butyl esters (FABE) were prepared from total lipid extracts. Fatty acids were separated and analyzed by GC by using a Varian capillary (3800) gas choromatograph (Varian Inc, Division of Agilent, Santa Clara, CA) with a flame ionization detector (FID) in a fused silica column (30 mm length×0.25 mm inner diameter) (Zebron FFAP; Phenomenex, Inc., Torrance, CA). Helium was used as the carrier gas and the gas line was equipped with an oxygen and water scrubber. The following temperature program was used: start at 65°C for 2 min, hold at 165°C for 0.40 min after ramping at 20°C/min, hold at 215°C for 6.6 min after ramping at 2°C/min, and hold at 250°C for 5 min after ramping at 5°C/min. Up to 80 different fatty acids were identified by following the methods of Iverson et al. (1997; 2002) of which the molecular identities were confirmed by gas chromatography and mass spectrometry (S. Budge, personal commun.[2]) by using standard chemicals run on both machines. Each fatty acid was described by using the nomenclature of *A:Bn-X*, where *A* is the number of carbon atoms, *B* is the number of double bonds, and *X* is the position of the double bond closest to the terminal methyl group. Peak identification was confirmed in each run, and results were integrated with Galaxie GC software (vers. 1.8.501.1, Varian, Inc., Palo Alto, CA).

[1] Stoddard, J. H. 1967. Studies of the condition (fatness) of herring. Fish. Res. Board Can. Manuscript No. 1042, 15 p.

[2] Budge, Suzanne. 2009. Canadian Institute of Fisheries Technology, Dalhousie University, Halifax, Nova Scotia, Canada B3J 2X4.

Statistical analysis of total lipid content

Statistical analysis was conducted by using SPSS, vers. 16.0 (SPSS, Inc., Chicago, IL) and Plymouth Routines in Multivariate Ecological Research (PRIMER 6, Primer-E, Ltd., Ivybridge, UK) statistical software and a significance level of 0.05 for each test performed. Error was reported as standard deviation. Analysis of covariance (ANCOVA) tests were evaluated for equality of variance by using Levene's test. Kolmogorov-Smirnov and Shapiro-Wilk normality tests were conducted on raw total percent lipid data. For comparisons of age classes, the age of each fish was estimated from length-at-age curves published in the literature (Penttila et al., 1989). Corrected Akaike information criteria (AIC_c) scores were calculated for linear, quadratic, and cubic distributions to determine the best fit for the relationship between total lipid content and fish size (Burnham and Anderson, 2002), and the remaining analyses were conducted by using the model of best fit. The normalized relative likelihood of any model to best represent the data is its Akaike weight, w_i, and lower w_i values indicate better model fits. The AIC model w_i statistics heavily favored the linear model (linear: w_i=0; quadratic: w_i=0.46; cubic: w_i=0.54), and therefore the linear model was used in subsequent regression analyses.

The relationship between total percent lipid (wet weight) and fish fork length over the entire size range of fish collected was examined with linear regression. Because size had a significant effect on total percent lipid (see *Results* section), the remaining analyses were conducted by using ANCOVA to account for this covariation. The annual, seasonal, and monthly variation in total percent lipid content of Atlantic herring was examined by ANCOVA. Only samples from 2006–07 were included in seasonal analyses because the winter of 2006–07 was the only winter in which samples were collected.

Statistical analysis of fatty acid composition

Fatty acid signatures of individual fish were compared by using PRIMER, vers. 6 software (Clarke, 1993; Clarke and Warwick, 2001; Clarke and Gorley, 2006). Of the suite of 67 fatty acids present in herring, a subset of 23 were selected and analyzed to determine whether patterns existed in fatty acid signatures in herring of different sizes, years, and seasons. These fatty acids were 14:0, 16:0, 16:1*n*-11, 16:1*n*-9, 16:1*n*-7, 16:1*n*-5, 18:1*n*-11, 18:1*n*-9, 18:2*n*-6, 18:3*n*-3, 18:4*n*-3, 20:1*n*-11, 20:1*n*-9, 20:1*n*-7, 20:4*n*-6, 20:4*n*-3, 20:5*n*-3, 22:1*n*-11, 22:1*n*-9, 22:1*n*-7, 22:5*n*-3, 22:6*n*-3, and 24:1*n*-9. These fatty acids were chosen if they were present in at least 95% of the individual fish analyzed. If a particular fatty acid was not detected in an individual, the concentration of that fatty acid was changed from zero to 0.005% because it was below the minimum detectable level (0.01%), but it was not so small that it would result in extreme outliers (Iverson et al., 2002). Individual fatty acids were standardized before analysis by dividing the value of each fatty acid in each sample by the standard deviation of that fatty acid in all samples and resemblance matrices were created on the basis of Bray-Curtis similarity.

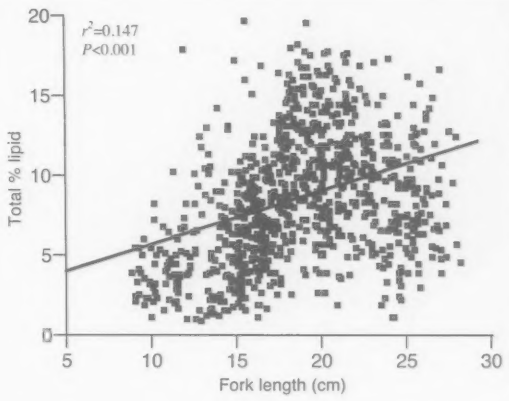

Figure 1

Bivariate scatterplot of total percent lipid by fork length for Atlantic herring (*Clupea harengus*, n=889). Although the linear r^2 value is low, the relationship is highly significant. The low r^2 value may be representative of the highly variable nature of the nutritional quality of herring in the Bay of Fundy ecosystem.

Nonmetric multidimensional scaling (MDS, 25 restarts, Kruskal scheme 1) analyses were conducted on the fatty acid profiles of all samples. MDS stress values range from 0 to 1. Low stress values indicate high confidence in the model, and stress values less than 0.2 were assumed to adequately represent the relationships of the samples in the model (Clark and Warwick, 2001). Analyses of similarities (ANOSIM, one-way, max. permutations=999) were conducted on all samples to evaluate the effect of fish age, year, and season on fatty acid signatures. Because similar patterns were observed when fish were separated first by age and then by year or season, all fish were pooled to examine annual and seasonal variability in fatty acid signatures to allow for higher power in the analyses. ANOSIM global r values range from 0 to 1, and higher global r values are more significant. One-way similarity percentages analysis (SIMPER, one-way, based on Bray-Curtis similarity, cut-off percentage=90) was conducted on all samples if the analysis of similarities was significant, to determine the fatty acids that contributed the most to the differences observed between groups.

Results

Total lipid content

A total of 889 individual fish collected between 2005 and 2008 were analyzed for trends in total lipid content (percentage of wet weight; Table 1). The linear regression of

Table 1

Number of fish sampled (total fish), and size range of Atlantic herring (*Clupea harengus*) analyzed for differences in total lipid content by year, season, and age class.

Year	Total fish	Size (cm)	Summer	Winter	Age 1	Age 2	Age 3	Age 4+
2005–2008	889	8.8–28.2	731	158	87	469	188	145
2005	113	9.0–25.0	113	0	2	66	37	8
2006	330	8.8–27.3	292	38	56	134	84	56
2007	334	10.7–28.2	214	120	26	206	37	65
2008	112	10.8–28.0	112	0	3	63	30	16

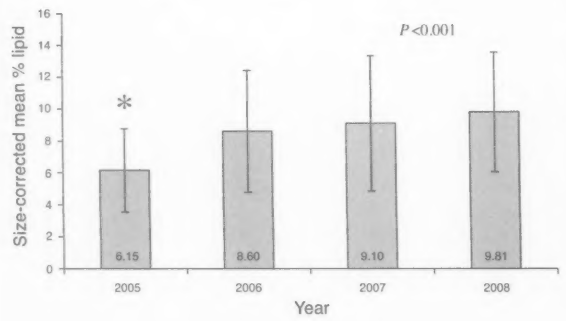

Figure 2

Size-corrected total lipid content in Atlantic herring (*Clupea harengus*) by sampling year (sample sizes: n_{2005}: 113, n_{2006}: 330, n_{2007}: 334, and n_{2008}:112). Error bars represent standard deviation; values inside bars graph are the yearly mean percent lipid.

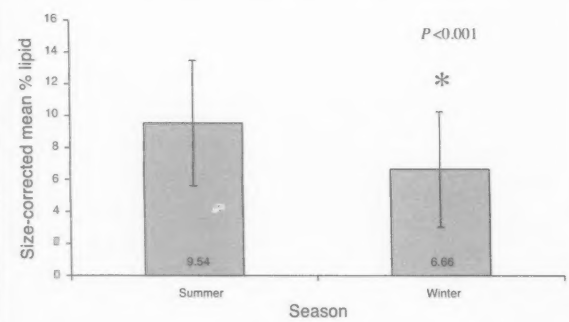

Figure 3

Size-corrected total lipid content by season for Atlantic herring (*Clupea harengus*) collected from 2006 through 2007 (n=158). Error bars represent standard deviation; values inside bars graph are the seasonal mean percent lipid.

total lipid content on fork length revealed a significant positive relationship (r^2=0.147, P<0.001, Fig. 1). The ANCOVA of total lipid content revealed significant differences (P<0.001) in the length-corrected lipid content of fish between years (Fig. 2). Multiple comparison tests (Bonferroni, α=0.05) showed that the total lipid content of fish from 2005 (6.15% ±2.61%, n=113) was significantly lower than the total lipid content of fish from 2006, 2007, and 2008 (P<0.001 for all comparisons), but fish from the latter three years were not different from each other (8.60% ±2.61%, n=330; 9.10% ±3.82%, n=334; and 9.81% ±3.75%), n=112, respectively; P>0.05). The ANCOVA of total lipid content by season was significant with summer fish having significantly more total lipid (9.54% ±3.93%, n=506) than winter fish (6.66% ±3.60%, n=158; P<0.001, Fig. 3).

Fatty acid composition

A total of 551 individual fish collected between 2005 and 2008 were analyzed for trends in fatty acid composition (Table 2). The ANOSIM of all fish showed a significant difference in fatty acid signatures of fish by age (global r=0.131, P<0.01, Fig. 4A). Figure 4A shows that age-1 and age-4+ fish group separately from age-2 and age-3 fish, but the clearest differences are seen between age-1 fish and all other age classes. The differences in the percent composition of these fatty acids by age can be seen in Table 3. For example, omega-3 and omega-6 fatty acids were significantly higher in concentration in age-1 fish than in age 2–4 fish (P<0.001, 25.88% ±6.42% and 20.73% ±3.57%, respectively), whereas long chain monounsaturated fatty acids (20:1n-11, 20:1n-9, 20:1n-7, 22:1n-11, 22:1n-9 and 22:1n-7) were higher in concentration in age 2–4 fish than in age-1 fish (P<0.001, 30.96% ±9.83% and 37.82% ±10.72%, respectively). However, the SIMPER analysis also showed that no fatty acid contributed more than 6.56% to the dissimilarity between the fatty acid signatures of fish by age, indicating that the variation observed

Table 2

Number of fish sampled (total fish) and size range of Atlantic herring (*Clupea harengus*) analyzed for differences in fatty acid signature by year, season, and age class.

Year	Total fish	Size (cm)	Summer	Winter	Age 1	Age 2	Age 3	Age 4+
2005–2008	551	8.8–28.2	480	71	70	272	131	78
2005	56	15.5–24.6	56	0	0	25	29	2
2006	260	8.8–27.3	225	35	52	108	60	40
2007	140	10.7–27.8	104	36	15	86	20	19
2008	95	10.8–28.0	95	0	3	53	23	16

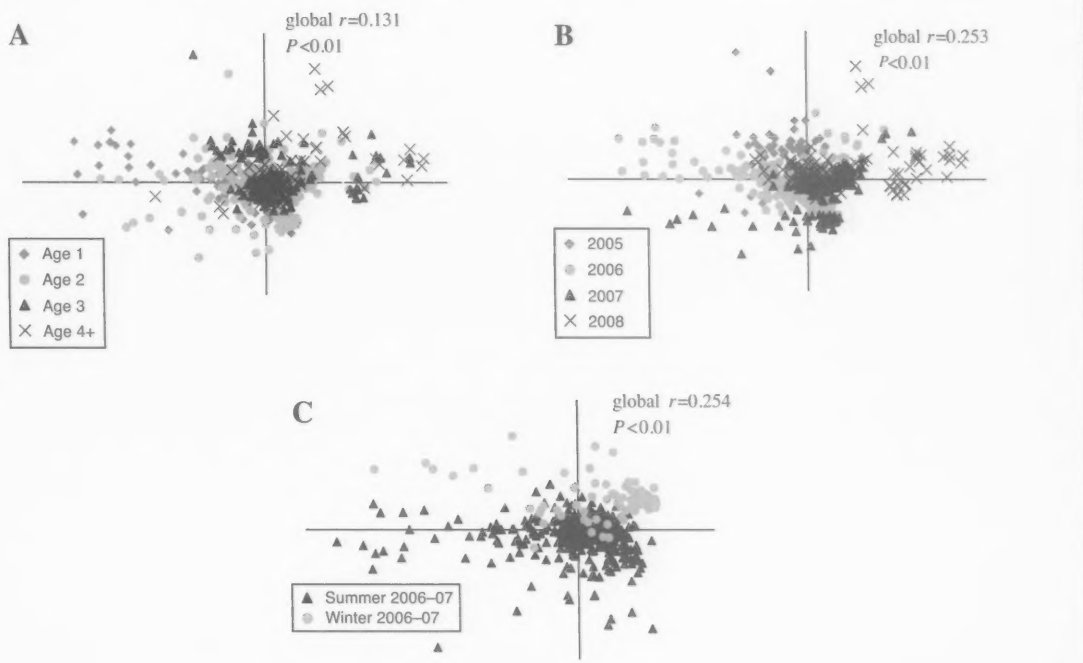

Figure 4

Multidimensional scaling plot of the fatty acid signatures of Atlantic herring (*Clupea harengus*) by (**A**) fish age, (**B**) sampling year, and (**C**) sampling season (2006–07 fish only). Symbols grouped together indicate similarity in fatty acid signatures between those symbols. Although all comparisons (age, year, and season) were significant, groupings were stronger by year (B) and season (C) than by age (A). Omega-3 and -6 and long chain monounsaturated fatty acids were important in distinguishing between the fatty acid signatures of fish ontogenetically, annually, and seasonally.

was in entire fatty acid signatures, not in just one or two individual fatty acids.

Significant differences were also found in the fatty acid signatures of fish by year (global r=0.253, P<0.01, Fig. 4B). Pairwise comparisons with ANOSIM indicated that fish from each year had significantly different fatty acid signatures (P<0.01), but the high r values for all pairwise tests that included fish from 2005 indicated that fish from 2005 were the most different in their fatty acid signatures (2005 vs. 2008: r=0.298; 2005 vs. 2007: 0.491; 2005 vs. 2006: 0.410; 2006 vs. 2007: 0.134; 2006 vs. 2008: 0.247; 2007 vs. 2008: 0.244). The separation of 2005 fish on the basis of fatty acid signatures was also evident from the results of the SIMPER analysis of fish by year. The average dissimilarities of comparisons including fish from 2005 were higher

Table 3

Age, sample size, mean percent composition, and standard error (SE) of all fatty acids that were included in non-parametric models to analyze Atlantic herring (*Clupea harengus*) for patterns in fatty acid signatures. Since significant differences were found in the fatty acid composition of fish by age, means for each age separately are shown as well as for all omega-3 (n-3) and omega-6 (n-6) fatty acids in the model.

		Mean % composition of fatty acid ±SE											
Age	n	14:0	16:0	16:1n-11	16:1n-9	16:1n-7	16:1n-5	18:1n-11	18:1n-9	18:2n-6	18:3n-3	18:4n-3	20:1n-11
1	70	7.61±1.67	14.38±2.56	0.06±0.02	0.11±0.03	4.26±0.84	0.27±0.05	0.53±0.40	6.70±1.54	1.06±0.21	0.56±0.34	1.66±0.79	1.05±0.57
2	272	8.32±1.09	12.45±1.58	0.06±0.04	0.10±0.02	4.85±1.08	0.28±0.05	0.63±0.72	5.61±1.39	1.07±0.28	0.62±0.48	1.96±1.04	1.10±0.51
3	131	8.07±0.73	12.27±1.05	0.08±0.07	0.11±0.02	5.48±1.16	0.26±0.07	0.99±1.43	5.46±1.64	1.05±0.45	0.82±0.57	2.22±1.03	1.13±0.61
4+	78	7.68±0.99	12.39±1.57	0.05±0.03	0.12±0.04	5.39±1.57	0.27±0.05	2.00±4.09	5.81±1.88	0.95±0.43	0.73±0.43	1.89±1.15	1.20±0.34

	Mean % composition of fatty acid ±SE												
Age	20:1n-9	20:1n-7	20:4n-6	20:4n-3	20:5n-3	22:1n-11	22:1n-9	22:1n-7	22:5n-3	22:6n-3	24:1n-9	Sum of all n-3	Sum of all n-6
1	10.87±3.62	0.21±0.06	0.46±0.19	0.39±0.07	7.33±2.40	17.97±6.03	0.69±0.19	0.17±0.06	1.07±2.62	12.44±4.51	0.78±0.24	24.09±7.01	1.79±0.31
2	13.78±2.46	0.23±0.06	0.27±0.15	0.45±0.13	6.82±1.79	21.46±3.78	0.96±0.32	0.15±0.07	0.78±0.53	8.32±3.13	0.66±0.24	19.51±4.06	1.59±0.36
3	13.54±1.61	0.27±0.11	0.25±0.08	0.49±0.57	6.73±1.20	21.75±2.39	1.03±0.23	0.18±0.05	0.86±0.53	7.30±1.10	0.57±0.36	19.07±2.29	1.59±0.43
4+	13.48±1.74	0.32±0.15	0.28±0.10	0.40±0.10	6.20±1.00	22.09±3.10	1.13±0.29	0.19±0.07	0.70±0.13	7.60±1.55	0.72±0.20	18.06±2.38	1.51±0.36

than comparisons including fish from the other three years (2005 vs. 2008: dissimilarity=18.15%; 2005 vs. 2007: 17.59%; 2005 vs. 2006: 16.36%; 2006 vs. 2007: 14.06%; 2006 vs. 2008: 16.10%; 2007 vs. 2008: 16.04%). As with the data on fatty acid signatures by fish age, the SIMPER analysis revealed that the separation of fish by year was also based on omega-3, -6, and long-chain polyunsaturated fatty acids (Table 4). However, in contrast to the age data, 16:1n-11 contributed to over 10% of the differences found in the fatty acid signatures of fish from 2005 in contrast to fish collected during the other years of the study. The reason for this strong difference in percent composition is unclear because this fatty acid has not been previously identified as biologically important.

Herring from 2006 and 2007 were analyzed for differences in fatty acid composition by season. The ANOSIM indicated significant differences in the fatty acid composition of fish by season (global r=0.254, P<0.01, Fig. 4C). The SIMPER analysis showed that omega-3 and -6 (specifically 20:5n-3) and long-chain monounsaturated fatty acids (specifically 20:1n-11 and 22:1n-11) were the most important fatty acids contributing to the differences in fatty acid signatures of fish by season (Table 4).

Discussion

Age was the strongest determinant of the total lipid content and fatty acid composition of Atlantic herring. Younger fish had less total lipid content, but this was paired with higher concentrations of certain classes of fatty acids, such as omega-3 and -6 fatty acids which are important for vertebrate growth and development early in life (Sargent et al., 1999; Szlinder-Richert et al., 2010.). This was in contrast to older fish, which had higher total lipid content paired with higher concentrations of long-chain monounsaturated fatty acids which are important for energy storage (Hadley, 1985). Although the r^2 value of the regression of fork length on total lipid content is relatively low, we believe this is indicative of the natural variability in the nutritional quality of Atlantic herring in this ecosystem. Although we do not know the direct cause of the ontogenetic variation in our sample, it is likely that small and large fish have different diets, especially considering the change in filtering ability as fish grow (Gibson, 1988). These differences in fatty acid composition could be manifested in one of two ways; either fish of different sizes are feeding on different prey items, or on different proportions of the same prey items (e.g., Iverson et al., 1997; 2002).

This study revealed significant annual variation in the lipid content and composition of herring. For example, 2005 fish had 37% less lipid than fish from 2006 through 2008, and their fatty acid signatures were also significantly different from fish collected in the other three years. Also, although not statistically

significant, fish from 2008 had the highest lipid content of any year in the study (Fig. 2) and also exhibited significant variation from the other years in their fatty acid signatures. Although significant differences were observed in the fatty acid composition of herring by year, these differences were not concentrated in any individual fatty acids (such as the biologically important polyunsaturated fatty acids) but were spread consistently throughout the entire suite of fatty acids sampled. These differences underscore the importance of measuring prey quality on annual scales to account for this variation. The source of the annual variation in total lipid content and fatty acid composition is not known and could be related to many factors including variation in prey availability or climatic shifts (Litz et al., 2010), but data for these factors are not currently available for the Bay of Fundy.

The seasonal variation in Atlantic herring lipid content and composition was not unexpected, considering the fall spawning habits of herring in the Bay of Fundy (Boyar et al., 1973). We found summer fish had significantly more lipid than winter fish (Fig. 3) and this high lipid content may reflect lipid storage in the summer before spawning occurs, and it may also reflect low prey availability in the winter for herring (Murison and Gaskin, 1989; Michaud and Taggart, 2007). However, almost all the fish in this study were sexually immature; therefore, even preparation for spawning may cause a shift in fatty acid composition. The differences in fatty acid composition may also be indicative of variation in the foraging habits of Atlantic herring throughout the year. The SIMPER analysis identified 20:5*n*-3 and 22:1*n*-11 as the most important fatty acids contributing to the seasonal differences in fatty acid signatures (Table 4). The data showed concentrations of omega-3 fatty acids necessary for growth and development (Sargent et al., 1988; Pond, 1998) are higher in summer fish than in winter fish. Specifically, the concentration of 20:5*n*-3 in winter fish was 4.24% ±1.41%, compared to 6.89% ±1.38% in summer fish. In contrast, winter fish had higher concentrations of long-chain monounsaturated fatty acids, typically used for energy storage over winter (Hadley, 1985), than did summer fish. Specifically, the concentration of 22:1*n*-11 in winter fish was 25.91% ±4.64, compared to 20.89% ±2.98% in summer fish, representing an increase of almost 25%. Overall,

Table 4

Year and season, sample size, mean percent composition, and standard error (SE) of all fatty acids that were included in non-parametric models to analyze Atlantic herring (*Clupea harengus*) for patterns in fatty acid signatures. Since significant differences were found in the fatty acid composition of fish by year and season, means for each year and season separately are shown as well as for all omega-3 (*n*-3) and omega-6 (*n*-6) fatty acids in the model. S=summer, W=winter.

		Mean % composition of fatty acid ±SE													
Year/Season	*n*	14:0	16:0	16:1*n*-11	16:1*n*-9	16:1*n*-7	16:1*n*-5	18:1*n*-11	18:1*n*-9	18:2*n*-6	18:3*n*3	18:4*n*-3	20:1*n*-11
2005/S	56	7.81±0.69	13.49±1.85	0.17±0.07	0.12±0.03	5.54±0.71	0.18±0.07	0.52±0.10	5.96±1.15	1.07±0.28	0.64±0.22	2.16±0.53	1.01±0.85
2006/S	225	7.93±1.09	13.10±1.91	0.05±0.02	0.10±0.03	4.79±1.09	0.27±0.04	0.51±0.24	6.45±1.32	1.17±0.22	0.69±0.37	2.25±0.92	0.98±0.44
2006–07/W	71	8.71±1.90	11.61±1.47	0.06±0.01	0.12±0.01	3.67±0.99	0.28±0.04	0.75±0.24	6.38±1.06	1.12±0.15	0.44±0.40	1.16±0.70	1.78±0.58
2007/S	104	8.31±0.58	11.87±0.94	0.04±0.01	0.11±0.02	5.14±0.94	0.33±0.04	0.53±0.40	5.08±1.11	1.08±0.25	0.49±0.49	1.97±1.26	1.03±0.18
2008/S	95	7.87±0.87	12.70±1.58	0.04±0.01	0.09±0.03	6.02±1.06	0.26±0.03	2.54±3.98	4.18±1.78	0.66±0.51	1.04±0.66	1.82±1.12	1.12±0.25

	Mean % composition of fatty acid ± SE												
Year/Season	20:1*n*-9	20:1*n*-7	20:4*n*-6	20:4*n*-3	20:5*n*-3	22:1*n*-11	22:1*n*-9	22:1*n*-7	22:5*n*-3	22:6*n*-3	24:1*n*9	Sum of all 1*n*-3	Sum of all 1*n*-6
2005/S	13.27±1.91	0.27±0.04	0.29±0.04	0.57±0.89	7.65±1.50	18.95±2.44	1.04±0.63	0.19±0.11	1.35±1.13	7.14±1.35	0.15±0.28	20.01±2.26	1.61±0.33
2006/S	12.02±2.45	0.24±0.08	0.33±0.18	0.44±0.09	7.02±1.43	20.36±4.00	0.88±0.22	0.17±0.04	0.85±1.49	9.61±3.55	0.75±0.25	21.55±4.66	1.79±0.27
2006–07/W	13.67±2.22	0.17±0.05	0.36±0.20	0.38±0.08	4.24±1.41	25.91±4.64	0.82±0.16	0.13±0.04	0.58±0.09	9.25±5.25	0.78±0.18	16.49±6.04	1.67±0.17
2007/S	15.70±1.73	0.26±0.09	0.20±0.04	0.45±0.08	6.75±0.99	21.42±1.68	1.12±0.16	0.17±0.04	0.71±0.11	7.06±1.10	0.67±0.13	18.03±2.09	1.59±0.30
2008/S	13.50±2.10	0.30±0.13	0.25±0.07	0.43±0.08	7.64±1.36	20.61±3.16	1.08±0.28	0.16±0.09	0.78±0.09	7.71±1.60	0.66±0.14	19.84±2.63	1.11±0.40

long-chain monounsaturated fatty acids were higher in concentration in the winter, and the omega-3 fatty acids were lower in winter. However, only concentrations of 20:5*n*-3, not the biologically important 22:6*n*-3, were observed to be lower in winter, indicating mobilization of 20:5*n*-3 or a shift in diet during winter.

The differences observed in total lipid content and fatty acid composition could also be a result of the differential allocation of resources to specific tissues within the body; however, this aspect of variability was not a goal of our research because Atlantic herring predators consume their prey whole. A small subset of large individuals (n=31, at least 21 cm in fork length) was examined for differences in total lipid content by tissue type, and muscle tissue was found to have significantly more total lipid content than gonad tissue (P<0.0001). However, because few of these individuals were sexually mature, these data indicate only that muscle tissue may be an important lipid store for fish as they begin to mature sexually.

Iverson et al. (2002) also identified ontogeny as the main factor responsible for the variation in the lipid content and fatty acid composition of Pacific herring (*Clupea pallasi*), and similar fatty acids (omega-3, -6, and long-chain monounsaturates) were identified as important in distinguishing between the fatty acid signatures of fish by age. Huynh et al. (2007) also found ontogenetic variation in the fatty acid signatures of Pacific herring fillets. As we found with the data from this study, Jensen et al. (2007) identified ontogeny, year, and season as important factors contributing to differences in the fatty acid composition of Baltic herring collected from 2001 through 2003. Budge et al. (2002) determined that the fatty acid signatures of Atlantic herring were significantly different from all other species found on the Scotian Shelf, Georges Bank, and the southern Gulf of St. Lawrence, with the exception of capelin (*Mallotus villosus*) and northern sand lance (*Ammodytes dubius*). The separation of Atlantic herring from other fish species in the Budge et al. study may be due to the high concentration of 22:1*n*-11 found in herring (17.27% ±5.68%) compared to other fish (haddock: 1.65% ±1.58%, mackerel: 6.0t% ±3.44%, pollock: 2.68% ±1.45%). We also found high concentrations of 22:1*n*-11 in the Atlantic herring examined; in fact, 22:1*n*-11 was the fatty acid in highest concentration in all fish (Tables 3 and 4). Combining previous work (Iverson et al., 2002; Jensen et al., 2007) on other ecosystems with the data presented here, it seems clear that there is significant variability in the nutritional quality of herring on ontogenetic, annual, and seasonal scales worldwide. In order to obtain a complete picture of prey quality, the total lipid content and fatty acid composition of the whole body, as well as body tissues (muscle, gonads), should be compared to identify possible differences due to sexual maturity stage. Further, these studies serve to emphasize that the characterization of prey from a physiological and biochemical perspective (quality) should be conducted synoptically with measures of biomass (quantity) to best determine the prey field of interest.

The variation in Atlantic herring nutritional quality observed in this study could have large impacts on the health of herring predators. During years or seasons of low lipid content, predators relying on herring would either have to spend more time foraging to meet energy demands or cope with less energy intake from the same amount of prey. The latter could result in a decline in body condition, health, or reproductive success if minimum caloric requirements are not met (e.g., Atkinson and Ramsay, 1995; Alonso-Alvarez and Tella, 2001). For example, Diamond and Devlin (2003) demonstrated a decline in breeding success of Arctic and common terns (*Sterna paradisaea, S. hirundo*) in the Bay of Fundy from 1995 through 2000 and directly linked it to a decline in lipid content of their main prey item, Atlantic herring. Although we do not know at which point, or whether, the lipid content of Atlantic herring falls below a level that would make them unprofitable for predators, the lowest mean percent lipid value observed in this study (6%) is still considered high for fish in general (compared to that for Atlantic cod [*Gadus morhua*]: 2.1%; haddock [*Melanogrammus aeglefinus*]: 1.4%; Atlantic mackerel [*Scomber scombrus*]: 3.4%; Atlantic pollock [*Pollachius pollachius*]: 3.0%; all values from Budge et al., 2002), many of which are important prey species despite their relatively low lipid content (Gannon et al., 1998; Pauly et al. 1998). Although it is likely that the lowest percentages observed in this study are still above this minimum level, the variation present in the nutritional quality of Atlantic herring has implications for the quality of food that predators are receiving. Predictability in the quantity and quality of available resources is an important element of food web dynamics, and some predators may depend heavily on the availability of a consistent type and level of energy intake. Such reliance can have serious implications for predators accustomed to high-energy prey; these predators may not be able to adjust to a high volume of low-quality food in place of a lower but more consistent amount of high-quality food, as has been shown in Steller sea lions (*Eumetopias jubatus*) by Rosen and Trites (2004).

The results of this study indicate significant ontogenetic, annual, and seasonal variation in the lipid content and composition of Atlantic herring from the Bay of Fundy. Herring are a critical prey species in the Bay of Fundy and the variation in lipid content and composition of these fish affects the nutritional quality of the prey that many upper predators in the Bay of Fundy are receiving. Because herring are a vital link between the upper and lower levels of the food chain, they are central to understanding the effects of variability in one species on the entire food web. Such variability has been shown to affect trophic dynamics in complex food webs across the globe (e.g., Duffy and Paul, 1992; Langvatn and Hanley, 1993; Toft and Wise, 1999; Rosen and Trites, 2004) and provides insight into the ecology and distribution of species in these environments. In the Bay of Fundy, predators of Atlantic herring are receiving nutritionally different "packages" depending

on which size of fish is eaten, and which season and year it is consumed in. The current study demonstrates the variability in the nutritional quality of species that may be assumed to offer consistent value in food webs and underscores the importance of characterizing species over broad temporal and developmental scales to capture this variability.

Acknowledgments

The authors thank the following, without whom this project would not have been possible: the fishermen of Grand Manan for herring samples, especially the Foster and Kinghorne families; J. Fife, G. Melvin, R. Stephenson, M. Powers (all from the Canadian Department of Fisheries and Ocean, St. Andrews Biological Station), L. Murison, and the Grand Manan Whale and Seabird Research Station staff for logistical and intellectual support; T. Hooper, D. Cooke, and K. Dugan at Connors Brothers, Inc., for sample collection; D. P. Gannon and F. Scharf for project development and assistance; and S. Budge for statistical support and guidance and for confirmation of peak identification. This work was supported through a Department of Fisheries and Oceans Herring Science Council research grant to H.A.L, and by the Grand Manan Whale and Seabird Research Station and the University of North Carolina Wilmington.

Literature cited

Alonso-Alvarez, C., and J. L. Tella.
2001. Effects of experimental food restriction and body mass changes on the avian T-cell-mediated immune response. Can. J. Zool. 79:101–105.

Anthony, V. C.
1972. Population dynamics of the Atlantic herring in the Gulf of Maine. Ph.D. diss., 266 p. Univ. Washington, Seattle, WA.

Anthony, V. C., and G. Waring.
1980. The assessment and management of the Georges Bank herring fishery. Rapp. P.-V. Reun.-Cons. Int. Explor. Mer 177:72–111.

Atkinson, S. N., and M. A. Ramsay.
1995. The effects of prolonged fasting of the body composition and reproductive success of female polar bears (*Ursus maritimus*). Funct. Ecol. 9:559–567.

Bishop, D. G., D. A. Ritz, G. W. Hosie, J. R. Kenrick and J. Olley.
1983. Fatty acid composition of the lipids of *Puffinus tenuirostris* (Temminck) in relation to its diet. J. Exp. Mar. Biol. Ecol. 71:17–26.

Boyar, H. C., R. R. Marak, F. E. Perkins, and R. A. Clifford
1973. Seasonal distribution and growth of larval herring (*Clupea harengus* L.) in the Georges Bank-Gulf of Maine area from 1962–1970. J. Cons. Int. Explor. Mer 35:36–51.

Bradford, R. G.
1993. Differential utilization of storage lipids and storage proteins by Northwest Atlantic herring (*Clupea harengus harengus*). J. Fish. Biol. 43:811–824.

Budge, S. M., S. J. Iverson, W. D. Bowen, and R. G. Ackman.
2002. Among- and within-species variability in fatty acid signatures of marine fish and invertebrates on the Scotian Shelf, Georges Bank, and southern Gulf of St. Lawrence. Can. J. Fish. Aquat. Sci. 59:886–898.

Budge, S. M., S. J. Iverson, and H. N. Koopman.
2006. Studying trophic ecology in marine ecosystems using fatty acids: A primer on analysis and interpretation. Mar. Mamm. Sci. 22:759–801.

Burnham, K. P., and D. R. Anderson.
2002. Model selection and inference: a practical approach. Springer, New York.

Chase, B. C.
2002. Differences in diet of Atlantic tuna (*Thunnus thynnus*) at five seasonal feeding grounds of the New England continental shelf. Fish. Bull. 100:168–180.

Clarke, K. R.
1993. Non-parametric multivariate analyses of changes in community structure. Aust. J. Ecol. 18:117–143.

Clarke, K. R., and R. N. Gorley.
2006. PRIMER, vers. 6: user manual/tutorial, 190 p. PRIMER-E: Plymouth, UK.

Clarke, K. R., and R. M. Warwick.
2001. Changes in marine communities: an approach to statistical analysis and interpretation, 2nd ed., 172 p. PRIMER-E: Plymouth, UK.

Colwell, M. A., and S. L. Landrum.
1993. Nonrandom shorebird distribution and fine-scale variation in prey abundance. Condor. 95:94–103.

Colton, J. B., Jr., W. G. Smith, A. W. Kendall Jr., P. L. Berrien, and M. P. Fahay.
1979. Principle spawning areas and times of marine fishes, Cape Sable to Cape Hatteras. Fish. Bull. 76:911–915.

Dalsgaard, J., M. St. John, G. Kattner, D. Muller-Navarra, and W. Hagen.
2003. Fatty acid trophic markers in the pelagic marine environment. Adv. Mar. Biol. 46:225–340.

De Silva, S. S.
1973. Food and feeding habits of the herring *Clupea harengus* and the sprat *C. sprattus* in inshore waters of the west coast of Scotland. Mar. Biol. 20:282–290.

Diamond, A. W., and C. M. Devlin.
2003. Seabirds as indicators of changes in marine ecosystems: ecological monitoring on Machias Seal Island. Environ. Monit. Assess. 88:153–175.

Duffy, J. E., and V. J. Paul.
1992. Prey nutritional quality and the effectiveness of chemical defenses against tropical reef fishes. Oecologia 90:333–339.

Folch, J., M. Lees, and G. H. Sloane-Stanley.
1957. A simple method for the isolation and purification of total lipids from animal tissues. J. Biol. Chem. 226:497–509.

Forsman, A., and L. E. Lindell.
1997. Responses of a predator to variation in prey abundance: survival and emigration of adders in relation to vole density. Can. J. Zool. 75:1099–1108.

Gannon, D. P., J. E. Craddock, and A. J. Read.
1998. Autumn food habits of harbor porpoises, *Phocoena phocoena*, in the Gulf of Maine. Fish Bull. 96:428–437.

Gibson, R. N.
1988. Development, morphometry and particle retention capability of the gill rakers in the herring, *Clupea harengus* L. J. Fish Biol. 32:949–962.

Greenstreet, S. P. R., J. A. McMillan, and E. Armstrong.
1998. Seasonal variation in the importance of pelagic fish in the diet of piscivorous fish in the Moray Firth,

NE Scotland: a response to variation in prey abundance? ICES J. Mar. Sci. 55:121–133.

Hadley, N. F.
1985. The adaptive role of lipids in biological systems, 319 p. John Wiley and Sons, New York.

Huynh, M. D., D.D. Kitts, C. Hu, and A. W. Trites.
2007. Comparison of fatty acid profiles of spawning and non-spawning Pacific herring, *Clupea harengus pallasi*. Comp. Biol. Phys. B 146:504–511.

Huynh, M. D., and D. D. Kitts.
2009. Evaluating nutritional quality of pacific fish species from fatty acid signatures. Food Chem. 114:912–918.

Iverson, S. J., K. J. Frost, and S. L. C. Lang.
2002. Fat content and fatty acid composition of forage fish and invertebrates in Prince William Sound, Alaska: factors contributing to among and within species variability. Mar. Ecol. Prog. Ser. 241:161–181.

Iverson, S. J., K. J. Frost and L. F. Lowry.
1997. Fatty acid signatures reveal fine scale structure of foraging distribution of harbor seals and their prey in Prince William Sound, Alaska. Mar. Ecol. Prog. Ser. 51:255–271.

Jensen, K. N., C. Jacobsen, and H. N. Nielsen.
2007. Fatty acid composition of herring (*Clupea harengus* L.): influence of time and place of catch on n-3 PUFA content. J. Sci. Food. Agr. 87:710–718.

Katona, S. K., V. Rough, and D. T. Richardson.
1993. A field guide to whales, porpoises, and seals from Cape Cod to Newfoundland, 316 p. Smithsonian Inst. Press, Washington and London.

Krebs, C. J., K. Danell, A. Angerbjörn, J. Agrell, D. Berteaux, K. A. Bråthen, Ö. Danell, S. Erlinge, V. Fedorov, K. Fredga, J. Hjältén, G. Högstedt, I. S. Jónsdóttir, A. J. Kenney, N. Kjellén, T. Nordin, H. Roininen, M. Svensson, M. Tannerfeldt, and C. Wiklund
2003. Terrestrial trophic dynamics in the Canadian Arctic. Can. J. Zool. 81:827–843.

Koopman, H. N.
2007. Phylogenetic, ecological and ontogenetic factors influencing the biochemical structure of the blubber of odontocetes. Mar. Biol. 151:277–291.

Langvatn, R., and T. A. Hanley.
1993. Feeding-patch choice by red deer in relation to foraging efficiency. Oecologia 95:164–170.

Litz, M. C., R. D. Brodeur, R. L. Emmett, S. S. Heppell, R. S. Rasmussen, L. O'Higgins, and M. S. Morris.
2010. The effects of variable oceanographic conditions on forage fish lipid content and fatty acid composition in the northern California Current. Mar. Ecol. Prog. Ser. 405:71–85.

Melvin, G. D., and R. L. Stephenson.
2007. The dynamics of a recovering fish stock: Georges Bank herring. ICES J. Mar. Sci. 64:69–82.

Messieh, S. N., R. Pottle, P. MacPherson, and T. Hurlbut.
1985. Spawning and exploitation of Atlantic herring (*Clupea harengus*) at Escuminac in the southwestern Gulf of St. Lawrence, spring 1983. J. Northw. Atl. Fish. Sci. 6:125–133.

Michaud, J., and C. T. Taggart.
2007. Lipid and gross energy content of North Atlantic right whale food, *Clanus finmarchicus*, in the Bay of Fundy. Endang. Species Res. 3:77–94.

Murison, L. D. and D. E. Gaskin.
1989. The distribution and right whales and zooplankton in the Bay of Fundy, Canada. Can. J. Zool. 67:1411–1420.

O'Brien, L., J. Burnett, and R. K. Mayo.
1993. Maturation of nineteen species of finfish off the northeast coast of the United States, 1985–1990. NOAA Tech. Rep. NMFS 133, 66 p.

Overholtz, W. J., and K. D. Friedland.
2002. Recovery of Maine-Georges Bank Atlantic herring (*Clupea harengus*) complex: perspectives based on bottom trawl survey data. Fish. Bull. 100:593–608.

Overholtz, W. J., and J. S. Link.
2007. Consumption impacts by marine mammals, fish, and seabirds on the Gulf of Maine—Georges Bank Atlantic herring (*Clupea harengus*) complex during the years 1977–2002. ICES J. Mar. Sci. 64:83–96.

Pauly, D., A. W. Trites, E. Capuli, and V. Christensen.
1998. Diet composition and trophic levels of marine mammals. ICES. J. Mar. Sci. 55:467–481.

Penttila, J. A., G. A. Nelson, and J. M. Burnett II.
1989. Guidelines for estimating lengths at age for 18 northwest Atlantic finfish and shellfish species. NOAA Tech. Memo. NMFS-F/NEC-66, 39 p.

Pond, C. M.
1998. The fats of life, 337 p. Cambridge University Press, Cambridge, UK.

Rosen, D. A. S., and A. W. Trites.
2004. Satiation and compensation for short-term changes in food quality and availability in young Steller sea lions (*Eumetopias jubatus*). Can. J. Zool. 82:1061–1069.

Sargent, J. R., R. J. Parkes, I. Mueller-Harvey, and R. J. Henderson.
1988. Lipid biomarkers in marine ecology. *In* Microbes in the sea (M. A. Sleigh, ed.), p. 119–138. Ellis Horwood Ltd., Chichester, UK.

Sargent, J., G. Bell, L. McEvoy, D. Tocher, and A. Estevez.
1999. Recent developments in the essential fatty acid nutrition of fish. Aquaculture. 177:191–199.

Szlinder-Richert, J., Z. Usydus, M. Wysznski, and M. Adamczyk.
2010. Variation in fat content and fatty-acid composition of the Baltic herring *Clupea harengus membras*. J. Fish Biol. 77: 585–599.

Sinclair, M., and M. J. Tremblay.
1984. Timing of spawning of Atlantic herring (*Clupea harengus harengus*). Can. J. Fish. Aquat. Sci. 39:288–295.

Toft, S., and D. H. Wise.
1999. Growth, development, and survival of a generalist predator fed single- and mixed-species diets of different quality. Oecologia 119:191–197.

Torcher, D. R., A. J. Fraser, J. R. Sargent, and J. C. Gamble.
1985. Fatty acid composition of phospholipids and neutrals lipids during embryonic and early larval development in Atlantic herring (*Clupea harengus*, L.) Lipids 20: 69–74.

Womble, J. N., and M. F. Singler.
2006. Seasonal availability of abundant, energy-rich prey influences the abundance and diet of a marine predator, the Steller sea lion *Eumetopias jubatus*. Mar. Ecol. Prog. Ser. 325:281–293.

Woo, K. J., K. H. Elliott, M. Davidson, A. J. Gaston, and G. K. Davoren.
2008. Individual specialization in diet by a generalist marine predator reflects specialization in foraging behaviour. J. Anim. Ecol. 77:1082–1091.

Estimates of body sizes at maturation and at sex change, and the spawning seasonality and sex ratio of the endemic Hawaiian grouper (*Hyporthodus quernus*, F. Epinephelidae)

Edward E. DeMartini (contact author)[1]

Alan R. Everson[2]

Ryan S. Nichols[1]

Email address for contact author: edward.demartini@noaa.gov

[1] National Marine Fisheries Service
Pacific Islands Fisheries Science Center
Hawaii Research Center
99-193 Aiea Heights Drive, Suite 417
Aiea, Hawaii 96701

[2] National Marine Fisheries Service
Pacific Islands Regional Office
1601 Kapiolani Boulevard, Suite 1110
Honolulu, Hawaii 96814

Abstract—A case study of the reproductive biology of the endemic Hawaiian grouper or hapu'upu'u (*Hyporthodus quernus*) is presented as a model for comprehensive future studies of economically important epinephelid groupers. Specimens were collected throughout multiple years (1978–81, 1992–93, and 2005–08) from most reefs and banks of the Northwestern Hawaiian Islands. The absence of small males, presence of atretic oocytes and brown bodies in testes of mature males, and both developed ovarian and testicular tissues in the gonads of five transitional fish provided evidence of protogynous hermaphroditism. No small mature males were collected, indicating that Hawaiian grouper are monandrous (all males are sex-changed females). Complementary microscopic criteria also were used to assign reproductive stage and estimate median body sizes (L_{50}) at female sexual maturity and at adult sex change from female to male. The L_{50} at maturation and at sex change was 580 ±8 (95% confidence interval [CI]) mm total length (TL) and 895 ±20 mm TL, respectively. The adult sex ratio was strongly female biased (6:1). Spawning seasonality was described by using gonadosomatic indices. Females began ripening in the fall and remained ripe through April. A February–June main spawning period that followed peak ripening was deduced from the proportion of females whose ovaries contained hydrated oocytes, postovulatory follicles, or both. Testes weights were not affected by season; average testes weight was only about 0.2% of body weight—an order of magnitude smaller than that for ovaries that peaked at 1–3% of body weight. The species' reproductive life history is discussed in relation to its management.

Manuscript submitted 24 July 2010.
Manuscript accepted 3 December 2010.
Fish. Bull. 109:123–134 (2011).

The views and opinions expressed or implied in this article are those of the author (or authors) and do not necessarily reflect the position of the National Marine Fisheries Service, NOAA.

Epinephelid groupers comprise about 160 species of economically valuable and ecologically important predatory fishes distributed worldwide in subtropical and tropical seas. They exhibit a variety of sexual patterns, including sequential hermaphroditism in which mature adults change sex (Erisman et al., 2010). The importance of information on adult sex ratio (Coleman et al., 1996; Heppell et al., 2006), spawning seasonality (Sadovy et al., 1994; Domeier and Colin, 1997), and body sizes at sexual maturity and at sex change (e.g., Pears et al., 2007) have been identified as important when developing management plans for sustainable extraction of sequentially hermaphroditic groupers. To date, however, comprehensive and self-contained evaluations based on all of these key life-history elements are rare. Few studies (e.g., Mackie, 2000; Chan and Sadovy, 2002; Erisman et al., 2010) have estimated body size at sex change, as well as size at first maturation for protogynous (female-first sex-changing) groupers, and few (e.g., Brule et al., 2003) have precisely quantified size at sex change. Only such comprehensive studies can provide the data necessary for meaningful exploration of patterns of sex and gonadal allocations that can provide additional insights into the behavioral responses of these fishes to fishing pressure (Alonzo and Mangel, 2005).

One of the more intriguing sex allocation patterns recently discovered for protogynous epinephelid groupers is the apparent covariation between adult body size and aggregation spawning. Medium- to large-body (>50 cm total length, TL) groupers of the genus *Epinephelus* and allied genera typically spawn in aggregations, while small-body species (e.g., within the genus *Cephalopholis*) tend not to spawn in aggregations (Sadovy et al., 1994; Sadovy, 1996). Some grouper species, moreover, have only one type of male, derived from sex-changed adult females (these species are termed "monandric"), whereas other species have an additional male type ("diandric") that is directly derived from the juvenile phase (Sadovy de Mitcheson and Liu, 2008).

The Hawaiian grouper (*Hyporthodus quernus*) (Seale) (Epinephelidae; Craig and Hastings, 2007; Smith and Craig, 2007) is endemic to the Hawaiian Islands and Johnston Atoll (a no-take zone within the Pacific Remote Island Area Monument since 2009, at 16°45'N lat., 169°31'W long.; Fig. 1) and is the only epinephelid indigenous to the Hawaiian Archipelago. The species has historically been a major component of both the North-

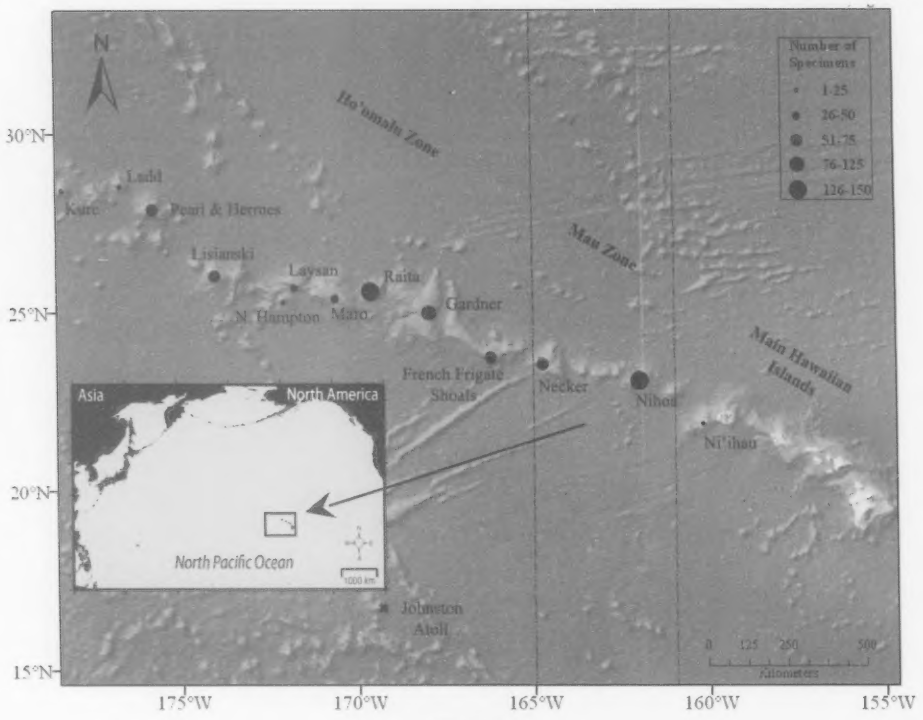

Figure 1

Map of the Hawaiian Archipelago and the North Pacific basin. The Main Hawaiian Islands bottomfish fishery zone and the Ho'omalu and Mau management zones of the former Northwestern Hawaiian bottomfish fishery are delineated by vertical dashed lines. Only fish collected from the Northwestern Hawaiian Islands and Niihau-Kauai (the island adjacent to and E-NE of Niihau)—i.e., west of about 160°W longitude—were evaluated for this study; >70% of these were from the Ho'omalu Zone, west of 165°W. The relative sizes of the black circles represent the number of Hawaiian grouper (*Hyporthodus quernus*) collected for analysis.

western Hawaiian Islands (NWHI) and Main Hawaiian Islands (MHI) handline bottomfisheries and, since closure of the fishery in both Ho'omalu and Mau Management Zones of the NWHI in June 2010, continues to be one of the targeted "deep-7" bottomfish species in the MHI. All deep-7 species have been protected by emergency fishery closures for 5 to 7 months during spring–summer of 2006–09 (http://www.hawaiibottomfish.info/index.htm). The MHI stocks of Hawaiian grouper have been identified as particularly stressed (Moffitt et al.[1]) based on the criterion of a low and recently declining SPR (spawning potential ratio: Goodyear, 1993) that has historically been used in Hawaii bottomfish stock assessments. Over the past half-decade, the catches of this grouper in the MHI have been variable and low compared to prior years, ranging from about 8000 to 16,000 pounds (3629–7257 kg; Moffitt et al.[1])—a small but valuable fraction of the recent (2007–2010) Total Allowable Catch limits set for MHI bottomfishes of 178–254 thousand pounds (80,740–115,200 kg) per year (http://www.hawaiibottomfish.info/BFnews_vol6_final.pdf; accessed July 2010). Like many large groupers (Huntsman et al., 1999), the Hawaiian grouper is a species of conservation concern (Morris et al., 2000). It is a slow growing, long-lived, and late maturing species (Nichols and DeMartini[2]), and preliminary evidence (Everson[3]) has indicated that, at least in the NWHI

[1] Moffitt, R., D. Kobayashi, and G. DiNardo. 2006. Status of Hawaiian bottomfish stocks, 2004. Pacific Islands Fisheries Science Center, National Marine Fisheries Service, NOAA Admin. Rep. NMFS-PIFSC-H-06-01, 45 p. Pac. Isl. Fish. Sci. Cent., 2570 Dole Street, Honolulu, HI 96822-2396.

[2] Nichols, R. S., and E. E. DeMartini. 2008. Preliminary estimates of age and growth for the endemic Hawaiian grouper (Hapu'upu'u, *Epinephelus quernus*, F. Serranidae). Pacific Islands Fisheries Science Center, National Marine Fisheries Service, NOAA Admin. Rep. NMFS-PIFSC H-08-06, 19 p. Pac. Isl. Fish. Sci. Cent., 2570 Dole Street, Honolulu, HI 96822-2396.

[3] Everson, A. R. 1992. Sexual identity and seasonal spawning of Hapu'upu'u, *Epinephelus quernus*, in Hawaii. Southwest Fisheries Science Center, National Marine Fisheries Service, NOAA Administrative Report NMFS-PIFSC H-92-13, 12 p. Southwest Fish. Sci. Cent., 2570 Dole Street, Honolulu, HI 96822-2396.

(Fig. 1)—the leeward low island region of the Hawaiian Archipelago—individuals are protogynous sequential hermaphrodites, like most epinephelids elsewhere (Shapiro, 1987; Sadovy and Domeier, 2005; Sadovy de Mitcheson and Liu, 2008). To date, however, data on body size at first sexual maturity, spawning seasonality, and adult sex ratio of Hawaiian grouper have not been adequately quantified, and information on its possible size-at-sex-change and sex and gonadal allocation patterns are lacking.

Our primary goal is to provide a comprehensive case study of the reproductive life history of Hawaiian grouper in the NWHI in which all of the aforementioned metrics are estimated (one of the few such studies so for any grouper). All of these metrics in combination are key elements necessary for conducting comprehensive reproductive studies of groupers elsewhere. We also evaluate the gonad indices of Hawaiian grouper in detail to explore possible relations among gonadal allocation pattern, male type, adult body size, and aggregation spawning.

Materials and methods

Fish collections and measurements

Hawaiian grouper were collected during three ("early," "mid-term," "recent") capture series. All captures were made with similar (hydraulic-powered) handline gear. Early specimens were caught by fisheries-independent research vessels during the period from May 1978 to August 1981. Mid-term specimens were obtained by fisheries-independent research cruises during August and December 1992 and June and September 1993. Most recent (October 2005–June 2008) specimens were purchased from contracted Hawaii-based commercial bottomfishing vessels and were fishery-dependent. All fish were collected from the NWHI, except 26 specimens (3.5% of all fish) collected from Niihau-Kauai at the northwestern edge of the MHI (Fig. 1). The limited availability of fish of a sufficient range of sizes from elsewhere in the MHI precluded separate analyses for fish from this region of relatively high fishing effort. For our analyses, we used a total 745 fish collected from the NWHI and Niihau-Kauai only (Fig. 1).

Body length (total length, TL, from tip of snout to posterior margin of caudal fin) was measured (mm) for each fish either aboard ship (research cruises) or at a fisheries laboratory ashore (for commercial specimens). The error of length measurements was about 0.5 cm. Fish were weighed (total round weight, RW, including all viscera, to 10 g) by using a bench scale. Additional details of specimen and shipboard data collection are provided elsewhere (Nichols and DeMartini[2]; Everson[3]) The Kolmogorov-Smirnov two-sample test (Zar, 1984) was used to compare body-length distributions and numbers of fish by month of collection between the total sample and a subsample used for histological examination.

Gonad extraction and processing

Both left and right lobes of gonads were either dissected from freshly caught specimens aboard the research ship or from iced fresh fish (commercial specimens) at a shore laboratory in Honolulu. Before further processing, gonads were weighed (to the nearest g). The gonads of 611 fish were examined microscopically. Histological slides were prepared for 604 fish including early and recent specimens (100 and 504 fish, respectively); no gonads from mid-term specimens were examined microscopically. In preparation for histological examination, gonads were first fixed in 10% (seawater buffered) formalin for a minimum of 2 months. A segment from the mid-region of one lobe (either left or right, random choice, including lumen and gonad wall) was then cut and placed in a histology cassette and sent to a contracted laboratory for further processing. The contractor then dehydrated tissues in an alcohol series, embedded them in paraffin wax, sectioned them at 6–7 microns, stained them with Harris's hematoxylin, and counter-stained them with eosin (Hunter and Macewicz, 1985). One slide of 2–6 (mode and median of 4) successive sections was prepared for each gonad specimen. The gonads of several ripe female specimens from the early series were prepared and examined for reproducibility of reproductive scores based on sections from the anterior, middle, and posterior regions of ovaries.

Sexual identity and reproductive status

Gonad appearance based on conventional macroscopic criteria (West, 1990) was insufficient to distinguish either sexual identity or maturation, and all determinations of sexual identity and maturation for Hawaiian grouper presented herein were based on standard microscopic criteria (West, 1990). After sexual identity was determined, each specimen was scored for reproductive stage by following a protocol (Table 1) similar to those used by others (Pears et al., 2007, and references therein) to evaluate gonadal stages of protogynous epinephelids. Key criteria included the presence of oogonia and primitive testicular tissue in the gonads of bisexual juveniles, the presence of brown body atretic structures in testes of mature sex-changed males as evidence of prior female function, and the occurrence of transitional individuals whose gonads contained both developing male and regressing female tissue types (Sadovy de Mitcheson and Liu, 2008). Fish were classified as mature females if ovaries were categorized at stages 3 through 6 (Table 1). The staging of oocytes was complemented by estimation of the median diameter of the largest mode of viable oocytes present in ovarian tissues by using a technique developed for Hawaiian bottomfishes (Lau and DeMartini, 1994). Size distributions of all yolked oocytes were described for a random subsample of ripe stage-5 fish and evaluated for multimodality by using the Kolmogorov-Smirnov one-sample test (Zar, 1984). Males were considered mature if at stage 7 or greater

Table 1

Diagnostic microscopic criteria (after Pears et al., 2007) and key to classification of sexual identity, maturation, and reproductive status of female and male Hawaiian grouper (*Hyporthodus quernus*), including gonadosomatic indices (*GSI*s) for each sex and diameter of the most advanced group of oocytes present in female ovaries. HYD=hydrated oocytes; POF=postovulatory follicles; *GFBW*=gonad-free body weight; *OD*=diameter of largest mode of viable oocytes; SE=standard error; *n*=sample size.

Gonadal maturity	Stage (0–10)	Microscopic characteristics	Mean ±SE (*n*) *GSI* (as % of *GFBW*)	Mean ±SE (*n*) *OD* (μm)	Mature? (yes/no)
Immature bisexual	0	Vestigial gonad: sex indeterminate; primitive sex cells of either one or both sexes present	0.08 ±0.009 (36)	44 ±9 (3)	no
Immature female	1	Undeveloped ovary: only primordial (weakly nucleate) oocytes present	0.08 ±0.007 (71)	76 ±3 (28)	no
Developing female	2	Ovaries contain perinucleolar (cortical alveoli-stage) oocytes with nucleolated nuclei	0.19 ±0.015 (85)	110 ±4 (22)	no
Ripening female	3	Oocytes largely previtellogenic; some eosin (pink) staining yolk vesicles	0.54 ±0.079 (13)	252 ±15 (13)	yes
Ripe female	4	Oocytes vitellogenic but not fully yolked; neither HYDs nor POFs present	0.70 ±0.129 (12)	313 ±13 (12)	yes
Imminent female	5A	Fully yolked oocytes; may have migratory nucleus; HYDs present	1.41 ±0.061 (151)	480 ±11 (29)	yes
Spawning female	5B	Fully yolked oocytes; POFs (or POFs and HYDs) present	0.23 ±0.281 (34)	533 ±12 (22)	yes
Resting female	6	Regressing or inactive, but previously spawned ovary: perinucleolar oocytes present; atretic oocytes, brown bodies, or both also present	0.48 ±0.031 (138)	111 ±6 (23)	yes
Transitional male	7	Gonad contains inactive ovarian tissue; brown bodies usually present along with developing testicular tissue (Sertoli cells in sperm crypts)	0.61 ±0.163 (5)	—	yes
Developing male	8	Recrudescing testes with spermatogonia; brown bodies may be present	0.21 ±0.016 (22)	—	yes
Active male	9	Ripe testes with spermatozoa in ducts or sinuses; brown bodies may still be present	0.21 ±0.015 (31)	—	yes
Resting male	10	Resting testes with evidence of prior spawning; sperm crypts present but no active spermatogenesis	0.32 ±0.102 (2)	—	yes

(Table 1). All histological preparations were examined by a single experienced reader (DeMartini).

Estimation of body sizes at maturation and at sex change

Nonlinear regression with maximum likelihood estimation was used to relate fish body lengths to sexual maturity and to size at sex change (Proc nlin; SAS for Windows, vers. 9.1, SAS Inst., Inc., Cary, NC). Specimens were binned by 10-mm length classes; the proportions mature (female, male) were then related to length class by using the 2-parameter logistic model,

$$P_x = 100 / (1 + \exp^{(a - b \cdot \mathrm{TL})}), \quad (1)$$

where a and b are fitted constants;
P_x = percentage mature at x TL; and
$L_{50} = (-a/b)$.

The proportions of mature and sex-changed fish were fitted by maximum likelihood by using Marquardt's algorithm. Mean proportions per 10-mm length class were weighted by square root of the respective sample size. Estimates of size at sexual maturity were further compared between early and recent collection series by using likelihood ratio statistics (Quinn and Deriso, 1999). A maximum likelihood chi-square test (Quinn and Keough, 2002) was used to compare adult sex ratios between collection series.

Spawning seasonality

Seasonality of spawning was gauged with a combination of gravimetric evidence of gonadal ripening and histological evidence of either recent or imminent spawning by females. A gonadosomatic index, $GSI=(GW/GFBW)\times100\%$, where GW=damp gonad weight and gonad-free body weight, $GFBW$=round weight minus GW, aggregated by month (years pooled) for each sex of adult fish, provided gravimetric evidence of gonadal growth. This simple (weight proportional) GSI was used to visualize temporal patterns. Because of the likely dynamic influence of reproductive stage on proportional gonad weight-to-body size, the calculation of a "relative gonad index" (RGI) was required in order to scale the relation across gonad maturation stages of mature females. This calculation removes the confounding influence of maturation stage on the gonad-to-body-size relation (Erickson et al., 1985). One-way ANCOVA (Zar, 1984) with month as a fixed factor (12 levels) and either TL or $GFBW$ as covariate was used to evaluate the potential effect of month on the RGI, controlling for fish size. ANCOVA was followed by a robust multiple comparison test (Ryan-Einot-Gabriel-Welsch [REGW] multiple-range test; Quinn and Keough, 2002) to quantitatively evaluate patterns among months. Plots of the proportional incidence for recently spawned and "imminent" (ready-to-spawn) females among all mature females constituted histological evidence of spawning by individual fish.

Results

Seventy percent of the Hawaiian grouper examined were from the Ho'omalu Zone, west of 165°W; another 26% were from the Mau Zone, between 165° and 161°W in the NWHI (Fig. 1). Fish from the early, mid-term, and recent series comprised about 18%, 11%, and 71%, respectively, of those collected. Fish were obtained in all months of the year (ranging from 20 in January to 108 fish in April); and the distribution of specimens among months of collection was indistinguishable between the parent sample and a subsample used for histological examination. The gonads of 20 (January) to 92 (April) specimens per month were examined microscopically. The mean and median body lengths of specimens was 661 mm TL (ranging from 241 to 1103 mm). Sizes of fish used for histological examination generally resembled those in the parent sample (mean=659 mm, median=652 mm, range 258 to 1103 mm TL; Kolmogorov-Smirnov two-sample test: $P>0.10$).

Comparisons of collection series

Estimated median body size at sexual maturation varied by barely 3 mm between the early (576.0 ±13.4 [standard error, SE] mm TL) and recent (579.1 ±4.0 mm TL) collection series. We considered this sufficient reason to pool samples, given the small magnitude of length measurement error, despite a marginally significant F-statistic ($F_{30,91}=1.97$, $P=0.02$). Estimates of adult sex ratios also were indistinguishable between these two collection series (maximum likelihood chi-square: $\chi^2=1.40$, df=1, $P=0.24$). Because neither metric differed between series, we pooled all fish collections and present single estimates for each of these and related variables based on all combined capture series.

Gonadal and sex allocation patterns

Gonadal patterns Four of the 604 specimens prepared for histological examination were alimentary tract tissues collected in error and were discarded. A small minority of the remaining 600 valid histological specimens were bisexual juveniles with vestigial gonads containing chromatin nucleolar oogonia, undeveloped spermatic tissue, or both (Fig. 2; Fig. 3, A and B). Most of these fish were <450 mm TL (Fig. 2). Among the remaining specimens whose gonads were more developed, about one-third of all females had immature but clearly all-female characteristics, another two-thirds were mature females, five were developing males with transitional gonads, and 55 (9.2%) were fully mature males (Table 1; Fig. 2; Fig. 3, C and D, E and F). Developing oocytes progressed from a cortical alveolus (perinucleolar) and previtellogenic stage through vitellogenesis and ovulation, with concomitant increases in ovarian mass and oocyte diameter (Table 1). The ovaries of each of three stage-5 females had multimodal size distributions of yolked or yolking oocytes (reject *Ho*: distribution unimodal normal; Kolmogorov-Smirnov one-sample test, all $P<0.001$; Fig. 3C). The gonads of all males contained from one to dozens of brown bodies; in many cases, these were recognizable as gamma-stage (Hunter and Macewicz, 1985) atretic structures (Fig. 3, E and F). No mature males smaller than 753 mm TL were encountered. Gonads were fused posteriorly and the gonads of fish of all sizes and each sex contained a membrane-lined ovary-like lumen (e.g., bisexual juveniles and mature males: Fig. 3, A and E). Maturation scores were identical and sizes of oocytes were indistinguishable from the respective anterior, middle, and posterior sections of the ovaries of three ripe females from the early collection series.

Body sizes at maturation and at sex change

Maturation Body size at first sexual maturation was estimated by using the pooled sample of all immature (bisexual and female) fish and all recognizably mature females. On the basis of Equation 1, proportional body length at 50% maturity was best described by the logistic equation

$$P_{50}=100 / (1 + \exp^{(0.0286 - 16.574 \cdot L_{50})}),$$

with $SE_a=0.003$, $SE_b=1.749$, $r^2=0.93$, $P<0.0001$, and $n=540$.

Body length (L_{50}) at female maturation was 580 ±8 mm TL (95% confidence interval [CI]) (Fig. 4). The respec-

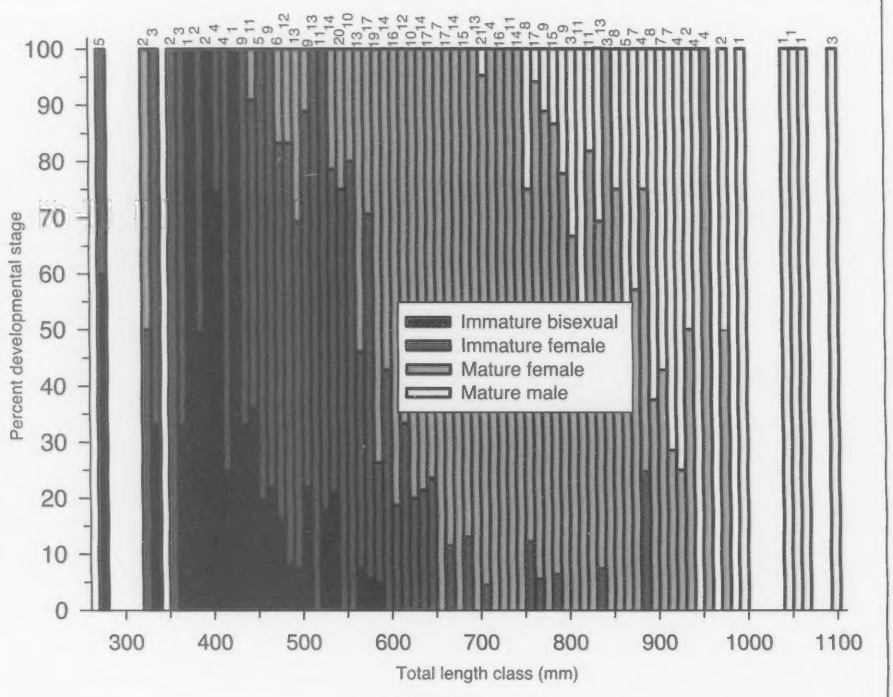

Figure 2

Proportions of immature bisexual, immature female, mature female, and mature male Hawaiian grouper (*Hyporthodus quernus*) present in each 10-mm length class of the 600-specimen subsample used for histological examination. Numbers above bars indicate numbers of specimens examined.

tive mean and median body lengths of all adult female specimens were 703 and 700 mm TL. The smallest and largest observed adult female individuals were 328 and 977 mm TL. The smallest female whose ovaries contained hydrated oocytes was 492 mm TL.

Sex change Body size at adult female-to-male sex change was appraised using all recognizably mature adult fish. The body length-at-female-to-male sex change relation was best described by the logistic equation

$$P_{50}=100 / (1+\exp^{(0.0153-13.653 \cdot L_{50})}),$$

with $SE_a=0.002$, $SE_b=1.858$, $r^2=0.80$, $P<0.0001$, and $n=397$.

Body length (L_{50}) at female-to-male sex change was 895 ±20 mm TL (95% CI) (Fig. 5). The mean and median body lengths of all adult male specimens were 895 and 891 TL, respectively. The smallest and largest adult male fish encountered were 753 and 1103 mm TL. The five transitional fish ranged from 760 to 913 mm TL. Many (38%) of the mature specimens were between the sizes of the smallest male and the largest female fish.

Spawning seasonality

The slopes of the relations between gonadal and body weights and between gonadal weights and body lengths did not differ among females in prespawning, spawning, and postspawning maturation stages (ANCOVA of *GFBW* and maturation stage effects on *GW*: *GFBW*-by-maturation and TL-by-maturation interaction effects—$F_{2,327}=2.36$ and 2.30, respectively; accept H_o: slopes equal at $P=0.10$). The intercepts of these same relations, however, differed (ANCOVA: maturation stage effects—$F_{2,329}=114.0$ and 113.2, respectively; reject H_o: intercepts equal at $P<0.0001$). The relation between gonadal weight and body length provided the better fit and TL was used in subsequent analyses of monthly patterns. In these analyses we used *RGI*s, in which the pooled slope of the *GW*-to-TL relation (2.69266) was the scaling factor. *RGI*s indicated that most females began ripening in December and maintained elevated ovarian masses of 1–3% *GFBW* through April (1-way ANCOVA: month effect on *RGI*—$F_{11,324}=6.86$; reject H_o: all months equal at $P<0.0001$). Ovary weights peaked in January–March (REGW multiple-range test: January–March highest; $P<0.03$). Analyses with simple

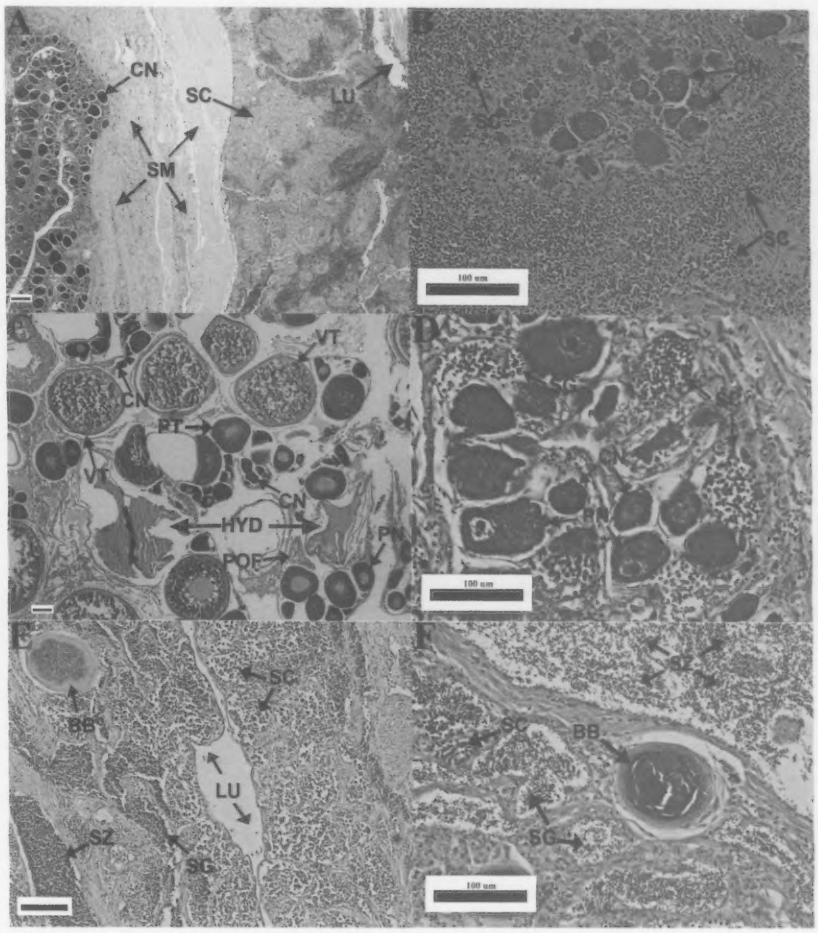

Figure 3

Photomicrographs of select representative gonads illustrating key reproductive stages of Hawaiian grouper (*Hyporthodus quernus*). (**A**) Vestigial bisexual, 333 mm total length (TL); (**B**) immature bisexual, 495 mm TL; (**C**) mature female, 624 mm TL; (**D**) transitional (female-male) mature fish, 913 mm TL; (**E**) mature male, 820 mm TL; and (**F**) mature male, 919 mm TL. CN=chromatin nucleolar oogonium; PN=perinucleolar oocyte; PT=previtellogenic oocyte; VT=vitellogenic oocyte; HYD= hydrated oocyte; POF= postovulatory follicle; SC=spermatocytes (Sertoli nurse cells); SG=spermatogonia; SZ=spermatozoa in sperm duct; SM=smooth muscle; BB=gamma-stage atretic "brown body"; LU=lumen. Black scale bars: 100 µm.

*GSI*s produced qualitatively similar results (Fig. 6) but the statistical clarity of monthly patterns improved when based on the more precise body-size–corrected *RGI*s.

The proportional incidence of active spawners, including "imminent" females ready to spawn (ovaries containing hydrated oocytes), recently spawned fish (ovaries containing recognizable [i.e., less-than-several-days-old; Fitzhugh and Hettler, 1995] postovulatory follicles), or both, also indicated a main February–June period of spawning with a peak in March (Fig. 7). Eleven (16%) of these 68 active spawners were captured outside of the February–June period (Fig. 7); nine of the 11 fish (caught during September–January) exceeded median body size at female maturity (range 550–833 mm). Adult female gonads averaged 1.35 and 1.15% of *GFBW* during the February–June peak and throughout the year, respectively (Fig. 6). Adult male gonads exhibited no seasonal change in weight and averaged 0.23% of *GFBW* throughout the year (Fig. 6).

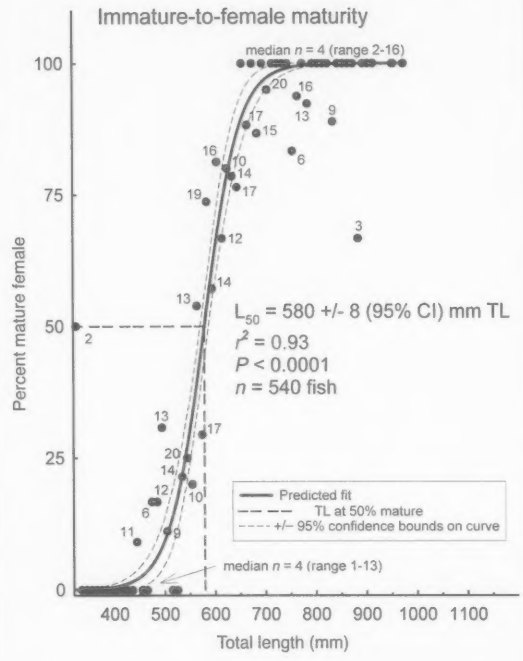
Immature-to-female maturity
median n = 4 (range 2-16)
Percent mature female
Total length (mm)
L50 = 580 +/- 8 (95% CI) mm TL
r2 = 0.93
P < 0.0001
n = 540 fish
Predicted fit
TL at 50% mature
+/- 95% confidence bounds on curve
median n = 4 (range 1-13)

Figure 4

Estimated total length (TL) at which 50% of Hawaiian grouper (*Hyporthodus quernus*) first attain sexual maturity as females (L_{50}); estimates are for 540 fish: 36 immature bisexuals, 167 immature females, 337 mature females. Solid circles represent mean percentage mature by 10-cm length class; number of fish specimens in each length class is noted adjacent to its corresponding circle. Solid curved line represents the predicted best fit model; curved dashed lines enclose the 95% confidence bounds of the fitted line. The perpendicular dashed lines indicate estimated body length at median (50%) female sexual maturity.

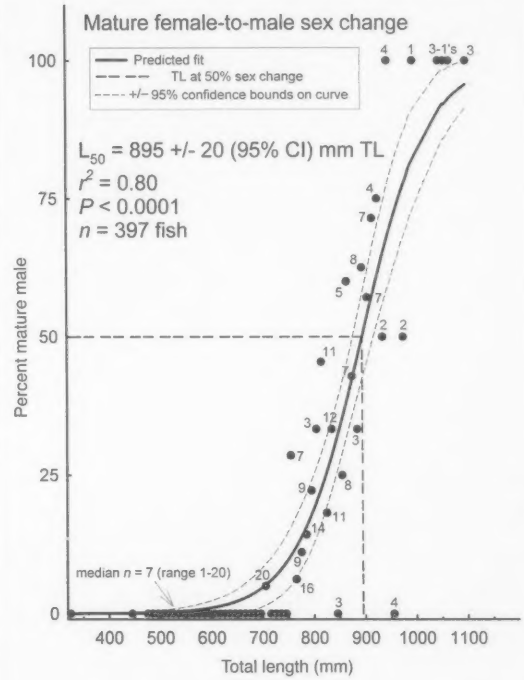
Mature female-to-male sex change
Predicted fit
TL at 50% sex change
+/- 95% confidence bounds on curve
L50 = 895 +/- 20 (95% CI) mm TL
r2 = 0.80
P < 0.0001
n = 397 fish
Percent mature male
Total length (mm)
median n = 7 (range 1-20)

Figure 5

Estimated body size (length, TL) at which 50% of Hawaiian grouper (*Hyporthodus quernus*; 397 adult fish) changed sex from female to male. Key to symbols and lines are given as in Figure 4, except the perpendicular dashed lines indicate body length at median (50%) female-to-male sex change.

Sex ratio

For all specimens whose sex was verified histologically, the adult sex ratio was highly female biased (6.1 females per male; χ^2=205, df=1, P<0.0001). The ratio became progressively less female biased at body lengths approaching the estimated median length at adult sex change from female to male.

Discussion and conclusions

Gonadal and sex allocation

Hawaiian grouper from the NWHI are protogynous sequential hermaphrodites. This conclusion is based on three lines of evidence: 1) the presence of undeveloped bisexual gonads in small (generally <45 cm TL) fish; 2) a total lack of small mature males; and 3) the presence of a lumen, posteriorly fused gonadal lobes, and brown body remnants of yolked oocytes in the gonads of relatively large mature males (Sadovy and Shapiro, 1987; Sadovy de Mitcheson and Liu, 2008). The Hawaiian grouper might be expected to be a functional gonochore (i.e., sexes separate in the adult without a postmaturational sex change) because the species has a subtropical distribution and nontropical species within primarily tropical, sex-changing lineages of serranids are often gonochores (DeMartini and Sikkel, 2006). There was no evidence to indicate this, however. Many primitive serranines and even some epinephelines (e.g., Nassau grouper [*Epinephelus striatus*]: Sadovy and Colin, 1995) are functional gonochores (Sadovy and Domeier, 2005; Sadovy de Mitcheson and Liu, 2008).

The total absence of small mature male Hawaiian grouper, despite the large number of sample fish collected in all seasons, over multiple years, and throughout much of its geographic distribution, further indicates that it is most likely monandrous. All males appear to be sex-changed females; primary males derived from bisexual juveniles were never encountered.

Diandrous species of epinephelines have been described (*Plectropomus leopardus* and *P. maculatus* [Adams, 2003]; *Epinephelus coioides* [Grandcourt et al., 2009]; *E. andersoni* [Fennessy and Sadovy, 2002]; *Cephalopholis boenak* [Liu and Sadovy, 2004]; *C. taeniops* [Siau, 1994]) but seem to constitute a minority of species within the subfamily Epinephelinae. Diandry appears to be better represented among small-bodied species and genera, whereas monandry exemplified by Hawaiian grouper is consistent with the general pattern for large-bodied groupers. Most known species of medium to large epinephelid groupers also are aggregation-spawners (Samoilys and Squire, 1994; Sadovy et al., 1994), but nothing is known of the spawning habits of Hawaiian grouper. Large (e.g., 7–12% [Erisman et al., 2007]) male *GSI*s are typical in groupers in which sperm competition occurs within multiple-male spawning aggregations. The relatively small (<1%) testes weights (compared to ovaries) of Hawaiian grouper are typical of protogynous species (Molloy et al., 2007) and indicate that it spawns in single-male spawning groups that lack intense sperm competition (Sadovy et al., 1994). Although inconsistent with multiple-male spawning groups, relatively small testes size might reflect pair-spawning within aggregations and cannot be used as evidence either for or against aggregation spawning in the species (Domeier and Colin, 1997). Growing evidence indicates that monandry and pair-spawning within aggregations are the norm for epinephelids that are large enough to migrate and can monopolize females while pair-spawning at low male densities. Diandry and multiple-male group-spawning is relatively prevalent in smaller-bodied species that cannot tolerate the predation risk of migration to aggregation sites and that experience sperm competition at relatively high male densities.

We caution that our evaluation of sex allocation patterns for Hawaiian grouper is limited to fish in the NWHI. Other sex and gonadal allocation patterns may exist for populations in the windward, high main Hawaiian Islands where, among other

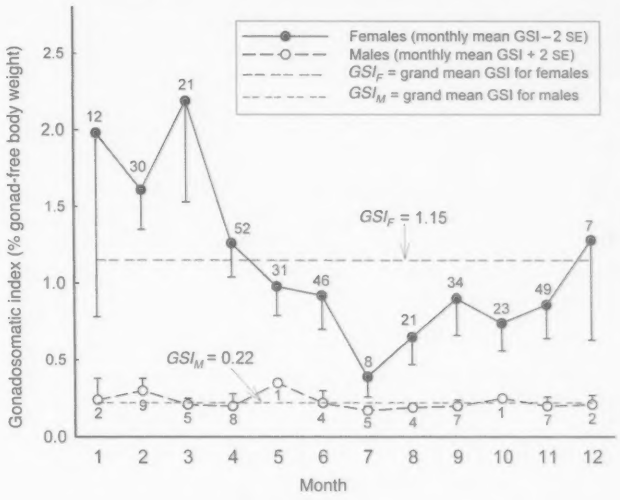
Females (monthly mean GSI – 2 SE)
Males (monthly mean GSI + 2 SE)
GSI_F = grand mean GSI for females
GSI_M = grand mean GSI for males
Gonadosomatic index (% gonad-free body weight)
GSI_F = 1.15
GSI_M = 0.22
Month

Figure 6

Monthly gonadosomatic indices for female (top: solid circles and line) and male (bottom: hollow circles and coarse dashed line) Hawaiian grouper (*Hyporthodus quernus*). The mean gonadosomatic indices for females (GSI_F) and males (GSI_M) are indicated by medium and fine dashed lines, respectively. The number either above or below each data point indicates sample size (number of fish). Vertical lines represent 2 standard errors (SE).

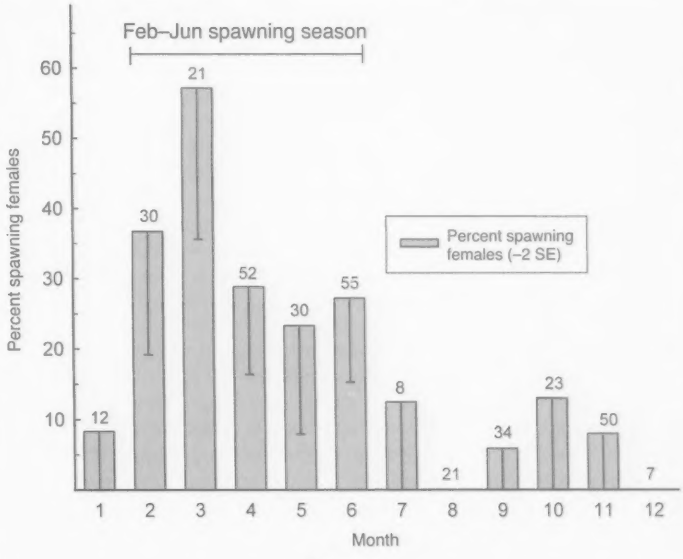

Figure 7

Proportional monthly incidence of actively spawning female Hawaiian grouper (*Hyporthodus quernus*) (i.e., those whose ovaries contained hydrated oocytes, postovulatory follicles, or both). The number above each histogram bar indicates sample size (number of fish). Vertical lines represent 2 standard errors (SE).

things, the species' depth distribution is appreciably deeper (DeMartini and Friedlander, 2004) and depth-related differences in benthic habitat are likely.

Body sizes at maturation and at sex change

All Hawaiian grouper apparently first mature as females at about 58 cm TL. Our estimate is close to a preliminary estimate (570.5 mm TL [Everson[3]]) based only on the same early series of histological slides. Maturation at 58 cm is equivalent to about 52% of a maximum body length of 110.6 cm TL (Seki, 1986). Most groupers mature at about 40–60% of maximum body length (Shapiro, 1987). A preliminary growth estimate for Hawaiian grouper (Nichols and DeMartini[2]) indicates that the median length at female maturation corresponds to an age of 6–7 yr.

On average, adult Hawaiian grouper change sex from female to male at about 89–90 cm TL. A preliminary growth curve indicates that this would be equivalent to an age of >20 yr, but size-at-age estimates for fish this large are imprecise (Nichols and DeMartini[2]) and any firm conclusion must await pending validations of older age estimates. Sex change thus occurs at about 81% of maximum body length. Our estimate of relative size at sex change approximates (perhaps coincidentally) the 80% predicted by using an empirical relationship between maximum body length and length at sex change derived by Allsop and West (2003) and based on data for diverse protogynous fish lineages.

Spawning seasonality and sex ratio

Evidence of spawning from gonad indices, together with estimates of the proportional incidence of spawning females, convincingly illustrates that Hawaiian grouper spawn in the NWHI during the first and second quarters of the calendar year, peak ripening occurs in December–April, and peak spawning follows several months later (in February–June). Relatively little reproduction occurs outside these months, although large females may begin to spawn in the fall. The multimodal size distribution of yolked oocytes indicates that individual females spawn more than once during a spawning season. Male Hawaiian grouper seem capable of spawning throughout the year. Most species of groupers spawn during a restricted period of year (Shapiro, 1987).

The highly female-biased adult sex ratio of Hawaiian grouper is typical of protogynous sequential hermaphrodites in which adult sex ratios are almost never male biased (Allsop and West, 2004; West, 2009). Species that do not change sex usually have adult sex ratios approximating unity (Charnov, 1982; Molloy et al., 2007). Our estimated 6-to-1 adult sex ratio for Hawaiian grouper is surely conservative because the targeting of larger adults by commercial fishermen is likely (i.e., catches are male biased), and most of our recent collection series were fishery-dependent samples. Fishery-dependent catches that are sex biased cannot be used to argue whether a fishery either has or has not induced changes in the operational sex ratio of a resource population.

Implications for fishery management

The life history information needed to better manage the Hawaiian grouper fishery in the MHI includes data on possible regional differences between fish in the MHI and NWHI. Little is known about geographic variation in sizes at maturity and at sex change among intraspecific populations of commercial species of sequential hermaphrodites, even though both potential and actual temporal changes reflecting varying magnitudes of exploitation are recognized (Heppell et al., 2006, and references cited therein). Our finding of equivalent body sizes at female maturation for the early versus recent NWHI collection series indicates that this fundamental aspect of the species' reproductive dynamics has not changed between the early 1980s and the mid-2000s in this region. This finding implies that the NWHI bottomfishery has not quantitatively altered the reproductive life-history of the species over the past several decades in the NWHI—perhaps reflecting the strongly regulated and capped levels of take in this region of the archipelago. In the MHI, however, body size has on average been smaller and the proportion of presumed immature fish has been greater for Hawaiian grouper caught in the MHI than in either the Mau or Ho'omalu Zone of the NWHI during the past two decades (Moffitt et al.[1]). The body sizes at female maturation and at female-to-male sex change of this species in the MHI, and evidence that they have recently declined, are currently unknown. Because of the likely but presently unquantified targeting of large Hawaiian grouper, there is a clear need to estimate body sizes at maturation and at sex change for the species in the MHI and to integrate such findings with those of this study. Characterizations of the growth rate and longevity of the Hawaiian grouper also need to be completed for each region and for the regions collectively.

Protogynous fishes, epinephelid groupers in particular (e.g., Adams et al., 2000; Coleman et al., 1996), are especially sensitive to changes in size and sex distributions as a result of harvesting (Alonzo and Mangel, 2004, 2005; Alonzo et al., 2008). Regional variations in key reproductive life history traits like sex ratio, body sizes at maturity and at sex change, and the occurrence of aggregation-spawning can profoundly influence population dynamics and the consequent effective management of protogynous stocks (Vincent and Sadovy, 1998). This is true regardless of whether the management scheme incorporates the use of no-take zones (e.g., the entire NWHI since 2010 and Johnston Atoll since 2009) or is limited to more conventional management measures like bag and size limits (Molloy et al., 2008). The latter unfortunately is impractical for a deep-water multispecies line fishery like the MHI bottomfishery in which barotrauma is a serious issue for all sizes of most species caught (Haight et al., 1993). Regional variation in stock structure may be especially important for

management of the MHI fishery because of the genetic differentiation of Hawaiian grouper that has been documented within the archipelago (Rivera et al., 2004).

Acknowledgments

We thank the many NOAA Fisheries biologists and technicians who processed specimens used in this study and the captains and crews of NOAA research vessels for their assistance. We acknowledge Federal Disaster Relief Project no. 657787, and the Pelagic Fisheries Research Program (University of Hawaii), for funding the purchase of recent specimens; A. Andrews and R. Humphreys for reviewing the draft manuscript; and M. McCracken for statistical advice. This article is dedicated to the memory of Julia P. Leung DeMartini, who photo-edited the final version of Figure 3; may her many memes continue to spread throughout the biological research community.

Literature cited

Adams, S.
2003. Morphological ontogeny of the gonad of three plectropomid species through sex differentiation and transition. J. Fish Biol. 63:22–36.

Adams, S., B. D. Mapstone, G. R. Russ, and C. R. Davies.
2000. Geographic variation in the sex ratio, sex specific size, and age structure of *Plectropomus leopardus* Serranidae) between reefs open and closed to fishing on the Great Barrier Reef. Can. J. Fish. Aquat. Sci. 57:1448–1458.

Allsop, D. J., and S. A. West.
2003. Constant relative age and size at sex change for sequentially hermaphroditic fish. J. Evol. Biol. 16:921–929.
2004. Sex-ratio evolution in sex changing animals. Evolution 58:1019–1027.

Alonzo, S. H., T. Ish, M. Key, A. D. MacCall, and M. Mangel.
2008. The importance of incorporating protogynous sex change into stock assessments. Bull. Mar. Sci. 83:163–179.

Alonzo, S. H., and M. Mangel.
2004. The effects of size-selective fisheries on the stock dynamics of and sperm limitation in sex-changing fish. Fish. Bull. 102:1–13.
2005. Sex-change rules, stock dynamics, and the performance of spawning-per-recruit measures in protogynous stocks. Fish. Bull. 103:229–245.

Brule, T., X. Renan, T. Colas-Marrufo, Y. Hauyon, and A. N. Tuz-Sulub.
2003. Reproduction in the protogynous black grouper (*Mycteroperca bonaci* (Poey)) from the southern Gulf of Mexico. Fish. Bull. 101:463–475.

Chan, T. T. C., and Y. Sadovy.
2002. Reproductive biology, age and growth in the chocolate hind, *Cephalopholis boenak* (Bloch, 1790), in Hong Kong. Mar. Freshw. Res. 53:791–803.

Charnov, E. L.
1982. The theory of sex allocation. Princeton Univ. Press, Princeton, NJ.

Coleman, F. C., C. C. Koenig, and L. A. Collins.
1996. Reproductive styles of shallow-water groupers (Pisces: Serranidae) in the eastern Gulf of Mexico and the consequences of fishing spawning aggregations. Environ. Biol. Fish. 47:129–141.

Craig, M. T., and P. A. Hastings.
2007. A molecular phylogeny of the groupers of the subfamily Epinephelinae (Serranidae) with a revised classification of the Epinephelini. Ichthyol. Res. 54: 1–17.

DeMartini, E. E., and A. M. Friedlander.
2004. Spatial patterns of endemism in shallow-water reef fish populations of the Northwestern Hawaiian Islands. Mar. Ecol. Prog. Ser. 271:281–296.

DeMartini, E. E., and P. C. Sikkel.
2006. Reproduction. *In* The ecology of marine fishes: California and adjacent waters (L. G. Allen, D. J. Pondella, and M. H. Horn, eds.), p. 483–523. Univ. Calif. Press, Berkeley.

Domeier, M. L., and P. L. Colin.
1997. Tropical reef fish spawning aggregations: defined and reviewed. Bull. Mar. Sci. 60:698–726.

Erickson, D. L., J. E. Hightower, and G. D. Grossman.
1985. The relative gonadal index: an alternative index for quantification of reproductive condition. Comp. Biochem. Physiol. 81A:117–120.

Erisman, B. E., M. L. Buckhorn, and P. A. Hastings.
2007. Spawning patterns in the leopard grouper, *Mycteroperca rosacea*, in comparison with other aggregating groupers. Mar. Biol. 151:1849–1861.

Erisman, B. E., M. T. Craig, and P. A. Hastings.
2010. Reproductive biology of the Panama graysby *Cephalopholis panamensis* (Teleostei: Epinephelidae). J. Fish Biol. 76:1312–1328.

Fennessy, S. T., and Y. Sadovy.
2002. Reproductive biology of a diandric protogynous hermaphrodite, the serranid *Epinephelus andersoni*. Mar. Freshw. Res. 53:147–158.

Fitzhugh, G. R., and W. F. Hettler.
1995. Temperature influence on postovulatory follicle degeneration in Atlantic menhaden. Fish. Bull. 93:568–572.

Goodyear, C. P.
1993. Spawning stock biomass per recruit in fisheries management: foundation and current use. *In* Risk evaluation and biological reference points for fisheries management. (S. J. Smith, J. J. Hunt, and D. Rivard, eds.), p. 67–81. Can. Spec. Publ. Fish. Aquat. Sci. 120.

Grandcourt, E. M., T. Z. Al Abdesalaam, F. Francis, A. T. Al Shamsi, and S. A. Hartmann.
2009. Reproductive biology and implications for management of the orange-spotted grouper *Epinephelus coioides* in the southern Arabian Gulf. J. Fish Biol. 74:820–841.

Haight, W. R., J. D. Parrish, and T. A. Hayes.
1993. Feeding ecology of deepwater lutjanid snappers at Penguin bank, Hawaii. Trans. Am. Fish. Soc. 122:328–347.

Heppell, S. S., S. A. Heppell, F. C. Coleman, and C. C. Coleman.
2006. Models to compare management options for a protogynous fish. Ecol. Appl. 16:238–249.

Hunter, J. R., and B. J. Macewicz.
1985. Measurement of spawning frequency in multiple spawning fishes. *In* An egg production method for estimating spawning biomass of pelagic fish: application to the northern anchovy, *Engraulis mordax* (R. Lasker, ed.), p. 79–94. NOAA Tech. Rep. NMFS 35.

Huntsman, G. R., J. Potts, R. W. Mays, and D. Vaughan.
1999. Groupers (Serranidae, Epinephelinae): endangered apex predators of reef communities. *In* Life in the slow lane: ecology and conservation of long-lived marine animals (J. A. Musick, ed.), p. 217–231. Am. Fish. Soc. Symp. 23, Am. Fish. Soc., Bethesda, MD.

Lau, B. B., and E. E. DeMartini.
1994. An evaluation of oocyte size in multiple regressions predicting gonad weight from body weight: a test using *Etelis carbunculus*. NOAA Tech. Memo. NMFS-SWFSC-212, 17 p.

Liu, M., and Y. Sadovy.
2004. Early gonadal development and primary males in the protogynous epinepheline, *Cephalopholis boenak*. J. Fish Biol. 65:987–1002.

Mackie, M.
2000. Reproductive biology of the halfmoon grouper, *Epinephelus rivulatus*, at Ningaloo Reef, Western Australia. Environ. Biol. Fish. 57:363–376.

Molloy, P. P., N. B. Goodwin, I. M. Cote, J. D. Reynolds, and M. J. G. Gage.
2007. Sperm competition and sex change: a comparative analysis across fishes. Evolution 61:640–652.

Molloy, P. P., J. D. Reynolds, M. J. G. Gage, I. Mosquiera, and I. B. Cote.
2008. Links between sex change and fish densities in protected areas. Biol. Conserv. 141:187–197.

Morris, A. V., C. M. Roberts, and J. P. Hawkins.
2000. The threatened status of groupers (Epinephelinae). Biodiv. Conserv. 9:919–942.

Pears, R. J., J. H. Choat, B. D. Mapstone, and G. A Begg.
2007. Reproductive biology of a large, aggregation-spawning serranid, *Epinephelus fuscoguttatus* (Forsskal): management implications. J. Fish Biol. 71:795–817.

Quinn, G. P., and M. J. Keough.
2002. Experimental design and data analysis for biologists, 537 p. Cambridge Univ. Press, Cambridge, UK.

Quinn, T. J., II, and R. B. Deriso.
1999. Quantitative fish dynamics, 542 p. Oxford Univ. Press, New York.

Rivera, M. A. J., C. D. Kelly, and G. K. Roderick.
2004. Subtle population genetic structure in the Hawai'i grouper, *Epinephelus quernus* (Serranidae) as revealed by mitrochondrial DNA analyses. Biol. J. Linn. Soc. 81:449–468.

Sadovy, Y.
1996. Reproduction of reef fishery species. *In* Reef fisheries (N. V. C. Polunin and C. M. Roberts, eds.), p. 15–59. Chapman and Hall, London.

Sadovy, Y., and P. L. Colin.
1995. Sexual development and sexuality in the Nassau grouper. J. Fish Biol. 46:961–976.

Sadovy, Y., and M. L. Domeier.
2005. Perplexing problems of sexual patterns in the fish genus *Paralabrax* (Serranidae, Serraninae). J. Zool. (Lond.) 267:121–133.

Sadovy, Y., A. Rosario, and A. Roman.
1994. Reproduction in an aggregating grouper, the red hind, *Epinephelus guttatus*. Environ. Biol. Fish. 41:269–286.

Sadovy, Y., and D.Y. Shapiro.
1987. Criteria for the diagnosis of hermaphroditism in fishes. Copeia 1987:136–156.

Sadovy de Mitcheson, Y., and M. Liu.
2008. Functional hermaphroditism in teleosts. Fish Fish. 9:1–43.

Samoilys, M. A., and L. C. Squire.
1994. Preliminary observations on the spawning behavior of coral trout *Plectropomus leopardus* (Pisces, Serranidae), on the Great Barrier Reef. Bull. Mar. Sci. 54:332–342.

Seki, M. P.
1986. Serranidae (*Epinephelus quernus*). *In* Fishery atlas of the Northwestern Hawaiian Islands. (R. N. Uchida and J. H. Uchiyama, eds.), p. 82–83. NOAA Tech. Rep. NMFS 38, 142 p.

Shapiro, D.Y.
1987. Reproduction in groupers. *In* Tropical snappers and groupers: biology and fisheries management (J. J. Polovina and S. Ralston, eds.), p. 295–327. Westview Press, Boulder, CO.

Siau, Y.
1994. Population structure, reproduction and sex-change in a tropical East Atlantic grouper. J. Fish Biol. 44:205–211.

Smith, W. L., and M. T. Craig.
2007. Casting the percomorph net widely: the importance of broad taxonomic sampling in the search for the placement of serranid and percid fishes. Copeia 2007:35–55.

Vincent, A. C. J., and Y. Sadovy.
1988. Reproductive ecology and the conservation and management of fishes. *In* Behavioral ecology and conservation biology (T. Caro, ed.), p. 209–245. Oxford Univ. Press, Oxford.

West, G.
1990. Methods of assessing ovarian development in fishes: a review. Austr. J. Mar. Freshw. Res. 41:199–222.

West, S.
2009. Sex allocation. Monographs in population biology. Princeton Univ. Press, Princeton, NJ.

Zar, J. H
1984. Biostatistical analysis, 2nd ed., 718 p. Prentice-Hall, Englewood Cliffs, NJ.

Errata

Fishery Bulletin 107:235–243.

Graham, Larissa J., Mark L. Botton, David Hata, Robert E. Loveland, and Brian R. Murphy
Prosomal-width-to-weight relationships in American horseshoe crabs (*Limulus polyphemus*): examining conversion factors used to estimate landings

Page 238, Equation 1. The *y*-intercept variable reads "*b*" and it should read "$\log_e(b)$."

Page 241, Table 3. The third entry horizontally in the boxhead of the table reads "b" and it should read "$\log_e(b)$." Likewise, "SE(*b*)" should read "SE[$\log_e(b)$]."

The table should read as follows:

Table 3

The number of individuals sampled (n), coefficient values (a, $\log_e(b)$), standard errors for values (SE[a], SE[$\log_e(b)$]), and correlation coefficient (r^2) of the relationship between prosomal width and weight for horseshoe crabs (*Limulus polyphemus*), $\log_e(Wt)=\log_e(PW)\times a+\log_e(b)$. Samples were collected during the Horseshoe Crab Research Center trawl survey (i.e., inshore continental shelf waters between New York and Virginia), spawning surveys (i.e., New Jersey, Delaware, New Hampshire), and the commercial fishery (i.e., Delaware). All regressions are significant (α=0.05).

	n	a	$\log_e(b)$	SE(a)	SE[$\log_e(b)$]	r^2
Female (all)	1025	2.98	–15.71	0.02	0.10	0.96
Females (mature)	802	2.65	–13.85	0.04	0.21	0.86
Females (immature)	223	2.85	–15.10	0.05	0.23	0.95
Males (all)	1055	2.89	–15.39	0.02	0.12	0.94
Males (mature)	931	2.97	–15.80	0.02	0.13	0.94
Males (immature)	124	2.58	–13.81	0.10	0.50	0.85

Fishery Bulletin

Guidelines for authors

Manuscript Preparation

Contributions published in *Fishery Bulletin* describe original research in marine fishery science, fishery engineering and economics, as well as the areas of marine environmental and ecological sciences (including modeling). Preference will be given to manuscripts that examine processes and underlying patterns. Descriptive reports, surveys, and observational papers may occasionally be published but should appeal to an audience outside the locale in which the study was conducted. Although all contributions are subject to peer review, responsibility for the contents of papers rests upon the authors and not on the editor or publisher. *Submission of an article implies that the article is original and is not being considered for publication elsewhere.* **Articles** may range from relatively short contributions (10–15 typed, double-spaced pages, tables and figures not included) to extensive contributions (20–30 typed pages). Manuscripts must be written in English; authors whose native language is not English are strongly advised to have their manuscripts checked by English-speaking colleagues before submission.

Title page should include authors' full names and mailing addresses and the senior author's telephone, fax number, and e-mail address, and a list of key words to describe the contents of the manuscript. **Abstract** should be limited to 200 words (one-half typed page), state the main scope of the research, and emphasize the author's conclusions and relevant findings. Do not review the methods of the study or list the contents of the paper. Because abstracts are circulated by abstracting agencies, it is important that they represent the research clearly and concisely. **Text** must be typed in 12 point Times New Roman font throughout. A brief introduction should convey the broad significance of the paper; the remainder of the paper should be divided into the following sections: **Materials and methods, Results, Discussion** (or **Conclusions**), and **Acknowledgments**. Headings within each section must be short, reflect a logical sequence, and follow the rules of multiple subdivision (i.e., there can be no subdivision without at least two items). The entire text should be intelligible to interdisciplinary readers; therefore, all acronyms, abbreviations, and technical terms should be written out in full the first time they are mentioned. Include FAO common names for species in the list of keywords and in the introduction. Regional common names may be used throughout the rest of the text if they are different from FAO common names which can be found at http://www.fishbase.org/search.html. Follow the U.S. Government Printing Office Style Manual (2000 ed.) and Scientific Style and Format: the CSE Manual for Authors, Editors, and Publishers (7th ed.) for editorial style; for fish nomenclature follow the most current issue of the American Fisheries Society's Common and Scientific Names of Fishes from the United States, Canada, and Mexico, 6th ed. Dates should be written as follows: 11 November 2000. Measurements should be expressed in metric units, e.g., 58 metric tons (t); if other units of measurement are used, please make this fact explicit to the reader. Write out the numbers zero through nine unless they form part of measurement units (e.g., nine fish but 9 mm). Refrain from using the shorthand slash (/), an ambiguous symbol, in the general text.

Equations and mathematical symbols Set equations from a standard mathematical program (MathType) or tool (Equation Editor in MS Word). LaTex is acceptable for more advanced computations. For mathematical symbols in the general text (α, χ^2, π, $\pm$, etc.), use the symbols provided by the MS Word program and italicize all variables. Do not use the photo mode when creating these symbols in the general text.

Literature cited comprises published works and those accepted for publication in peer-reviewed literature (in press). Follow the name and year system for citation format in the "Literature cited" section (that is say, citations should be listed alphabetically by the authors' last names, and then by year if there is more than one citation with the same authorship). If there is a sequence of citations in the text, list chronologically: (Smith, 1932; Green, 1947; Smith and Jones, 1985). Abbreviations of serials should conform to abbreviations given in Cambridge Scientific Abstracts (http://www.csa.com/ids70/serials_source_list.php?ab=biolclast-set-c). Authors are responsible for the accuracy and completeness of all citations. Literature citation format: Author (last name, followed by first-name initials). Year. Title of report or manuscript. Abbreviated title of the series to which it belongs. Always include number of pages. Cite all software and special equipment or chemical solutions used in the study, not in a footnote but within parentheses in the text (e.g., SAS, vers. 6.03, SAS Inst., Inc., Cary, NC).

Tables are often overused in scientific papers; it is seldom necessary or even desirable to present all the data associated with a study. Tables should not be excessive in size and must be cited in numerical order in the text. Headings should be short but ample enough to allow the table to be intelligible on its own. All unusual symbols must be explained in the table legend. Other incidental comments may be footnoted with italic numeral footnote markers. Use asterisks to indicate significance in statistical data. Do not type table legends on a separate page; place them above the table data. *Do not submit tables in photo mode.*

Figures include line illustrations, photographs (or slides), and computer-generated graphs and must be cited in numerical order in the text. Graphics should aid in the comprehension of the text, but they should be limited to presenting patterns rather than raw data. Figures should not exceed one figure for every four pages of text. Figures must be labeled with author's

name and number of the figure. Avoid placing labels vertically (except for *y* axis). Figure legends should explain all symbols and abbreviations and should be double-spaced on a separate page at the end of the manuscript. Color is allowed in figures to show morphological differences among species (for species identification), to show stain reactions, and to show gradations in temperature contours within maps. Color is discouraged in graphs, and for the few instances where color may be allowed, the use of color will be determined by the Managing Editor.

- Zeros should precede all decimal points for values less than one.
- Sample size, *n*, should be italicized.
- Capitalize the first letter of the first word in all labels within figures.
- Do not use overly large font sizes in maps and for units of measurements along axes in figures.
- Do not use bold fonts or bold lines in figures.
- Do not place outline rules around graphs.
- Use a comma in numbers of five digits or more (e.g. 13,000 but 3000).
- Maps require a North arrow and degrees latitude-longitude (e.g., 170°E).

Failure to follow these guidelines and failure to correspond with editors in a timely manner will delay publication of a manuscript.

Copyright law does not apply to *Fishery Bulletin*, which falls within the public domain. However, if an author reproduces any part of an article from *Fishery Bulletin* in his or her work, reference to source is considered correct form (e.g., Source: Fish. Bull. 97:105).

Submission

Submit manuscript online at http://mc.manuscriptcentral.com/fisherybulletin. Commerce Department personnel should submit papers under a completed NOAA Form 25-700. For further details on electronic submission, please contact the Scientific Editorial Office directly at

julie.scheurer@noaa.gov

Once the manuscript has been accepted for publication, you will be asked to submit a final electronic copy of your manuscript. When requested, the text and tables should be submitted in Word format. Figures should be sent as PDF files, Windows metafiles, tiff files, or EPS files. Send a copy of figures in the original software if conversion to any of these formats yields a degraded version.

Questions? If you have questions regarding these guidelines, please contact the Managing Editor, Sharyn Matriotti, at

Sharyn.Matriotti@noaa.gov

Questions regarding manuscripts under review should be addressed to Julie Scheurer, Associate Editor.

Fishery Bulletin

Subscription form

Superintendent of Documents **Publications** Order Form

*5178

☐ YES, please send me the following publications:

____ Subscriptions to *Fishery Bulletin*
for $36.00 per year ($50.40 foreign)

The total cost of my order is $ _____ . Prices include regular domestic postage and handling and are subject to change.

_____
(Company or Personal Name) (Please type or print)

_____
(Additional address/attention line)

_____
(Street address)

_____
(City, State, ZIP Code)

_____
(Daytime phone including area code)

_____
(Purchase Order No.)

Charge your order. IT'S EASY!

VISA

MasterCard

Please Choose Method of Payment:

☐ Check Payable to the Superintendent of Documents
☐ GPO Deposit Account ☐☐☐☐☐☐☐–☐
☐ VISA or MasterCard Account
☐☐☐☐☐☐☐☐☐☐☐☐☐☐☐☐
☐☐☐☐ (Credit card expiration date)

To fax your orders (202) 512-2250

_____
(Authorizing Signature)

Mail To: Superintendent of Documents
P.O. Box 371954, Pittsburgh, PA 15250-7954

Thank you for your order!
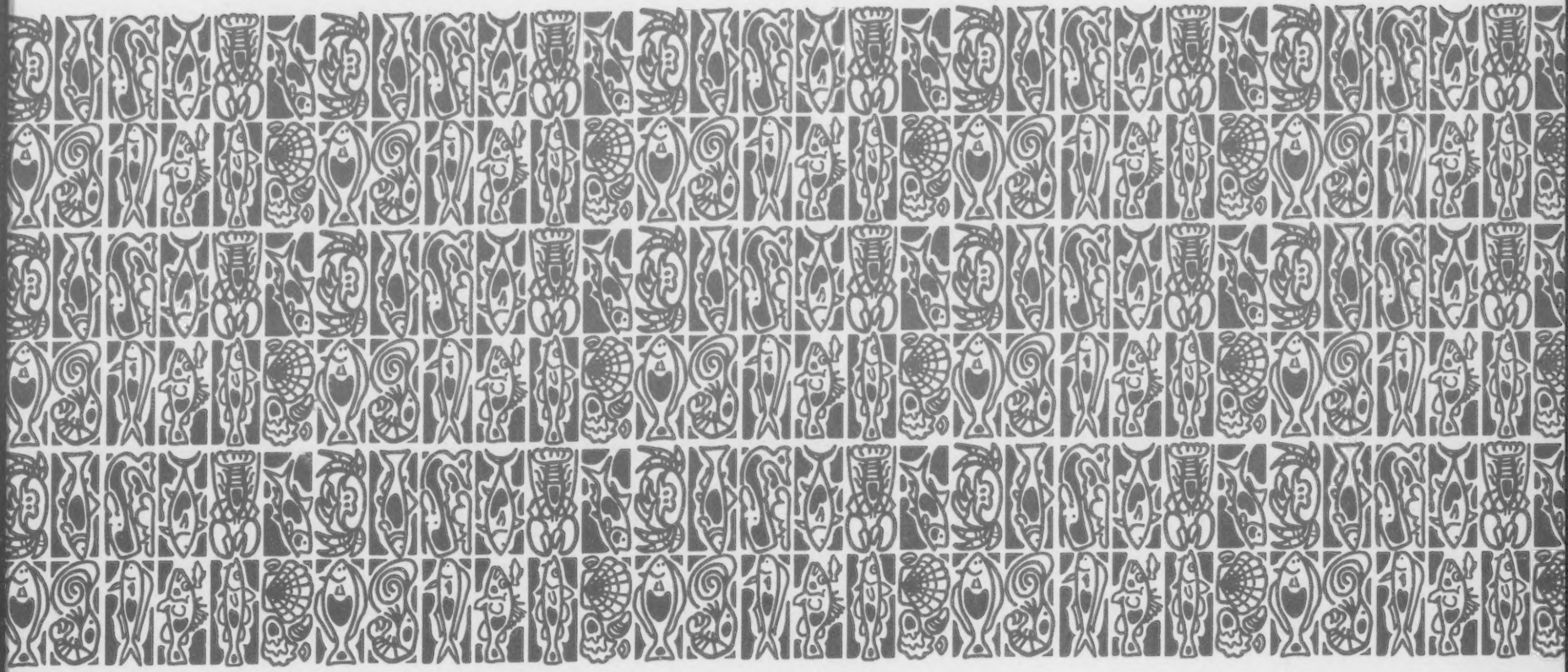
Also available online at http://bookstore.gpo.gov/collections/fishery-bulletin